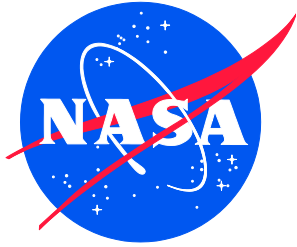


NASA/TM–2020-220568/Volume II/Part 5



# Nondestructive Evaluation (NDE) Methods and Capabilities Handbook

*Volume II Appendices — Appendix E Volume 4*

*Patricia A. Howell, Editor  
Langley Research Center, Hampton, Virginia*

APPROVED FOR PUBLIC RELEASE

February 2020

## NASA STI Program . . . in Profile

Since its founding, NASA has been dedicated to the advancement of aeronautics and space science. The NASA scientific and technical information (STI) program plays a key part in helping NASA maintain this important role.

The NASA STI program operates under the auspices of the Agency Chief Information Officer. It collects, organizes, provides for archiving, and disseminates NASA's STI. The NASA STI program provides access to the NTRS Registered and its public interface, the NASA Technical Reports Server, thus providing one of the largest collections of aeronautical and space science STI in the world. Results are published in both non-NASA channels and by NASA in the NASA STI Report Series, which includes the following report types:

- **TECHNICAL PUBLICATION.** Reports of completed research or a major significant phase of research that present the results of NASA Programs and include extensive data or theoretical analysis. Includes compilations of significant scientific and technical data and information deemed to be of continuing reference value. NASA counter-part of peer-reviewed formal professional papers but has less stringent limitations on manuscript length and extent of graphic presentations.
- **TECHNICAL MEMORANDUM.** Scientific and technical findings that are preliminary or of specialized interest, e.g., quick release reports, working papers, and bibliographies that contain minimal annotation. Does not contain extensive analysis.
- **CONTRACTOR REPORT.** Scientific and technical findings by NASA-sponsored contractors and grantees.

- **CONFERENCE PUBLICATION.** Collected papers from scientific and technical conferences, symposia, seminars, or other meetings sponsored or co-sponsored by NASA.
- **SPECIAL PUBLICATION.** Scientific, technical, or historical information from NASA programs, projects, and missions, often concerned with subjects having substantial public interest.
- **TECHNICAL TRANSLATION.** English-language translations of foreign scientific and technical material pertinent to NASA's mission.

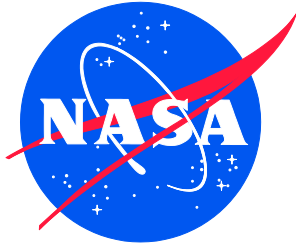
Specialized services also include organizing and publishing research results, distributing specialized research announcements and feeds, providing information desk and personal search support, and enabling data exchange services.

For more information about the NASA STI program, see the following:

- Access the NASA STI program home page at <http://www.sti.nasa.gov>
- E-mail your question to [help@sti.nasa.gov](mailto:help@sti.nasa.gov)
- Phone the NASA STI Information Desk at 757-864-9658

- Write to:  
NASA STI Information Desk  
Mail Stop 148  
NASA Langley Research Center  
Hampton, VA 23681-2199

NASA/TM–2020-220568/Volume II/Part 5



# Nondestructive Evaluation (NDE) Methods and Capabilities Handbook

*Volume II Appendices — Appendix E Volume 4*

*Patricia A. Howell, Editor  
Langley Research Center, Hampton, Virginia*

National Aeronautics and  
Space Administration

Langley Research Center  
Hampton, Virginia 23681-2199

APPROVED FOR PUBLIC RELEASE

February 2020

**The material is based upon work supported by NASA under Award Nos.  
NNL09AA00A and 80LARC17C0004**

The use of trademarks or names of manufacturers in the report is for accurate reporting and does not constitute an official endorsement, either expressed or implied, of such products or manufacturers by the National Aeronautics and Space Administration.

Available from:

NASA STI Program / Mail Stop 148  
NASA Langley Research Center  
Hampton, VA 23681-2199  
Fax: 757-864-6500



## Table of Contents

E.61 Specimen #61: NASA-03-Folded-Tow-002 .....	1
E.61.1 Method: Pulse-Echo Ultrasound Testing (PEUT) .....	1
E.61.2 Method: Single-Sided Infrared Thermography (SSIR).....	4
E.61.3 Method: Through-Transmission Infrared Thermography (TTIR) .....	7
E.61.4 Method: Single-Side Flash Thermography (SSFT-TSR).....	10
E.62 Specimen #62: NASA-03-Missing-Tow-001 .....	12
E.62.1 Method: Pulse-Echo Ultrasound Testing (PEUT) .....	12
E.62.2 Method: Single-Sided Infrared Thermography (SSIR).....	15
E.62.3 Method: Through-Transmission Infrared Thermography (TTIR) .....	18
E.62.4 Method: Single-Side Flash Thermography (SSFT-TSR).....	21
E.63 Specimen #63: NASA-03-Missing-Tow-002 .....	23
E.63.1 Method: Pulse-Echo Ultrasound Testing (PEUT) .....	23
E.63.2 Method: Single-Sided Infrared Thermography (SSIR).....	26
E.63.3 Method: Through-Transmission Infrared Thermography (TTIR) .....	29
E.63.4 Method: Single-Side Flash Thermography (SSFT-TSR).....	32
E.64 Specimen #64 – NASA-03-Bridged Joggle-001 – Not Tested .....	34
E.65 Specimen #65 – NASA-03-Bridged-Joggle-002 – Not Tested.....	34
E.66 Specimen #66 – NASA-03-Bridged-Joggle-003 – Not Tested.....	34
E.67 Specimen #67 – NASA-03-Bridged-Joggle-004 – Not Tested.....	34
E.68 Specimen #68: NAA-03-FOD-Panel-001:.....	34
E.68.1 Method: Pulse-Echo Ultrasound Testing (PEUT) .....	35
E.68.2 Method: Through-Transmission Ultrasound Testing (TTUT).....	37
E.68.3 Method: Pulse Echo Ultrasound Testing (PEUT).....	38
E.69 Specimen #69: NASA-03-Porosity-Panel-001 .....	39
E.69.1 Method: Pulse-Echo Ultrasound Testing (PEUT) .....	40
E.69.2 Method: Pulse-Echo Ultrasound Testing (PEUT) .....	42
E.69.3 Method: Through-Transmission Ultrasound Testing (TTUT).....	45
E.69.4 Method: Single-Sided Infrared Thermography (SSIR).....	48
E.69.5 Method: Through-Transmission Infrared Thermography (TTIR) .....	51
E.70 Specimen #70: NASA-03-Porosity-Panel-002 .....	54
E.70.1 Method: Pulse-Echo Ultrasound Testing (PEUT) .....	55
E.70.2 Method: Pulse-Echo Ultrasound Testing (PEUT) .....	58
E.70.3 Method: Through-Transmission Ultrasound Testing (TTUT).....	61
E.70.4 Method: Single-Sided Infrared Thermography (SSIR).....	63
E.70.5 Method: Through-Transmission Infrared Thermography (TTIR) .....	67
E.71 Specimen #71A&B: NASA-03-Porosity-Panel-003.....	70
E.71.1 Method: Pulse-Echo Ultrasound Testing (PEUT) .....	71
E.71.2 Method: X-ray Computed Tomography (XCT).....	74
E.71.3 Method: Pulse-Echo Ultrasound Testing (PEUT) .....	77
E.71.4 Method: Through-Transmission Ultrasound Testing (TTUT).....	80
E.71.5 Method: Single-Sided Infrared Thermography (SSIR).....	82
E.71.6 Method: Through-Transmission Infrared Thermography (TTIR) .....	86
E.72 Specimen #72A&B: NASA-03-Porosity-Panel-004.....	89
E.72.1 Method: Pulse-Echo Ultrasound Testing (PEUT) .....	90
E.72.2 Method: X-ray Computed Tomography (XCT).....	93
E.72.3 Method: Pulse-Echo Ultrasound Testing (PEUT) .....	96
E.72.4 Method: Through-Transmission Ultrasound Testing (TTUT).....	99
E.72.5 Method: Single-Side Infrared Thermography (SSIR).....	101
E.72.6 Method: Through-Transmission Infrared Thermography (TTIR) .....	104

E.73 Specimen #73 – NASA-005-STANDARD-001 – Not Tested.....	107
E.74 Specimen #74 – NASA-005-STANDARD-002 – Not Tested.....	107
E.75 Specimen #75 – NASA-005-Wrinkle-001 – Not Tested .....	108
E.76 Specimen #76 – NASA-05-Wrinkle-002 – Not Tested .....	108
E.77 Specimen #77 – NASA-005-Porosity-001 – Not Tested.....	108
E.78 Specimen #78 – NASA-005-Porosity-002 – Not Tested.....	108
E.79 Specimen #79: NASA-005-Porosity-003.....	108
E.79.1 Method: Pulse-Echo Ultrasound Testing (PEUT) .....	108
E.80 Specimen #80 – NASA-005-Porosity-004 – Not Tested.....	110
E.81 Specimen #81: Boeing Impact QI_45 8ply 6x5 Impact 1 .....	111
E.81.1 Method: X-ray Computed Tomography (XCT).....	111
E.81.2 Method: X-ray Computed Radiography (CR) .....	115
E.81.3 Method: Pulse-Echo Ultrasound Testing (PEUT) .....	117
E.82 Specimen #82: Boeing Impact QI_45 8ply 3x6 Impact 1 .....	121
E.82.1 Method: X-ray Computed Tomography .....	122
E.82.2 Method: X-ray Computed Radiography (CR) .....	122
E.82.3 Method: Pulse-Echo Ultrasound Testing (PEUT) .....	122
E.82.4 Method: X-ray Computed Tomography (XCT).....	125
E.83 Specimen #83: Boeing Impact QI_45 8ply 3x6 Impact 2.....	129
E.83.1 Method: X-ray Computed Tomography (XCT).....	129
E.83.2 Method: X-ray Computed Radiography (CR) .....	129
E.83.3 Method: Pulse-Echo Ultrasound Testing (PEUT) .....	129
E.83.4 Method: X-ray Computed Tomography (XCT).....	132
E.84 Specimen #84 – QI_45 8ply Impact 1 – Not Tested.....	136
E.85 Specimen #85: Boeing Impact QI_45 8ply 22x22 Impact 1 .....	136
E.85.1 Method: X-ray Computed Tomography (XCT).....	137
E.85.2 Method: X-ray Computed Radiography (CR) .....	141
E.85.3 Method: Electronics Shearography with Vacuum Excitation.....	143
E.85.4 Method: X-Ray Backscatter.....	145
E.86 Specimen #86: Boeing Impact QI_45 16ply 6x6 Impact 1 .....	148
E.86.1 Method: X-ray Computed Tomography (XCT).....	148
E.86.2 Method: X-ray Computed Radiography (CR) .....	151
E.86.3 Method: Pulse-Echo Ultrasound Testing (PEUT) .....	154
E.87 Specimen #87: Boeing Impact QI_45 16ply 3x5 Impact 1 .....	158
E.87.1 Method: Pulse-Echo Ultrasound Testing (PEUT) .....	158
E.88 Specimen #88: Boeing Impact QI_45 16ply 3x5 Impact 2.....	164
E.88.1 Method: Pulse-Echo Ultrasound Testing (PEUT) .....	164
E.88.2 Method: X-ray Computed Tomography (XCT).....	167
E.89 Specimen #89: Boeing Impact QI_45 16ply 22x22 Impact 1.....	170
E.90 Specimen #90: Boeing Impact QI_45 24ply 6x6 Impact 1 .....	170
E.90.1 Method: X-ray Computed Tomography (XCT).....	171
E.90.2 Method: X-ray Computed Radiography (CR) .....	174
E.90.3 Method: Pulse-Echo Ultrasound Testing (PEUT) .....	177
E.91 Specimen #91: Boeing Impact QI_45 24ply 3x5 Impact 1 .....	181
E.91.1 Method: Pulse-Echo Ultrasound Testing (PEUT) .....	182
E.91.2 Method: X-ray Computed Tomography (XCT).....	185
E.92 Specimen #92: Boeing Impact QI_45 24ply 3x5 Impact 2.....	188
E.92.1 Method: Pulse-Echo Ultrasound Testing (PEUT) .....	188
E.92.2 Method: X-ray Computed Tomography (XCT).....	192
E.93 Specimen #93: Boeing Impact QI_45 32ply 6x6 Impact 1 .....	196

E.93.1	Method: X-ray Computed Tomography .....	197
E.93.2	Method: X-ray Computed Radiography (CR) .....	200
E.93.3	Method: Pulse-Echo Ultrasound Testing (PEUT)) .....	202
E.94	Specimen #94: Boeing Impact QI_45 32ply 3x5 Impact 1 .....	207
E.94.1	Method: Pulse-Echo Ultrasound Testing (PEUT) .....	207
E.94.2	Method: X-ray Computed Tomography (XCT).....	210
E.95	Specimen #95: Boeing Impact QI_45 32ply 3x5 Impact 2.....	214
E.95.1	Method: Pulse-Echo Ultrasound Testing (PEUT) .....	214
E.96	Specimen #96: Boeing Impact TC1 18ply 6x6 Impact 1 .....	221
E.96.1	Method: X-ray Computed Tomography (XCT).....	222
E.96.2	Method: X-ray Computed Radiography (CR) .....	225
E.96.3	Method: Pulse-Echo Ultrasound Testing (PEUT) .....	228
E.97	Specimen #97: Boeing Impact TC1 18ply 3x5 Impact 1 .....	232
E.97.1	Method: Pulse-Echo Ultrasound Testing (PEUT) .....	233
E.97.2	Method: X-ray Computed Tomography (XCT).....	235
E.98	Specimen #98: Boeing Impact TC1 18ply 3x5 Impact 2 .....	238
E.98.1	Method: Pulse-Echo Ultrasound Testing (PEUT) .....	238
E.98.2	Method: X-ray Computed Tomography (XCT).....	241

## List of Figures

Figure E.61-1.	Photographs of Specimen #61: NASA 03 Folded Tow 002. ....	1
Figure E.61-2.	Ultrasonic system components. ....	2
Figure E.61-3.	Specimen orientation within testing apparatus. ....	2
Figure E.61-4.	UT image showing folded tows in the bulk of the specimen. ....	3
Figure E.61-5.	UT image showing a second view of folded tows in the bulk of the specimen. ....	4
Figure E.61-6.	SSIR setup.....	5
Figure E.61-7.	NASA-03-Folded-Tow-002 sample.....	6
Figure E.61-8.	SSIR inspection of NASA-03-Folded-Tow-002 sample processed with PCA from frame 50 (0.83s) to 1249 (20.82s).....	6
Figure E.61-9.	TTIR setup.....	8
Figure E.61-10.	NASA-03-Folded-Tow-002 sample.....	9
Figure E.61-11.	TTIR inspection of NASA-03-Folded-Tow-002 sample processed with PCA from frame 100 (1.67s) to 1249 (20.82s).....	9
Figure E.61-12.	SSFT system with TSR.....	11
Figure E.61-13.	TSR 1 <sup>st</sup> derivative at 24.41 sec of #61- Fold Ply #12. ....	11
Figure E.62-1.	Photographs of Specimen #61: NASA 03 Missing Tow 001. ....	12
Figure E.62-2.	Ultrasonic system components. ....	13
Figure E.62-3.	Specimen orientation within testing apparatus. ....	13
Figure E.62-4.	UT image showing missing tows near the surface of the specimen. ....	14
Figure E.62-5.	UT image showing evidence of missing tows. ....	15
Figure E.62-6.	SSIR setup.....	16
Figure E.62-7.	NASA-03-Missing-Tow-001 sample.....	17
Figure E.62-8.	SSIR inspection of NASA-03-Missing-Tow-001 sample processed with PCA from frame 100 (1.67s) to 999 (16.65s).....	17
Figure E.62-9.	TTIR setup.....	19
Figure E.62-10.	NASA-03-Missing-Tow-001 sample.....	20
Figure E.62-11.	TTIR inspection of NASA-03-Missing-Tow-001 sample processed with PCA from frame 50 (0.83s) to 250 (4.17s).....	20
Figure E.62-12.	SSFT System with TSR .....	22
Figure E.62-13.	TSR 1 <sup>st</sup> derivative at 20.18 sec of #62-Missing Toe Ply #23.....	22
Figure E.63-1.	Photographs of Specimen #63: NASA 03 Missing Tow 002. ....	23

Figure E.63-2.	Ultrasonic system components. ....	24
Figure E.63-3.	Specimen orientation within testing apparatus. ....	24
Figure E.63-4.	UT image showing missing tows in the bulk of the specimen.....	25
Figure E.63-5.	UT image showing missing tows in the bulk of the specimen.....	26
Figure E.63-6.	SSIR setup.....	27
Figure E.63-7.	NASA-03-Missing-Tow-002 sample. ....	28
Figure E.63-8.	SSIR inspection of NASA-03-Missing-Tow-002 sample processed with PCA from frame 100 (1.67s) to 999 (16.65s).....	28
Figure E.63-9.	TTIR setup. ....	30
Figure E.63-10.	NASA-03-Missing-Tow-002 sample. ....	31
Figure E.63-11.	TTIR inspection of NASA-03-Missing-Tow-002 sample processed with PCA from frame 50 (0.83s) to 250 (4.17s).....	31
Figure E.63-12.	SSFT system with TSR.....	33
Figure E.63-13.	TSR 1 <sup>st</sup> derivative at 6.54 sec of #63- Missing Toe Ply #12.....	33
Figure E.68-1.	Photographs of Specimen #68: NASA-03-FOD-Panel-001. ....	35
Figure E.68-2.	PEUT setup in Test-Tech scanning tank.....	35
Figure E.68-3.	PEUT C-scans at 2.25 MHz for steps 1-6 (Internal Gate). ....	36
Figure E.68-4.	PEUT C-scans at 2.25 MHz for steps 1-6 (BW Gate). ....	37
Figure E.68-5.	TTUT C-scans at 5.0 MHz showing square-shaped Grafoil targets. ....	38
Figure E.68-6.	PEUT amplitude C-scans at 5.0 MHz for shallow steps.....	39
Figure E.68-7.	PEUT Time-of-Flight C-scans at 5.0 MHz for shallow steps.....	39
Figure E.69-1.	Photographs of Specimen #69: NASA 03 Porosity Panel 001. ....	39
Figure E.69-2.	Ultrasonic system components. ....	40
Figure E.69-3.	UT image of porosity within the sample.....	41
Figure E.69-4.	UT image of porosity deeper within the sample. ....	42
Figure E.69-5.	PEUT setup in Test-Tech scanning tank.....	43
Figure E.69-6.	PEUT C-scans at 2.25 MHz (Internal Gate). ....	44
Figure E.69-7.	PEUT C-scans at 2.25 MHz (BW Gate). ....	44
Figure E.69-8.	PEUT C-scans at 5.0 MHz (Internal Gate). ....	45
Figure E.69-9.	PEUT C-scans at 5.0 MHz (BW Gate). ....	45
Figure E.69-10.	TTUT setup in Test-Tech scanning tank. ....	46
Figure E.69-11.	TTUT C-scans at 1 MHz.....	47
Figure E.69-12.	TTUT C-scans at 2.25 MHz.....	47
Figure E.69-13.	SSIR schematic. ....	48
Figure E.69-14.	Photo of SSIR setup. ....	49
Figure E.69-15.	SSIR image of Specimen #69. ....	50
Figure E.69-16.	Intensity curve showing heat dispersion over time for Specimen #69.....	50
Figure E.69-17.	TTIR schematic.....	51
Figure E.69-18.	Photo of TTIR setup. ....	52
Figure E.69-19.	Temperature curve showing the dispersion of heat over time during image capture. ....	53
Figure E.69-20.	Histogram showing frequency of thermal diffusivity values.....	53
Figure E.69-21.	Image of thermal diffusivity post processing.....	54
Figure E.70-1.	Photographs of Specimen #70: NASA 03 Porosity Panel 002. ....	55
Figure E.70-2.	Ultrasonic system components. ....	55
Figure E.70-3.	UT image of porosity within the sample.....	57
Figure E.70-4.	B-scan of specimen showing location and prevalence of defects. ....	57
Figure E.70-5.	UT image of porosity within the sample.....	58
Figure E.70-6.	PEUT setup in Test-Tech scanning tank.....	59
Figure E.70-7.	PEUT C-scans at 2.25 MHz (Internal Gate). ....	60
Figure E.70-8.	PEUT C-scans at 2.25 MHz (BW Gate). ....	60
Figure E.70-9.	PEUT C-scans at 5.0 MHz (Internal Gate). ....	61

Figure E.70-10. PEUT C-scans at 5.0 MHz (BW Gate).....	61
Figure E.70-11. TTUT setup in Test-Tech scanning tank. ....	62
Figure E.70-12. TTUT C-scans at 1 MHz.....	63
Figure E.70-13. TTUT C-scans at 2.25 MHz.....	63
Figure E.70-14. SSIR schematic. ....	64
Figure E.70-15. Photo of SSIR setup. ....	65
Figure E.70-16. SSIR image of Specimen #70. ....	66
Figure E.70-17. Intensity curve showing heat dispersion over time for Specimen #70.....	66
Figure E.70-18. TTIR schematic.....	67
Figure E.70-19. Photo of TTIR setup. ....	68
Figure E.70-20. Temperature curve showing the dispersion of heat over time during image capture. ....	69
Figure E.70-21. Histogram showing frequency of thermal diffusivity values.....	69
Figure E.70-22. Image of thermal diffusivity post processing.....	70
Figure E.71-1. Photographs of Specimen #71: NASA-03-Porosity-Panel-003. ....	71
Figure E.71-2. Ultrasonic system components. ....	71
Figure E.71-3. UT image of porosity within the sample.....	73
Figure E.71-4. UT image of porosity within the sample.....	73
Figure E.71-5. XCT system components. ....	74
Figure E.71-6. Slice direction nomenclature.....	75
Figure E.71-7. Test setup showing specimen orientation. ....	75
Figure E.71-8. XCT of Specimen #71 A (top) and B (bottom) showing porosity at different resolutions.....	77
Figure E.71-9. XCT of Specimen #71 from the z-view (left) and y-view (right). ....	77
Figure E.71-10. PEUT setup in Test-Tech scanning tank.....	78
Figure E.71-11. PEUT C-scans at 1.0 MHz.....	79
Figure E.71-12. PEUT C-scans at 2.25 MHz.....	79
Figure E.71-13. PEUT C-scans at 5.0 MHz.....	80
Figure E.71-14. TTUT setup in Test-Tech scanning tank. ....	81
Figure E.71-15. TTUT C-scans at 1 MHz.....	82
Figure E.71-16. TTUT C-scans at 2.25 MHz.....	82
Figure E.71-17. SSIR schematic. ....	83
Figure E.71-18. Photo of SSIR setup. ....	84
Figure E.71-19. SSIR image of Specimen #71. ....	85
Figure E.71-20. Intensity curve showing heat dispersion over time for Specimen #71.....	85
Figure E.71-21. TTIR schematic.....	86
Figure E.71-22. Photo of TTIR setup. ....	87
Figure E.71-23. Temperature curve showing the dispersion of heat over time during image capture. ....	88
Figure E.71-24. Histogram showing frequency of thermal diffusivity values.....	88
Figure E.71-25. Image of thermal diffusivity post processing.....	89
Figure E.72-1. Photographs of Specimen #72: NASA-03-Porosity-Panel-004. ....	90
Figure E.72-2. Ultrasonic system components. ....	90
Figure E.72-3. UT image of porosity within the sample.....	92
Figure E.72-4. UT image of porosity at a greater depth within the sample. ....	92
Figure E.72-5. XCT system components. ....	93
Figure E.72-6. Slice direction nomenclature.....	94
Figure E.72-7. Test setup showing specimen orientation. ....	94
Figure E.72-8. XCT of specimen #72 A (top) and B (bottom) showing porosity at different resolutions.....	96
Figure E.72-9. XCT of Specimen #72 from the z-view (left) and y-view (right). ....	96
Figure E.72-10. PEUT setup in Test-Tech scanning tank.....	97
Figure E.72-11. PEUT C-scans at 1.0 MHz.....	98

Figure E.72-12. PEUT C-scans at 2.25 MHz.....	98
Figure E.72-13. PEUT C-scans at 5.0 MHz.....	99
Figure E.72-14. TTUT setup in Test-Tech scanning tank. ....	99
Figure E.72-15. TTUT C-scans at 1 MHz.....	100
Figure E.72-16. TTUT C-scans at 2.25 MHz.....	101
Figure E.72-17. SSIR schematic. ....	102
Figure E.72-18. Photo of SSIR setup. ....	102
Figure E.72-19. SSIR image of Specimen #72. ....	103
Figure E.72-20. Intensity curve showing heat dispersion over time for Specimen #72.....	104
Figure E.72-21. TTIR schematic.....	105
Figure E.72-22. Photo of TTIR setup. ....	105
Figure E.72-23. Temperature curve showing the dispersion of heat over time during image capture. ....	106
Figure E.72-24. Histogram showing frequency of thermal diffusivity values.....	106
Figure E.72-25. Image of thermal diffusivity post processing.....	107
Figure E.79-1. Photographs of Specimen #79: NASA 005 Porosity 003. ....	108
Figure E.79-2. Ultrasonic system components. ....	109
Figure E.79-3. PEUT image of large porosity throughout the side wall of the specimen. ....	110
Figure E.81-1. Photographs of radii delamination standard. ....	111
Figure E.81-2. XCT system components. ....	112
Figure E.81-3. Slice direction nomenclature.....	113
Figure E.81-4. Microfocus XCT setup for impact damage standards.....	114
Figure E.81-5. CT slice view of 8-ply impact damage panels 81 (a), 82 (b), and 83 (c).....	114
Figure E.81-6. X-ray CR imaging.....	116
Figure E.81-7. Laboratory setup of impact plate standards for CR imaging. ....	116
Figure E.81-8. Flash filtered CR image of 8-ply impact panels. ....	117
Figure E.81-9. Ultrasonic system components. ....	117
Figure E.81-10. Specimen baseline inspection orientation.....	118
Figure E.81-11. 10-MHz baseline image. ....	119
Figure E.81-12. 10-MHz post-impact image. ....	121
Figure E.82-1. Ultrasonic system components. ....	122
Figure E.82-2. Specimen baseline inspection orientation.....	123
Figure E.82-3. 10-MHz baseline image. ....	124
Figure E.82-4. 10-MHz post-impact image. ....	125
Figure E.82-5. XCT system components. ....	126
Figure E.82-6. Slice direction nomenclature.....	127
Figure E.82-7. Impact specimen test stand setup.....	127
Figure E.82-8. CT slice normal to the thickness direction show delaminations and matrix cracking (left). CT slice normal to the front surface shows delaminations between plies (right). ....	129
Figure E.83-1. Ultrasonic system components. ....	130
Figure E.83-2. Specimen baseline inspection orientation.....	131
Figure E.83-3. 10-MHz baseline image. ....	131
Figure E.83-4. 10-MHz post-impact image. ....	132
Figure E.83-5. XCT system components. ....	133
Figure E.83-6. Slice direction nomenclature.....	134
Figure E.83-7. Impact specimen test stand setup.....	134
Figure E.83-8. CT slice normal to the thickness direction shows 1 delamination approximately 30% through the thickness from the impact surface (left). CT slice normal to the front surface shows small delaminations between plies (right). ....	136
Figure E.85-1. Photographs of impact panel reference standards 8-ply (a) and 16-ply (b). ....	137
Figure E.85-2. XCT system components. ....	138
Figure E.85-3. Slice direction nomenclature.....	139

Figure E.85-4.	Microfocus XCT setup for impact panel standard.	140
Figure E.85-5.	Slice view of impact standards showing top surface indent on 8-ply (a) and 16-ply (b).	140
Figure E.85-6.	Slice view of impact standards showing bottom surface compression damage on 8-ply (a) and 16-ply (b).	141
Figure E.85-7.	X-ray CR imaging.	142
Figure E.85-8.	Laboratory setup of impact plate standards for CR imaging.	142
Figure E.85-9.	Flash filtered CR images of 8-ply (a) and 16-ply (b) impact panels.	143
Figure E.85-10.	Shearography camera and speckle laser patterns.	144
Figure E.85-11.	a) shearography image of subsurface disbonds and b) surface deformation caused from vacuum excitation.	144
Figure E.85-12.	Shearography inspection system with vacuum excitation.	145
Figure E.85-13.	Nucsafe portable X-ray Backscatter system.	146
Figure E.85-14.	X-ray Backscatter imaging.	147
Figure E.85-15.	X-ray Backscatter image of 8-ply impact damage panel.	147
Figure E.86-1.	Photographs of radii delamination standard.	148
Figure E.86-2.	XCT system components.	149
Figure E.86-3.	Slice direction nomenclature.	150
Figure E.86-4.	Microfocus XCT setup for impact damage standards.	151
Figure E.86-5.	CT slice view of 16-ply impact damage panels 86 (a), 87 (b), and 88 (c).	151
Figure E.86-6.	X-ray CR imaging.	153
Figure E.86-7.	Laboratory setup of impact plate standards for CR imaging.	153
Figure E.86-8.	Flash filtered CR image of 16-ply impact panels.	154
Figure E.86-9.	Ultrasonic system components.	154
Figure E.86-10.	Specimen baseline inspection orientation.	155
Figure E.86-11.	10-MHz baseline image.	156
Figure E.86-12.	10-MHz post-impact image.	158
Figure E.87-1.	Ultrasonic system components.	159
Figure E.87-2.	Specimen baseline inspection orientation.	160
Figure E.87-3.	10-MHz baseline image.	160
Figure E.87-4.	10-MHz post-impact image.	161
Figure E.87-5.	XCT system components.	162
Figure E.87-6.	Slice direction nomenclature.	162
Figure E.87-7.	Impact specimen test stand setup.	163
Figure E.87-8.	CT slice normal to the thickness direction show delaminations and matrix cracking (left). CT slice normal to the front surface shows delaminations between plies (right).	164
Figure E.88-1.	Ultrasonic system components.	165
Figure E.88-2.	Specimen baseline inspection orientation.	166
Figure E.88-3.	10-MHz baseline image.	166
Figure E.88-4.	10-MHz post-impact image.	167
Figure E.88-5.	XCT system components.	168
Figure E.88-6.	Slice direction nomenclature.	168
Figure E.88-7.	Impact specimen test stand setup.	169
Figure E.88-8.	CT slice normal to the thickness direction show delaminations and matrix cracking (left). CT slice normal to the front surface shows delaminations between plies (right).	170
Figure E.90-1.	Photographs of radii delamination standard.	171
Figure E.90-2.	XCT system components.	172
Figure E.90-3.	Slice direction nomenclature.	173
Figure E.90-4.	Microfocus XCT setup for impact damage standards.	174
Figure E.90-5.	CT slice view of 24-ply impact damage panels 90 (a), 91 (b), and 92 (c).	174
Figure E.90-6.	X-ray CR imaging.	176

Figure E.90-7. Laboratory setup of impact plate standards for CR imaging. ....	176
Figure E.90-8. Flash filtered CR image of 24-ply impact panels. ....	177
Figure E.90-9. Ultrasonic system components. ....	177
Figure E.90-10. Specimen baseline inspection orientation. ....	178
Figure E.90-11. 10-MHz baseline image. ....	179
Figure E.90-12. 10-MHz post-impact image. ....	181
Figure E.91-1. Ultrasonic system components. ....	182
Figure E.91-2. Specimen post-impact inspection orientation. ....	183
Figure E.91-3. Baseline PEUT was not performed on this sample. ....	183
Figure E.91-4. 10-MHz post-impact image. ....	184
Figure E.91-5. XCT system components. ....	185
Figure E.91-6. Slice direction nomenclature. ....	186
Figure E.91-7. Impact specimen test stand setup. ....	186
Figure E.91-8. CT slice normal to the thickness direction show delaminations and matrix cracking (left). CT slice normal to the front surface shows delaminations between plies (right). ....	188
Figure E.92-1. Ultrasonic system components. ....	189
Figure E.92-2. Specimen baseline inspection orientation. ....	190
Figure E.92-3. 10-MHz baseline image. ....	191
Figure E.92-4. 10-MHz post-impact image. ....	192
Figure E.92-5. XCT system components. ....	193
Figure E.92-6. Slice direction nomenclature. ....	194
Figure E.92-7. Impact specimen test stand setup. ....	194
Figure E.92-8. CT slice normal to the thickness direction show delaminations and matrix cracking (left). CT slice normal to the front surface shows delaminations between plies (right). ....	196
Figure E.93-1. Photographs of radii delamination standard. ....	196
Figure E.93-2. XCT system components. ....	198
Figure E.93-3. Slice direction nomenclature. ....	198
Figure E.93-4. Microfocus XCT setup for impact damage standards. ....	199
Figure E.93-5. CT slice view of 32-ply impact damage panels 93 (a), 94 (b), and 95 (c). ....	199
Figure E.93-6. X-ray CR imaging. ....	201
Figure E.93-7. Laboratory setup of impact plate standards for CR imaging. ....	201
Figure E.93-8. Flash filtered CR image of 32-ply impact panels. ....	202
Figure E.93-9. Ultrasonic system components. ....	203
Figure E.93-10. Specimen baseline inspection orientation. ....	204
Figure E.93-11. 10-MHz baseline image. ....	205
Figure E.93-12. 10-MHz post-impact image. ....	207
Figure E.94-1. Ultrasonic system components. ....	208
Figure E.94-2. Specimen baseline inspection orientation. ....	209
Figure E.94-3. 10-MHz baseline image. ....	209
Figure E.94-4. 10-MHz post-impact image. ....	210
Figure E.94-5. XCT system components. ....	211
Figure E.94-6. Slice direction nomenclature. ....	212
Figure E.94-7. Impact specimen test stand setup. ....	212
Figure E.94-8. CT slice normal to the thickness direction show delaminations and matrix cracking (left). CT slice normal to the front surface shows delaminations between plies (right). ....	214
Figure E.95-1. Ultrasonic system components. ....	215
Figure E.95-2. Specimen baseline inspection orientation. ....	216
Figure E.95-3. Baseline PEUT was not performed on this sample. ....	216
Figure E.95-4. 10-MHz post-impact image. ....	217
Figure E.95-5. XCT system components. ....	218
Figure E.95-6. Slice direction nomenclature. ....	219



Figure E.95-7.	Impact specimen test stand setup. ....	219
Figure E.95-8.	CT slice normal to the thickness direction show no damage (left). CT slice normal to the front surface shows no damage plies (right). ....	221
Figure E.96-1.	Photographs of radii delamination standard. ....	222
Figure E.96-2.	XCT system components. ....	223
Figure E.96-3.	Slice direction nomenclature. ....	224
Figure E.96-4.	Microfocus XCT setup for impact damage standards. ....	225
Figure E.96-5.	CT slice view of 18-ply impact damage panels 96 (a), 97 (b), and 98 (c). ....	225
Figure E.96-6.	X-ray CR imaging. ....	226
Figure E.96-7.	Laboratory setup of impact plate standards for CR imaging. ....	227
Figure E.96-8.	Flash filtered CR image of 18-ply impact panels. ....	228
Figure E.96-9.	Ultrasonic system components. ....	228
Figure E.96-10.	Specimen baseline inspection orientation. ....	229
Figure E.96-11.	10-MHz baseline image. ....	230
Figure E.96-12.	10-MHz post-impact image. ....	232
Figure E.97-1.	Ultrasonic system components. ....	233
Figure E.97-2.	Specimen baseline inspection orientation. ....	234
Figure E.97-3.	10-MHz baseline image. ....	234
Figure E.97-4.	10-MHz post-impact image. ....	235
Figure E.97-5.	XCT system components. ....	236
Figure E.97-6.	Slice direction nomenclature. ....	236
Figure E.97-7.	Impact specimen test stand setup. ....	237
Figure E.97-8.	CT slice normal to the thickness direction show delaminations and matrix cracking (left). CT slice normal to the front surface shows delaminations between plies (right). ....	238
Figure E.98-1.	Ultrasonic system components. ....	239
Figure E.98-2.	Specimen baseline inspection orientation. ....	240
Figure E.98-3.	10-MHz baseline image. ....	240
Figure E.98-4.	10-MHz post-impact image. ....	241
Figure E.98-5.	XCT system components. ....	242
Figure E.98-6.	Slice direction nomenclature. ....	243
Figure E.98-7.	Impact specimen test stand setup. ....	243
Figure E.98-8.	CT slice normal to the thickness direction show delaminations and matrix cracking (left). CT slice normal to the front surface shows delaminations between plies (right). ....	245

## List of Tables

Table E.61-1.	Data collection settings. ....	2
Table E.62-1.	Data collection settings. ....	13
Table E.63-1.	Data collection settings. ....	24
Table E.68-1.	Equipment settings for 2.25 MHz scan. ....	36
Table E.68-2.	Equipment settings for 5.0 MHz scan. ....	36
Table E.68-3.	Equipment settings for 5 MHz scan. ....	38
Table E.68-4.	Equipment settings for 5.0 MHz scan. ....	39
Table E.69-1.	Data collection settings. ....	40
Table E.69-2.	Equipment settings for 2.25 MHz scan. ....	43
Table E.69-3.	Equipment settings for 5.0 MHz scan. ....	43
Table E.69-4.	Equipment settings for 1.0 MHz scan. ....	46
Table E.69-5.	Equipment settings for 2.25 MHz scan. ....	46
Table E.69-6.	Equipment settings for SSIR scan. ....	49
Table E.69-7.	Equipment settings for TTIR scan. ....	52

Table E.70-1.	Data collection settings.....	56
Table E.70-2.	Equipment settings for 2.25 MHz scan.....	59
Table E.70-3.	Equipment settings for 5.0 MHz scan.....	59
Table E.70-4.	Equipment settings for 1.0 MHz scan.....	62
Table E.70-5.	Equipment settings for 2.25 MHz scan.....	62
Table E.70-6.	Equipment settings for SSIR scan.....	65
Table E.70-7.	Equipment settings for TTIR scan.....	68
Table E.71-1.	Data collection settings.....	72
Table E.71-2.	Data collection settings.....	76
Table E.71-3.	Equipment settings for 1.0 MHz scan.....	78
Table E.71-4.	Equipment settings for 2.25 MHz scan.....	78
Table E.71-5.	Equipment settings for 5.0 MHz scan.....	78
Table E.71-6.	Equipment settings for 1.0 MHz scan.....	81
Table E.71-7.	Equipment settings for 2.25 MHz scan.....	81
Table E.71-8.	Equipment settings for SSIR scan.....	84
Table E.71-9.	Equipment settings for TTIR scan.....	87
Table E.72-1.	Data collection settings.....	91
Table E.72-2.	Data collection settings.....	95
Table E.72-3.	Equipment settings for 1.0 MHz scan.....	97
Table E.72-4.	Equipment settings for 2.25 MHz scan.....	97
Table E.72-5.	Equipment settings for 5.0 MHz scan.....	97
Table E.72-6.	Equipment settings for 1.0 MHz scan.....	100
Table E.72-7.	Equipment settings for 2.25 MHz scan.....	100
Table E.72-8.	Equipment settings for SSIR scan.....	103
Table E.72-9.	Equipment settings for TTIR scan.....	106
Table E.79-1.	Data collection settings.....	109
Table E.81-1.	Data collection settings.....	111
Table E.81-2.	Imaging and exposure parameters.....	115
Table E.81-3.	Post-impact inspection settings.....	118
Table E.82-1.	Post-impact inspection settings.....	123
Table E.82-2.	Data collection settings.....	128
Table E.83-1.	Post-impact inspection settings.....	130
Table E.83-2.	Data collection settings.....	135
Table E.85-1.	Data collection settings.....	137
Table E.85-2.	Imaging and exposure parameters.....	141
Table E.85-3.	Inspection time and vacuum.....	143
Table E.85-4.	Imaging and exposure parameters.....	145
Table E.86-1.	Data collection settings.....	148
Table E.86-2.	Imaging and exposure parameters.....	152
Table E.86-3.	Post-impact inspection settings.....	155
Table E.87-1.	Post-impact inspection settings.....	159
Table E.87-2.	Data collection settings.....	163
Table E.88-1.	Post-impact inspection settings.....	165
Table E.88-2.	Data collection settings.....	169
Table E.90-1.	Data collection settings.....	171
Table E.90-2.	Imaging and exposure parameters.....	175
Table E.90-3.	Post-impact inspection settings.....	178
Table E.91-1.	Post-impact inspection settings.....	182
Table E.91-2.	Data collection settings.....	187
Table E.92-1.	Post-impact inspection settings.....	189
Table E.92-2.	Data collection settings.....	195

Table E.93-1.	Data collection settings.....	197
Table E.93-2.	Imaging and exposure parameters. ....	200
Table E.93-3.	Post-impact inspection settings.....	203
Table E.94-1.	Post-impact inspection settings.....	208
Table E.94-2.	Data collection settings.....	213
Table E.95-1.	Post-impact inspection settings.....	215
Table E.95-2.	Data collection settings.....	220
Table E.96-1.	Data collection settings.....	222
Table E.96-2.	Imaging and exposure parameters. ....	226
Table E.96-3.	Post-impact inspection settings.....	229
Table E.97-1.	Post-impact inspection settings.....	233
Table E.97-2.	Data collection settings.....	237
Table E.98-1.	Post-impact inspection settings.....	239
Table E.98-2.	Data collection settings.....	244

## Nomenclature

$\mu\text{A}$	Microampere
$\mu\text{m}$	Micrometer/Micron
$\mu\text{s}$	Microseconds
1D	One-Dimensional
2D	Two-Dimensional
3D	Three-Dimensional
ABS	Acrylonitrile Butadiene Styrene
ACAD	Air Coupled Acoustic Drive
ACC	Advanced Composites Consortium
ACP	Advanced Composites Project
ACT	Air Coupled Transducer
ADR	Assisted Defect Recognition
AFP	Automated fiber placement
AISI	American Iron and Steel Institution
AMT	Active Microwave Thermography
ANSI	American National Standards Institute
APF	Automated Fiber Placement
ARC	Ames Research Center
ASME	American Society of Mechanical Engineers
ASNT	American Society of Nondestructive Testing
ASTM	American Society for Testing and Materials
ATL	Automated Tape Lay-Up
AWG	Arbitrary Waveform Generator
AWS	American Welding Society
BMS	Boeing Material Specification
BSI	British Standards Institution
BVID	Barely Visible Impact Damage
BW	Back Wall
C	Celsius
CAD	Computer-Aided Design
CAFA	Combined Analytical Finite Element Approach
CCD	Charge-coupled Device
CDRH	Center for Devices and Radiological Health
CFRP	Carbon Fiber Reinforced Polymer
CMOS	complementary metal oxide semiconductor
CNN	Convolutional Neural Network
$\text{CO}_2$	Carbon Dioxide
COPV	Composite Over-Wrap Pressure Vessel
CPV	Composite Pressure Vessel
CR	Computed Radiography
CST	Charge Simulation Technique
CT	Computed Tomography
CTE	Coefficient of Thermal Expansion
DAQ	Data Acquisition
dB	Decibel
dB/in	Decibels Per Inch
DDA	Digital Detector Array
DOF	Degree of Freedom
DR	Digital Radiography
DRC	Digital Radiography Center
ECT	Eddy Current Thermography
EFIT	Elastodynamic Finite Integration Technique

FBH	Flat-bottom holes
FD	Finite Difference
FDA	Food and Drug Administration
FEA	Finite Element Analysis
FEM	Finite Element Method
FEP	Fluorinated Ethylene Propylene
FLIR	Forward-looking Infrared
FMC	Full Matrix Capture
FOD	Foreign Object Debris
FOV	Field of View
ft-lbs	Foot Pounds
GE	General Electric
GHz	Gigahertz
GN <sub>2</sub>	Gaseous Nitrogen
gsm	Grams per square meter
GWUT	Guided Wave Ultrasound
Hz	Hertz
ID	Inner Diameter
IDIQ	Indefinite Delivery/Indefinite Quantity
IEC	International Electrotechnical Commission
IML	Inner Mold Line
in	Inch
in/min	Inches per Minute
InSb	Indium Antimonide
ipm	Images per Minute
IR	Infrared
IRT	Infrared Thermography
ISTIS	<i>In Situ</i> Thermal Inspection System
J/cm <sup>2</sup>	Joules Per Square Centimeter
K	Kelvin
KeV	Kiloelectron Volt
kg	Kilograms
kg/cm <sup>2</sup>	kilogram per square centimeter
kHz	Kilohertz
kV	Kilovolts
kW	kilowatt
LaRC	Langley Research Center
LBI	Laser Bond Inspection
LMCO	Lockheed-Martin Company
LPS	Local Positioning System
LST	Line Scanning Thermography
LT	Lock-In Thermography
m <sup>2</sup>	Square Meter
m <sup>2</sup> /hr	Meters Square per Hour
mA	Miliampere
MECAD	Mechanically Coupled Acoustic Drive
MGBM	Multi-Gaussian Beam Model
MHz	Megahertz
mHz	Millihertz
mK	Millikelvin
mm	Millimeter
MPa	Megapascals
ms	Meter per Second
MS/s	Megasamples/second

msec	Millisecond
MSFC	Marshall Space Flight Center
NAS	National Aerospace Standard
NASA	National Aeronautics and Space Administration
Nd:Glass	Neodymium Glass Laser
NDE	Nondestructive Evaluation
NDI	Nondestructive Inspection
NDT	Nondestructive Test
NEDT	Noise Equivalent Differential Temperature
NGIS	Northrop Grumman Innovation Systems
nm	Nanometer
ns	Nanosecond
OEM	Original Equipment Manufacturer
OML	Outer Mold Line
ONR	Office of Naval Research
OSHA	Occupational Safety and Health Administration
PA	Phased Array
PCA	Principal Component Analysis
PEUT	Pulse Echo Ultrasound
PMC	Polymer Matrix Composite
PML	Perfectly Matched Layer
POC	Point of Contact
PoD	Probability of Detection
PPT	Pulsed-Phase Thermography
psi	Pounds Per Square Inch
PT	Pressure-Sensitive Tape
PTFE	Polytetrafluoroethylene (Teflon™)
PVDF	polyvinylidene fluoride
PWI	Plane Wave Imaging
PW-UTC	Pratt Whitney – United Technology Corporation
PZT	Piezoelectric Sensors/Transducer
R&D	Research and Development
RAH	Refresh After Heat
RBH	Refresh Before Heat
RGB	Red, Green, and Blue
RMS	Root Mean Squared
ROI	Region of Interest
RPF	Release Ply Fabric
RSG	Rotated-Staggered Grid
RVE	Representative Volume Element
s	Seconds
SAE	Society of Automotive Engineers
SAFE	Semi-Analytical Finite Element
SAR	Synthetic Aperture Radar
sec	Seconds
SHM	Structural Health Monitoring
SLDV	Scanning Laser Doppler Vibrometer
SMAAART	Structures, Materials, Aerodynamics, Aerothermodynamics, and Acoustics Research and Technology
SME	Subject Matter Expert
SNR	Signal to Noise Ratio
SOFI	Spray on Foam Insulation
SoP	State-of-Practice
sq. ft/hr	square foot per hour

SSFT	Single-Side Flash Thermography
SSIR	Single-Sided Infrared Thermography
SVD	Singular Value Decomposition
TC2	Technical Challenge 2
TDRS	Time Domain Reflectometry Systems
TFM	Total Focus Method
T <sub>g</sub>	Glass Transition Temperature
THz	Terahertz
TPS	Thermal Protection System
TSR	Thermographic Signal Reconstruction
TT	Through Transmission
TTIR	Through-Transmission Infrared Thermography
TTUT	Through-Transmission Ultrasound
TWI	Thermal Wave Imaging System
USC	University of South Carolina
UT	Ultrasound
VaRTM	Variation Resin Transfer Molding
VSHM	Visualized Structural Health Monitoring
XCT	X-ray Computed Tomography

## Appendix E Individual Test Reports by Specimen (Sections 61–98)

☆☆☆	Not Suitable for this Specimen
★★☆	Marginally suitable for this Specimen, or only provides qualitative information
★★★	Highly successful for this Specimen, including quantifiable information

### E.61 Specimen #61: NASA-03-Folded-Tow-002

Structure	Material	Details	Dimensions (inches)	Partner Methods	
Fiber placed panel	IM7/8552-1 Slit Tape	Flat panel Folded Tow - mid	16 × 16 × 0.15	NASA	E.61.1 PEUT E.61.2 SSIR E.61.3 TTIR
				TWI	E.61.4 SSFT



*Figure E.61-1. Photographs of Specimen #61: NASA 03 Folded Tow 002.*

#### E.61.1 Method: Pulse-Echo Ultrasound Testing (PEUT)

##### E.61.1.1 Partner: NASA

##### E.61.1.2 Technique Applicability: ★★★

PEUT is able to detect the folded tows in this specimen.

##### E.61.1.3 Laboratory Setup

Immersion Ultrasonic Testing: NASA Langley Research Center (LaRC) uses a custom-designed single-probe ultrasonic scanning system. The system has an 8-axis motion controller, a multi-axis gantry robot mounted above a medium-size water tank, a dual-channel, 16-bit, high-speed digitizer, and an off-the-shelf ultrasonic pulser receiver. The system can perform Through-Transmission (TT) Ultrasound (TTUT) and Pulse-echo Ultrasound (PEUT) inspections. TT inspection employs two aligned ultrasonic probes, one transmitter, and one receiver, placed on either side of a test specimen. Pulse-echo inspection is a single-sided method where a single ultrasonic probe is both transmitter and receiver. In each method, data are acquired while raster scanning the ultrasonic probe(s) in relation to a part. Figure E.61-2 shows a simplified block diagram of a scanning Pulse-echo inspection.



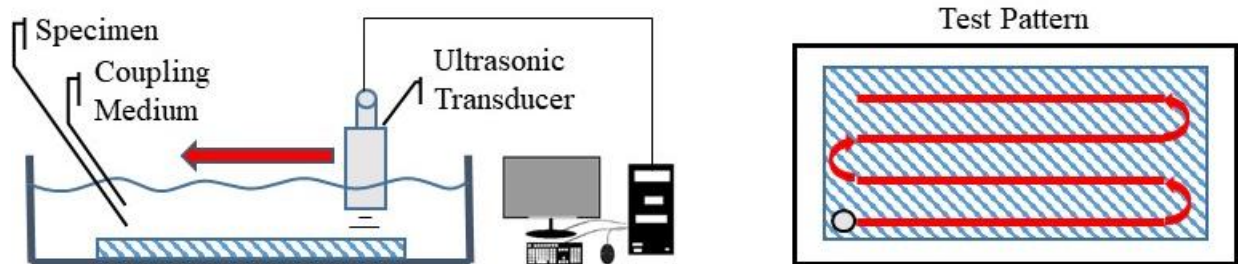


Figure E.61-2. Ultrasonic system components.

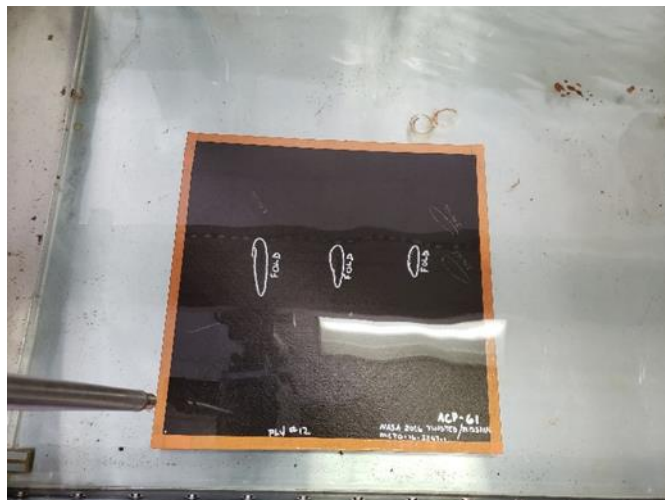


Figure E.61-3. Specimen orientation within testing apparatus.

#### E.61.1.4 Equipment List and Specifications:

- Pulsar/Receiver: Olympus 5073PR
- Digitizer: AlazarTech ATS9462, dual channel, 16 bit, 180 MS/s
- Sensor: Olympus 2-inch spherical focus immersion ultrasonic transducer
- Motion system: open looped stepper motor based X-YY-Z gantry robot
- Motion Controller: Galil DMC-4183
- Acquisition Software: FastScan, custom developed at NASA LaRC
- Signal Processing Software: DataViewer, custom developed at NASA LaRC

#### E.61.1.5 Settings

Table E.61-1. Data collection settings.

Resolution horizontal [in/pixel]	0.02
Resolution vertical [in/pixel]	0.02
Probe frequency [MHz]	5
Focal Length [in]	1.9
Array Dimensions [pixels]	751 × 736

The specimen is placed flat against the zero position of the tank raised above the glass bottom by several metal washers. The test probe is computer-controlled and correlated to the position on the sample. It is also focused to a point 1 mm below the surface of the test material. The specimen remains in place while the transducer follows a preprogrammed test grid across the surface as indicated in Figure E.61-2. At each point, ultrasonic data are collected from individual pulses.

Larger step sizes between data collection result in lower image resolution. These data points are reconstructed into a data cube displaying spatial coordinates as time progresses. 2D reconstruction of the collection of ultrasonic responses create flattened slices at varying depths within the material.

#### E.61.1.6 Inspection Results

Specimen #61, is a fiber placed flat panel fabricated from IM7/8552-1 Slit Tape with the objective of achieving folded tows within the bulk of the sample. PEUT was performed on this specimen in NASA's immersion tank specified above.

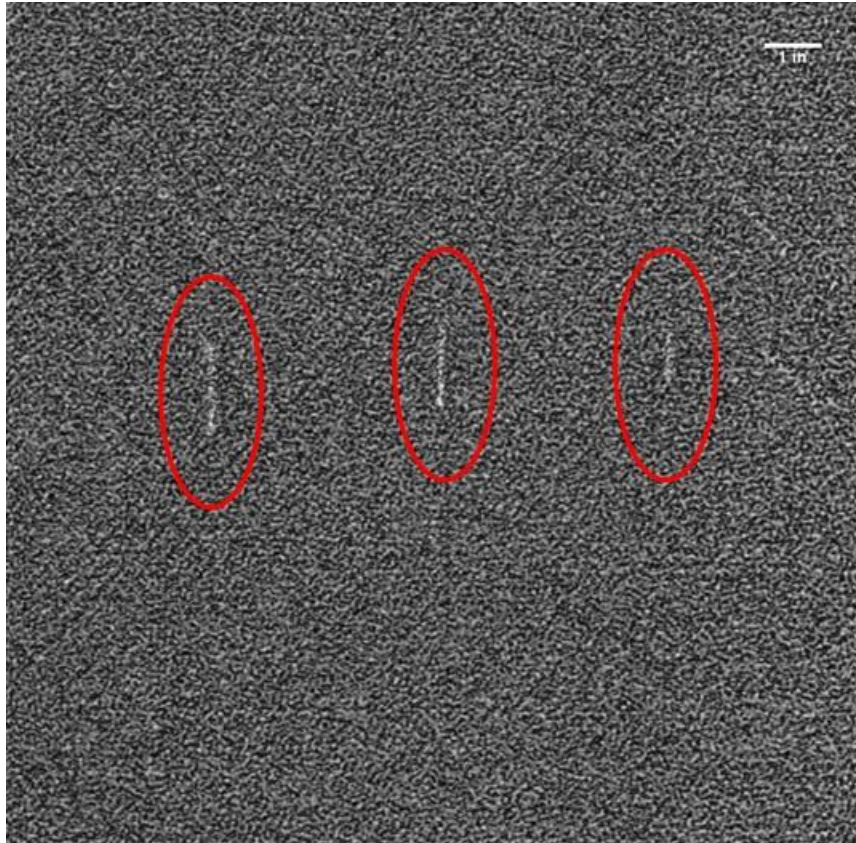


*Figure E.61-4. UT image showing folded tows in the bulk of the specimen.*

In Figures E.61-4 and E.61-5 evidence of three folded tows in the material appear in the middle of the specimen. The fiber folds reflect and cause perturbations in the acoustic waves that differ from the pattern representing the bulk of the material. This difference, while small, makes visual detection of the folded tows possible. These defects were detected at a depth of 0.064 inch roughly halfway through the composite part. The edge of sample is wrapped in tape due to the sharp edges. Additionally, Figure E.61-5 shows three fiber splices.

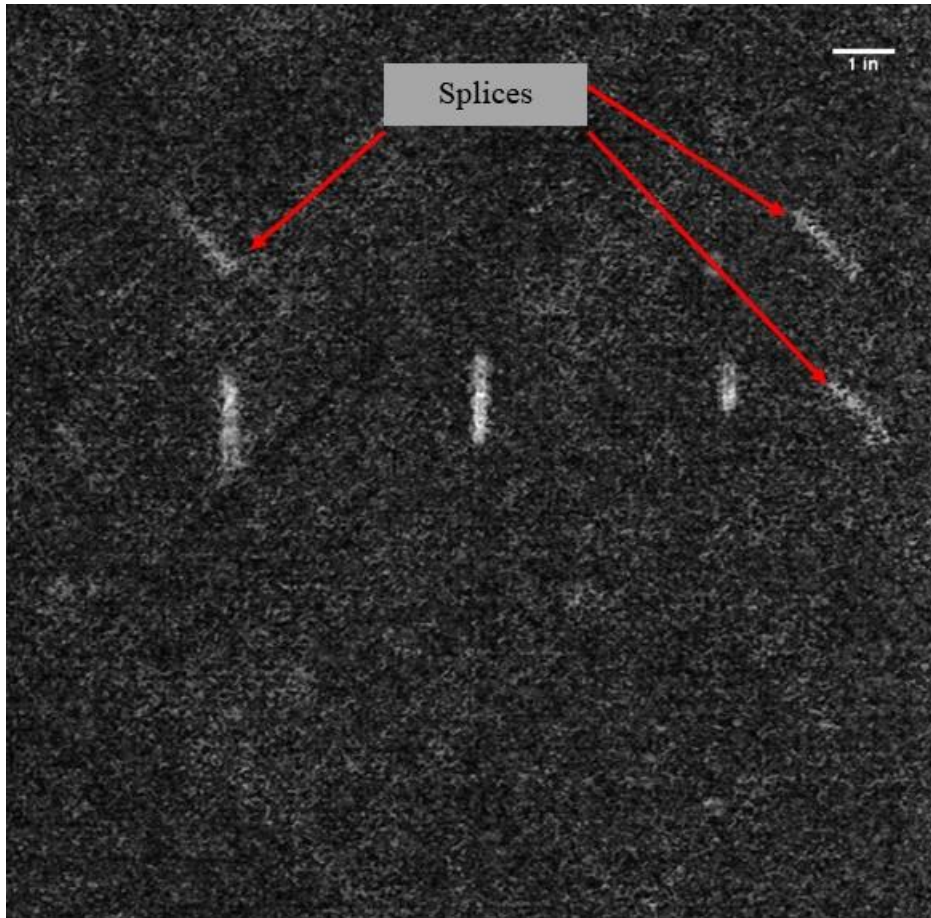


*Figure E.61-5. UT image showing a second view of folded tows in the bulk of the specimen.*

**E.61.2 Method: Single-Sided Infrared Thermography (SSIR)**

**E.61.2.1 Partner: NASA**

**E.61.2.2 Technique Applicability: ★★☆☆**

SSIR Thermography was capable of detecting the folded tows.

**E.61.2.3 Equipment List and Specifications:**

- Thermal Wave Imaging (TWI) System
- TWI System flash heat source using Speedotron power supplies.
- SC6000 Forward Looking Infrared (FLIR) camera,  $640 \times 512$  Indium Antimonide (InSb) array, Noise Equivalent Differential Temperature (NEDT)  $< 20$  mK
- 25 mm Germanium Optics

**E.61.2.4 Settings:**

- 60 Hz Frame Rate
- Flash on frame #10
- Total number of Frames 1499
- Total data acquisition time of 24.98 sec
- The camera/hood was positioned to view the entire sample



### E.61.2.5 Laboratory Setup

A commercially available flash thermography system was used for the inspection. The flash thermography system consisted of two linear flash tubes mounted within a hood. An infrared (IR) camera was mounted at the back of the hood viewing through a circular hole between the flash tubes and were positioned to view the hood opening. In this configuration, the flash lamps heated an area equal to the hood opening and the IR camera captured the thermal response. The IR camera operates in the mid-wave IR band (3–5  $\mu\text{m}$ ) and is configured with a 25-mm germanium lens. The focal plane array size for the camera is  $640 \times 512$  with a detector pitch size of  $14 \times 14 \mu\text{m}$ .

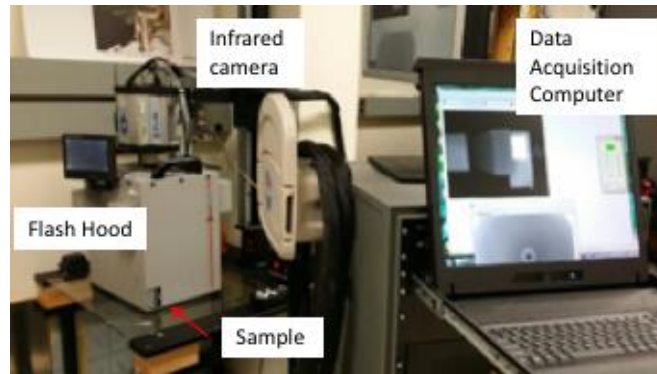


*Figure E.61-6. SSIR setup.*

### E.61.2.6 Principal Component Analysis

Principal component analysis (PCA) is common for processing of thermal data [1–3]. This algorithm is based on decomposition of the thermal data into its principal components or eigenvectors. Singular value decomposition is a routine used to find the singular values and corresponding eigenvectors of a matrix. Since thermal Nondestructive Evaluation (NDE) signals are slowly decaying waveforms, the predominant variations of the entire data set are usually contained in the first or second eigenvectors, and thus account for most of the data variance of interest. The principle components are computed by defining a data matrix  $A$ , for each data set, where the time variations are along the columns and the spatial image pixel points are row-wise. The matrix  $A$  is adjusted by dividing the maximum value (normalization) and subtracting the mean along the time dimension. The covariance matrix is defined as the  $A^T * A$ . The covariance matrix is now a square matrix of number of images used for processing. The covariance matrix can then be decomposed using singular value decomposition as:

$$\text{covariance matrix} = A^T A = V * S * V^T$$

where  $S$  is a diagonal matrix containing the square of the singular values and  $V$  is an orthogonal matrix, which contains the basis functions or eigenvectors describing the time variations. The eigenvectors can be obtained from the columns of  $V$ . The PCA inspection image is calculated by dot product multiplication of the selected eigenvector times the temperature response (data matrix  $A$ ), pixel by pixel.

### E.61.2.7 Inspection Results

The 1499 frames of data (24.98 sec) were processed using iterations of different time windows. The processing of frames 50 to 1249 corresponding to a time window of 0.83–20.82 sec yielded the best results. The three folded towels named A, B, and C were detected and are shown in Figure

E.61-8. A time delay of 0.83 sec allowed enough time after the flash for the heat to flow into the sample and 20.82 sec was sufficient to provide good contrast of the defects. The second eigenvector was used to produce the final inspection images shown in Figure E.61-8. Without prior knowledge of the existence of defect A, it is unclear that it would have been categorized as a flaw as its signal is very faint.

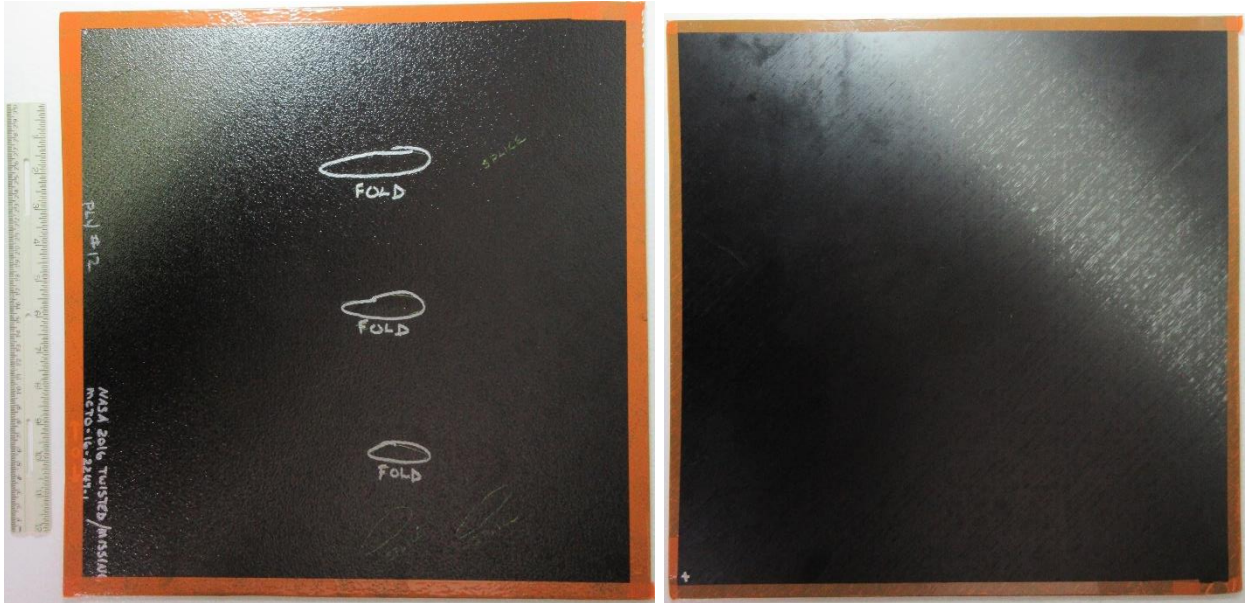


*Figure E.61-7. NASA-03-Folded-Tow-002 sample.*

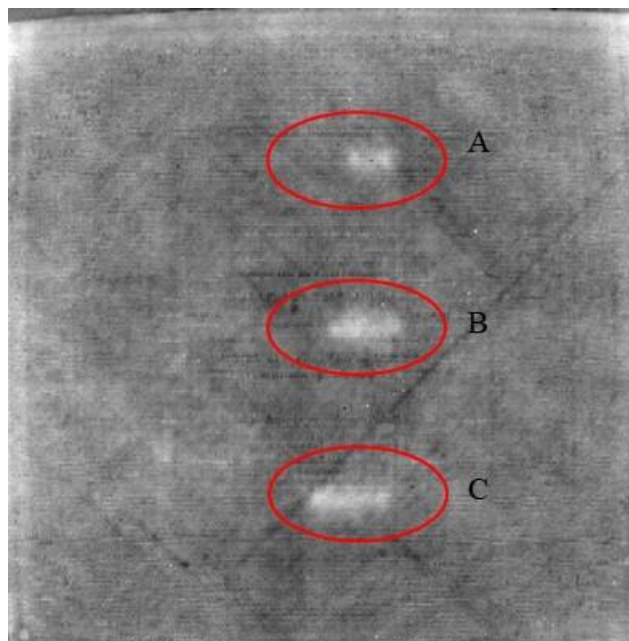


*Figure E.61-8. SSIR inspection of NASA-03-Folded-Tow-002 sample processed with PCA from frame 50 (0.83s) to 1249 (20.82s).*

### E.61.2.8 References

- [1] Rajic, N.: “Principal Component Thermography for Flaw Contrast Enhancement and Flaw Depth Characterization in Composite Structures,” *Composite Structures*, Vol. 58, pp. 521-528, 2002.
- [2] Zalameda, J. N.; Bolduc S.; and Harman R.: “Thermal Inspection of a Composite Fuselage Section using a Fixed Eigenvector Principal Component Analysis Method,” Proc. *SPIE* 10214, *Thermosense: Thermal Infrared Applications XXXIX*, 102140H, 5 May 2017.
- [3] Cramer, K. E.; and Winfree, W. P.: “Fixed Eigenvector Analysis of Thermographic NDE Data”, Proceedings of *SPIE, Thermosense XXXIII*, edited by Morteza Safai and Jeff Brown, Vol. 8013, 2011.
- [4] Shephard, S. M.: “Flash Thermography of Aerospace Composites,” *IV Conferencia Panamerica de END*, Buenos Aires – October (2007).

### E.61.3 Method: Through-Transmission Infrared Thermography (TTIR)

#### E.61.3.1 Technique Applicability: ★★☆☆

TTIR Thermography was capable of detecting the folded tows.

#### E.61.3.2 Equipment List and Specifications:

- TWI System
- TWI System flash heat source using Balcar power supply externally triggered by TWI system.
- SC6000 FLIR camera,  $640 \times 512$  InSb array, NEDT < 20 mK
- 25 mm Germanium Optics

#### E.61.3.3 Settings:

- 60 Hz Frame Rate
- Flash on frame #10
- Total number of Frames 2000
- Total data acquisition time of 33.33 sec
- IR camera was positioned to view the entire sample

#### E.61.3.4 Laboratory Setup

The TT thermal inspection system setup is shown in Figure E.61-9. The test specimen is placed between the heat source and the IR camera. The lamp used to induce the heat was a commercially available photographic flash lamp powered by a 6,400-Joule power supply (manufactured by Balcar). The camera used was a FLIR SC6000 with a  $640 \times 512$  InSb array operating in the 3- to 5- $\mu\text{m}$  IR band. The image data frame rate was 60 image frames per second. The computer records the IR image of the specimen immediately prior to the firing of the flash lamp (for emissivity correction), then the thermal response of the specimen at a user defined sampling rate and for a user defined duration is acquired.

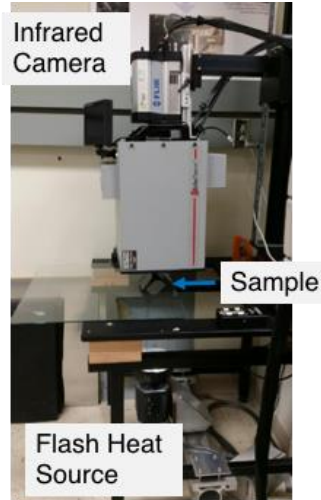


**Figure E.61-9. TTIR setup.**

### **E.61.3.5 Principal Component Analysis**

PCA is common for processing of thermal data [1–3]. This algorithm is based on decomposition of the thermal data into its principal components or eigenvectors. Singular value decomposition is a routine used to find the singular values and corresponding eigenvectors of a matrix. Since thermal NDE signals are slowly decaying waveforms, the predominant variations of the entire data set are usually contained in the first or second eigenvectors, and thus account for most of the data variance of interest. The principle components are computed by defining a data matrix  $A$ , for each data set, where the time variations are along the columns and the spatial image pixel points are row-wise. The matrix  $A$  is adjusted by dividing the maximum value (normalization) and subtracting the mean along the time dimension. The covariance matrix is defined as the  $A^T * A$ . The covariance matrix is now a square matrix of number of images used for processing. The covariance matrix can then be decomposed using singular value decomposition as:

$$\text{covariance matrix} = A^T A = V * S * V^T$$

Where  $S$  is a diagonal matrix containing the square of the singular values and  $V$  is an orthogonal matrix, which contains the basis functions or eigenvectors describing the time variations. The eigenvectors can be obtained from the columns of  $V$ . The PCA inspection image is calculated by dot product multiplication of the selected eigenvector times the temperature response (data matrix  $A$ ), pixel by pixel.

### **E.61.3.6 Inspection Results**

The 2000 frames of data (33.33 sec) were processed using iterations of different time windows. The processing of frames 50 to 250 corresponding to a time window of 0.83–4.17 sec yielded the best result, and is shown in Figure E.61-11. Possible defects, labeled A through D were detected.





**Figure E.61-10. NASA-03-Folded-Tow-002 sample.**

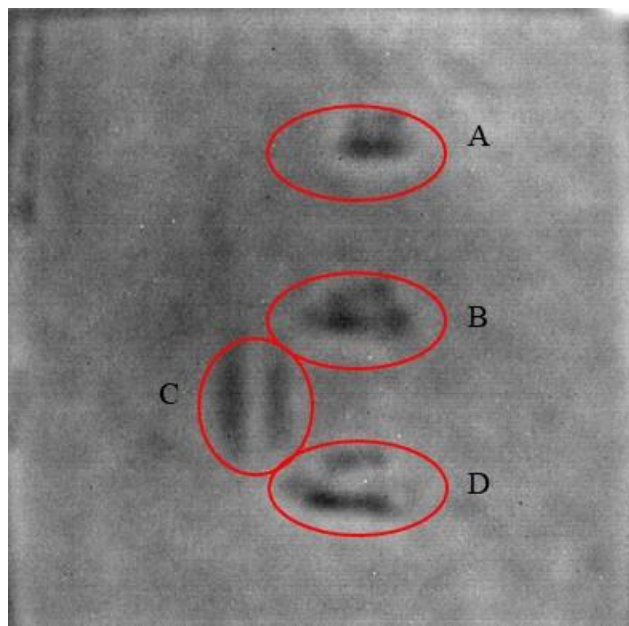


**Figure E.61-11. TTIR inspection of NASA-03-Folded-Tow-002 sample processed with PCA from frame 100 (1.67s) to 1249 (20.82s).**

### **E.61.3.7 References**

- [1] Rajic, N.: "Principal Component Thermography for Flaw Contrast Enhancement and Flaw Depth Characterization in Composite Structures," *Composite Structures*, Vol. 58, pp. 521-528, 2002.
- [2] Zalameda, J. N.; Bolduc S.; and Harman R.: "Thermal Inspection of a Composite Fuselage Section using a Fixed Eigenvector Principal Component Analysis Method," Proc. *SPIE* 10214, *Thermosense: Thermal Infrared Applications XXXIX*, 102140H, 5 May 2017.



- [3] Cramer, K. E.; and Winfree, W. P.: “Fixed Eigenvector Analysis of Thermographic NDE Data”, Proceedings of *SPIE, Thermosense XXXIII*, edited by Morteza Safai and Jeff Brown, Vol. 8013, 2011.

#### **E.61.4 Method: Single-Side Flash Thermography (SSFT-TSR)**

##### **E.61.4.1 Partner: Thermal Wave Imaging, Inc.\***

\*TWI was not part of the Advanced Composites Consortium (ACC) but reviewed specimens.

##### **E.61.4.2 Technique Applicability: ★★★**

SSFT-TSR is capable of detecting subsurface anomalies in this specimen that could be the result of delamination, voids or porosity. All indications appear in the head-on image, but more accurate sizing is achieved by inspecting the flat surfaces separately.

##### **E.61.4.3 Laboratory Setup:**

The sample was inspected with a commercially available flash thermography system (EchoTherm®, Thermal Wave Imaging, Inc.), equipped with 2 linear xenon flash/reflector assemblies mounted in a reflective hood optimized to provide uniform output at the 10-inch × 14-inch exit aperture. Each lamp is powered by a 6 kJ power supply that allows truncation of the flash to a rectangular pulse with duration <1 msec. A cryogenically cooled IR camera is mounted to view the plane of the hood exit aperture, with the camera lens positioned at the plane of the flashlamps. Excitation, data capture and processing and analysis using TSR are controlled at the system console using Virtuoso software.

##### **E.61.4.4 Equipment List and Specifications:**

- EchoTherm® Flash Thermography System
- 2 linear xenon flash lamps and power supplies (6 kJ each)
- TWI Precision Flash Control (truncation to 4 msec rectangular pulse)
- A6100sc FLIR camera, 640 × 512 InSb array, NEDT < 20 mK
- 13 mm Germanium Lens
- TWI Virtuoso® software

##### **E.61.4.5 Settings:**

- 30 Hz Frame Rate
- 10 Preflash Frames
- 1800 total frames
- 7 Polynomial order
- 60-sec data acquisition time
- Field of View (FOV): 10-inch × 14-inch

Settings were determined following the recommendations in ASTM E2582-14. Acquisition duration was set according to the time of the break from linearity ( $t^* \sim 8$  sec) due to the back wall (BW) for typical points in the log time history. The acquisition period was then set to 30 sec ( $3 \times t^*$ ), per ASTM E2582-14.

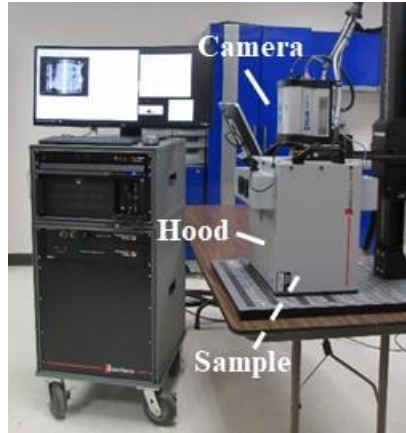


*Figure E.61-12. SSFT system with TSR.*

#### **E.61.4.6 Thermographic Signal Reconstruction (TSR)**

After acquisition, captured data are processed using TSR to reduce temporal noise, enhance deviation from normal cooling behavior and allow segmentation of the data based on signal attributes. For each pixel, the average of 10 frames immediately preceding the flash pulse is subtracted from the pixel time history, and a 7<sup>th</sup> order polynomial is fit to the logarithmically scaled result using least squares. First and 2<sup>nd</sup> derivatives of the result are calculated and the derivative images are displayed in the Virtuoso software. Derivative signals associated normal areas of the sample exhibit minimal activity over the duration of the acquisition. Signals associated with subsurface anomalies typically behave identically to the normal signals until a particular time (dependent on host material characteristics and the depth of the feature) after which their behavior deviates from normal (the degree of the deviation depends on the relative difference in the thermal properties of the anomaly and the surrounding normal matrix).

#### **E.61.4.7 Inspection Results**

Three subsurface indications were observed and confirmed to be subsurface by their late divergence in the logarithmic temperature time plot. The 1<sup>st</sup> derivative at 24.41 sec was used to produce the final inspection images shown in Figure E.61-13.

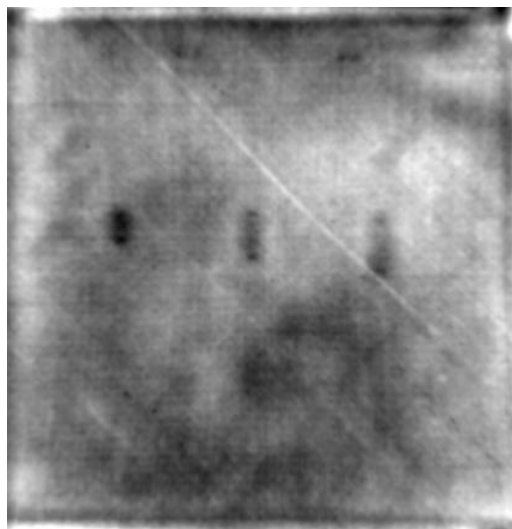


*Figure E.61-13. TSR 1<sup>st</sup> derivative at 24.41 sec of #61- Fold Ply #12.*

### E.61.4.8 References

- [1] ASNT: *ASNT Aerospace NDT Industry Handbook*, Chapter 11, “Thermography,” Nov 2014.
- [2] ASTM International: “Standard Practice for Infrared Flash Thermography of Composite Panels and Repair Patches,” *ASTM E2582–07*, 2007.
- [3] Shepard, S.; and Frenberg, M.: “Thermographic Detection and Characterization of Flaws in Composite Materials,” *Materials Evaluation*, ASNT, July 2014.
- [4] Hou, Y.; Lhota, J. R.; and Golden, T. J. M.: “Automated processing of thermographic derivatives for quality assurance,” *Opt. Eng.*, Vol. 46, 051008, 2007.
- [5] *Temporal noise reduction, compression and analysis of data sequences*, U.S. Patent 6,516,084.

### E.62 Specimen #62: NASA-03-Missing-Tow-001

Structure	Material	Details	Dimensions (inches)	Partner Methods	
Fiber placed panel	IM7/8552-1 Slit Tape	Flat panel Missing Tow – 1ply	16 × 16 × 0.15	NASA	E.62.1 PEUT E.62.2 SSIR E.62.3 TTIR
				TWI	E.62.4 SSFT

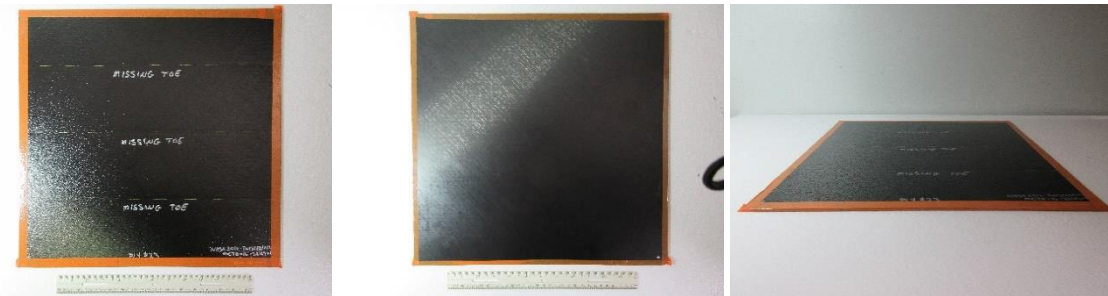


Figure E.62-1. Photographs of Specimen #61: NASA 03 Missing Tow 001.

#### E.62.1 Method: Pulse-Echo Ultrasound Testing (PEUT)

##### E.62.1.1 Partner: NASA

##### E.62.1.2 Technique Applicability: ★★★

PEUT is able to detect the missing tows in this specimen.

##### E.62.1.3 Laboratory Setup

Immersion Ultrasonic Testing: NASA LaRC uses a custom-designed single-probe ultrasonic scanning system. The system has an 8-axis motion controller, a multi-axis gantry robot mounted above a medium-size water tank, a dual-channel, 16-bit, high-speed digitizer, and an off-the-shelf ultrasonic pulser receiver. The system can perform TTUT and PEUT inspections. TT inspection employs two aligned ultrasonic probes, one transmitter, and one receiver, placed on either side of a test specimen. Pulse-echo inspection is a single-sided method where a single ultrasonic probe is both transmitter and receiver. In each method, data are acquired while raster scanning the ultrasonic probe(s) in relation to a part. Figure E.62-2 shows a simplified block diagram of a scanning Pulse-echo inspection.

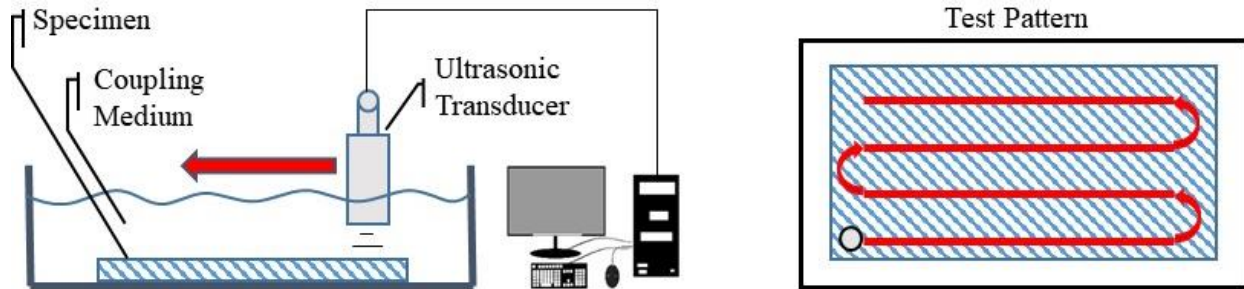


Figure E.62-2. Ultrasonic system components.

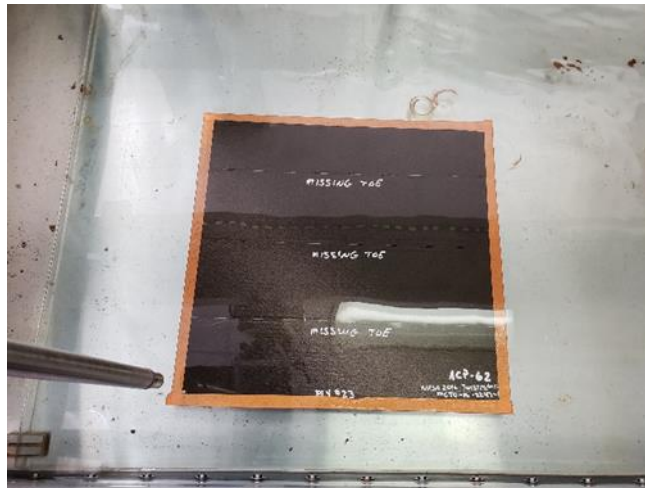


Figure E.62-3. Specimen orientation within testing apparatus.

#### E.62.1.4 Equipment List and Specifications:

- Pulser/Receiver: Olympus 5073PR
- Digitizer: AlazarTech ATS9462, dual channel, 16-bit, 180 MS/s
- Sensor: Olympus 2-inch spherical focus immersion ultrasonic transducer
- Motion system: open looped stepper motor based X-YY-Z gantry robot
- Motion Controller: Galil DMC-4183
- Acquisition Software: FastScan, custom developed at NASA LaRC
- Signal Processing Software: DataViewer, custom developed at NASA LaRC

#### E.62.1.5 Settings

Table E.62-1. Data collection settings.

Resolution horizontal [in/pixel]	0.02
Resolution vertical [in/pixel]	0.02
Probe frequency [MHz]	5
Focal Length [in]	1.9
Array Dimensions [pixels]	751 × 716

The specimen is placed flat against the zero position of the tank raised above the glass bottom by several metal washers. The test probe is computer-controlled and correlated to the position on the sample. It is also focused to a point 1 mm below the surface of the test material. The specimen remains in place while the transducer follows a preprogrammed test grid across the surface as

indicated in Figure E.62-2. At each point, ultrasonic data are collected from individual pulses. Larger step sizes between data collection result in lower image resolution. These data points are reconstructed into a data cube displaying spatial coordinates as time progresses. 2D reconstruction of the collection of ultrasonic responses create flattened slices at varying depths within the material.

#### **E.62.1.6 Inspection Results**

Specimen #62, is a fiber placed flat panel fabricated from IM7/8552-1 Slit Tape with the objective of achieving missing tows beneath the first ply of the sample. PEUT was performed on this specimen in NASA's immersion tank specified above.

In Figure E.62-4, evidence of three missing tows in the material appear equidistant throughout the specimen. The changing fiber geometry reflects and cause perturbations in the acoustic waves that differ from the pattern representing the bulk of the material. This difference, while small, makes visual detection of the folded tows possible. These defects were detected just below the first ply of the composite nearly indistinguishable from the surface reflection. Figure E.62-5 is located farther into the specimen and shows the residual acoustic pattern caused from the missing tows.

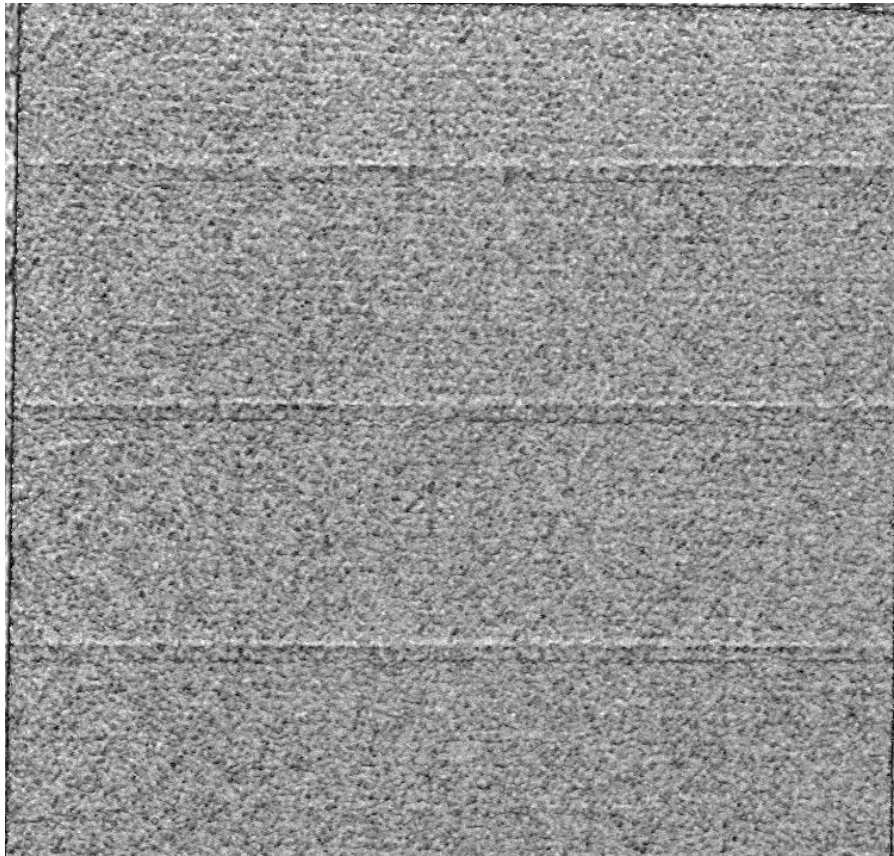


*Figure E.62-4. UT image showing missing tows near the surface of the specimen.*

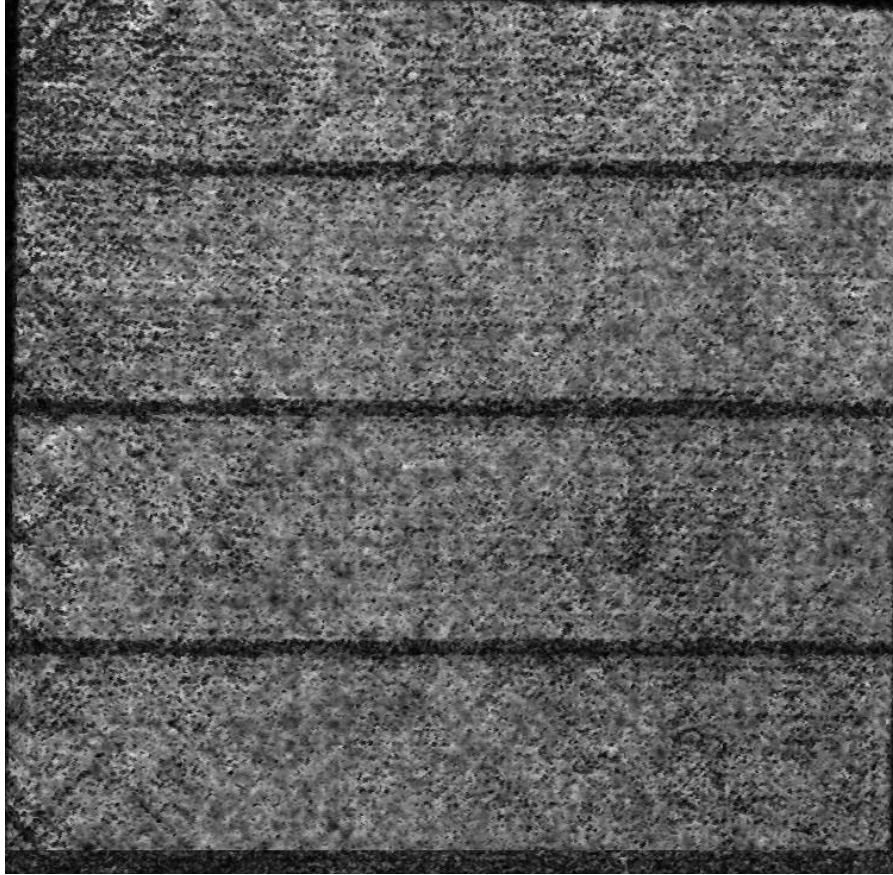


*Figure E.62-5. UT image showing evidence of missing tows.*

**E.62.2 Method: Single-Sided Infrared Thermography (SSIR)**

**E.62.2.1 Partner: NASA**

**E.62.2.2 Technique Applicability: ☆☆☆**

SSIR Thermography show signs of missing tows. The signal is very faint.

**E.62.2.3 Equipment List and Specifications:**

- TWI System
- TWI System flash heat source using Speedotron power supplies.
- SC6000 FLIR camera,  $640 \times 512$  InSb array, NEDT  $< 20$  mK
- 25 mm Germanium Optics

**E.62.2.4 Settings:**

- 60 Hz Frame Rate
- Flash on frame #10
- Total number of Frames 1499
- Total data acquisition time of 24.98 sec
- The camera/hood was positioned to view the entire sample



### E.62.2.5 Laboratory Setup

A commercially available flash thermography system was used for the inspection. The flash thermography system consisted of two linear flash tubes mounted within a hood. An IR camera was mounted at the back of the hood viewing through a circular hole between the flash tubes and were positioned to view the hood opening. In this configuration, the flash lamps heated an area equal to the hood opening and the IR camera captured the thermal response. The IR camera operates in the mid-wave IR band (3–5  $\mu\text{m}$ ) and is configured with a 25-mm germanium lens. The focal plane array size for the camera is  $640 \times 512$  with a detector pitch size of  $14 \times 14 \mu\text{m}$ .

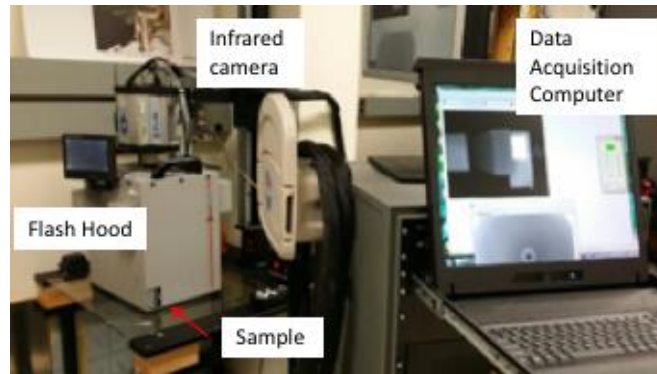


*Figure E.62-6. SSIR setup.*

### E.62.2.6 Principal Component Analysis

PCA is common for processing of thermal data [1–3]. This algorithm is based on decomposition of the thermal data into its principal components or eigenvectors. Singular value decomposition is a routine used to find the singular values and corresponding eigenvectors of a matrix. Since thermal NDE signals are slowly decaying waveforms, the predominant variations of the entire data set are usually contained in the first or second eigenvectors, and thus account for most of the data variance of interest. The principle components are computed by defining a data matrix  $A$ , for each data set, where the time variations are along the columns and the spatial image pixel points are row-wise. The matrix  $A$  is adjusted by dividing the maximum value (normalization) and subtracting the mean along the time dimension. The covariance matrix is defined as the  $A^T A$ . The covariance matrix is now a square matrix of number of images used for processing. The covariance matrix can then be decomposed using singular value decomposition as:

$$\text{covariance matrix} = A^T A = V * S * V^T$$

where  $S$  is a diagonal matrix containing the square of the singular values and  $V$  is an orthogonal matrix, which contains the basis functions or eigenvectors describing the time variations. The eigenvectors can be obtained from the columns of  $V$ . The PCA inspection image is calculated by dot product multiplication of the selected eigenvector times the temperature response (data matrix  $A$ ), pixel by pixel.

### E.62.2.7 Inspection Results

The 1499 frames of data (24.98 sec) were processed using iterations of different time windows. The processing of frames 100 to 999 corresponding to a time window of 1.67–16.65 sec yielded the best results. The three possible missing tows named A, B, and C are shown in Figure E.62-8. However, without prior knowledge of their presence, they could have easily gone undetected due

to their faint signal. The second eigenvector was used to produce the final inspection images shown in Figure E.62-8.

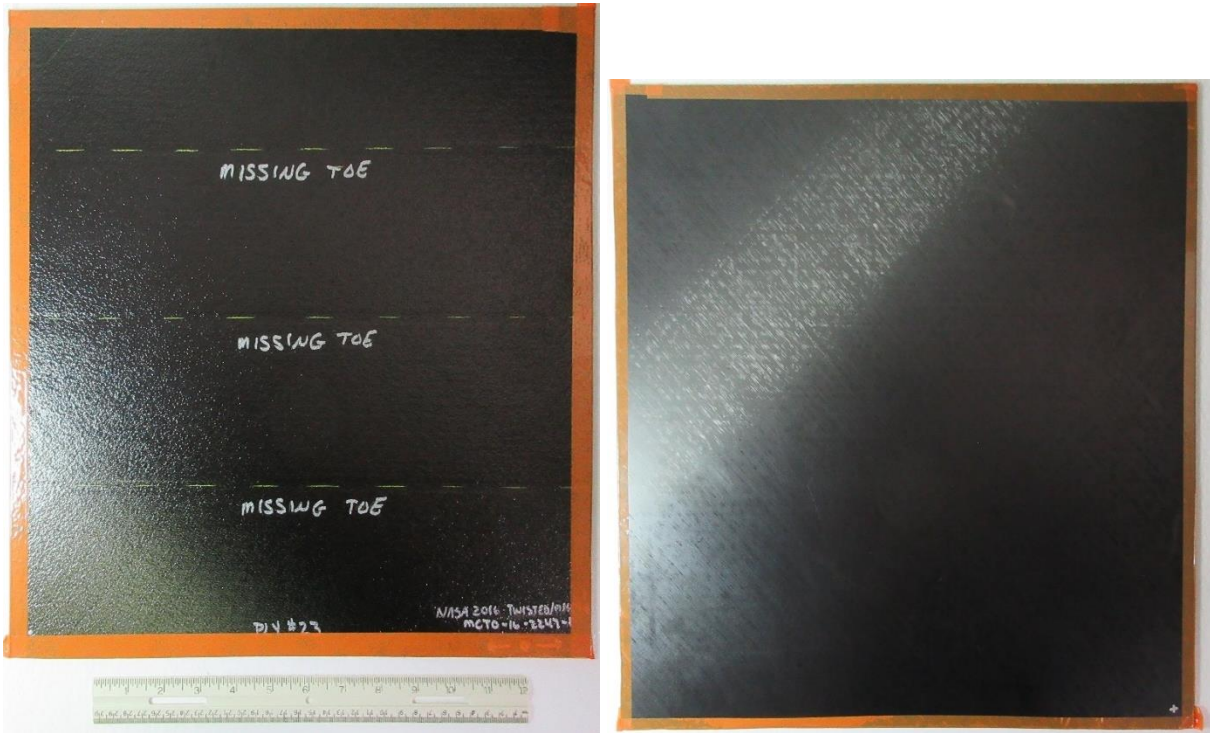


*Figure E.62-7. NASA-03-Missing-Tow-001 sample.*

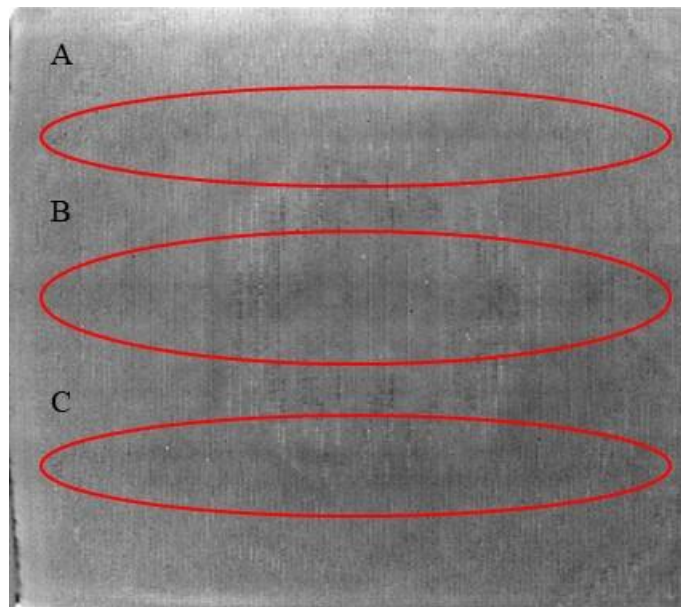


*Figure E.62-8. SSIR inspection of NASA-03-Missing-Tow-001 sample processed with PCA from frame 100 (1.67s) to 999 (16.65s).*

#### E.62.2.8 References

- [1] Rajic, N.: "Principal Component Thermography for Flaw Contrast Enhancement and Flaw Depth Characterization in Composite Structures," *Composite Structures*, Vol. 58, pp. 521-528, 2002.



- [2] Zalameda, J. N.; Bolduc S.; and Harman R.: “Thermal Inspection of a Composite Fuselage Section using a Fixed Eigenvector Principal Component Analysis Method,” Proc. *SPIE* 10214, *Thermosense: Thermal Infrared Applications XXXIX*, 102140H, 5 May 2017.
- [3] Cramer, K. E.; and Winfree, W. P.: “Fixed Eigenvector Analysis of Thermographic NDE Data”, Proceedings of *SPIE, Thermosense XXXIII*, edited by Morteza Safai and Jeff Brown, Vol. 8013, 2011.

### **E.62.3 Method: Through-Transmission Infrared Thermography (TTIR)**

#### **E.62.3.1 Partner: NASA**

#### **E.62.3.2 Technique Applicability: ★★☆☆**

TTIR thermography was capable of detecting the missing tows.

#### **E.62.3.3 Equipment List and Specifications:**

- TWI System
- TWI System flash heat source using Balcar power supply externally triggered by TWI system.
- SC6000 FLIR camera,  $640 \times 512$  InSb array, NEDT  $< 20$  mK
- 25 mm Germanium Optics

#### **E.62.3.4 Settings:**

- 60Hz Frame Rate
- Flash on frame #10
- Total number of Frames 2000
- Total data acquisition time of 33.33 sec
- IR camera was positioned to view the entire sample

#### **E.62.3.5 Laboratory Setup**

The TT thermal inspection system setup is shown in Figure E.62-9. The test specimen is placed between the heat source and the IR camera. The lamp used to induce the heat was a commercially available photographic flash lamp powered by a 6,400-Joule power supply (manufactured by Balcar). The camera used was a FLIR SC6000 with a  $640 \times 512$  InSb array operating in the 3- to 5- $\mu\text{m}$  IR band. The image data frame rate was 60 image frames per second. The computer records the IR image of the specimen immediately prior to the firing of the flash lamp (for emissivity correction), and then the thermal response of the specimen at a user defined sampling rate and for a user defined duration is acquired.

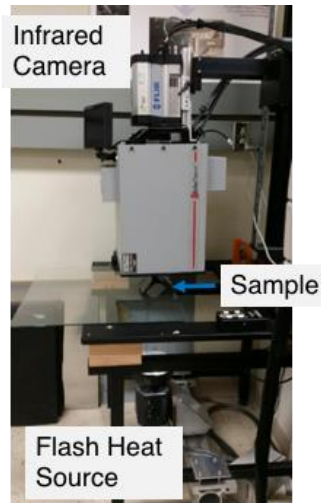


**Figure E.62-9. TTIR setup.**

### **E.62.3.6 Principal Component Analysis**

PCA is common for processing of thermal data [1–3]. This algorithm is based on decomposition of the thermal data into its principal components or eigenvectors. Singular value decomposition is a routine used to find the singular values and corresponding eigenvectors of a matrix. Since thermal NDE signals are slowly decaying waveforms, the predominant variations of the entire data set are usually contained in the first or second eigenvectors, and thus account for most of the data variance of interest. The principle components are computed by defining a data matrix  $A$ , for each data set, where the time variations are along the columns and the spatial image pixel points are row-wise. The matrix  $A$  is adjusted by dividing the maximum value (normalization) and subtracting the mean along the time dimension. The covariance matrix is defined as the  $A^T * A$ . The covariance matrix is now a square matrix of number of images used for processing. The covariance matrix can then be decomposed using singular value decomposition as:

$$\text{covariance matrix} = A^T A = V * S * V^T$$

where  $S$  is a diagonal matrix containing the square of the singular values and  $V$  is an orthogonal matrix, which contains the basis functions or eigenvectors describing the time variations. The eigenvectors can be obtained from the columns of  $V$ . The PCA inspection image is calculated by dot product multiplication of the selected eigenvector times the temperature response (data matrix  $A$ ), pixel by pixel.

### **E.62.3.7 Inspection Results**

The 2000 frames of data (33.33 sec) were processed using iterations of different time windows. The processing of frames 50 to 250 corresponding to a time window of 0.83–4.17 sec yielded the best result, and is shown in Figure E.62.11. Possible defects, labeled A through G were detected. A, B, and C are linear and run across the entire width of the test sample. D, E, and F are also linear, but centered in the middle of the test sample. These three defects are possibly due to the writing seen on the panel in Figure E.62-10. The different shape of area G could indicate there is a separate type of defect found in this region.



**Figure E.62-10. NASA-03-Missing-Tow-001 sample.**

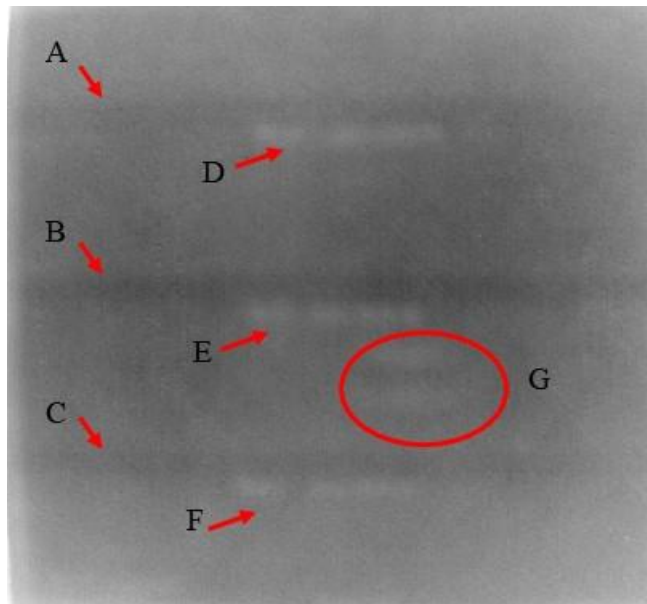


**Figure E.62-11. TTIR inspection of NASA-03-Missing-Tow-001 sample processed with PCA from frame 50 (0.83s) to 250 (4.17s).**

#### **E.62.3.8 References**

- [1] Rajic, N.: "Principal Component Thermography for Flaw Contrast Enhancement and Flaw Depth Characterization in Composite Structures," *Composite Structures*, Vol. 58, pp. 521-528, 2002.

- [2] Zalameda, J. N.; Bolduc S.; and Harman R.: “Thermal Inspection of a Composite Fuselage Section using a Fixed Eigenvector Principal Component Analysis Method,” Proc. *SPIE* 10214, *Thermosense: Thermal Infrared Applications XXXIX*, 102140H, 5 May 2017.
- [3] Cramer, K. E.; and Winfree, W. P.: “Fixed Eigenvector Analysis of Thermographic NDE Data”, Proceedings of *SPIE, Thermosense XXXIII*, edited by Morteza Safai and Jeff Brown, Vol. 8013, 2011.

#### **E.62.4 Method: Single-Side Flash Thermography (SSFT-TSR)**

##### **E.62.4.1 Partner: Thermal Wave Imaging, Inc.\***

\*TWI was not part of the ACC but reviewed specimens.

##### **E.62.4.2 Technique Applicability: ★★★**

SSFT-TSR is capable of detecting subsurface anomalies in this specimen that could be the result of delamination, voids or porosity. All indications appear in the head-on image, but more accurate sizing is achieved by inspecting the flat surfaces separately.

##### **E.62.4.3 Laboratory Setup:**

The sample was inspected with a commercially available flash thermography system (EchoTherm®, Thermal Wave Imaging, Inc.), equipped with 2 linear xenon flash/reflector assemblies mounted in a reflective hood optimized to provide uniform output at the 10-inch × 14-inch exit aperture. Each lamp is powered by a 6 kJ power supply that allows truncation of the flash to a rectangular pulse with duration <1 msec. A cryogenically cooled IR camera is mounted to view the plane of the hood exit aperture, with the camera lens positioned at the plane of the flashlamps. Excitation, data capture and processing and analysis using TSR are controlled at the system console using Virtuoso software.

##### **E.62.4.4 Equipment List and Specifications:**

- EchoTherm® Flash Thermography System
- 2 linear xenon flash lamps and power supplies (6 kJ each)
- TWI Precision Flash Control (truncation to 4 msec rectangular pulse)
- A6100sc FLIR camera, 640 × 512 InSb array, NEDT < 20 mK
- 13 mm Germanium Lens
- TWI Virtuoso® software

##### **E.62.4.5 Settings:**

- 30 Hz Frame Rate
- 10 Preflash Frames
- 1800 total frames
- 7 Polynomial order
- 60-sec data acquisition time
- FOV: 10-inch × 14-inch

Settings were determined following the recommendations in ASTM E2582-14. Acquisition duration was set according to the time of the break from linearity ( $t^* \sim 8$  sec) due to the BW for typical points in the log time history. The acquisition period was then set to 30 sec ( $3 \times t^*$ ), per ASTM E2582-14.

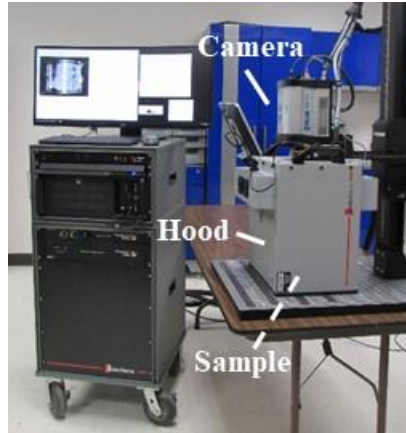


*Figure E.62-12. SSFT System with TSR*

#### **E.62.4.6 Thermographic Signal Reconstruction (TSR)**

After acquisition, captured data are processed using TSR to reduce temporal noise, enhance deviation from normal cooling behavior and allow segmentation of the data based on signal attributes. For each pixel, the average of 10 frames immediately preceding the flash pulse is subtracted from the pixel time history, and a 7<sup>th</sup> order polynomial is fit to the logarithmically scaled result using least squares. First and 2<sup>nd</sup> derivatives of the result are calculated and the derivative images are displayed in the Virtuoso software. Derivative signals associated normal areas of the sample exhibit minimal activity over the duration of the acquisition. Signals associated with subsurface anomalies typically behave identically to the normal signals until a particular time (dependent on host material characteristics and the depth of the feature) after which their behavior deviates from normal (the degree of the deviation depends on the relative difference in the thermal properties of the anomaly and the surrounding normal matrix).

#### **E.62.4.7 Inspection Results**

Three subsurface indications were observed and confirmed to be subsurface by their late divergence in the logarithmic temperature time plot. The 1<sup>st</sup> derivative at 20.18 sec was used to produce the final inspection images shown in Figure E.62-13.

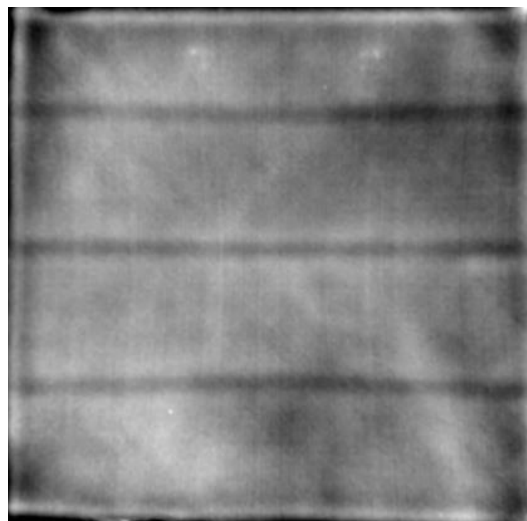


*Figure E.62-13. TSR 1<sup>st</sup> derivative at 20.18 sec of #62-Missing Toe Ply #23.*

**E.62.4.8 References**

- [1] ASNT: *ASNT Aerospace NDT Industry Handbook*, Chapter 11, “Thermography,” Nov 2014.
- [2] ASTM International: “Standard Practice for Infrared Flash Thermography of Composite Panels and Repair Patches,” *ASTM E2582–07*, 2007.
- [3] Shepard, S.; and Frenberg, M.: “Thermographic Detection and Characterization of Flaws in Composite Materials,” *Materials Evaluation*, ASNT, July 2014.
- [4] Hou, Y.; Lhota, J. R.; and Golden, T. J. M.: “Automated processing of thermographic derivatives for quality assurance,” *Opt. Eng.*, Vol. 46, 051008, 2007.
- [5] *Temporal noise reduction, compression and analysis of data sequences*, U.S. Patent 6,516,084.

**E.63 Specimen #63: NASA-03-Missing-Tow-002**

Structure	Material	Details	Dimensions (inches)	Partner Methods	
Fiber placed panel	IM7/8552-1 Slit Tape	Flat panel Missing Tow – Mid	16 × 16 × 0.15	NASA	E.63.1 PEUT E.63.2 SSIR E.63.3 TTIR
				TWI	E.63.4 SSFT

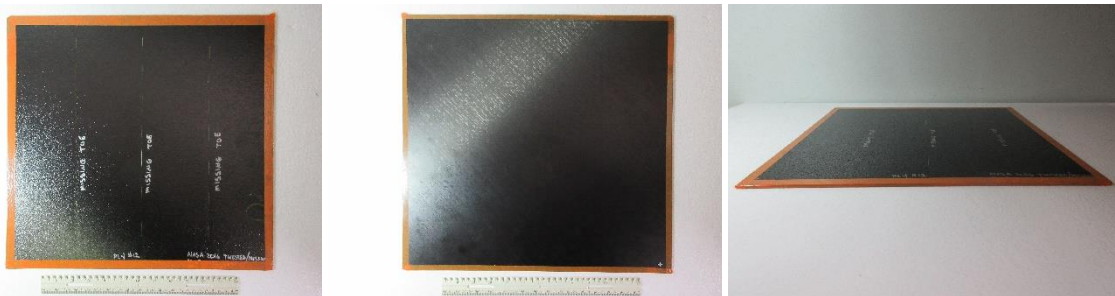


*Figure E.63-1. Photographs of Specimen #63: NASA 03 Missing Tow 002.*

**E.63.1 Method: Pulse-Echo Ultrasound Testing (PEUT)**

**E.63.1.1 Partner: NASA**

**E.63.1.2 Technique Applicability: ★★★**

PEUT is capable of detecting the missing tows in this specimen.

**E.63.1.3 Laboratory Setup**

Immersion Ultrasonic Testing: NASA LaRC uses a custom-designed single-probe ultrasonic scanning system. The system has an 8-axis motion controller, a multi-axis gantry robot mounted above a medium-size water tank, a dual-channel, 16-bit, high-speed digitizer, and an off-the-shelf ultrasonic pulser receiver. The system can perform TTUT and PEUT inspections. TT inspection employs two aligned ultrasonic probes, one transmitter, and one receiver, placed on either side of a test specimen. Pulse-echo inspection is a single-sided method where a single ultrasonic probe is both transmitter and receiver. In each method, data are acquired while raster scanning the ultrasonic probe(s) in relation to a part. Figure E.63-2 shows a simplified block diagram of a scanning Pulse-echo inspection.



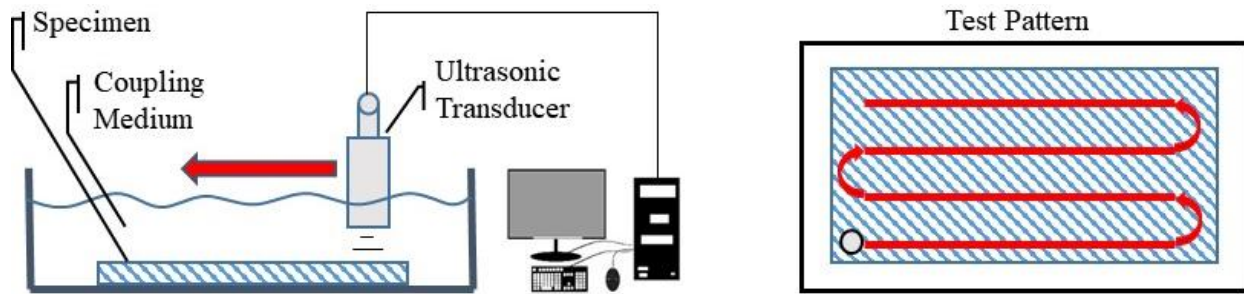


Figure E.63-2. Ultrasonic system components.

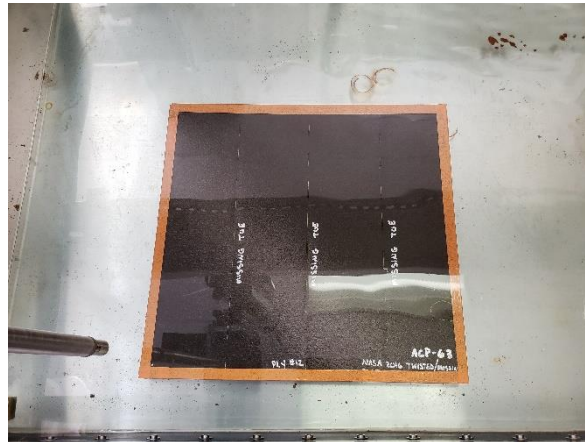


Figure E.63-3. Specimen orientation within testing apparatus.

#### E.63.1.4 Equipment List and Specifications:

- Pulsar/Receiver: Olympus 5073PR
- Digitizer: AlazarTech ATS9462, dual channel, 16 bit, 180 MS/s
- Sensor: Olympus 2-inch spherical focus immersion ultrasonic transducer
- Motion system: open looped stepper motor based X-YY-Z gantry robot
- Motion Controller: Galil DMC-4183
- Acquisition Software: FastScan, custom developed at NASA LaRC
- Signal Processing Software: DataViewer, custom developed at NASA LaRC

#### E.63.1.5 Settings

Table E.63-1. Data collection settings.

Resolution (horizontal) [in/pixel]	0.02
Resolution (vertical) [in/pixel]	0.02
Probe frequency [MHz]	5
Focal Length [in]	1.9
Array Dimensions [pixels]	751 × 711

The specimen is placed flat against the zero position of the tank raised above the glass bottom by several metal washers. The test probe is computer-controlled and correlated to the position on the sample. It is also focused to a point one mm below the surface of the test material. The specimen remains in place while the transducer follows a preprogrammed test grid across the surface as indicated in Figure E.63-2. At each point, ultrasonic data are collected from individual pulses. Larger step sizes between data collection result in lower image resolution. These data points are

reconstructed into a data cube displaying spatial coordinates as time progresses. 2D reconstruction of the collection of ultrasonic responses create flattened slices at varying depths within the material.

#### **E.63.1.6 Inspection Results**

Specimen #63 is a fiber placed flat panel fabricated from IM7/8552-1 Slit Tape with the objective of achieving missing tows in the middle of the sample. PEUT was performed on this specimen in NASA's immersion tank specified above.

In Figure E.63-4 evidence of three missing tows in the material appear equidistant throughout the specimen. The changing fiber geometry reflects and cause perturbations in the acoustic waves that differ from the pattern representing the bulk of the material. This difference, while small, makes visual detection of the folded tows possible. These defects were detected roughly halfway throughout the sample at 0.06 inch. Figure E.63-5 is located farther into the specimen and shows the residual acoustic pattern caused from the missing tows.

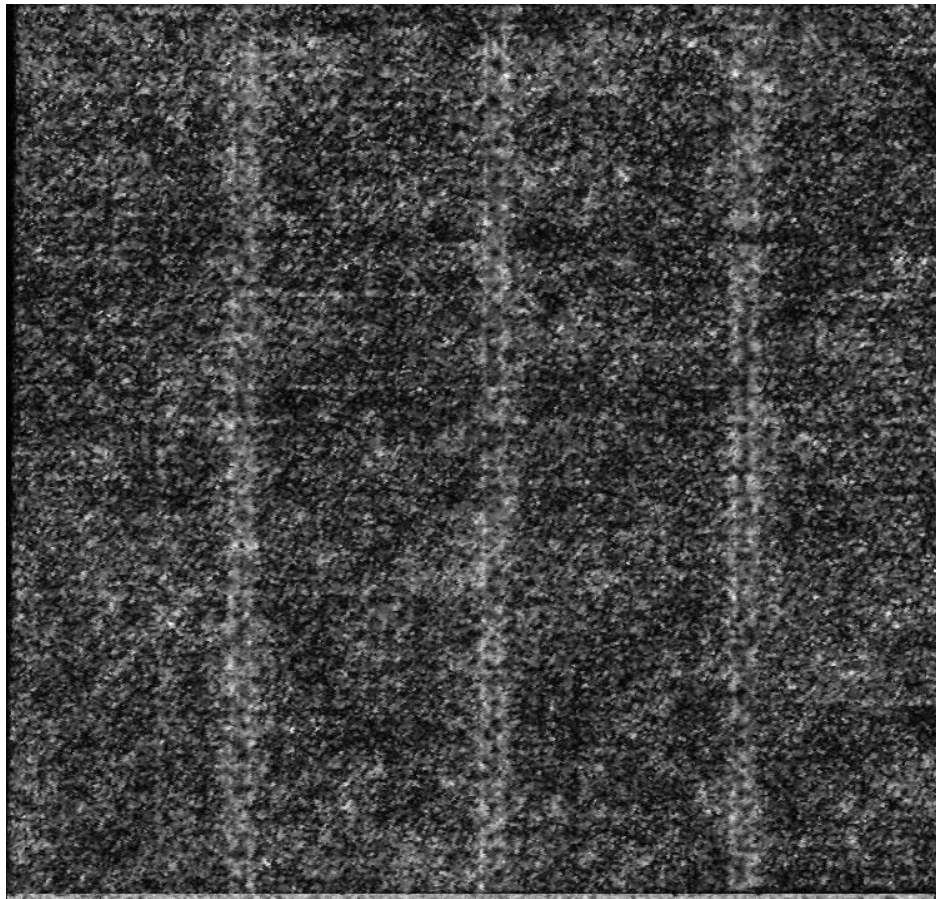


*Figure E.63-4. UT image showing missing tows in the bulk of the specimen.*



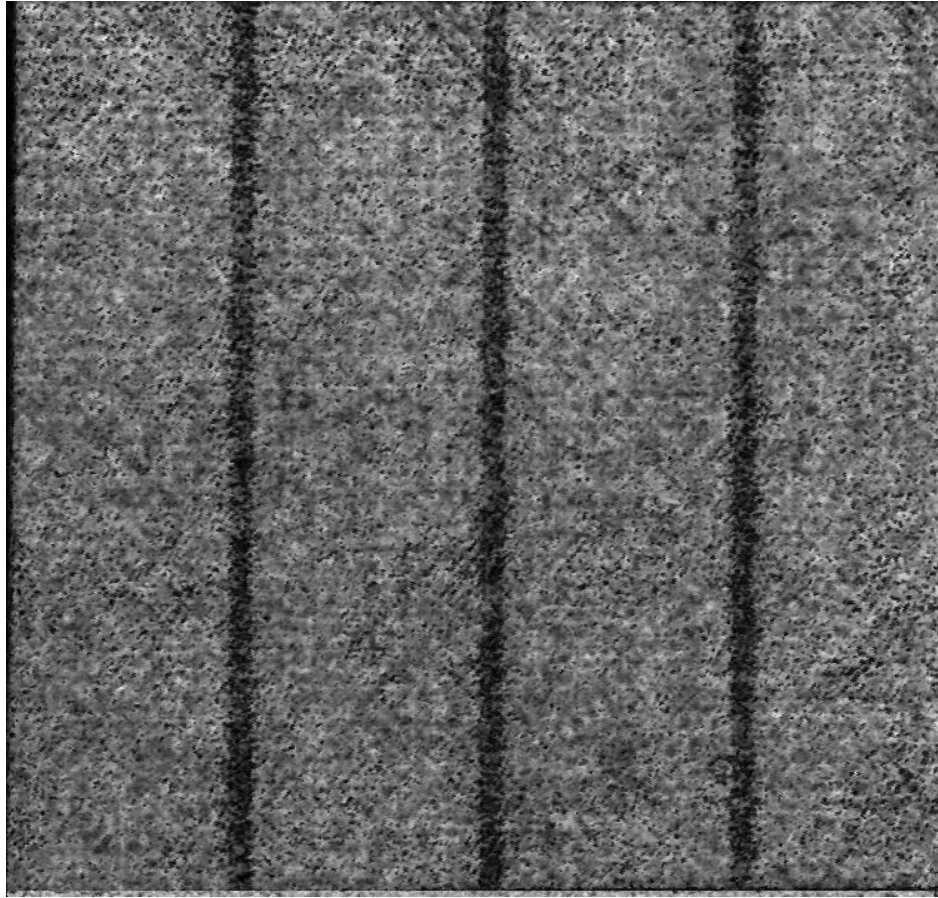


*Figure E.63-5. UT image showing missing tows in the bulk of the specimen.*

## **E.63.2 Method: Single-Sided Infrared Thermography (SSIR)**

### **E.63.2.1 Partner: NASA**

### **E.63.2.2 Technique Applicability: ★☆☆**

SSIR thermography was capable of detecting the missing tows. The signal is very faint.

### **E.63.2.3 Equipment List and Specifications:**

- TWI System
- TWI System flash heat source using Speedotron power supplies.
- SC6000 FLIR camera,  $640 \times 512$  InSb array, NEDT  $< 20$  mK
- 25 mm Germanium Optics

### **E.63.2.4 Settings:**

- 60 Hz Frame Rate
- Flash on frame #10
- Total number of Frames 1499
- Total data acquisition time of 24.98 sec
- The camera/hood was positioned to view the entire sample

### E.63.2.5 Laboratory Setup:

A commercially available flash thermography system was used for the inspection. The flash thermography system consisted of two linear flash tubes mounted within a hood. An IR camera was mounted at the back of the hood viewing through a circular hole between the flash tubes and were positioned to view the hood opening. In this configuration, the flash lamps heated an area equal to the hood opening and the IR camera captured the thermal response. The IR camera operates in the mid-wave IR band (3–5  $\mu\text{m}$ ) and is configured with a 25-mm germanium lens. The focal plane array size for the camera is  $640 \times 512$  with a detector pitch size of  $14 \times 14 \mu\text{m}$ .

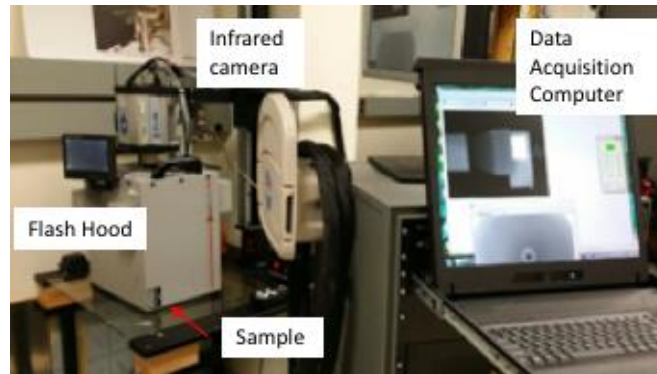


*Figure E.63-6. SSIR setup.*

### E.63.2.6 Principal Component Analysis

PCA is common for processing of thermal data [1–3]. This algorithm is based on decomposition of the thermal data into its principal components or eigenvectors. Singular value decomposition is a routine used to find the singular values and corresponding eigenvectors of a matrix. Since thermal NDE signals are slowly decaying waveforms, the predominant variations of the entire data set are usually contained in the first or second eigenvectors, and thus account for most of the data variance of interest. The principle components are computed by defining a data matrix  $A$ , for each data set, where the time variations are along the columns and the spatial image pixel points are row-wise. The matrix  $A$  is adjusted by dividing the maximum value (normalization) and subtracting the mean along the time dimension. The covariance matrix is defined as the  $A^T A$ . The covariance matrix is now a square matrix of number of images used for processing. The covariance matrix can then be decomposed using singular value decomposition as:

$$\text{covariance matrix} = A^T A = V * S * V^T$$

where  $S$  is a diagonal matrix containing the square of the singular values and  $V$  is an orthogonal matrix, which contains the basis functions or eigenvectors describing the time variations. The eigenvectors can be obtained from the columns of  $V$ . The PCA inspection image is calculated by dot product multiplication of the selected eigenvector times the temperature response (data matrix  $A$ ), pixel by pixel.

### E.63.2.7 Inspection Results

The 1499 frames of data (24.98 sec) were processed using iterations of different time windows. The processing of frames 100 to 999 corresponding to a time window of 1.67–16.65 sec yielded the best results. The three missing tows named A, B, and C were detected and are shown in Figure E.63-8. However, without prior knowledge of their presence, they could have easily gone

undetected due to their faint signal. The second eigenvector was used to produce the final inspection images shown in Figure E.63-7.



**Figure E.63-7. NASA-03-Missing-Tow-002 sample.**

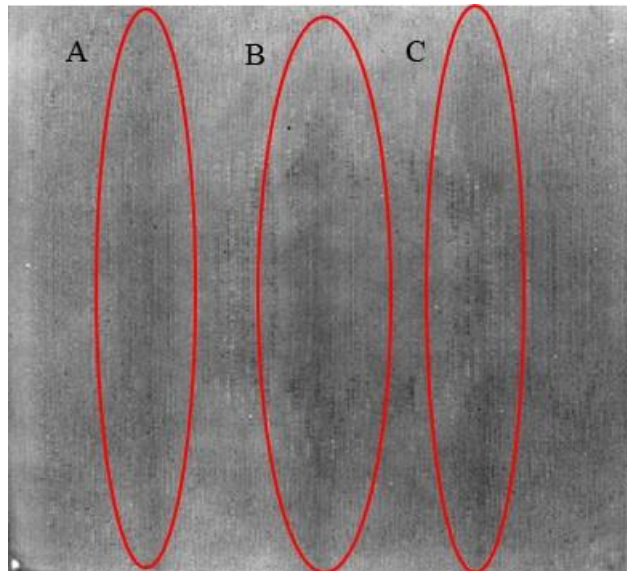


**Figure E.63-8. SSIR inspection of NASA-03-Missing-Tow-002 sample processed with PCA from frame 100 (1.67s) to 999 (16.65s).**

#### **E.63.2.8 References**

- [1] Rajic, N.: “Principal Component Thermography for Flaw Contrast Enhancement and Flaw Depth Characterization in Composite Structures,” *Composite Structures*, Vol. 58, pp. 521-528, 2002.
- [2] Zalameda, J. N.; Bolduc S.; and Harman R.: “Thermal Inspection of a Composite Fuselage Section using a Fixed Eigenvector Principal Component Analysis Method,” Proc. *SPIE* 10214, *Thermosense: Thermal Infrared Applications XXXIX*, 102140H, 5 May 2017.

- [3] Cramer, K. E.; and Winfree, W. P.: “Fixed Eigenvector Analysis of Thermographic NDE Data”, Proceedings of *SPIE, Thermosense XXXIII*, edited by Morteza Safai and Jeff Brown, Vol. 8013, 2011.

### **E.63.3 Method: Through-Transmission Infrared Thermography (TTIR)**

#### **E.63.3.1 Partner: NASA**

#### **E.63.3.2 Technique Applicability: ★★☆☆**

TTIR Thermography was capable of detecting the missing tows.

#### **E.63.3.3 Equipment List and Specifications:**

- TWI System
- TWI System flash heat source using Balcar power supply externally triggered by TWI system.
- SC6000 FLIR camera,  $640 \times 512$  InSb array, NEDT  $< 20$  mK
- 25 mm Germanium Optics

#### **E.63.3.4 Settings:**

- 60 Hz Frame Rate
- Flash on frame #10
- Total number of Frames 2000
- Total data acquisition time of 33.33 sec
- IR camera was positioned to view the entire sample

#### **E.63.3.5 Laboratory Setup**

The TT thermal inspection system setup is shown in Figure E.63-9. The test specimen is placed between the heat source and the IR camera. The lamp used to induce the heat was a commercially available photographic flash lamp powered by a 6,400-Joule power supply (manufactured by Balcar). The camera used was a FLIR SC6000 with a  $640 \times 512$  InSb array operating in the 3- to 5- $\mu\text{m}$  IR band. The image data frame rate was 60 image frames per second. The computer records the IR image of the specimen immediately prior to the firing of the flash lamp (for emissivity correction), and then the thermal response of the specimen at a user defined sampling rate and for a user defined duration is acquired.

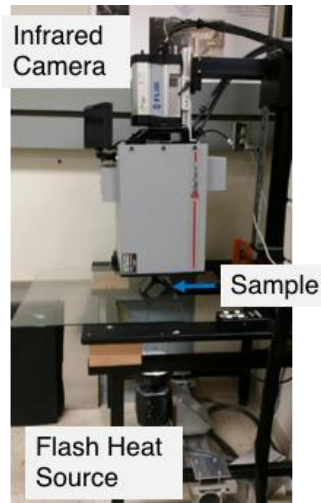


**Figure E.63-9. TTIR setup.**

### **E.63.3.6 Principal Component Analysis**

PCA is common for processing of thermal data [1–3]. This algorithm is based on decomposition of the thermal data into its principal components or eigenvectors. Singular value decomposition is a routine used to find the singular values and corresponding eigenvectors of a matrix. Since thermal NDE signals are slowly decaying waveforms, the predominant variations of the entire data set are usually contained in the first or second eigenvectors, and thus account for most of the data variance of interest. The principle components are computed by defining a data matrix  $A$ , for each data set, where the time variations are along the columns and the spatial image pixel points are row-wise. The matrix  $A$  is adjusted by dividing the maximum value (normalization) and subtracting the mean along the time dimension. The covariance matrix is defined as the  $A^T * A$ . The covariance matrix is now a square matrix of number of images used for processing. The covariance matrix can then be decomposed using singular value decomposition as:

$$\text{covariance matrix} = A^T A = V * S * V^T$$

where  $S$  is a diagonal matrix containing the square of the singular values and  $V$  is an orthogonal matrix, which contains the basis functions or eigenvectors describing the time variations. The eigenvectors can be obtained from the columns of  $V$ . The PCA inspection image is calculated by dot product multiplication of the selected eigenvector times the temperature response (data matrix  $A$ ), pixel by pixel.

### **E.63.3.7 Inspection Results**

The 2000 frames of data (33.33 sec) were processed using iterations of different time windows. The processing of frames 50 to 250 corresponding to a time window of 0.83–4.17 sec yielded the best result, and is shown in Figure E.63-11. Possible defects, labeled A through G were detected. A, B, and C are linear and run across the entire length of the test sample. D, E, and F are also linear, but centered in the middle of the test sample. These three defects are possibly due to the writing seen on the panel in Figure E.63-10. The different shape of area G could indicate there is a separate type of defect found in this region.



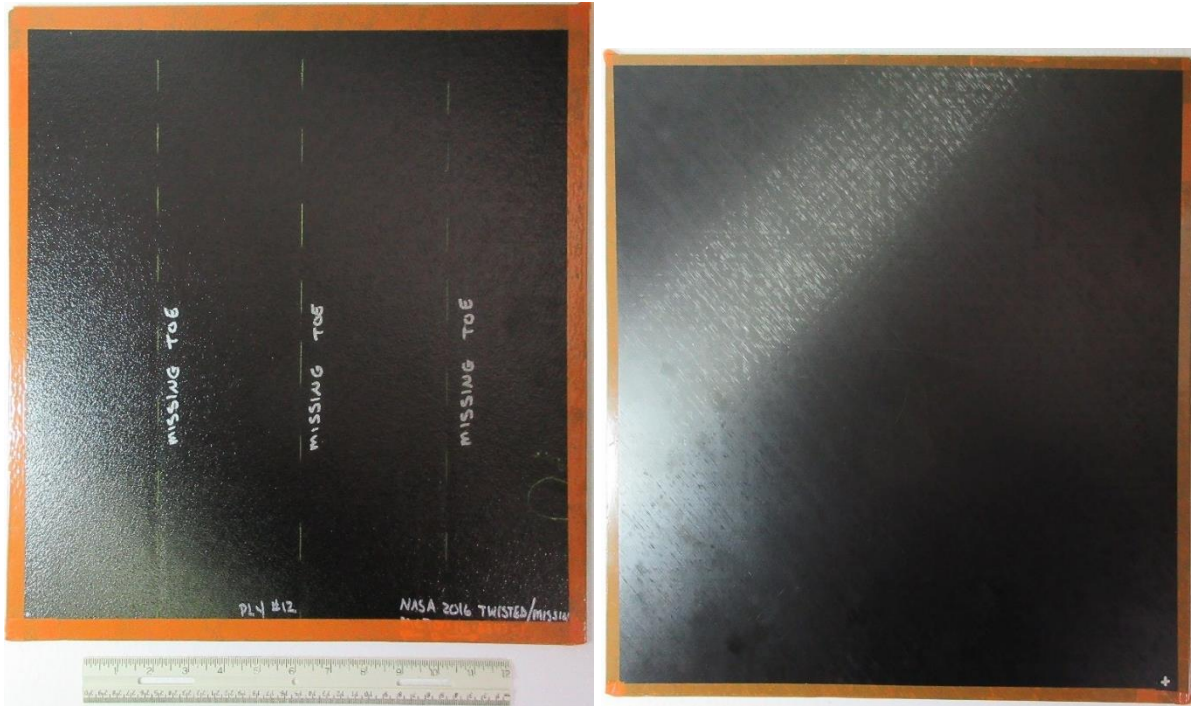


Figure E.63-10. NASA-03-Missing-Tow-002 sample.

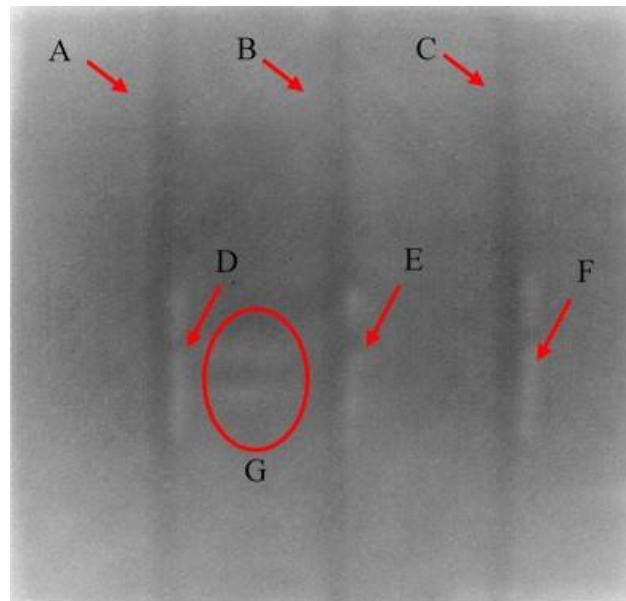


Figure E.63-11. TTIR inspection of NASA-03-Missing-Tow-002 sample processed with PCA from frame 50 (0.83s) to 250 (4.17s).

### E.63.3.8 References

- [1] Rajic, N.: "Principal Component Thermography for Flaw Contrast Enhancement and Flaw Depth Characterization in Composite Structures," *Composite Structures*, Vol. 58, pp. 521-528, 2002.
- [2] Zalameda, J. N.; Bolduc S.; and Harman R.: "Thermal Inspection of a Composite Fuselage Section using a Fixed Eigenvector Principal Component Analysis Method," Proc. *SPIE* 10214, *Thermosense: Thermal Infrared Applications XXXIX*, 102140H, 5 May 2017.

- [3] Cramer, K. E.; and Winfree, W. P.: “Fixed Eigenvector Analysis of Thermographic NDE Data”, Proceedings of *SPIE, Thermosense XXXIII*, edited by Morteza Safai and Jeff Brown, Vol. 8013, 2011.

#### **E.63.4 Method: Single-Side Flash Thermography (SSFT-TSR)**

##### **E.63.4.1 Partner: Thermal Wave Imaging, Inc.\***

\*TWI was not part of the ACC but reviewed specimens.

##### **E.63.4.2 Technique Applicability: ★★★**

SSFT-TSR is capable of detecting subsurface anomalies in this specimen that could be the result of delamination, voids or porosity. All indications appear in the head-on image, but more accurate sizing is achieved by inspecting the flat surfaces separately.

##### **E.63.4.3 Laboratory Setup:**

The sample was inspected with a commercially available flash thermography system (EchoTherm®, Thermal Wave Imaging, Inc.), equipped with two linear xenon flash/reflector assemblies mounted in a reflective hood optimized to provide uniform output at the 10-inch × 14-inch exit aperture. Each lamp is powered by a 6 kJ power supply that allows truncation of the flash to a rectangular pulse with duration <1 msec. A cryogenically cooled IR camera is mounted to view the plane of the hood exit aperture, with the camera lens positioned at the plane of the flashlamps. Excitation, data capture and processing and analysis using TSR are controlled at the system console using Virtuoso software.

##### **E.63.4.4 Equipment List and Specifications:**

- EchoTherm® Flash Thermography System
- 2 linear xenon flash lamps and power supplies (6 kJ each)
- TWI Precision Flash Control (truncation to 4 msec rectangular pulse)
- A6100sc FLIR camera, 640 × 512 InSb array, NEDT < 20 mK
- 13 mm Germanium Lens
- TWI Virtuoso® software

##### **E.63.4.5 Settings:**

- 30 Hz Frame Rate
- 10 Preflash Frames
- 1800 total frames
- 7 Polynomial order
- 60-sec data acquisition time
- FOV: 10-inch × 14-inch

Settings were determined following the recommendations in ASTM E2582-14. Acquisition duration was set according to the time of the break from linearity ( $t^* \sim 8$  sec) due to the BW for typical points in the log time history. The acquisition period was then set to 30 sec ( $3 \times t^*$ ), per ASTM E2582-14.

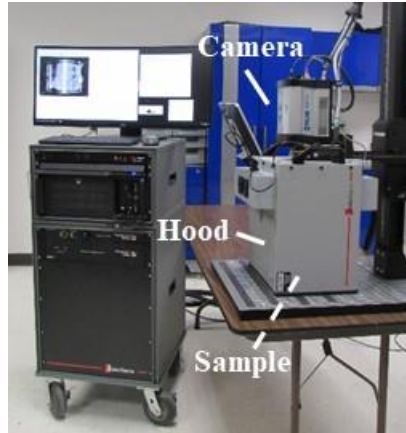


*Figure E.63-12. SSFT system with TSR*

#### **E.63.4.6 Thermographic Signal Reconstruction (TSR)**

After acquisition, captured data are processed using TSR to reduce temporal noise, enhance deviation from normal cooling behavior and allow segmentation of the data based on signal attributes. For each pixel, the average of 10 frames immediately preceding the flash pulse is subtracted from the pixel time history, and a 7<sup>th</sup> order polynomial is fit to the logarithmically scaled result using least squares. First and 2<sup>nd</sup> derivatives of the result are calculated and the derivative images are displayed in the Virtuoso software. Derivative signals associated normal areas of the sample exhibit minimal activity over the duration of the acquisition. Signals associated with subsurface anomalies typically behave identically to the normal signals until a particular time (dependent on host material characteristics and the depth of the feature) after which their behavior deviates from normal (the degree of the deviation depends on the relative difference in the thermal properties of the anomaly and the surrounding normal matrix).

#### **E.63.4.7 Inspection Results**

Three subsurface indications were observed and confirmed to be subsurface by their late divergence in the logarithmic temperature time plot. The 1<sup>st</sup> derivative at 6.54 sec was used to produce the final inspection images shown in Figure E.63-13.

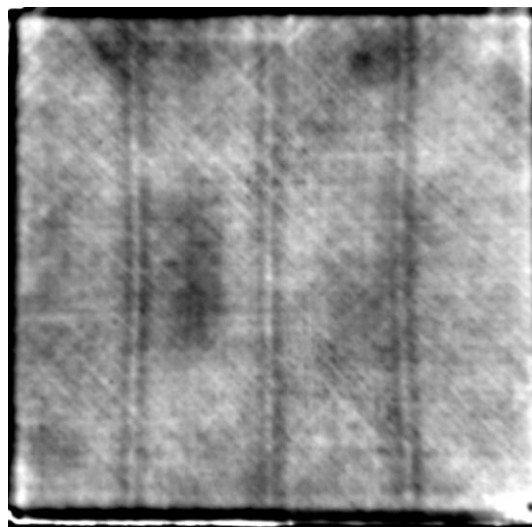


*Figure E.63-13. TSR 1<sup>st</sup> derivative at 6.54 sec of #63- Missing Toe Ply #12.*



**E.63.4.8 References**

- [1] ASNT: *ASNT Aerospace NDT Industry Handbook*, Chapter 11, “Thermography,” Nov 2014.
- [2] ASTM International: “Standard Practice for Infrared Flash Thermography of Composite Panels and Repair Patches,” *ASTM E2582–07*, 2007.
- [3] Shepard, S.; and Frenberg, M.: “Thermographic Detection and Characterization of Flaws in Composite Materials,” *Materials Evaluation*, ASNT, July 2014.
- [4] Hou, Y.; Lhota, J. R.; and Golden, T. J. M.: “Automated processing of thermographic derivatives for quality assurance,” *Opt. Eng.*, Vol. 46, 051008, 2007.
- [5] *Temporal noise reduction, compression and analysis of data sequences*, U.S. Patent 6,516,084.

**E.64 Specimen #64 – NASA-03-Bridged Joggle-001 – Not Tested**

Structure	Material	Details	Dimensions (inches)	Partner Methods
AFP Fiber Placed panel	IM7/8552-1 Slit Tape	Flange with bridging in joggle	12 × 9 × 1.3	Not Tested

**E.65 Specimen #65 – NASA-03-Bridged-Joggle-002 – Not Tested**

Structure	Material	Details	Dimensions (inches)	Partner Methods
AFP Fiber Placed panel	IM7/8552-1 Slit Tape	Flange with bridging in joggle	12 × 9 × 1.3	Not Tested

**E.66 Specimen #66 – NASA-03-Bridged-Joggle-003 – Not Tested**

Structure	Material	Details	Dimensions (inches)	Partner Methods
AFP Fiber Placed panel	IM7/8552-1 Slit Tape	Flange with bridging in joggle	12 × 9 × 1.3	Not Tested

**E.67 Specimen #67 – NASA-03-Bridged-Joggle-004 – Not Tested**

Structure	Material	Details	Dimensions (inches)	Partner Methods
AFP Fiber Placed panel	IM7/8552-1 Slit Tape	Flange with bridging in joggle	12 × 9 × 1.3	Not Tested

**E.68 Specimen #68: NAA-03-FOD-Panel-001:**

Structure	Material	Details	Dimensions (inches)	Partners Methods	
Fiber Placed Panel	IM7/8552-1 Slit Tape w/ IM7/8552 Fabric Outer Mold Line (OML)	FOD Panel	19 × 43 × 0.3	NGIS	E.68.1 PEUT
				GE	E.68.2 TTUT E.68.3 PEUT

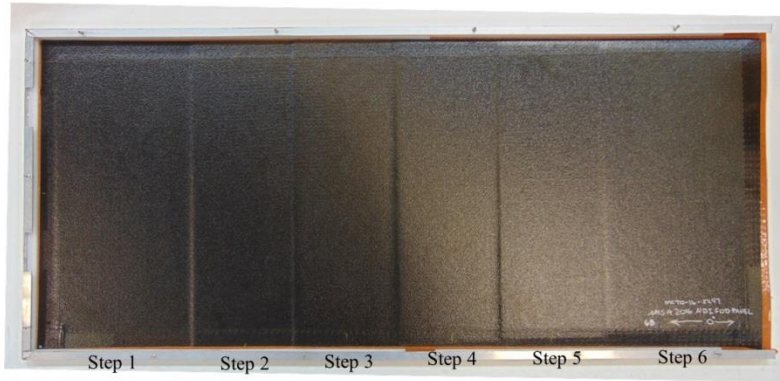


*Figure E.68-1. Photographs of Specimen #68: NASA-03-FOD-Panel-001.*

**E.68.1 Method: Pulse-Echo Ultrasound Testing (PEUT)**

**E.68.1.1 Partner: NGIS**

**E.68.1.2 Technique Applicability: ★★★**

Water-coupled PEUT scans were performed to demonstrate the feasibility of detecting defects in thick carbon-composite laminates on a stepped-thickness panel with foreign object debris (FOD) placed throughout and laminate thickness ranging from 0.1 to 1.0 inch. Scans were performed from the flat tool-side to determine detection dependency on both defect depth and diameter. Different frequencies including 2.25 MHz and 5.0 MHz were sampled to observe frequency dependence.

**E.68.1.3 Laboratory Setup**

PEUT scans were performed in the Test-Tech 3-axis scanning tank using a water-squirter method. For each panel, water nozzle and column diameter was optimized to achieve optimal signal-to-noise ratio (SNR) and defect detection (if defects existed).

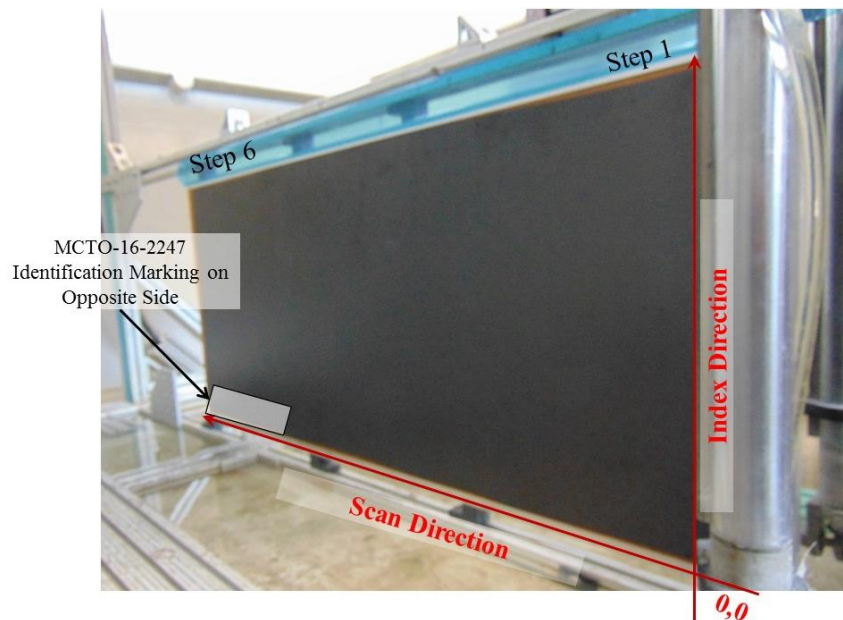


*Figure E.68-2. PEUT setup in Test-Tech scanning tank.*

#### E.68.1.4 Equipment List and Specifications:

- Test-Tech 3-axis scanning tank
- Olympus 5077PR Square Wave Pulsar/Receiver
- Transducer frequencies: 2.25, 5.0 MHz

#### E.68.1.5 Settings

*Table E.68-1. Equipment settings for 2.25 MHz scan.*

Transducer	Brand	Model	Freq. (MHz)	Element Dia. (in.)	Water Column Dia. (in.)			Outer Dia. (in.)		
Transmitter	KB-Aerotech	Alpha	2.25	0.25	0.25			0.5		
Pulsar/Receiver	PRF	Voltage	Freq. (MHz)		HPF (MHz)	LPF (MHz)	Rtune	Ttune	Attn	Range
Olympus	Ext	100	2-2.25		1	10	N/A	N/A	N/A	N/A
	Gain (dB)	11 for Steps 1-6								

*Table E.68-2. Equipment settings for 5.0 MHz scan.*

Transducer	Brand	Model	Freq. (MHz)	Element Dia. (in.)	Water Column Dia. (in.)			Outer Dia. (in.)		
Transmitter	Krautkramer	Benchmark	5	0.25	0.25			0.5		
Pulsar/Receiver	PRF	Voltage	Freq. (MHz)		HPF	LPF (MHz)	Rtune	Ttune	Attn	Range
Olympus	Ext	100	5-6		Out	10	N/A	N/A	N/A	N/A
	Gain (dB)	"-3 for Steps 1-6								

#### E.68.1.6 Inspection Results

Not all defects or BWs were detected for all measured frequencies as shown below. For example, for higher frequency PEUT, thicker step panels were too thick and attenuating. For lower frequency PEUT on thinner panels, internal and BW signals could not be individually resolved due to the relatively large wavelength. Scans were performed and data quality was verified by producing C-scans for the different panels.

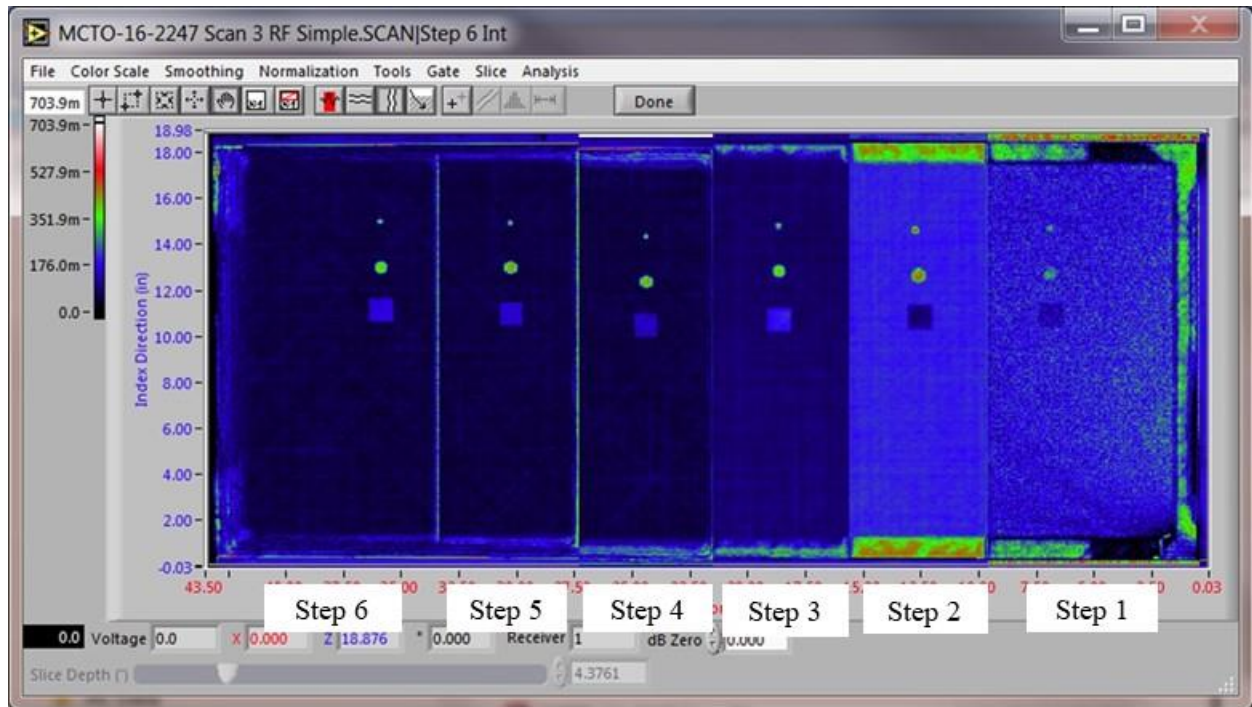


*Figure E.68-3. PEUT C-scans at 2.25 MHz for steps 1-6 (Internal Gate).*

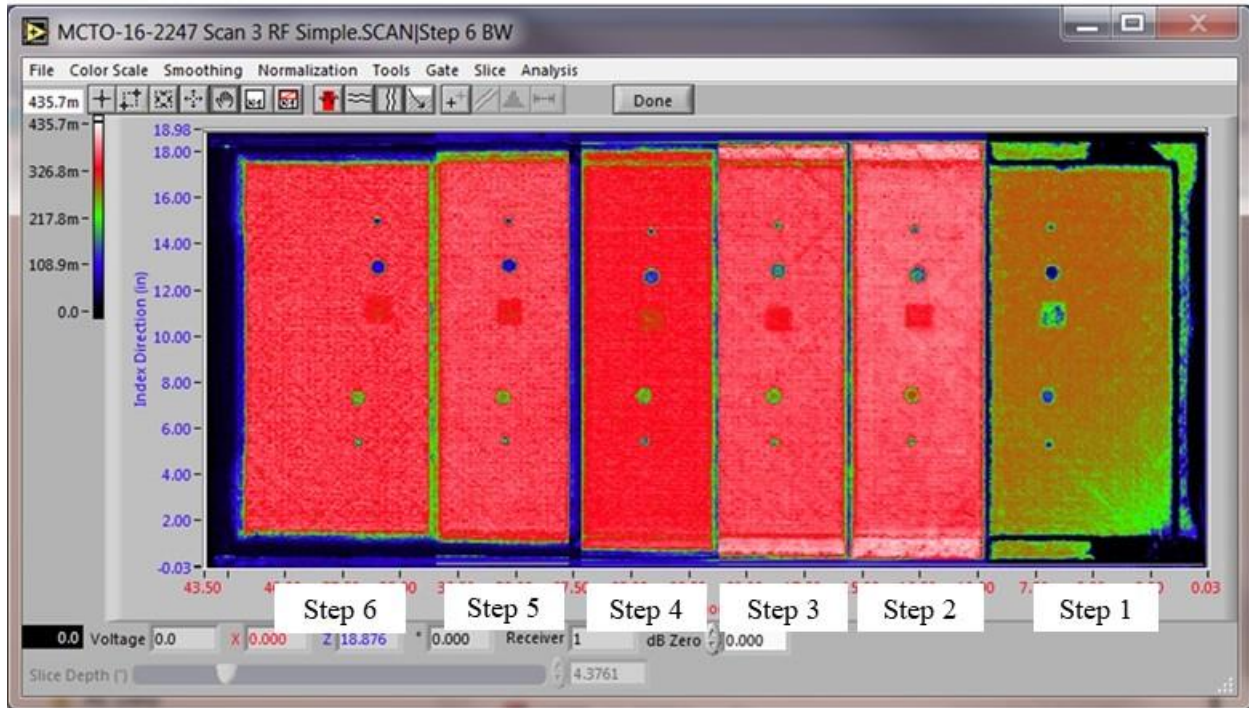


*Figure E.68-4. PEUT C-scans at 2.25 MHz for steps 1-6 (BW Gate).*

## **E.68.2 Method: Through-Transmission Ultrasound Testing (TTUT)**

### **E.68.2.1 Partner: GE Aviation**

### **E.68.2.2 Technique Applicability: ★★★**

Immersion TTUT scan was performed at 5 MHz on the stepped panel to demonstrate detection of thin Grafoil targets which were not detectable at lower frequencies. Shim-type foreign material are not detectable if thickness is less than 1/10<sup>th</sup> the transducer wavelength.

### **E.68.2.3 Laboratory Setup**

TTUT scans were performed in the OKOS 6-axis scanning tank using the immersion method. Transmission was performed on the flat tool side of the panel and received from the bagged stepped side. Gain was adjusted to receive a 50% amplitude signal from the thinnest step. A snapshot of the C-scan is provided below to show detection of square-shaped Grafoil targets.

### **E.68.2.4 Equipment List and Specifications:**

- OKOS 6-axis scanning tank
- JSR DPR35G Spike Pulser/Receiver
- Transducer Frequencies: 5 MHz



### E.68.2.5 Settings

*Table E.68-3. Equipment settings for 5 MHz scan.*

Transducer	Brand	Model	Freq. (MHz)	Element Dia. (in.)	Water path (in.)	Focal Length (in)
Transmitter	Olympus	V320	5	0.5	2	2
Receiver	Olympus	V320	5	0.5	2	2
Pulser/Receiver	PRF	Voltage	Damping	Energy	LPF (MHz)	HPF (MHz)
JSR DPR35G	Ext.	100	1000	0	1	10

### E.68.2.6 Inspection Results

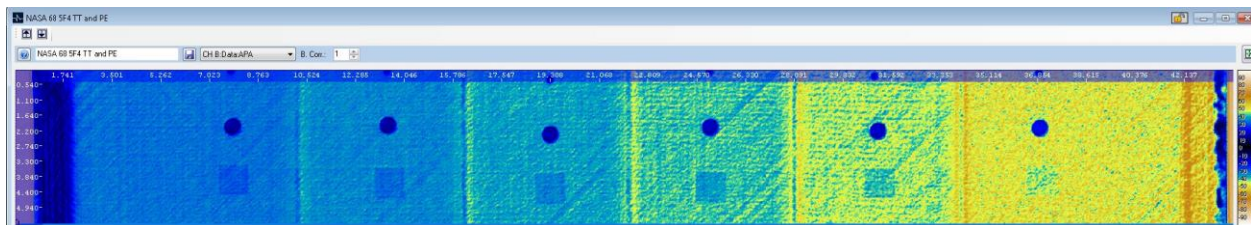


*Figure E.68-5. TTUT C-scans at 5.0 MHz showing square-shaped Grafoil targets.*

### E.68.3 Method: Pulse Echo Ultrasound Testing (PEUT)

#### E.68.3.1 Partner: GE Aviation

#### E.68.3.2 Technique Applicability: ★★★

Additional immersion PEUT scans were performed to demonstrate the feasibility of detecting defects by using time-of-flight data. Scans were performed from the flat tool-side, using data gates to select various depths of interest.

#### E.68.3.3 Laboratory Setup

PEUT scans were performed in the OKOS 6-axis scanning tank using the immersion method. For each panel, the gain setting was selected to set the peak signal from targets or BW to 80%.

#### E.68.3.4 Equipment List and Specifications:

- OKOS 6-axis scanning tank
- JSR DPR35G Spike Pulser/Receiver
- Transducer Frequencies: 5 MHz

### E.68.3.5 Settings

Table E.68-4. Equipment settings for 5.0 MHz scan.

Transducer	Brand	Model	Freq. (MHz)	Element Dia. (in.)	Water path (in.)	Focal Length (in)
Transmitter	Olympus	V307	5	1	2	2
Pulser/Receiver	PRF	Voltage	Damping	Energy	LPF (MHz)	HPF (MHz)
JSR DPR35G	Ext.	100	1000	0	1	10

### E.68.3.6 Inspection Results

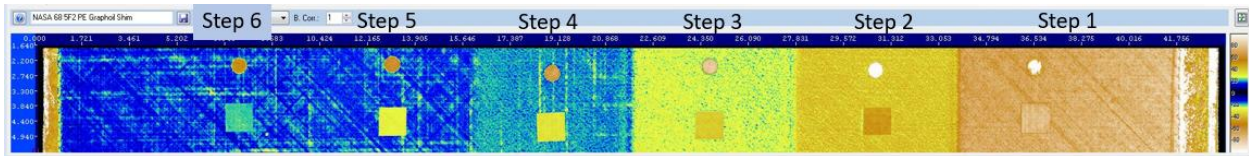


Figure E.68-6. PEUT amplitude C-scans at 5.0 MHz for shallow steps. BW amplitude is observed in steps 1–4.

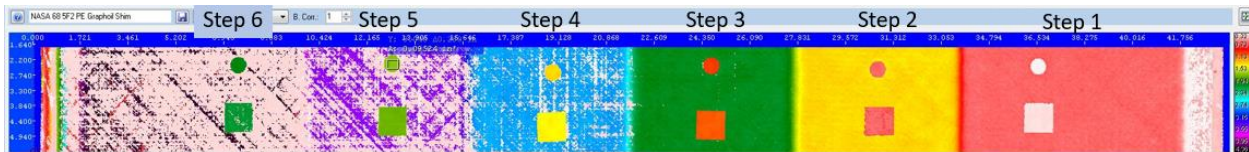


Figure E.68-7. PEUT Time-of-Flight C-scans at 5.0 MHz for shallow steps. Uniform target depth is seen in steps 2-6, uniform BW depth is observed in steps 1–4. Disruption of BW depth in steps 1–4 indicate presence of target.

### E.69 Specimen #69: NASA-03-Porosity-Panel-001

Structure	Material	Details	Dimensions (inches)	Partner Methods	
				NASA	E.69.1 PEUT
Fiber Placed Panel	IM7/8552-1 Slit Tape w/ IM7/8552 Fabric OML	Flat Panel with porosity	15 × 17.5 × 0.15	NGIS	E.69.2 PEUT
					E.69.3 TTUT
					E.69.4 SSIR
					E.69.5 TTIR

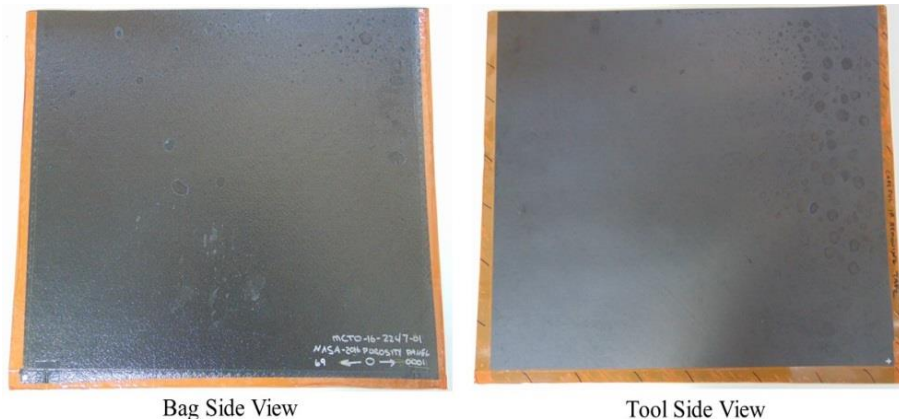


Figure E.69-1. Photographs of Specimen #69: NASA 03 Porosity Panel 001.



## E.69.1 Method: Pulse-Echo Ultrasound Testing (PEUT)

### E.69.1.1 Partner: NASA

### E.69.1.2 Technique Applicability: ★★☆☆

PEUT is able to detect some instances of porosity in this sample.

### E.69.1.3 Laboratory Setup

Immersion Ultrasonic Testing: NASA LaRC uses a custom-designed single-probe ultrasonic scanning system. The system has an 8-axis motion controller, a multi-axis gantry robot mounted above a medium-size water tank, a dual-channel, 16-bit, high-speed digitizer, and an off-the-shelf ultrasonic pulser receiver. The system can perform TTUT and PEUT inspections. TT inspection employs two aligned ultrasonic probes, one transmitter, and one receiver, placed on either side of a test specimen. Pulse-echo inspection is a single-sided method where a single ultrasonic probe is both transmitter and receiver. In each method, data are acquired while raster scanning the ultrasonic probe(s) in relation to a part. Figure E.69-2 shows a simplified block diagram of a scanning Pulse-echo inspection.

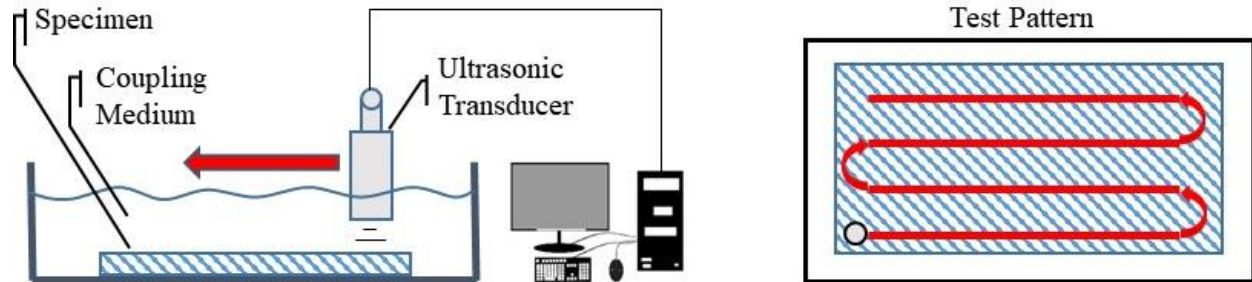


Figure E.69-2. Ultrasonic system components.

### E.69.1.4 Equipment List and Specifications:

- Pulser/Receiver: Olympus 5073PR
- Digitizer: AlazarTech ATS9462, dual channel, 16 bit, 180 MS/s
- Sensor: Olympus 2-inch spherical focus immersion ultrasonic transducer
- Motion system: open looped stepper motor based X-YY-Z gantry robot
- Motion Controller: Galil DMC-4183
- Acquisition Software: FastScan, custom developed at NASA LaRC
- Signal Processing Software: DataViewer, custom developed at NASA LaRC

### E.69.1.5 Settings

Table E.69-1. Data collection settings.

Resolution (horizontal) [in/pixel]	0.02
Resolution (vertical) [in/pixel]	0.02
Probe frequency [MHz]	5
Focal Length [in]	1.9
Array Dimensions [pixels]	851 × 751

The specimen is placed flat against the zero position of the tank raised above the glass bottom by several metal washers. The test probe is computer-controlled and correlated to the position on the

sample. It is also focused to a point one mm below the surface of the test material. The specimen remains in place while the transducer follows a preprogrammed test grid across the surface as indicated in Figure E.69-2. At each point, ultrasonic data are collected from individual pulses. Larger step sizes between data collection result in lower image resolution. These data points are reconstructed into a data cube displaying spatial coordinates as time progresses. 2D reconstruction of the collection of ultrasonic responses create flattened slices at varying depths within the material.

#### **E.69.1.6 Inspection Results**

Specimen #69 is a fiber placed flat panel fabricated from IM7/8552-1 Slit Tape with the objective of achieving porosity throughout the sample. PEUT was performed on this specimen in NASA's immersion tank specified above.

Figure E.69-3 is at a depth of 0.086 inch and shows a few instances of porosity as indicated. The larger porosity appears white initially as the air pocket reflects acoustic waves creating a strong early response. The striations seen in Figure E.69-3 and Figure E.69-4 are the fiber directions of the individual plies.

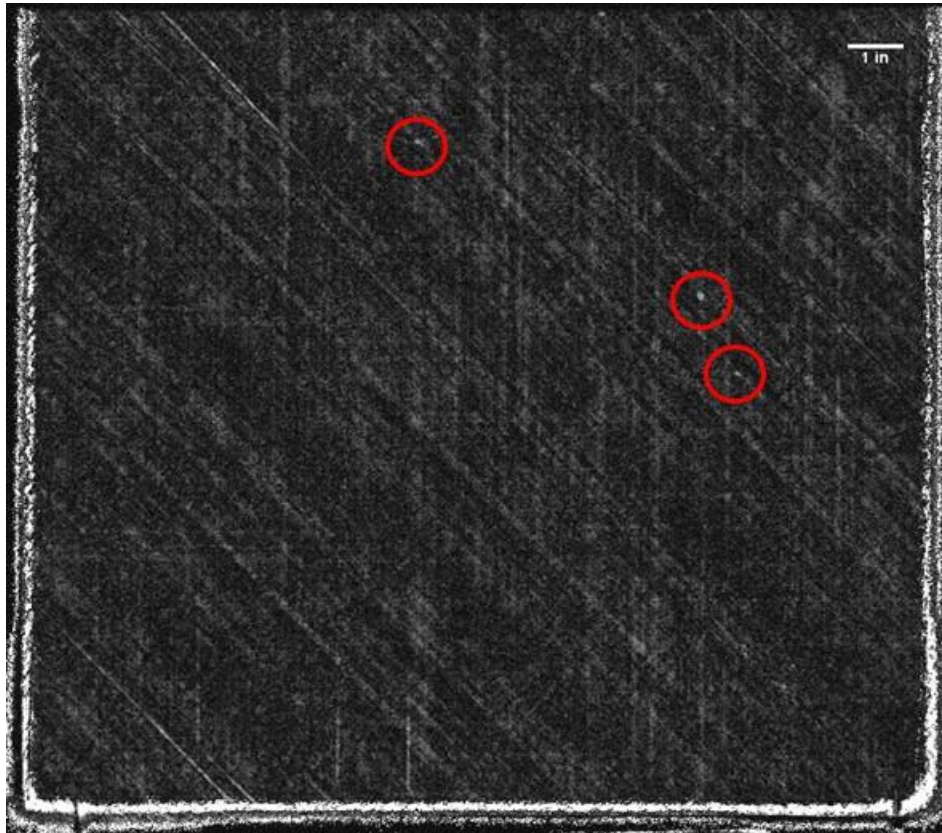


*Figure E.69-3. UT image of porosity within the sample.*

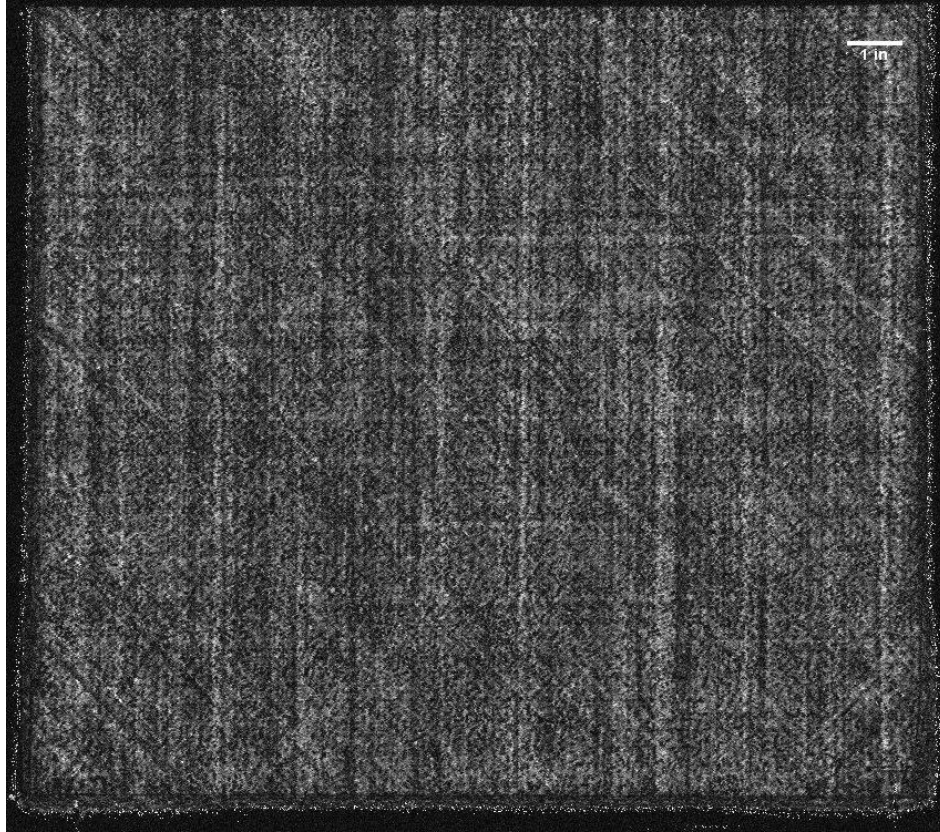


*Figure E.69-4. UT image of porosity deeper within the sample.*

**E.69.2 Method: Pulse-Echo Ultrasound Testing (PEUT)**

**E.69.2.1 Partner: NGIS**

**E.69.2.2 Technique Applicability: ★★★**

PEUT scans were performed on the flat tool side of the panel in order to detect defects.

**E.69.2.3 Laboratory Setup**

PEUT scans performed in the Test-Tech 3-axis scanning tank used the water-squirter method. For each panel, use of optimum water nozzle and column diameter achieved optimal SNR and defect detection (if defects existed).

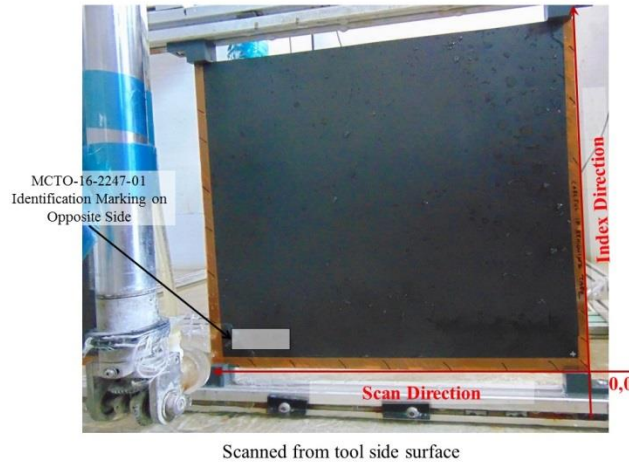


**Figure E.69-5. PEUT setup in Test-Tech scanning tank.**

**E.69.2.4 Equipment List and Specifications:**

- Test-Tech 3-axis scanning tank
- Olympus 5077PR Square Wave Pulsar/Receiver
- Transducers (2.25, 5.0 MHz)

**E.69.2.5 Settings**

**Table E.69-2. Equipment settings for 2.25 MHz scan.**

Transducer	Brand	Model	Freq. (MHz)	Element Dia. (in.)	Water Column Dia. (in.)			Outer Dia. (in.)		
Transmitter	KB-Aerotech	Alpha	2.25	0.25	0.25			0.5		
Pulsar/Receiver	PRF	Voltage	Freq. (MHz)		HPF (MHz)	LPF (MHz)	Rtune	Ttune	Attn	Range
Olympus	Ext	100	2-2.25		Out	Full BW	N/A	N/A	N/A	N/A
	Gain (dB)	14								

**Table E.69-3. Equipment settings for 5.0 MHz scan.**

Transducer	Brand	Model	Freq. (MHz)	Element Dia. (in.)	Water Column Dia. (in.)			Outer Dia. (in.)		
Transmitter	Krautkramer	Benchmark	5	0.25	0.25			0.5		
Pulsar/Receiver	PRF	Voltage	Freq. (MHz)		HPF	LPF (MHz)	Rtune	Ttune	Attn	Range
Olympus	Ext	100	5-6		Out	Full BW	N/A	N/A	N/A	N/A
	Gain (dB)	-5								

**E.69.2.6 Inspection Results**

Scans were performed and data quality was verified by producing C-scans for the different panels. Front wall and multiple BW reflections were resolved at both 2.25 MHz and 5 MHz.



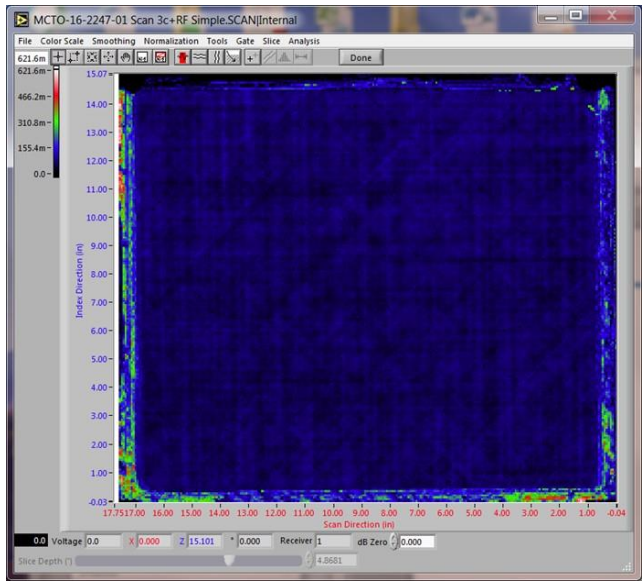
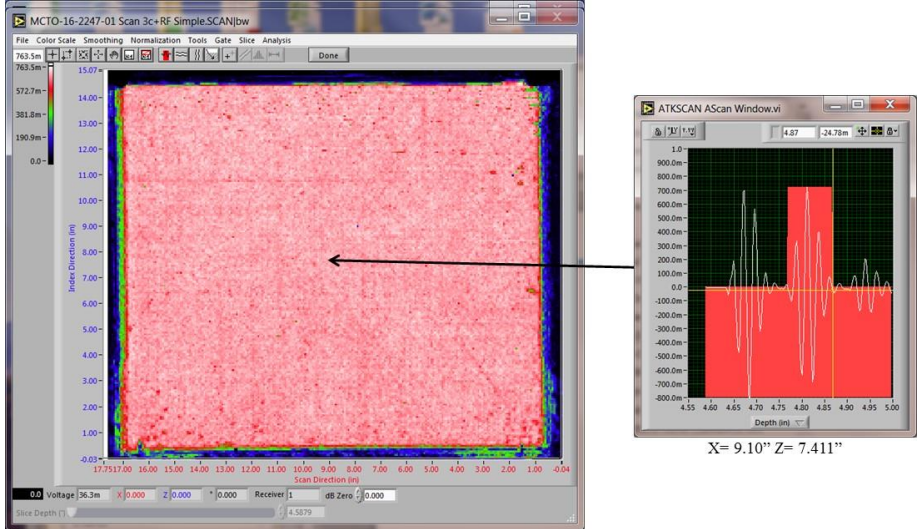


Figure E.69-6. PEUT C-scans at 2.25 MHz (Internal Gate).



MCTO-16-2247-01 Scan 3c Backwall Gate

Figure E.69-7. PEUT C-scans at 2.25 MHz (BW Gate).

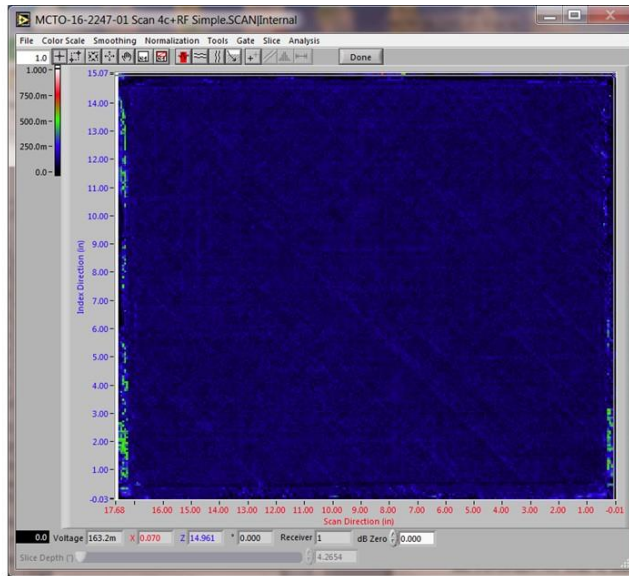


Figure E.69-8. PEUT C-scans at 5.0 MHz (Internal Gate).

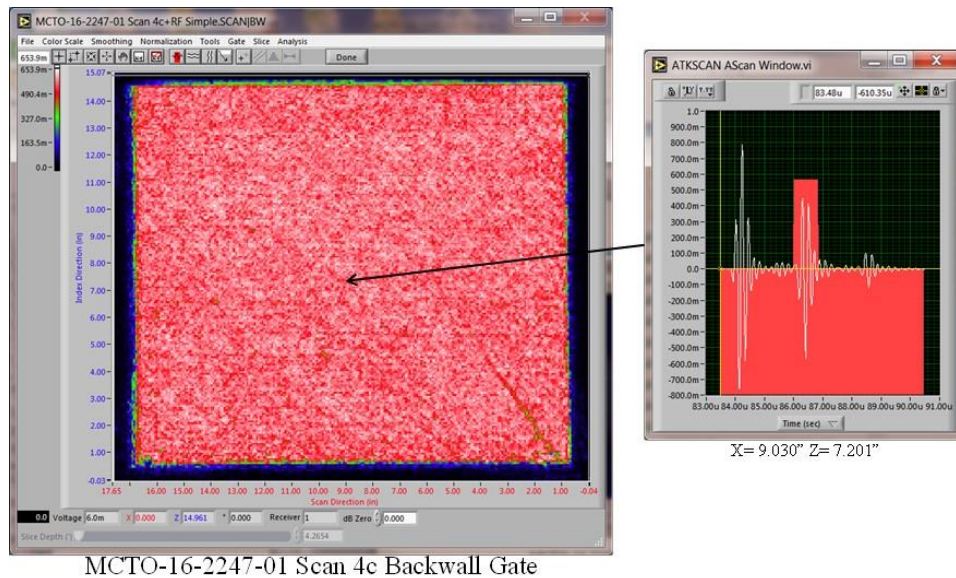


Figure E.69-9. PEUT C-scans at 5.0 MHz (BW Gate).

### E.69.2.7 References

- [1] Workman, Gary L; and Kishoni, Doron: *Nondestructive Testing Handbook*, Third. Edited by Patrick O Moore. Vol. 7. American Society for Nondestructive Testing (ANST), 2007.

### E.69.3 Method: Through-Transmission Ultrasound Testing (TTUT)

#### E.69.3.1 Partner: NGIS

#### E.69.3.2 Technique Applicability: ★★★

TTUT scans were performed on the stepped panel in order to detect defects. Depth of defect cannot be determined with this method.



### E.69.3.3 Laboratory Setup

TTUT scans were performed in the Test-Tech 3-axis scanning tank using a water-squirter method. Transmission was performed on the flat tool side of the panel and received from the bagged stepped side of the panel. For each panel, water nozzle and column diameter was optimized to achieve optimal SNR and defect detection (if defects existed).

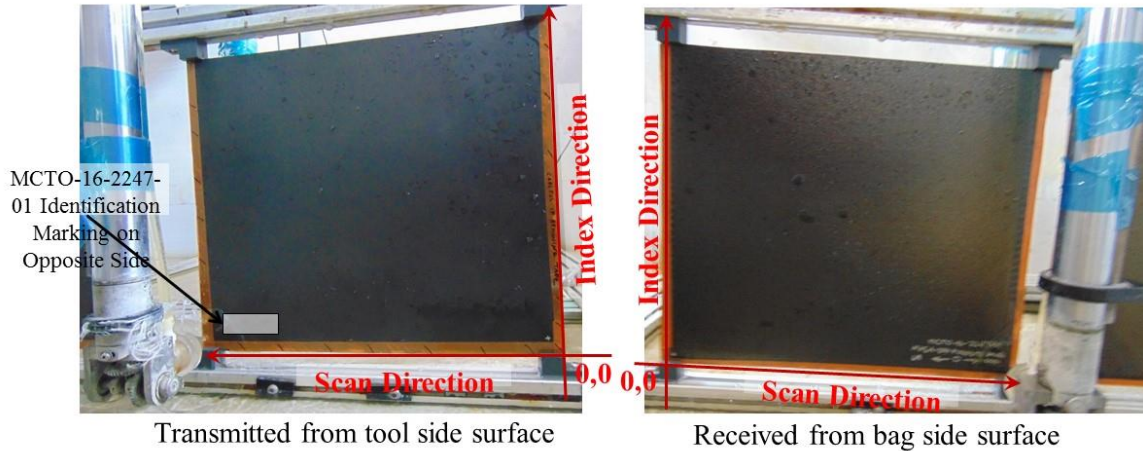


Figure E.69-10. TTUT setup in Test-Tech scanning tank.

### E.69.3.4 Equipment List and Specifications:

- Test-Tech 3-axis scanning tank
- Olympus 5077PR Square Wave Pulsar/Receiver
- Transducer Pairs (1.0, 2.25 MHz)

### E.69.3.5 Settings

Table E.69-4. Equipment settings for 1.0 MHz scan.

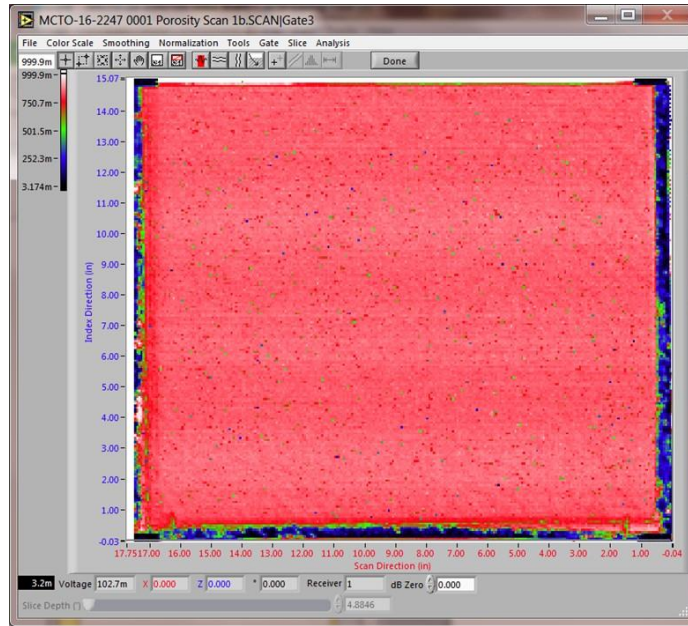
Transducer	Brand	Model	Freq. (MHz)	Element Dia. (in.)	Water Column Dia. (in.)			Outer Dia. (in.)		
Transmitter	Sonic	IBK I-2	1	0.5	0.25			0.5		
Receiver	Sonic	IBK I-2	1	0.5	0.25			0.5		
Pulsar/Receiver	PRF	Voltage	Freq. (MHz)		HPF	LPF (MHz)	Rtune	Ttune	Attn	Range
Olympus	Ext	100	1.0		Out	Full BW	N/A	N/A	N/A	N/A
	Gain (dB)	28								

Table E.69-5. Equipment settings for 2.25 MHz scan.

Transducer	Brand	Model	Freq. (MHz)	Element Dia. (in.)	Water Column Dia. (in.)			Outer Dia. (in.)		
Transmitter	KB-Aerotech	Alpha	2.25	0.25	0.25			0.5		
Receiver	KB-Aerotech	Alpha	2.25	0.25	0.25			0.5		
Pulsar/Receiver	PRF	Voltage	Freq. (MHz)		HPF (MHz)	LPF (MHz)	Rtune	Ttune	Attn	Range
Olympus	Ext	100	2-2.25		Out	Full BW	N/A	N/A	N/A	N/A
	Gain (dB)	13								

### E.69.3.6 Inspection Results

TTUT C-scans and signals exhibited very low attenuation at both 1 MHz and 2.25 MHz.



**Figure E.69-11. TTUT C-scans at 1 MHz.**

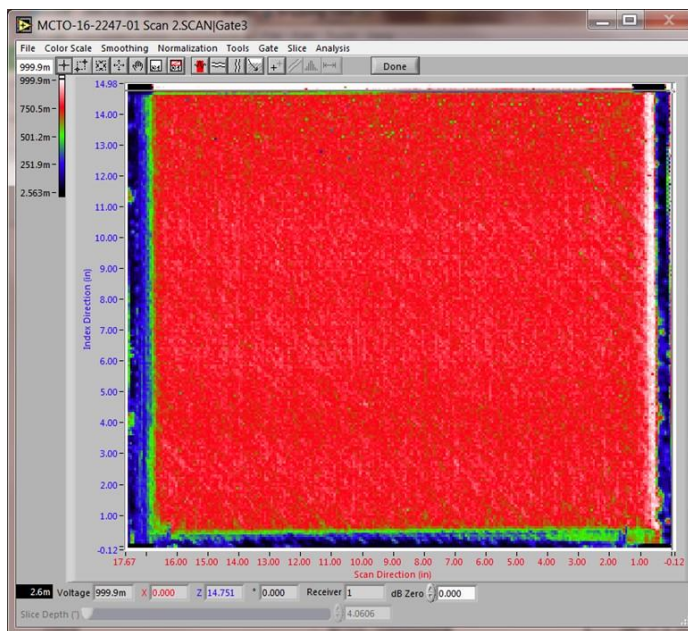


**Figure E.69-12. TTUT C-scans at 2.25 MHz.**

### E.69.3.7 References

- [1] Workman, Gary L; and Kishoni, Doron: *Nondestructive Testing Handbook*, Third. Edited by Patrick O Moore. Vol. 7. American Society for Nondestructive Testing (ANST), 2007.

## E.69.4 Method: Single-Sided Infrared Thermography (SSIR)

### E.69.4.1 Partner: NGIS

### E.69.4.2 Technique Applicability: ★☆☆

The thermal response produced by single-sided thermographic inspection has been determined to be dominated by factors other than porosity. It was found that slight variations in thickness and localized thermal property variation dominated the surface temperature compared to material's porosity. For this reason, single-sided inspection is not recommend as a technique for discriminating porosity.

### E.69.4.3 Laboratory Setup

Single-sided thermography images were acquired using a FLIR SC6000 IR camera setup. The thermal camera is mounted to the back of the flash hood and mounted in a fixed location on an optical table. The panel is held vertically within a fixture that slides across a linear track between captures in order to ensure total coverage. Paper light shields were constructed for the fixture to block flash spillover around the edges of the panel.

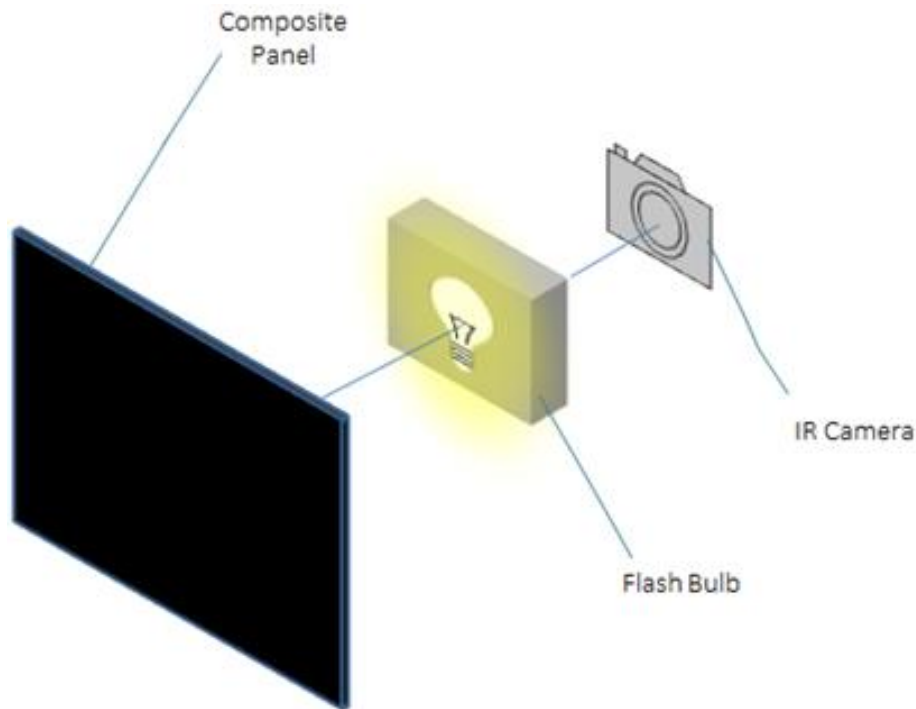


*Figure E.69-13. SSIR schematic.*



*Figure E.69-14. Photo of SSIR setup.*

**E.69.4.4 Equipment List and Specifications:**

- FLIR SC6000 IR camera, mid wavelength IR sensor (3.0- to 5.0- $\mu\text{m}$ )
- Flash power supplies, hood, and lamps
- EchoTherm® V8 Software

**E.69.4.5 Settings**

*Table E.69-6. Equipment settings for SSIR scan.*

Flash Duration (ms)	30
Capture Elapsed Time (s)	55.8
Camera Frequency (Hz)	13.28
Integration Time (s)	2



**E.69.4.6 Inspection Results**

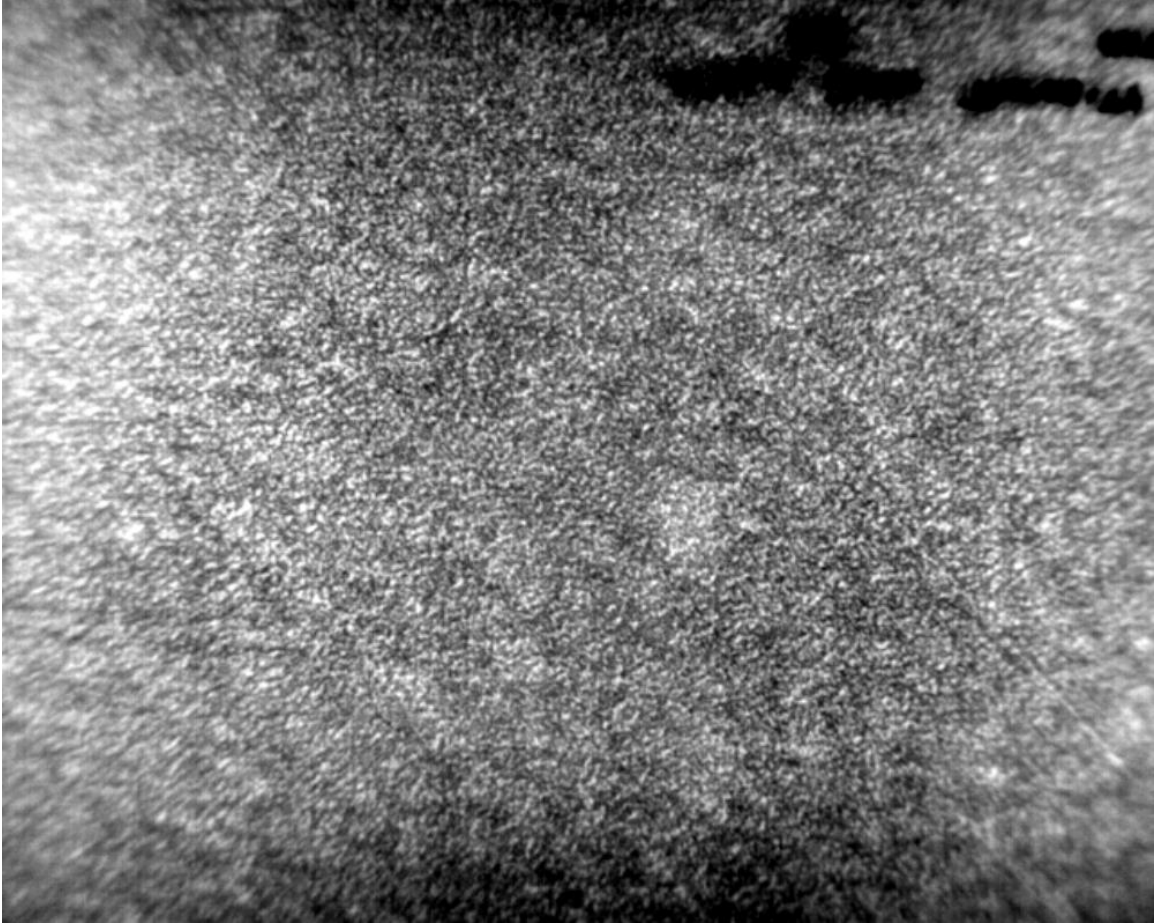


*Figure E.69-15. SSIR image of Specimen #69.*

**Porosity Panel #1**

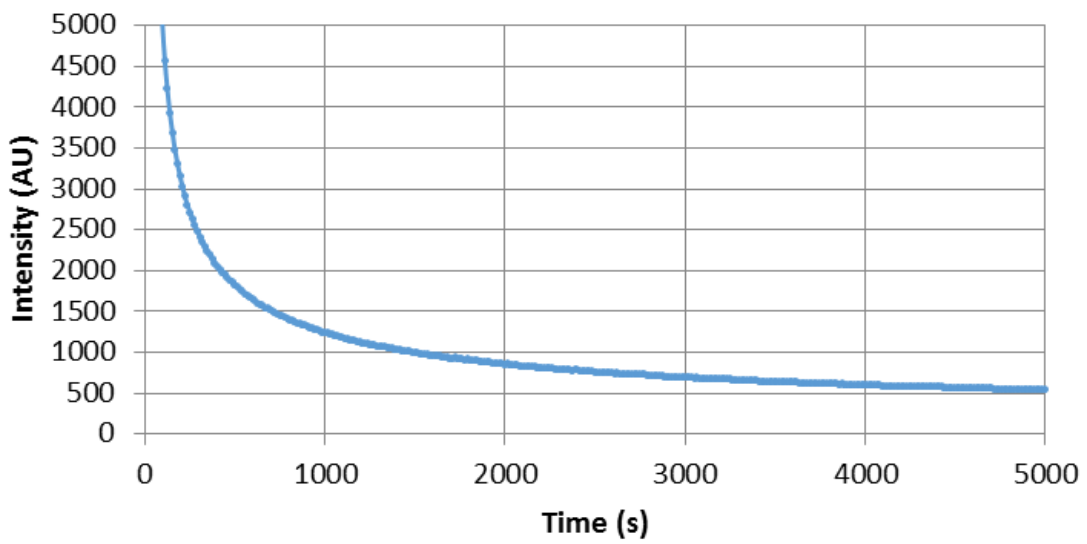


*Figure E.69-16. Intensity curve showing heat dispersion over time for Specimen #69.*

#### E.69.4.7 References

- [1] Parker, W. J.; Jenkins, R. J.; Butler, C. P.; and Abbott, G. L.: "Method of Determining Thermal Diffusivity, Heat Capacity and Thermal Conductivity," *Journal of Applied Physics*, 32 (9): 1679, Bibcode:1961JAP....32.1679P. doi:10.1063/1.1728417, 1961.

#### E.69.5 Method: Through-Transmission Infrared Thermography (TTIR)

##### E.69.5.1 Partner: NGIS

##### E.69.5.2 Technique Applicability: ★★★

TTIR Thermography is used to create thermal diffusivity maps of the material. This is similar to flash thermal diffusivity measurement (ASTM E1461-13). Thermal diffusivity is directly proportional to specific volume, which is highly effected by porosity level. Therefore, TT thermal diffusivity maps provide a method for evaluating porosity, assuming a calibration is acquired. However, care should be taken in the applicability of thermal diffusivity measurements for porosity estimation as geometric effects for complex geometries can effect results. Thermal diffusivity of samples with variable thicknesses can be difficult as the lateral conduction effects the 1D assumption used by the technique.

##### E.69.5.3 Laboratory Setup

TT thermography images were acquired using a FLIR SC6000 IR camera setup. The flash hood is mounted in a fixed location on an optical table. The thermal camera is mounted on a tripod with the panel between it and the flash hood. The panel is held vertically within a fixture that slides across a linear track between captures in order to ensure total coverage. Paper light shields were constructed for the fixture to block flash spillover around the edges of the panel.

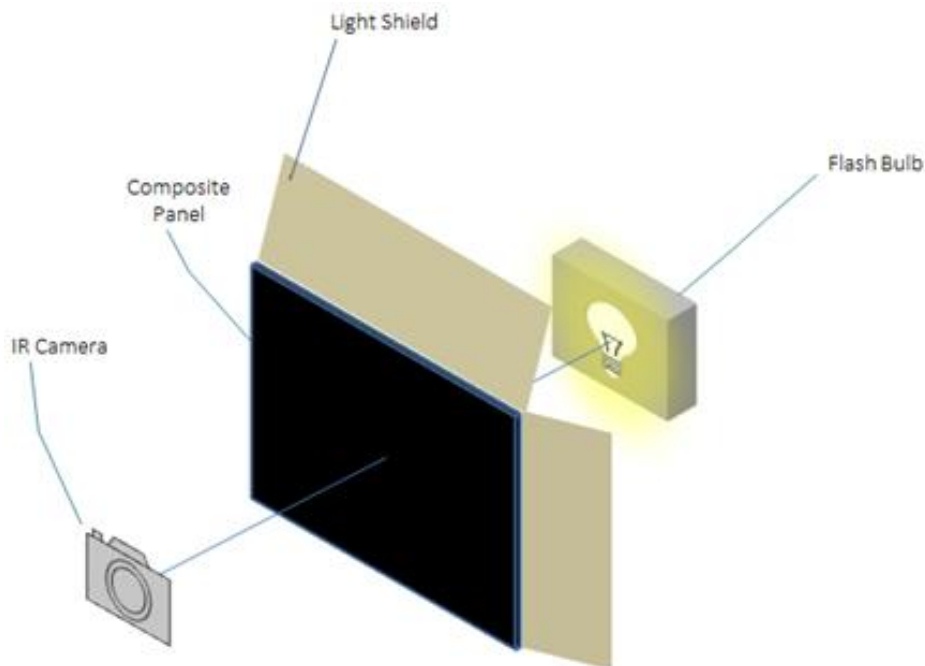


*Figure E.69-17. TTIR schematic.*





*Figure E.69-18. Photo of TTIR setup.*

**E.69.5.4 Equipment List and Specifications:**

- FLIR SC6000 IR camera, mid wavelength IR sensor (3.0- to 5.0- $\mu\text{m}$ )
- Flash power supplies, hood, and lamps
- EchoTherm® V8 Software

**E.69.5.5 Settings**

*Table E.69-7. Equipment settings for TTIR scan.*

Panel Thickness (mm)	3.63
Flash Duration (ms)	30
Capture Elapsed Time (s)	33.49
Camera Frequency (Hz)	5.51
Integration Time (s)	2

**E.69.5.6 Inspection Results**

Images were captured and the thermal diffusivity data were processed. Lower thermal diffusivity correlates to higher levels of porosity. Less variation in the histogram of thermal diffusivity shows consistent porosity across the total area.

## Specimen #69

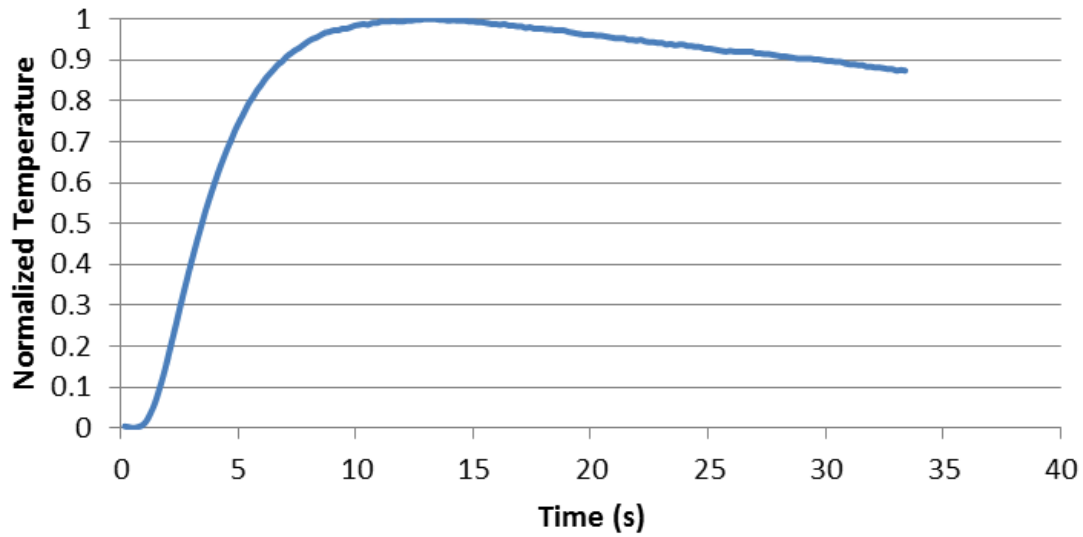


Figure E.69-19. Temperature curve showing the dispersion of heat over time during image capture.

## Specimen #69

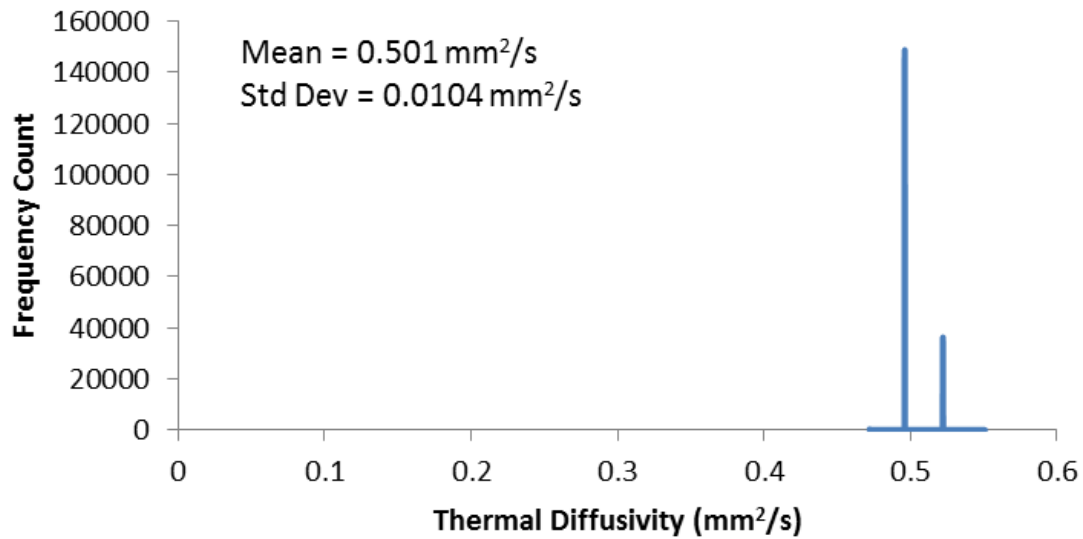


Figure E.69-20. Histogram showing frequency of thermal diffusivity values. Tighter point spread shows consistent porosity throughout panel and a low standard deviation shows low porosity levels.

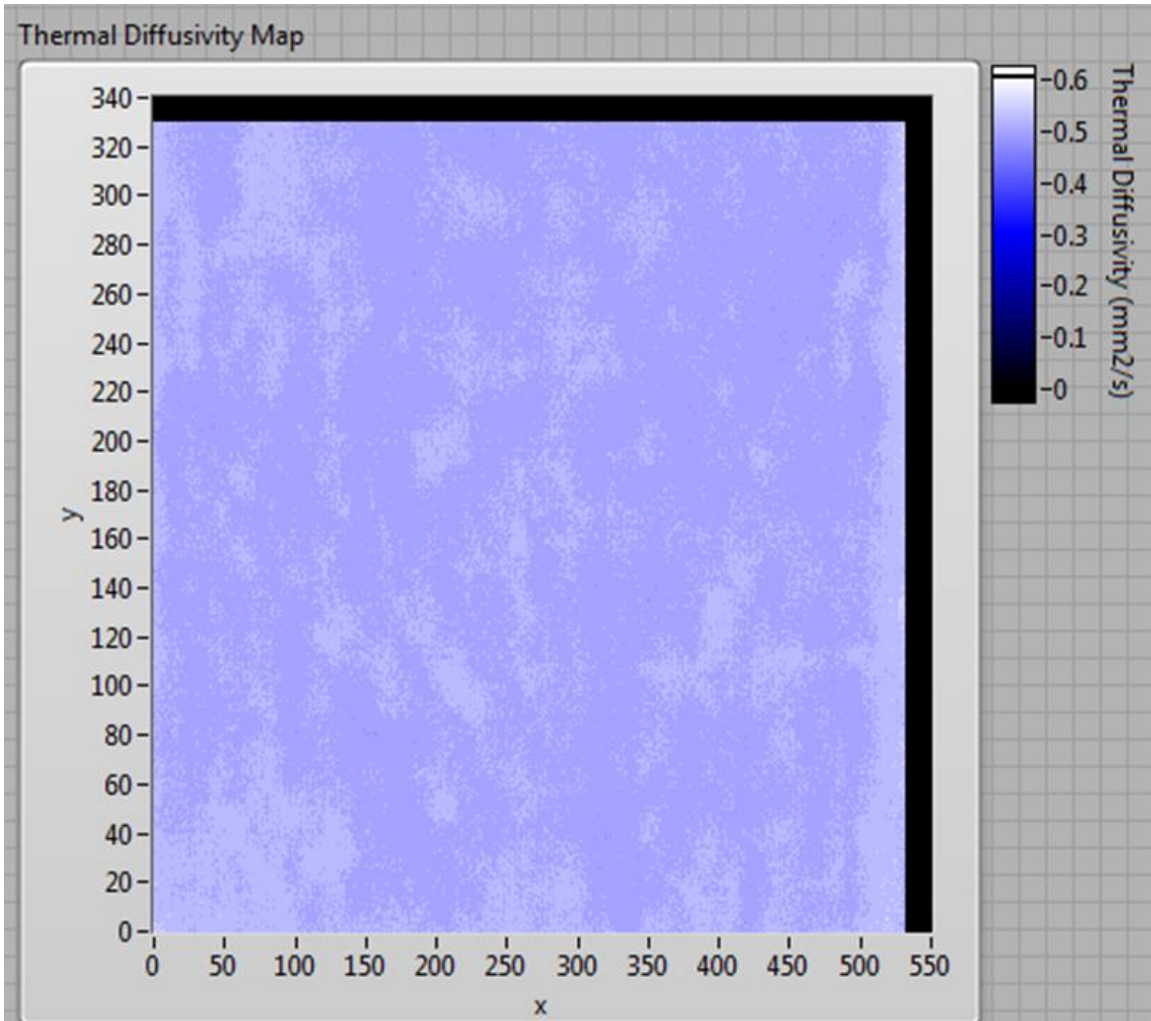


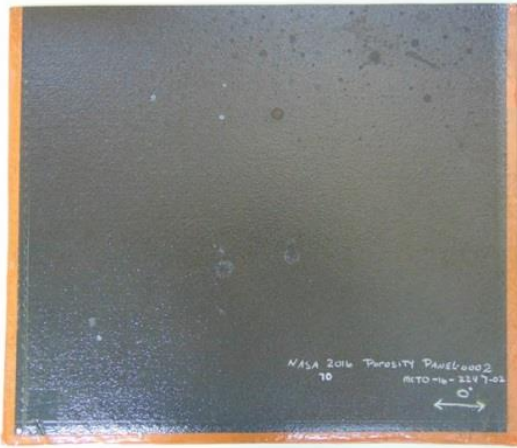
Figure E.69-21. Image of thermal diffusivity post processing.

**E.69.5.7 References**

- [2] Parker, W. J.; Jenkins, R. J.; Butler, C. P.; and Abbott, G. L.: “Method of Determining Thermal Diffusivity, Heat Capacity and Thermal Conductivity,” *Journal of Applied Physics*, 32 (9): 1679, Bibcode:1961JAP....32.1679P. doi:10.1063/1.1728417, 1961.

**E.70 Specimen #70: NASA-03-Porosity-Panel-002**

Structure	Material	Details	Dimensions (inches)	Partner Methods	
Fiber Placed Panel	IM7/8552-1 Slit Tape w/ IM7/8552 Fabric OML	Flat Panel with porosity	15 × 17.5 × 0.15	NASA	E.70.1 PEUT
				NGIS	E.70.2 PEUT E.70.3 TTUT E.70.4 SSIR E.70.5 TTIR



Bag Side View



Tool Side View

*Figure E.70-1. Photographs of Specimen #70: NASA 03 Porosity Panel 002.*

**E.70.1 Method: Pulse-Echo Ultrasound Testing (PEUT)**

**E.70.1.1 Partner: NASA**

**E.70.1.2 Technique Applicability: ★★★**

PEUT detected the porosity in this specimen.

**E.70.1.3 Laboratory Setup**

Immersion Ultrasonic Testing: NASA LaRC uses a custom-designed single-probe ultrasonic scanning system. The system has an 8-axis motion controller, a multi-axis gantry robot mounted above a medium-size water tank, a dual-channel, 16-bit, high-speed digitizer, and an off-the-shelf ultrasonic pulser receiver. The system can perform TTUT and PEUT inspections. TT inspection employs two aligned ultrasonic probes, one transmitter, and one receiver, placed on either side of a test specimen. Pulse-echo inspection is a single-sided method where a single ultrasonic probe is both transmitter and receiver. In each method, data are acquired while raster scanning the ultrasonic probe(s) in relation to a part. Figure E.70-2 shows a simplified block diagram of a scanning Pulse-echo inspection.

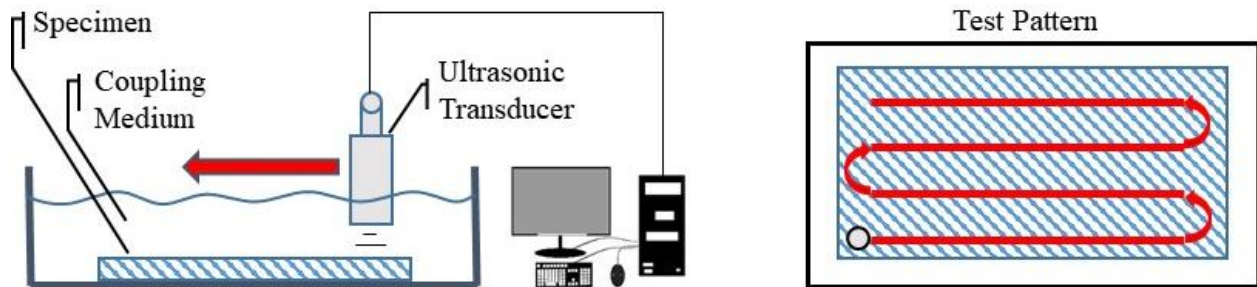


*Figure E.70-2. Ultrasonic system components.*

**E.70.1.4 Equipment List and Specifications:**

- Pulser/Receiver: Olympus 5073PR
- Digitizer: AlazarTech ATS9462, dual channel, 16 bit, 180 MS/s
- Sensor: Olympus 2-inch spherical focus immersion ultrasonic transducer

- Motion system: open looped stepper motor based X-YY-Z gantry robot
- Motion Controller: Galil DMC-4183
- Acquisition Software: FastScan, custom developed at NASA LaRC
- Signal Processing Software: DataViewer, custom developed at NASA LaRC

### E.70.1.5 Settings

*Table E.70-1. Data collection settings.*

Resolution (horizontal) [in/pixel]	0.02
Resolution (vertical) [in/pixel]	0.02
Probe frequency [MHz]	10
Focal Length [in]	2
Array Dimensions [pixels]	851 × 751

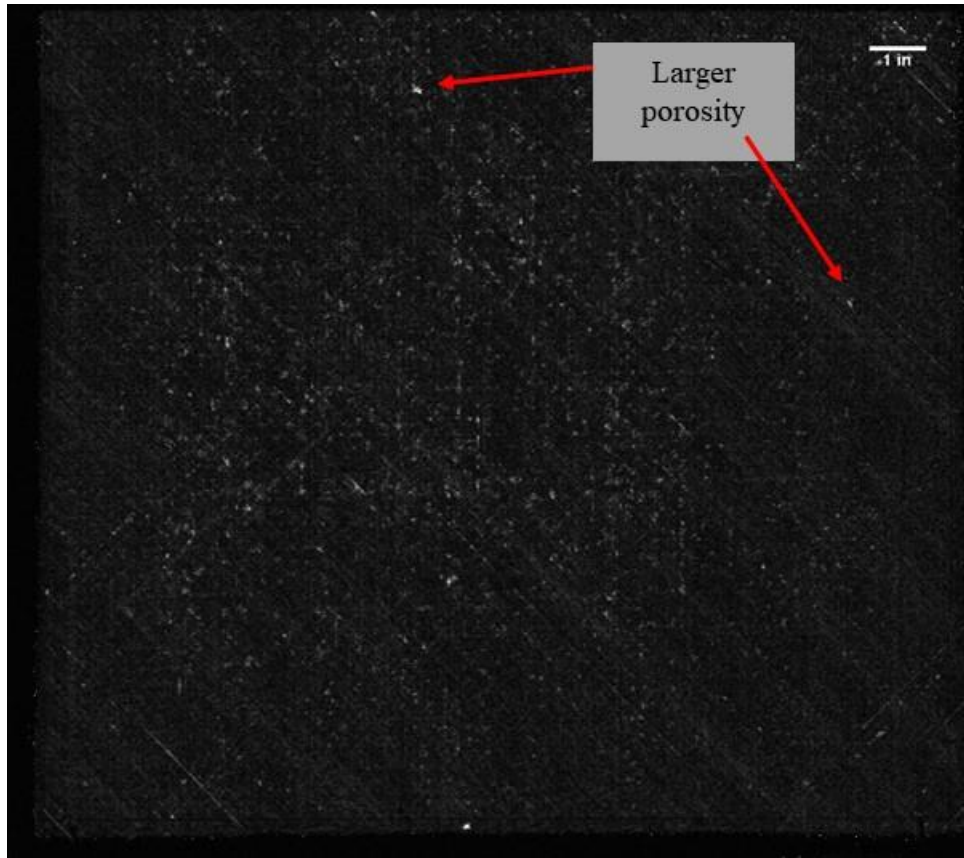
The specimen is placed flat against the zero position of the tank raised above the glass bottom by several metal washers. The test probe is computer-controlled and correlated to the position on the sample. It is also focused to a point one mm below the surface of the test material. The specimen remains in place while the transducer follows a preprogrammed test grid across the surface as indicated in Figure E.70-2. At each point, ultrasonic data are collected from individual pulses. Larger step sizes between data collection result in lower image resolution. These data points are reconstructed into a data cube displaying spatial coordinates as time progresses. 2D reconstruction of the collection of ultrasonic responses create flattened slices at varying depths within the material.

### E.70.1.6 Inspection Results

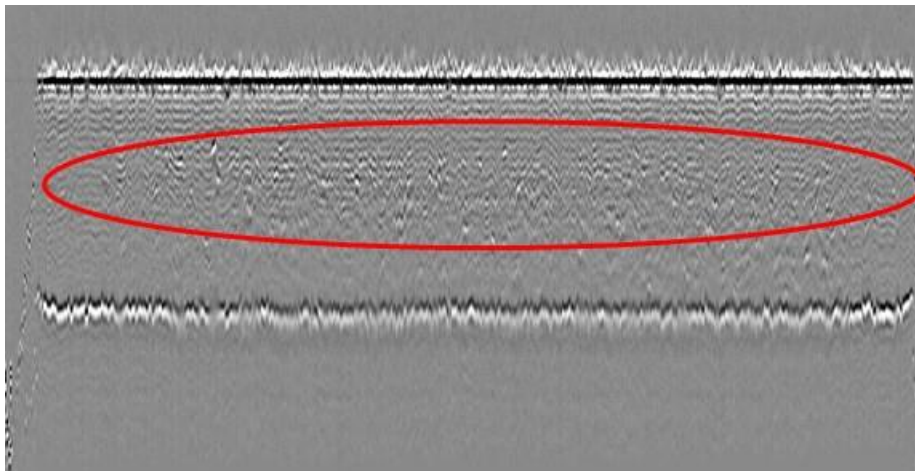
Specimen #70, is a fiber placed flat panel fabricated from IM7/8552-1 Slit Tape with the objective of achieving porosity throughout the sample. PEUT was performed on this specimen in NASA’s immersion tank specified above.

Figure E.70-3 is at a depth of 0.045 inch and shows a multiple instances of porosity as indicated. The larger porosity appears white initially as the air pocket reflects acoustic waves creating a strong early response. Visually this is demonstrated by the nebulous dark regions in Figure E.70-5. The striations seen in Figures E.70-3 and E.70-5 are the fiber directions of the individual plies. The B-scan is a crosssection of the material, all of the variations in the horizontal represent defects within the specimen. The majority of the porosity is located at throughout the middle of the sample.





*Figure E.70-3. UT image of porosity within the sample.*



*Figure E.70-4. B-scan of specimen showing location and prevalence of defects.*



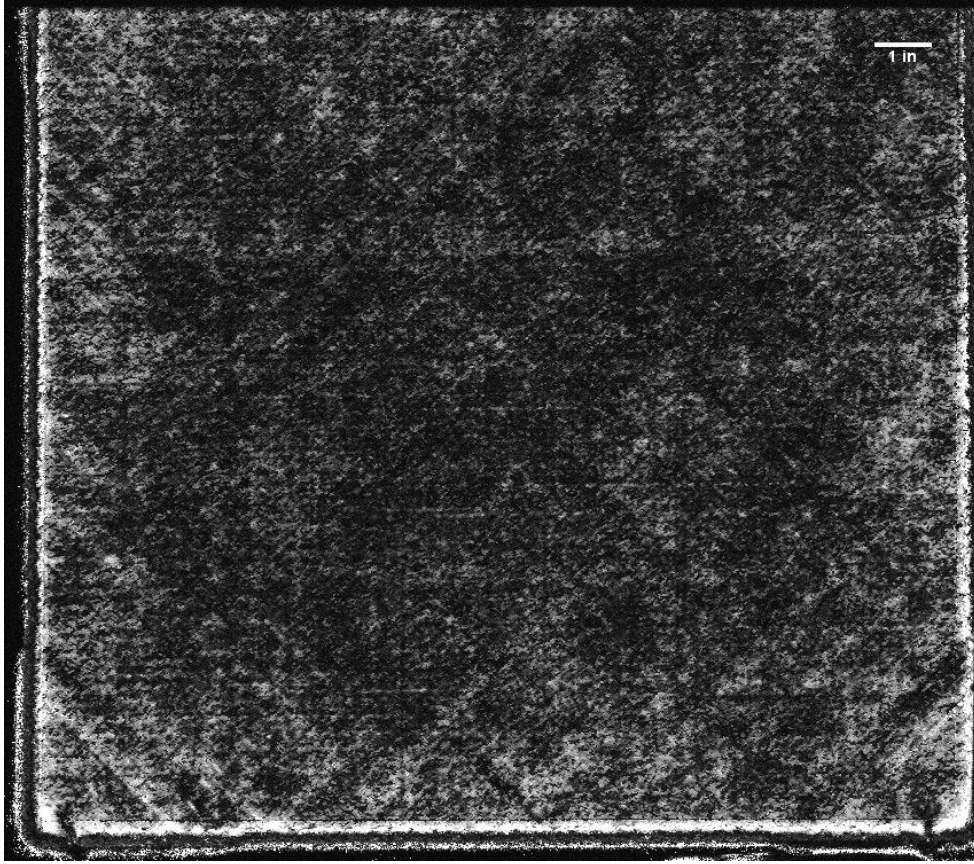


*Figure E.70-5. UT image of porosity within the sample.*

**E.70.2 Method: Pulse-Echo Ultrasound Testing (PEUT)**

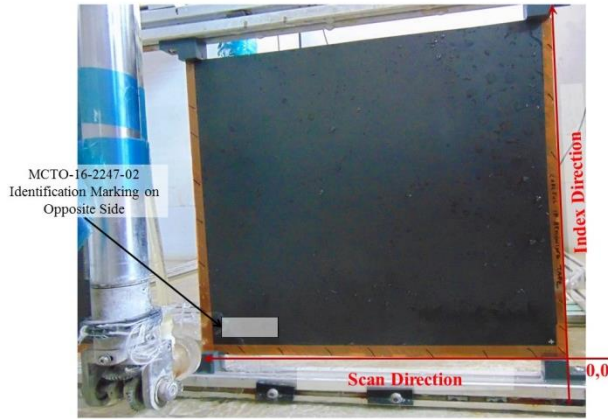
**E.70.2.1 Partner: NGIS**

**E.70.2.2 Technique Applicability: ★★★**

PEUT scans were performed on the flat tool side of the panel in order to detect defects.

**E.70.2.3 Laboratory Setup**

PEUT scans performed in the Test-Tech 3-axis scanning tank used the water-squirter method. For each panel, use of optimum water nozzle and column diameter achieved optimal SNR and defect detection (if defects existed).



Scanned from tool side surface

**Figure E.70-6. PEUT setup in Test-Tech scanning tank.**

#### E.70.2.4 Equipment List and Specifications:

- Test-Tech 3-axis scanning tank
- Olympus 5077PR Square Wave Pulsar/Receiver
- Transducers (2.25, 5.0 MHz)

#### E.70.2.5 Settings

**Table E.70-2. Equipment settings for 2.25 MHz scan.**

Transducer	Brand	Model	Freq. (MHz)	Element Dia. (in.)	Water Column Dia. (in.)			Outer Dia. (in)		
Transmitter	KB-Aerotech	Alpha	2.25	0.25	0.25			0.5		
Pulsar/Receiver	PRF	Voltage	Freq. (MHz)		HPF (MHz)	LPF (MHz)	Rtune	Ttune	Attn	Range
Olympus	Ext	100	2-2.25		Out	Full BW	N/A	N/A	N/A	N/A
	Gain (dB)	14								

**Table E.70-3. Equipment settings for 5.0 MHz scan.**

Transducer	Brand	Model	Freq. (MHz)	Element Dia. (in.)	Water Column Dia. (in.)			Outer Dia. (in)		
Transmitter	Krautkramer	Benchmark	5	0.25	0.25			0.5		
Pulsar/Receiver	PRF	Voltage	Freq. (MHz)		HPF	LPF (MHz)	Rtune	Ttune	Attn	Range
Olympus	Ext	100	5-6		Out	Full BW	N/A	N/A	N/A	N/A
	Gain (dB)	-3								

#### E.70.2.6 Inspection Results

Scans were performed and data quality was verified by producing C-scans for the different panels. Front wall and BW reflections were resolved at both 2.25 MHz and 5 MHz.

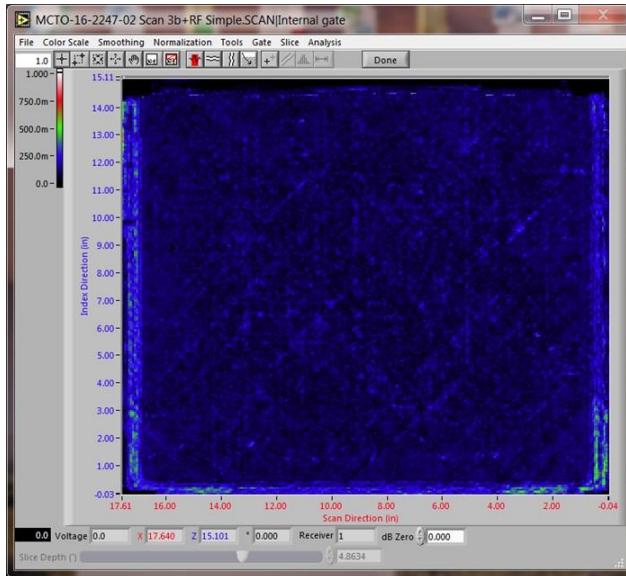
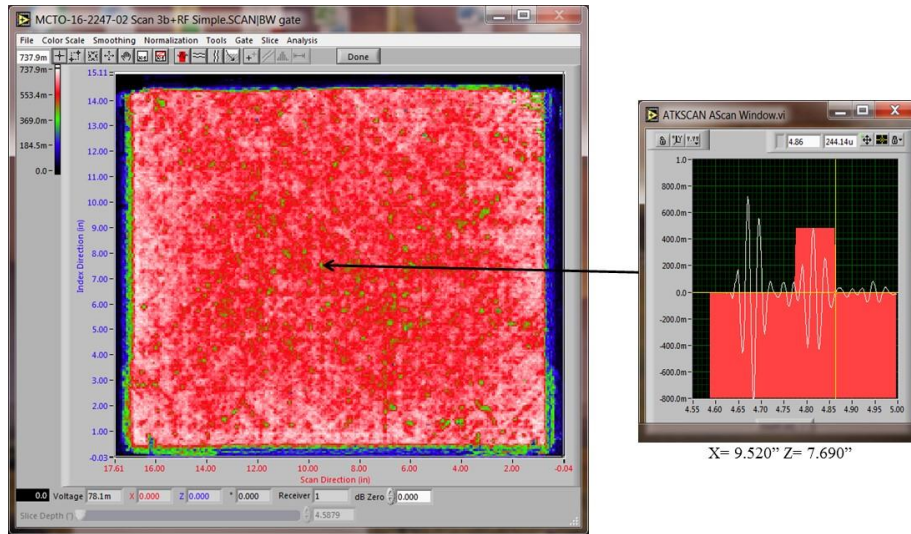


**Figure E.70-7. PEUT C-scans at 2.25 MHz (Internal Gate).**



MCTO-16-2247-02 Scan 3b Backwall Gate

**Figure E.70-8. PEUT C-scans at 2.25 MHz (BW Gate).**

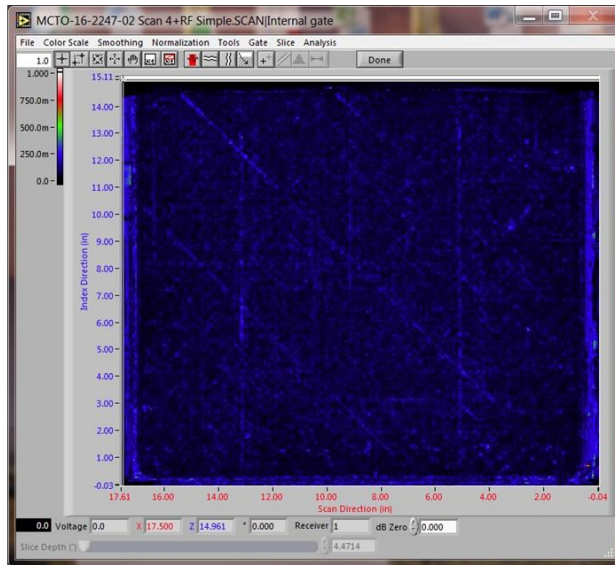
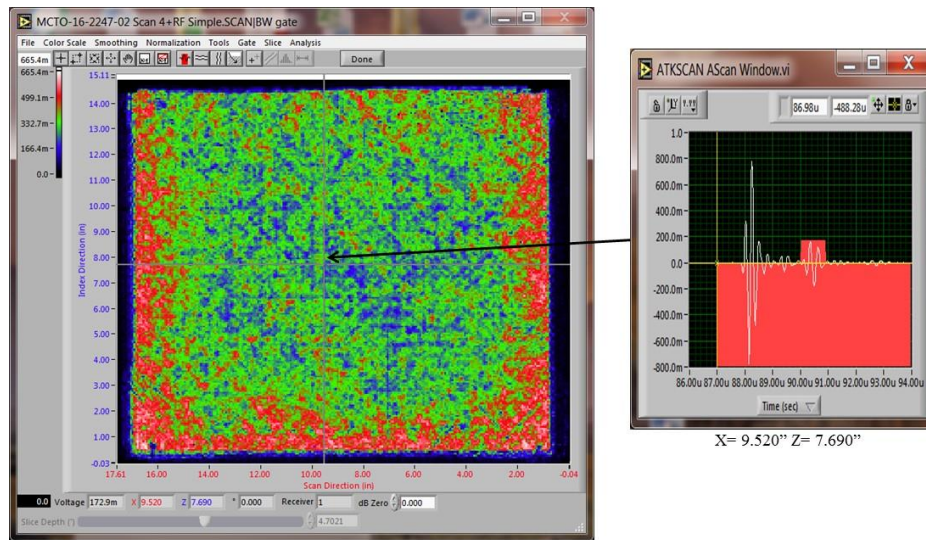


Figure E.70-9. PEUT C-scans at 5.0 MHz (Internal Gate).



MCTO-16-2247-02 Scan 4 Backwall Gate

Figure E.70-10. PEUT C-scans at 5.0 MHz (BW Gate).

### E.70.2.7 References

- [1] Workman, Gary L; and Kishoni, Doron: *Nondestructive Testing Handbook*, Third. Edited by Patrick O Moore. Vol. 7. American Society for Nondestructive Testing (ANST), 2007.

### E.70.3 Method: Through-Transmission Ultrasound Testing (TTUT)

#### E.70.3.1 Partner: NGIS

#### E.70.3.2 Technique Applicability: ★★★

TTUT scans were performed on the stepped panel in order to detect defects. Depth of defect cannot be determined with this method.



### E.70.3.3 Laboratory Setup

TTUT scans were performed in the Test-Tech 3-axis scanning tank using a water-squirter method. Transmission was performed on the flat tool side of the panel and received from the bagged stepped side of the panel. For each panel, water nozzle and column diameter was optimized to achieve optimal SNR and defect detection (if defects existed).

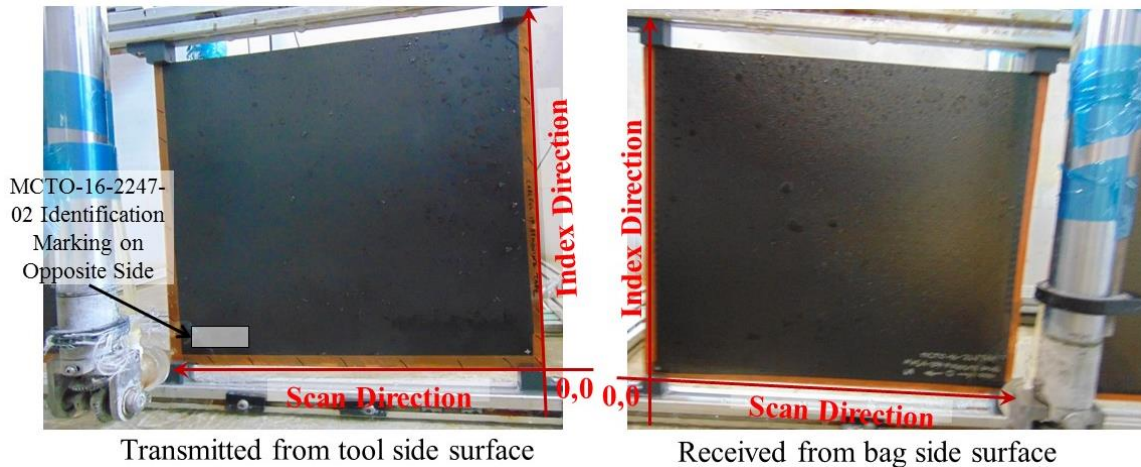


Figure E.70-11. TTUT setup in Test-Tech scanning tank.

### E.70.3.4 Equipment List and Specifications:

- Test-Tech 3-axis scanning tank
- Olympus 5077PR Square Wave Pulsar/Receiver
- Transducer Pairs (1.0, 2.25 MHz)

### E.70.3.5 Settings

Table E.70-4. Equipment settings for 1.0 MHz scan.

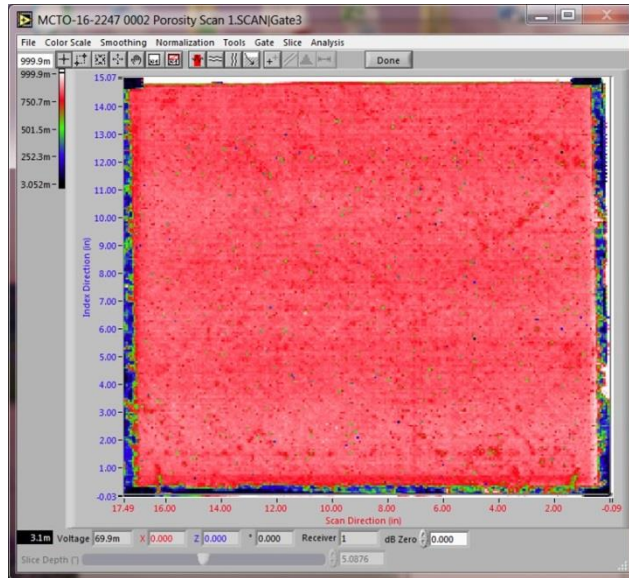
Transducer	Brand	Model	Freq. (MHz)	Element Dia. (in.)	Water Column Dia (in.)			Outer Dia. (in)		
Transmitter	Sonic	IBK I-2	1	0.5	0.25			0.5		
Receiver	Sonic	IBK I-2	1	0.5	0.25			0.5		
Pulsar/Receiver	PRF	Voltage	Freq. (MHz)		HPF	LPF (MHz)	Rtune	Ttune	Attn	Range
Olympus	Ext	100	1.0		Out	10	N/A	N/A	N/A	N/A
	Gain (dB)	28								

Table E.70-5. Equipment settings for 2.25 MHz scan.

Transducer	Brand	Model	Freq. (MHz)	Element Dia. (in.)	Water Column Dia (in.)			Outer Dia. (in)		
Transmitter	KB-Aerotech	Alpha	2.25	0.25	0.25			0.5		
Receiver	KB-Aerotech	Alpha	2.25	0.25	0.25			0.5		
Pulsar/Receiver	PRF	Voltage	Freq. (MHz)		HPF (MHz)	LPF (MHz)	Rtune	Ttune	Attn	Range
Olympus	Ext	100	2-2.25		Out	Full BW	N/A	N/A	N/A	N/A
	Gain (dB)	13								

### E.70.3.6 Inspection Results

TTUT C-scans and signals exhibited moderate attenuation at both 1 MHz and 2.25 MHz.



**Figure E.70-12. TTUT C-scans at 1 MHz.**

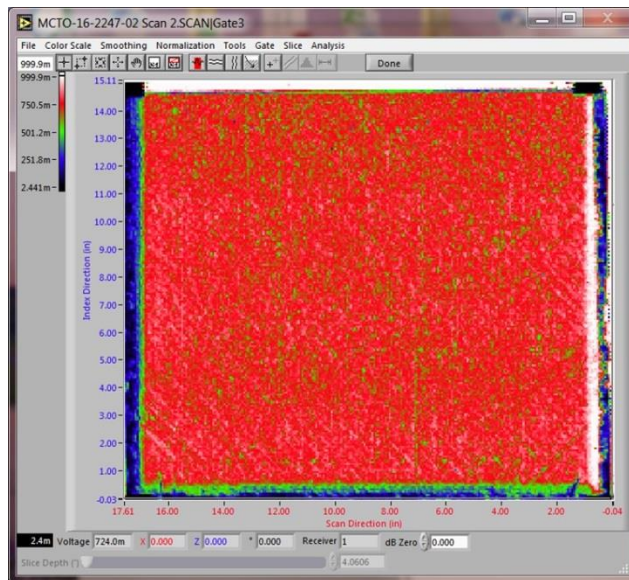


**Figure E.70-13. TTUT C-scans at 2.25 MHz.**

### **E.70.3.7 References**

- [1] Workman, Gary L; and Kishoni, Doron: *Nondestructive Testing Handbook*, Third. Edited by Patrick O Moore. Vol. 7. American Society for Nondestructive Testing (ANST), 2007.

### **E.70.4 Method: Single-Sided Infrared Thermography (SSIR)**

#### **E.70.4.1 Partner: NGIS**

#### **E.70.4.2 Technique Applicability: ★☆☆**

The thermal response produced by single-sided thermographic inspection has been determined to be dominated by factors other than porosity. It was found that slight variations in thickness and localized thermal property variation dominated the surface temperature compared to material's



porosity. For this reason, single-sided inspection is not recommend as a technique for discriminating porosity.

### E.70.4.3 Laboratory Setup

Single-sided thermography images were acquired using a FLIR SC6000 IR camera setup. The thermal camera is mounted to the back of the flash hood and mounted in a fixed location on an optical table. The panel is held vertically within a fixture that slides across a linear track between captures in order to ensure total coverage. Paper light shields were constructed for the fixture to block flash spillover around the edges of the panel.

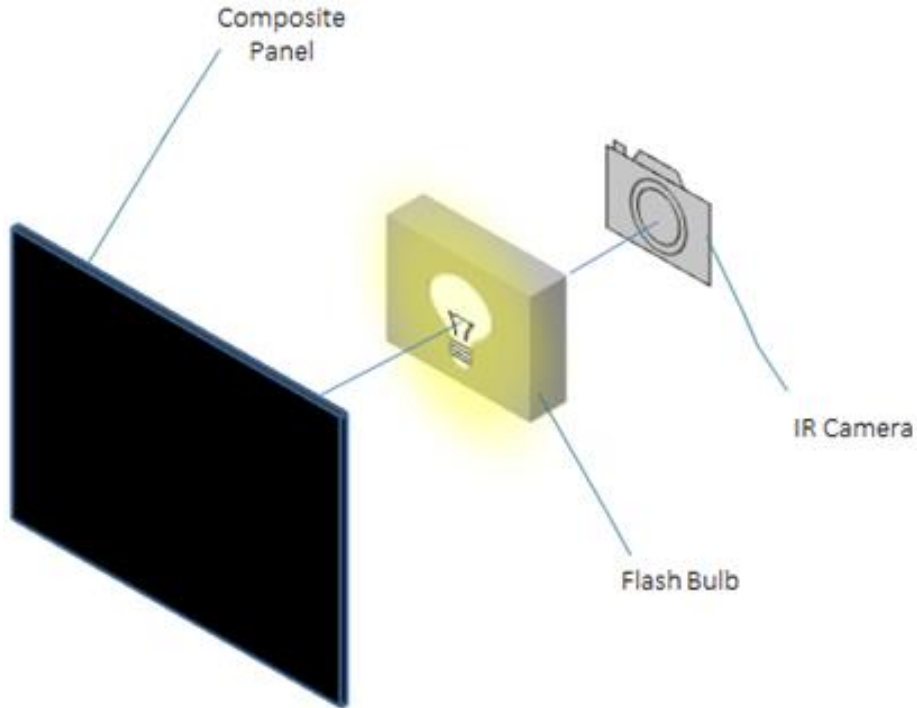


*Figure E.70-14. SSIR schematic.*



*Figure E.70-15. Photo of SSIR setup.*

**E.70.4.4 Equipment List and Specifications:**

- FLIR SC6000 IR camera, mid wavelength IR sensor (3.0- to 5.0- $\mu\text{m}$ )
- Flash power supplies, hood, and lamps
- EchoTherm® V8 Software

**E.70.4.5 Settings**

*Table E.70-6. Equipment settings for SSIR scan.*

Flash Duration (ms)	30
Capture Elapsed Time (s)	60.1
Camera Frequency (Hz)	12.33
Integration Time (s)	1

**E.70.4.6 Inspection Results**

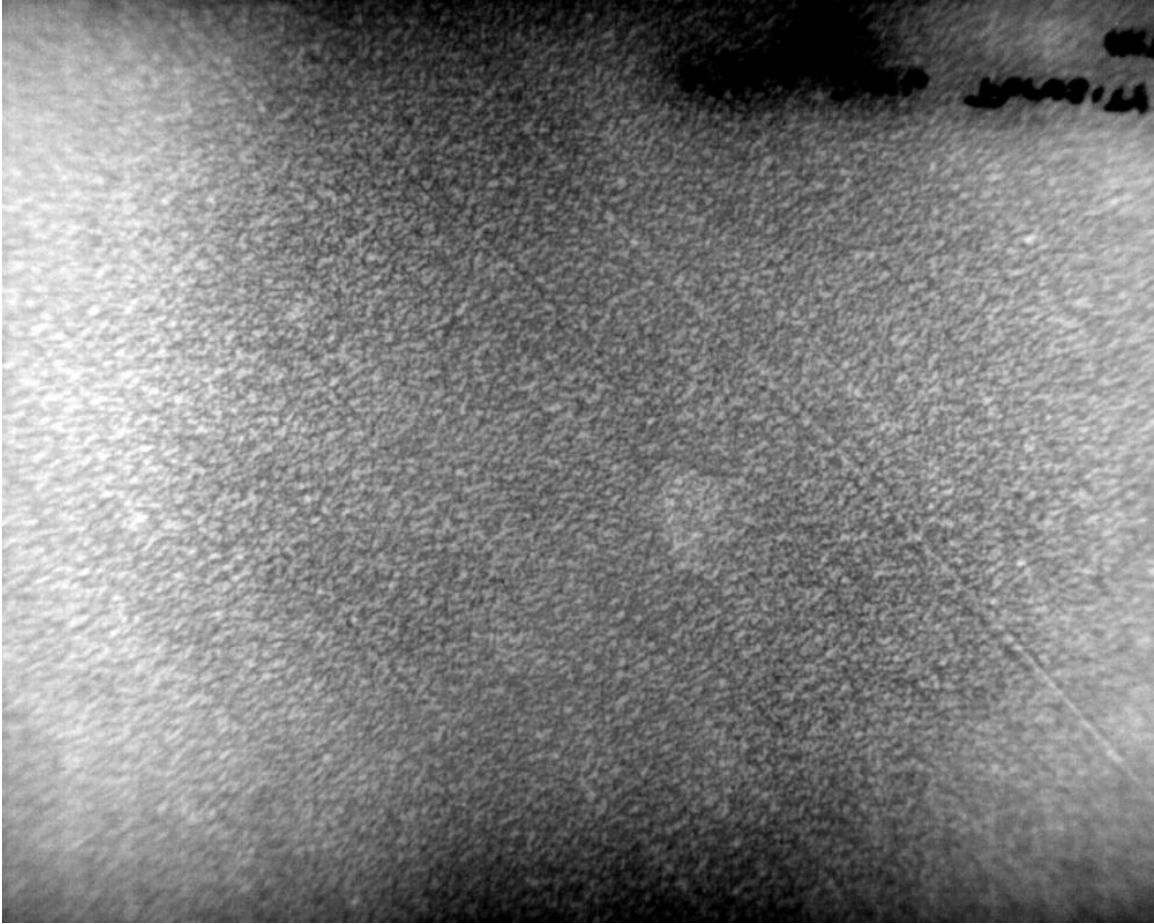


*Figure E.70-16. SSIR image of Specimen #70.*

**Porosity Panel #2**

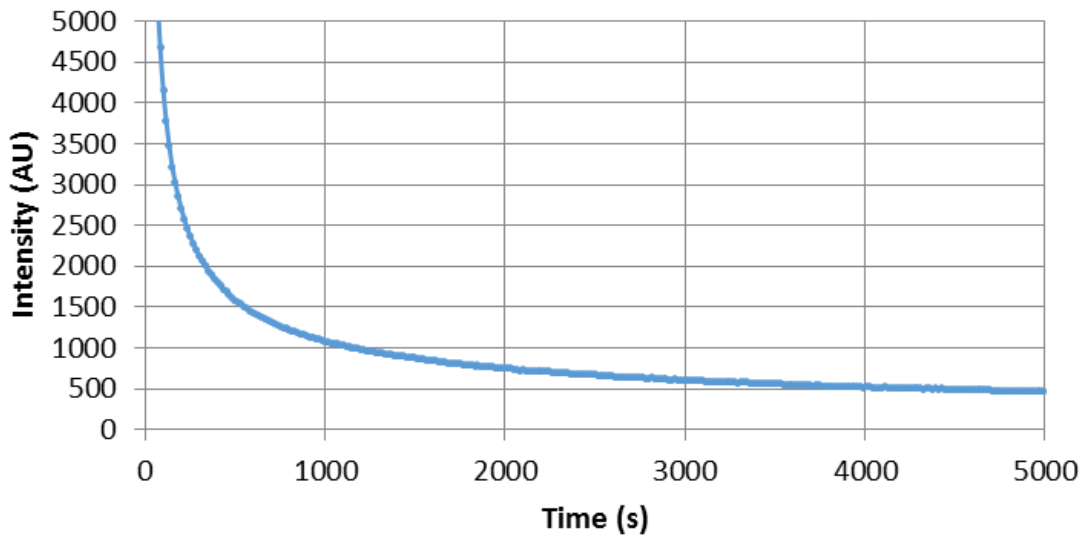


*Figure E.70-17. Intensity curve showing heat dispersion over time for Specimen #70.*

#### E.70.4.7 References

- [1] Parker, W. J.; Jenkins, R. J.; Butler, C. P.; and Abbott, G. L.: "Method of Determining Thermal Diffusivity, Heat Capacity and Thermal Conductivity," *Journal of Applied Physics*, 32 (9): 1679, Bibcode:1961JAP....32.1679P. doi:10.1063/1.1728417, 1961.

#### E.70.5 Method: Through-Transmission Infrared Thermography (TTIR)

##### E.70.5.1 Partner: NGIS

##### E.70.5.2 Technique Applicability: ★★★

##### E.70.5.3 Laboratory Setup

TT thermography images were acquired using a FLIR SC6000 IR camera setup. The flash hood is mounted in a fixed location on an optical table. The thermal camera is mounted on a tripod with the panel between it and the flash hood. The panel is held vertically within a fixture that slides across a linear track between captures in order to ensure total coverage. Paper light shields were constructed for the fixture to block flash spillover around the edges of the panel.

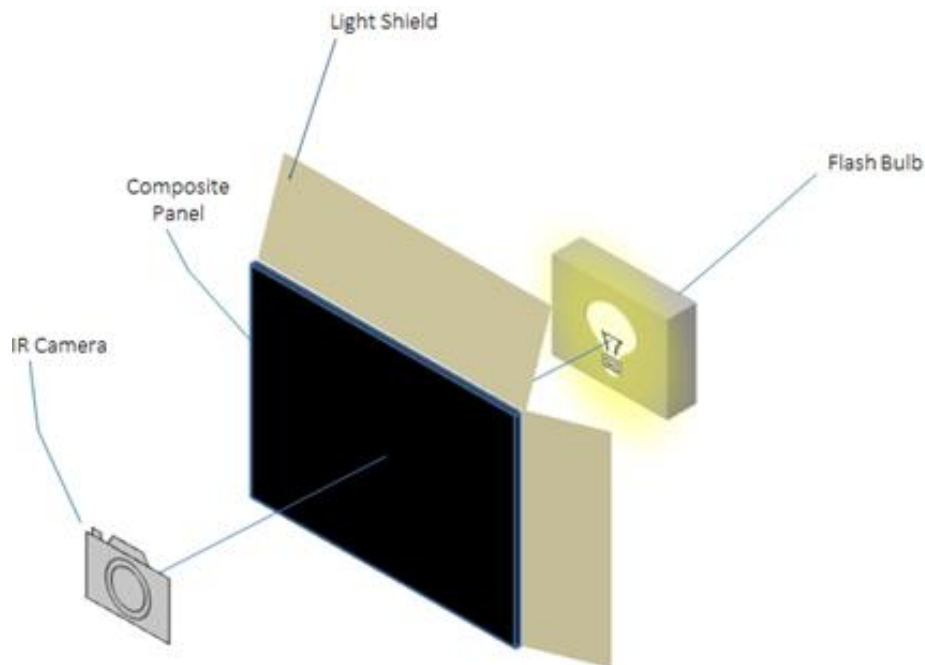


*Figure E.70-18. TTIR schematic.*



*Figure E.70-19. Photo of TTIR setup.*

**E.70.5.4 Equipment List and Specifications:**

- FLIR SC6000 IR camera, mid wavelength IR sensor (3.0- to 5.0- $\mu\text{m}$ )
- Flash power supplies, hood, and lamps
- EchoTherm® V8 Software

**E.70.5.5 Settings**

*Table E.70-7. Equipment settings for TTIR scan.*

Panel Thickness (mm)	3.63
Flash Duration (ms)	30
Capture Elapsed Time (s)	33.49
Camera Frequency (Hz)	5.51
Integration Time (s)	2

**E.70.5.6 Inspection Results**

Images were captured and the thermal diffusivity data were processed. Lower thermal diffusivity correlates to higher levels of porosity. Less variation in the histogram of thermal diffusivity shows consistent porosity across the total area.

## Specimen #70

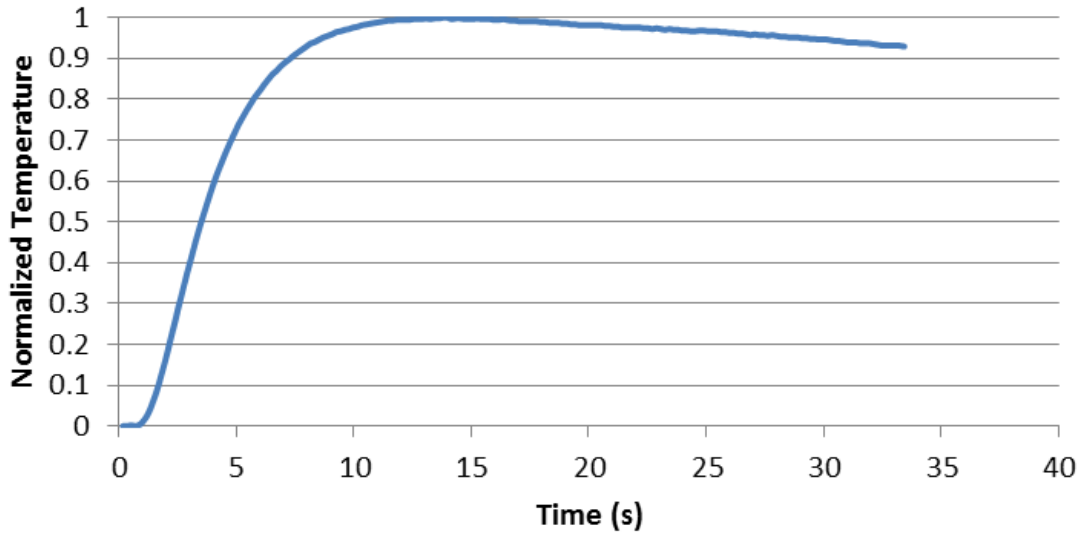


Figure E.70-20. Temperature curve showing the dispersion of heat over time during image capture.

## Specimen #70

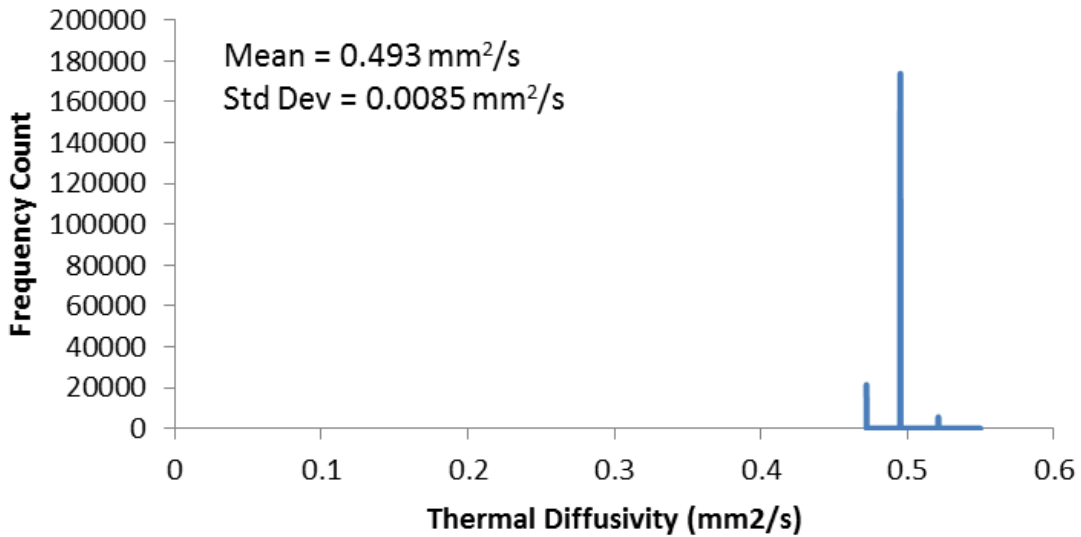


Figure E.70-21. Histogram showing frequency of thermal diffusivity values. Tighter point spread shows consistent porosity throughout panel and a low standard deviation shows low porosity levels.



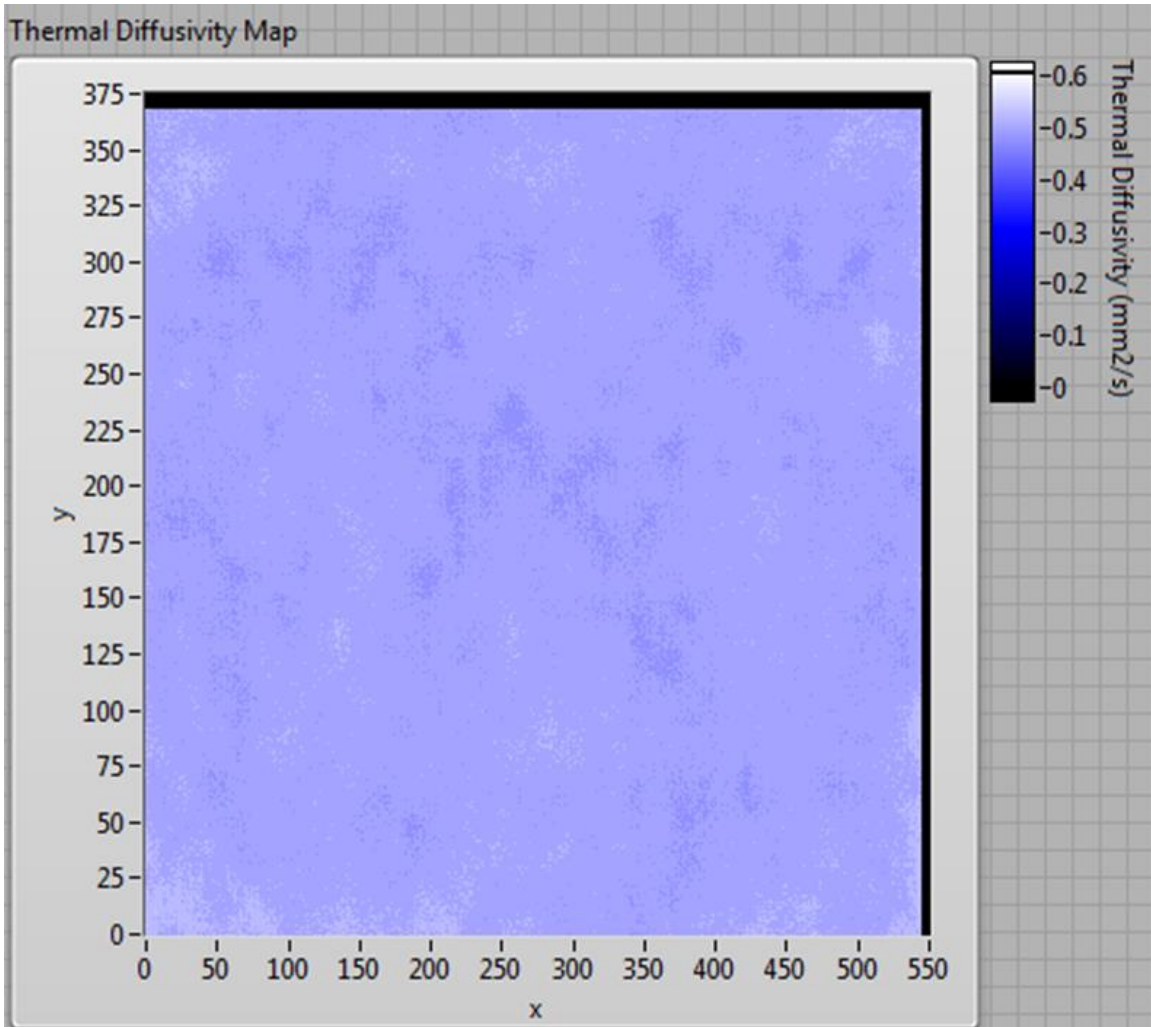


Figure E.70-22. Image of thermal diffusivity post processing.

**E.70.5.7 References**

- [1] Parker, W. J.; Jenkins, R. J.; Butler, C. P.; and Abbott, G. L.: “Method of Determining Thermal Diffusivity, Heat Capacity and Thermal Conductivity,” *Journal of Applied Physics*, 32 (9): 1679, Bibcode:1961JAP....32.1679P. doi:10.1063/1.1728417, 1961.

**E.71 Specimen #71A&B: NASA-03-Porosity-Panel-003**

Structure	Material	Details	Dimensions (inches)	Partner Methods	
Fiber Placed Panel	M7/8552-1 Slit Tape w/ IM7/8552 Fabric OML	Flat Panel with high porosity	14 × 16 × 0.15	NASA	E.71.1 PEUT E.71.2 XCT
				NGIS	E.71.3 PEUT E.71.4 TTUT E.71.5 SSIR E.71.6 TTIR

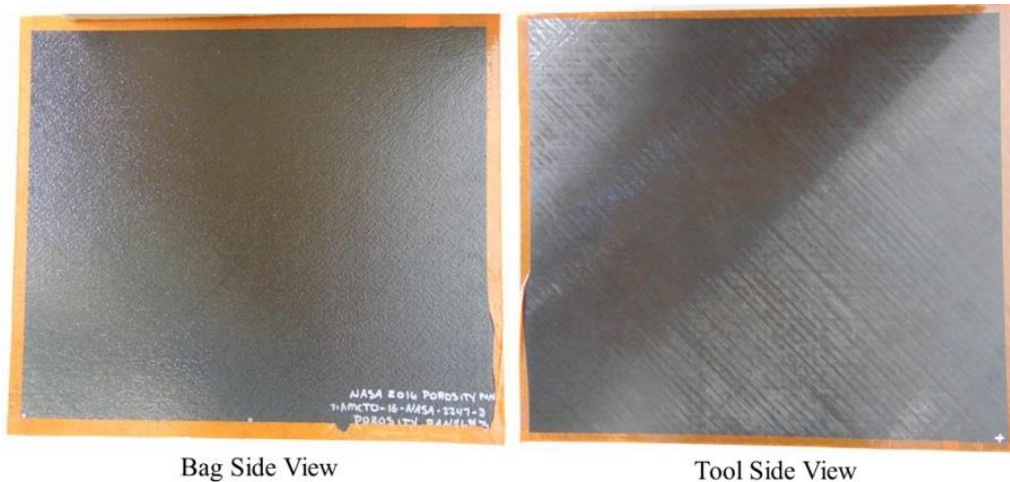


*Figure E.71-1. Photographs of Specimen #71: NASA-03-Porosity-Panel-003.*

**E.71.1 Method: Pulse-Echo Ultrasound Testing (PEUT)**

**E.71.1.1 Partner: NASA**

**E.71.1.2 Technique Applicability: ★★★**

PEUT detected the porosity in this specimen.

**E.71.1.3 Laboratory Setup**

Immersion Ultrasonic Testing: NASA LaRC uses a custom-designed single-probe ultrasonic scanning system. The system has an 8-axis motion controller, a multi-axis gantry robot mounted above a medium-size water tank, a dual-channel, 16-bit, high-speed digitizer, and an off-the-shelf ultrasonic pulser receiver. The system can perform TTUT and PEUT inspections. TT inspection employs two aligned ultrasonic probes, one transmitter, and one receiver, placed on either side of a test specimen. Pulse-echo inspection is a single-sided method where a single ultrasonic probe is both transmitter and receiver. In each method, data are acquired while raster scanning the ultrasonic probe(s) in relation to a part. Figure E.71-2 shows a simplified block diagram of a scanning Pulse-echo inspection

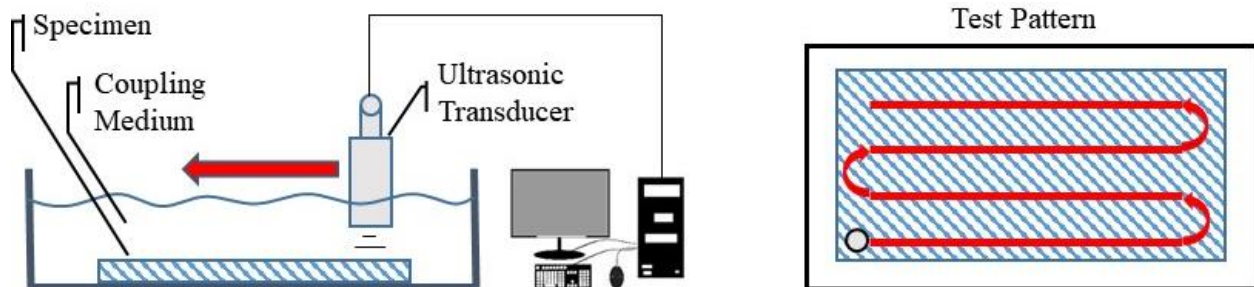


*Figure E.71-2. Ultrasonic system components.*

**E.71.1.4 Equipment List and Specifications:**

- Pulser/Receiver: Olympus 5073PR
- Digitizer: AlazarTech ATS9462, dual channel, 16 bit, 180 MS/s
- Sensor: Olympus 2-inch spherical focus immersion ultrasonic transducer
- Motion system: open looped stepper motor based X-YY-Z gantry robot

- Motion Controller: Galil DMC-4183
- Acquisition Software: FastScan, custom developed at NASA LaRC
- Signal Processing Software: DataViewer, custom developed at NASA LaRC

#### E.71.1.5 Settings

*Table E.71-1. Data collection settings.*

Resolution (horizontal) [in/pixel]	0.01
Resolution (vertical) [in/pixel]	0.01
Probe frequency [MHz]	10
Focal Length [in]	2
Array Dimensions [pixels]	676 × 581

The specimen is placed flat against the zero position of the tank raised above the glass bottom by several metal washers. The test probe is computer-controlled and correlated to the position on the sample. It is also focused to a point 1 mm below the surface of the test material. The specimen remains in place while the transducer follows a preprogrammed test grid across the surface as indicated in Figure E.71-2. At each point, ultrasonic data are collected from individual pulses. Larger step sizes between data collection result in lower image resolution. These data points are reconstructed into a data cube displaying spatial coordinates as time progresses. 2D reconstruction of the collection of ultrasonic responses create flattened slices at varying depths within the material.

#### E.71.1.6 Inspection Results

Specimen #71, is a fiber placed flat panel fabricated from IM7/8552-1 Slit Tape with the objective of achieving porosity throughout the sample. PEUT was performed on this specimen in NASA’s immersion tank specified above.

Figure E.71-3 is at a depth of 0.038 inch and shows multiple instances of porosity as indicated. The larger porosity appears white initially as the air pocket reflects acoustic waves creating a strong early response. Visually this is demonstrated by the nebulous dark regions in Figure E.71-4. The striations seen in Figures E.71-3 and E.71-4 are the fiber directions of the individual plies.

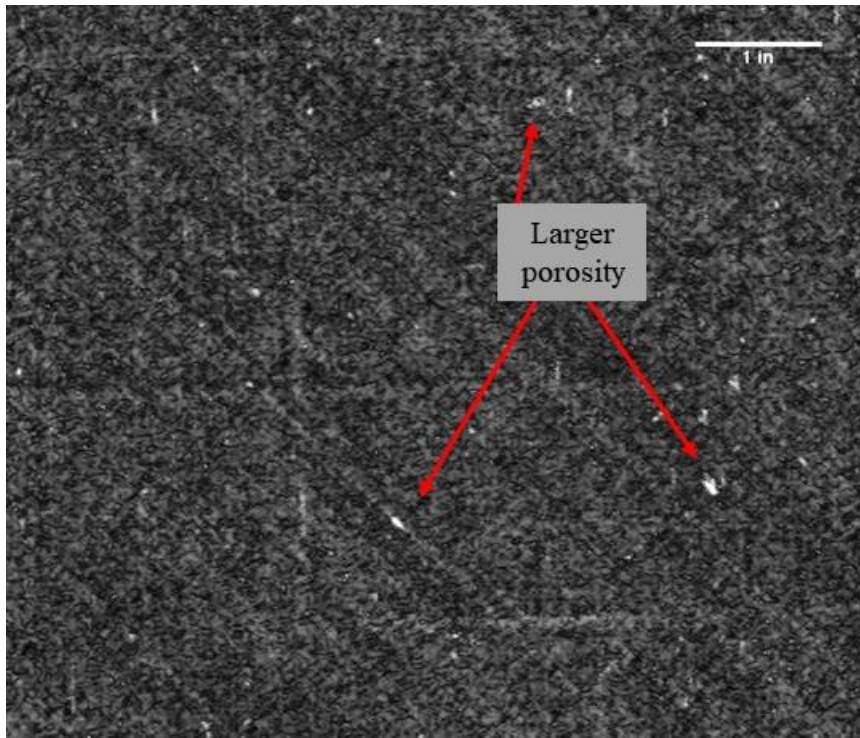


*Figure E.71-3. UT image of porosity within the sample.*

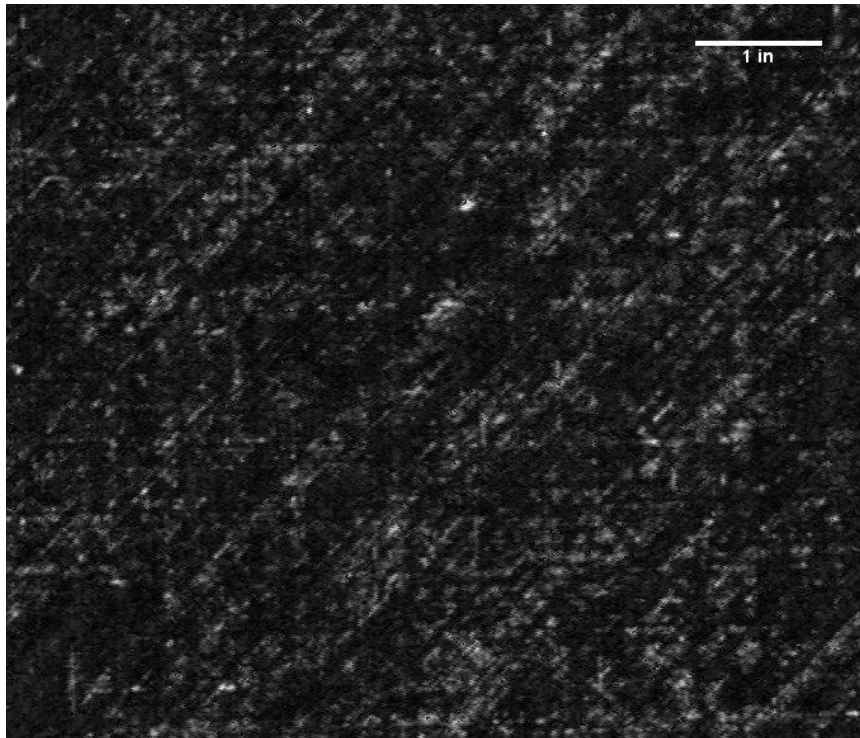


*Figure E.71-4. UT image of porosity within the sample.*

## E.71.2 Method: X-ray Computed Tomography (XCT)

### E.71.2.1 Partner: NASA

### E.71.2.2 Technique Applicability: ★★★

X-ray CT (XCT) is capable of imaging the high porosity in this specimen.

### E.71.2.3 Laboratory Setup

The microfocus XCT system at NASA LaRC is a commercially available Avonix (Nikon C2) Metrology System designed for high-resolution NDE inspections. The system is an advanced microfocus X-ray system, capable of resolving details down to 5  $\mu\text{m}$ , and with magnifications up to 60X. Supplied as complete, the system is a large-dimension radiation enclosure with X-ray source, specimen manipulator, and an amorphous silica detector, as shown in Figure E.71-5. The imaging controls are housed in a separate control console. The detector is a Perkin-Elmer, 16-bit, amorphous-silicon digital detector with a  $2000 \times 2000$ -pixel array.

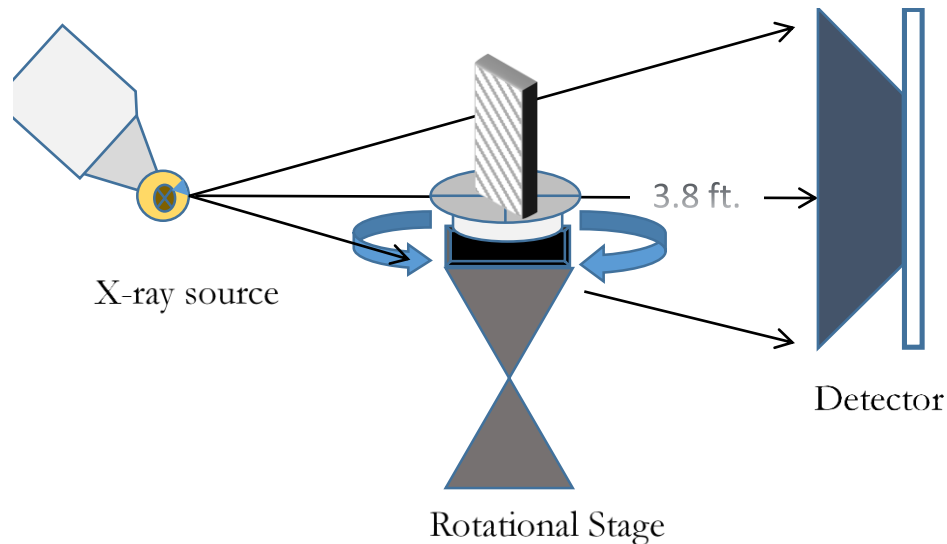


*Figure E.71-51. XCT system components.*

A consistent Cartesian coordinate system is used to define slice direction as illustrated in Figure E.71-6. Slices normal to the X-, Y-, and Z-directions are shown in Figure E.71-6a, b, and c, respectively.



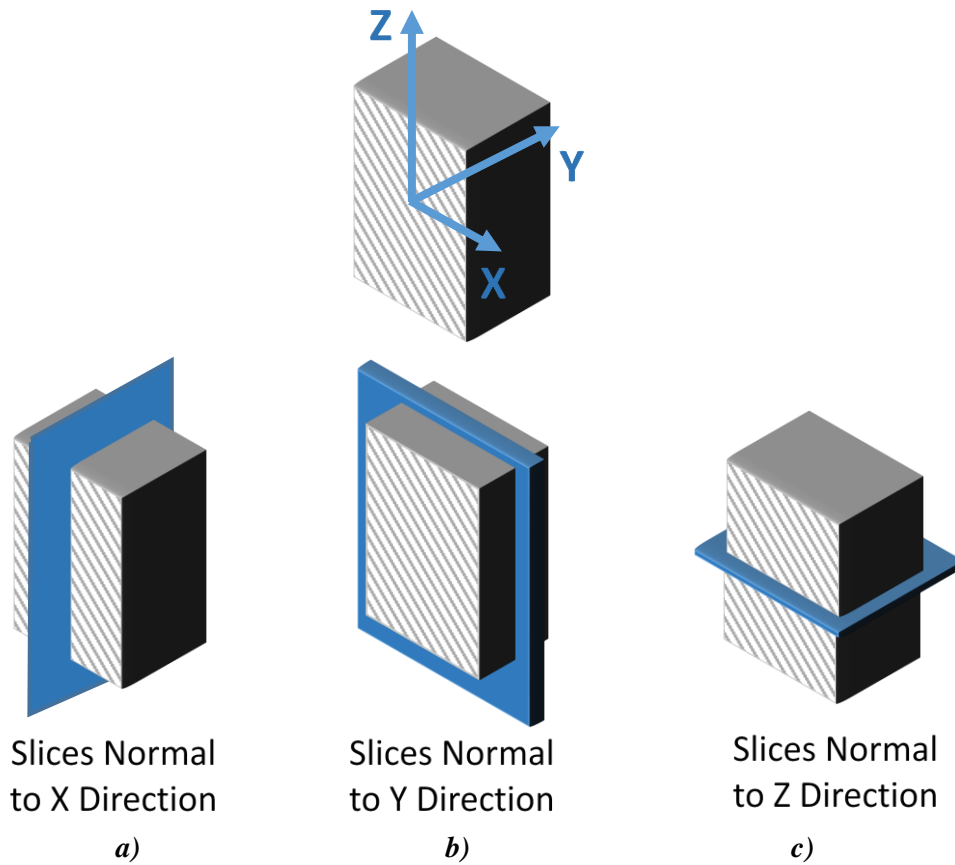


*Figure E.71-6. Slice direction nomenclature.*

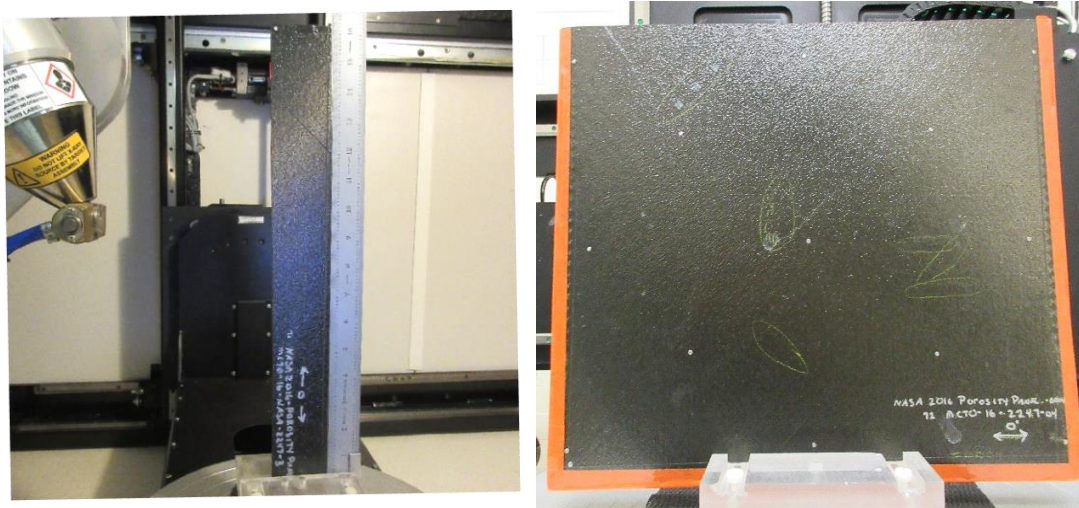


*Figure E.71-7. Test setup showing specimen orientation.*

#### **E.71.2.4 Equipment List and Specifications:**

- Avonix 225 CT System
- 225 kV microfocus X-ray source with 5- $\mu$ m focal spot size
- 15 or 30 kg Capacity 5 axis fully programmable manipulator.
- Detector: Perkin Elmer XRD 1621 – 2000  $\times$  2000 pixels with 200  $\mu$ m pitch



- 10- $\mu\text{m}$  spatial resolution for specimens 1.5 cm wide
- Thin panels 10  $\times$  10 inch – full volume 200- $\mu\text{m}$  spatial resolution

### E.71.2.5 Settings

*Table E.71-2. Data collection settings.*

Source Energy	120 kV
Current	100 $\mu\text{A}$
Magnification	1.30 X
Filter	NF
# Rotational angles	3142
Exposure time / frame	1.0 sec
Max Histogram Grey Level	22 K
# Averages	8
Resolution ( $\mu\text{m}$ )	154.162 $\mu\text{m}$
Array Dimensions (pixels)	Set 1: 1999 $\times$ 362 $\times$ 1998 Set 2: 1998 $\times$ 686 $\times$ 1997

The specimen is placed vertically (rotated about the smallest dimension) on the rotational stage located between the radiation source and the detector. The rotational stage is computer-controlled and correlated to the position of the sample. As the sample is rotated the full 360° (~0.11° increments), the detector collects radiographs at each rotated angle as the X-ray path intersects the sample. 3D reconstruction of the collection of radiographs produces a volume of data that can then be viewed along any plane in the volume. The closer the sample can be placed to the X-ray source, the higher the spatial resolution that can be obtained.

### E.71.2.6 Inspection Results

Specimen #71 had two components labeled A and B, A being the large bulk section of the material and B a 2 by 16-inch piece cut from the top. These were imaged separately at different distances from the source to produce scans of differing resolution. Figure E.71-8 shows scans from the same direction of the large specimen A and several scans from B stitched together using image registration techniques. Gross porosity and some delaminations are evident in both scans, but some of the smaller defects are lost on the large-scale specimen.

The porosity in Figure E.71-8 and Figure E.71-9 is represented by the small darker areas within the sample. This porosity pervades nearly every slice of the specimen and are easily detected. In Figure E.71-9 there is also evidence of missing tows in the bottom left of the y-view as well as more instances of porosity peppered across the specimen. The cross-stitched pattern on the y-view image is a result of the viewing angle not being perfectly normal with the specimen layers. A perfectly normal view is near impossible to achieve in this specimen as it is very thin and the amount of defects cause bowing.

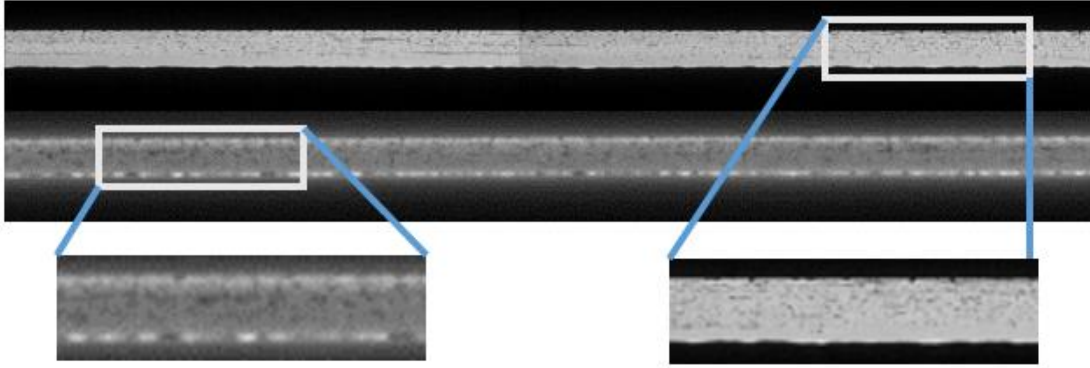


*Figure E.71-8. XCT of Specimen #71 A (top) and B (bottom) showing porosity at different resolutions.*

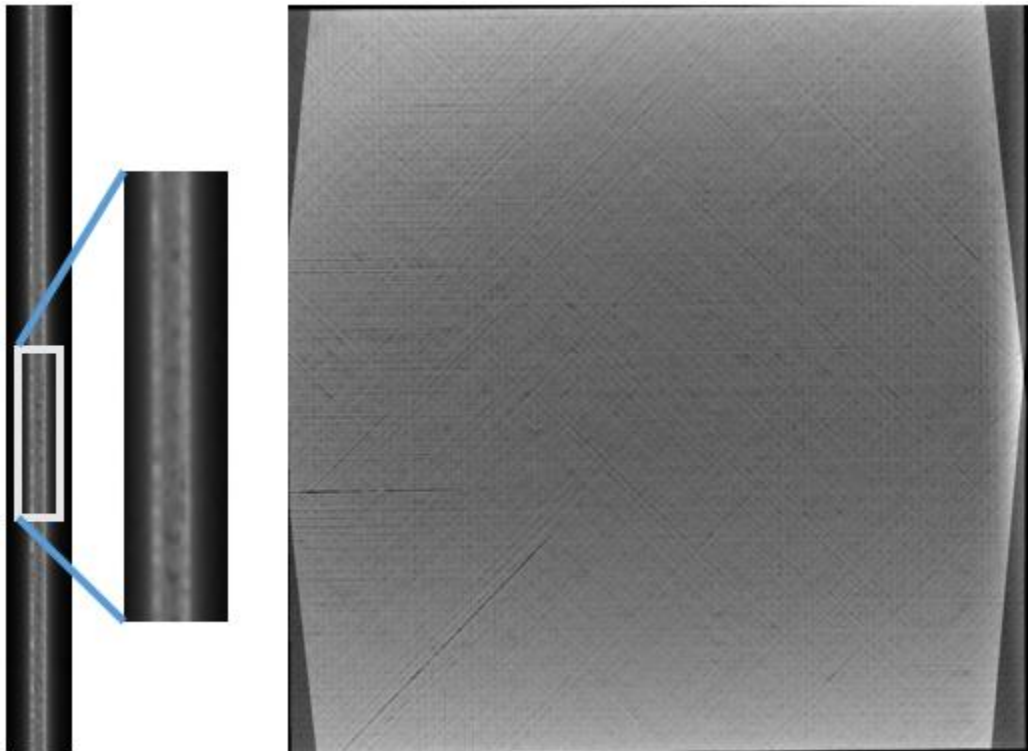


*Figure E.71-9. XCT of Specimen #71 from the z-view (left) and y-view (right).*

**E.71.3 Method: Pulse-Echo Ultrasound Testing (PEUT)**

**E.71.3.1 Partner: NGIS**

**E.71.3.2 Technique Applicability: ★★★**

PEUT scans were performed on the flat tool side of the panel in order to detect defects.

**E.71.3.3 Laboratory Setup**

PEUT scans performed in the Test-Tech 3-axis scanning tank used the water-squirter method. For each panel, use of optimum water nozzle and column diameter achieved optimal SNR and defect detection (if defects existed).



Figure E.71-10. PEUT setup in Test-Tech scanning tank.

#### E.71.3.4 Equipment List and Specifications:

- Test-Tech 3-axis scanning tank
- Olympus 5077PR Square Wave Pulsar/Receiver
- Transducer Frequencies: (1, 2.25, and 5 MHz)

#### E.71.3.5 Settings

Table E.71-3. Equipment settings for 1.0 MHz scan.

Transducer	Brand	Model	Freq. (MHz)	Element Dia. (in.)	Water Column Dia (in.)			Outer Dia. (in)		
Transmitter	Krautkramer	Benchmark	1	0.25	0.25			0.5		
Pulsar/Receiver	PRF	Voltage	Freq. (MHz)		HPF	LPF (MHz)	Rtune	Ttune	Attn	Range
Olympus	Ext	100	1.0		Out	Full BW	N/A	N/A	N/A	N/A

Table E.71-4. Equipment settings for 2.25 MHz scan.

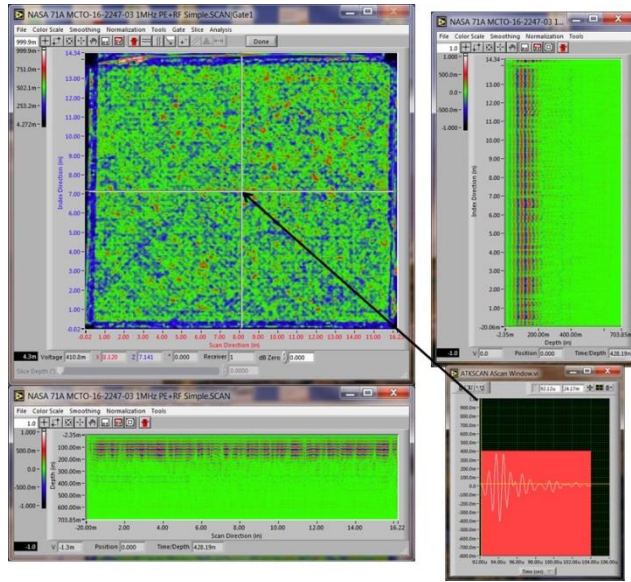
Transducer	Brand	Model	Freq. (MHz)	Element Dia. (in.)	Water Column Dia (in.)			Outer Dia. (in)		
Transmitter	KB-Aerotech	Alpha	2.25	0.25	0.25			0.5		
Pulsar/Receiver	PRF	Voltage	Freq. (MHz)		HPF (MHz)	LPF (MHz)	Rtune	Ttune	Attn	Range
Olympus	Ext	100	2-2.25		Out	Full BW	N/A	N/A	N/A	N/A
	Gain (dB)	16								

Table E.71-5. Equipment settings for 5.0 MHz scan.

Transducer	Brand	Model	Freq. (MHz)	Element Dia. (in.)	Water Column Dia (in.)			Outer Dia. (in)		
Transmitter	Krautkramer	Benchmark	5	0.25	0.25			0.5		
Pulsar/Receiver	PRF	Voltage	Freq. (MHz)		HPF	LPF (MHz)	Rtune	Ttune	Attn	Range
Olympus	Ext	100	5-6		Out	Full BW	N/A	N/A	N/A	N/A
	Gain (dB)	-6								

#### E.71.3.6 Inspection Results

Scans were performed and data quality was verified by producing C-scans for the different panels. Back-wall signals were not resolved or detected at any frequency due to high attenuation.



**Figure E.71-11. PEUT C-scans at 1.0 MHz.**

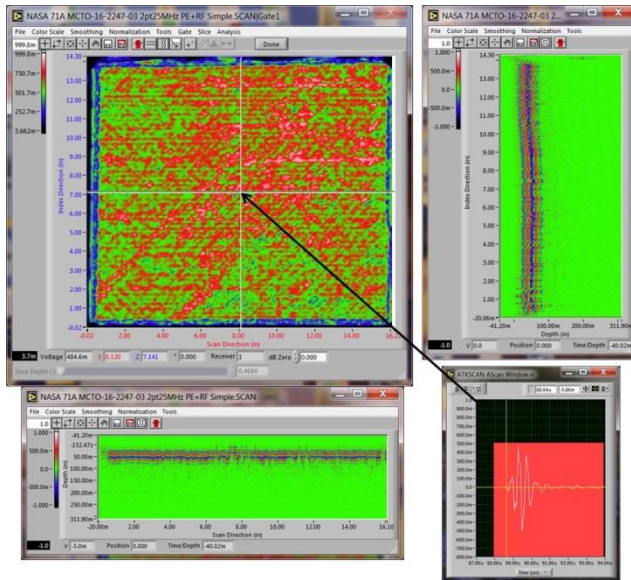


**Figure E.71-12. PEUT C-scans at 2.25 MHz.**

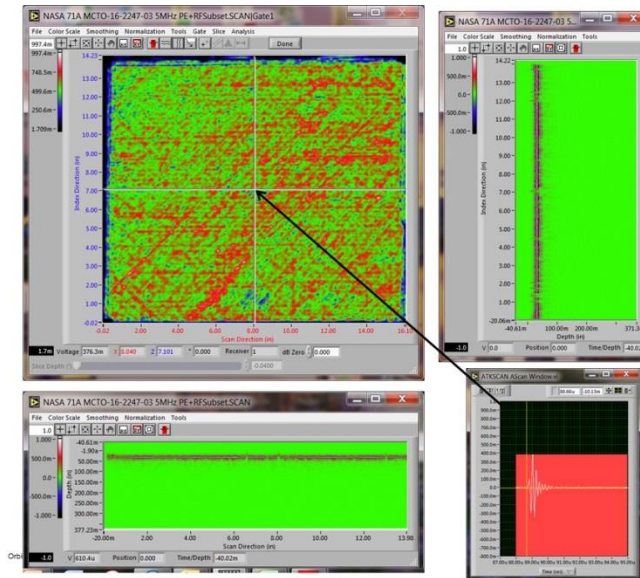


Figure E.71-13. PEUT C-scans at 5.0 MHz.

### E.71.3.7 References

- [1] Workman, Gary L; and Kishoni, Doron: *Nondestructive Testing Handbook*, Third. Edited by Patrick O Moore. Vol. 7. American Society for Nondestructive Testing (ANST), 2007.

### E.71.4 Method: Through-Transmission Ultrasound Testing (TTUT)

#### E.71.4.1 Partner: NGIS

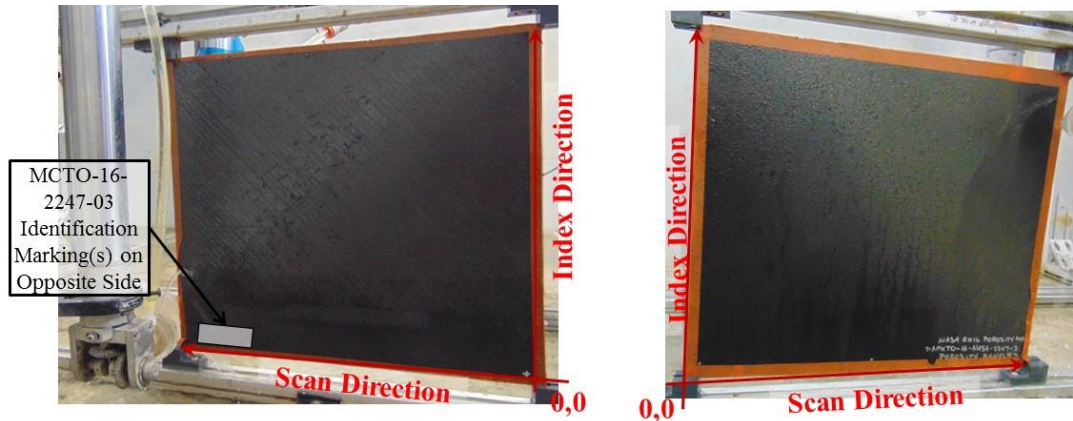
#### E.71.4.2 Technique Applicability: ★★★

TTUT scans were performed on the stepped panel in order to detect defects. Depth of defect cannot be determined with this method.

#### E.71.4.3 Laboratory Setup

TTUT scans were performed in the Test-Tech 3-axis scanning tank using a water-squirter method. Transmission was performed on the flat tool side of the panel and received from the bagged stepped side of the panel. For each panel, water nozzle and column diameter was optimized to achieve optimal SNR and defect detection (if defects existed).





Transmitted from tool side surface

Received from bag side surface

**Figure E.71-14. TTUT setup in Test-Tech scanning tank.**

**E.71.4.4 Equipment List and Specifications:**

- Test-Tech 3-axis scanning tank
- Olympus 5077PR Square Wave Pulsar/Receiver
- Transducer Pairs (1.0, 2.25 MHz)

**E.71.4.5 Settings**

**Table E.71-6. Equipment settings for 1.0 MHz scan.**

Transducer	Brand	Model	Freq. (MHz)	Element Dia. (in.)	Water Column Dia. (in.)			Outer Dia. (in)		
Transmitter	Sonic	IBK I-2	1	0.5	0.25			0.5		
Receiver	Sonic	IBK I-2	1	0.5	0.25			0.5		
Pulsar/Receiver	PRF	Voltage	Freq. (MHz)		HPF	LPF (MHz)	Rtune	Ttune	Attn	Range
Olympus	Ext	100	1.0		Out	Full BW	N/A	N/A	N/A	N/A
	Gain (dB)	31								

**Table E.71-7. Equipment settings for 2.25 MHz scan.**

Transducer	Brand	Model	Freq. (MHz)	Element Dia. (in.)	Water Column Dia. (in.)			Outer Dia. (in)		
Transmitter	KB-Aerotech	Alpha	2.25	0.25	0.25			0.5		
Receiver	KB-Aerotech	Alpha	2.25	0.25	0.25			0.5		
Pulsar/Receiver	PRF	Voltage	Freq. (MHz)		HPF (MHz)	LPF (MHz)	Rtune	Ttune	Attn	Range
Olympus	Ext	100	2-2.25		Out	Full BW	N/A	N/A	N/A	N/A
	Gain (dB)	23								

**E.71.4.6 Inspection Results**

Transmitted signals were detected, but panels exhibited relatively high attenuation at 1 MHz and 2.25 MHz.

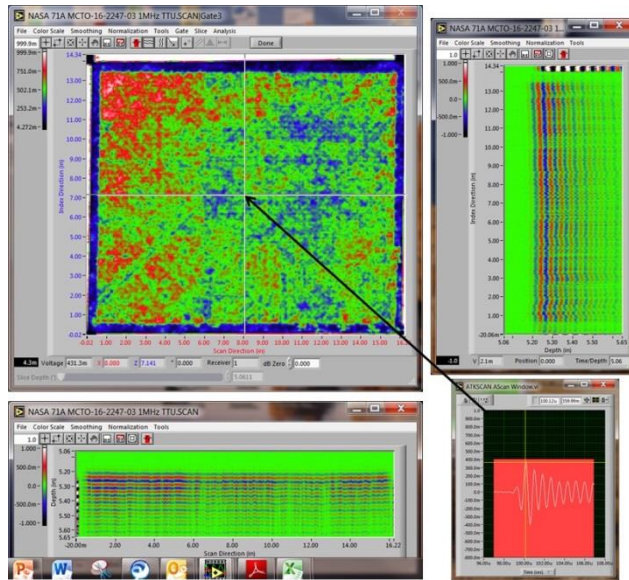


Figure E.71-15. TTUT C-scans at 1 MHz.

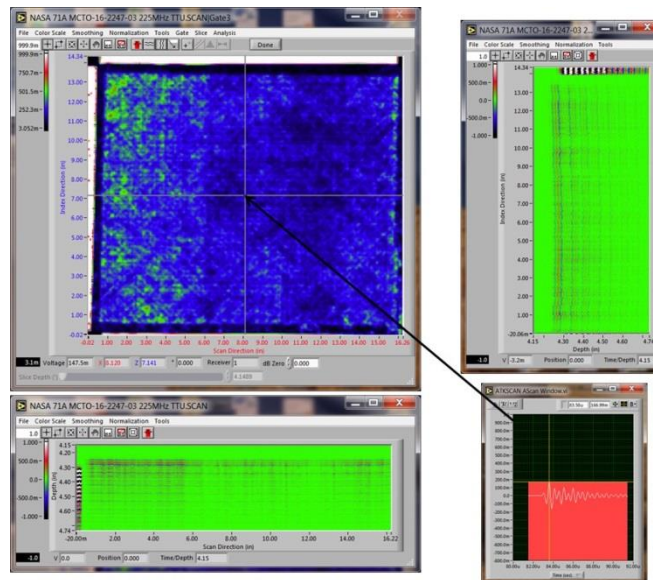


Figure E.71-16. TTUT C-scans at 2.25 MHz.

#### E.71.4.7 References

- [1] Workman, Gary L; and Kishoni, Doron: *Nondestructive Testing Handbook*, Third. Edited by Patrick O Moore. Vol. 7. American Society for Nondestructive Testing (ANST), 2007.

#### E.71.5 Method: Single-Sided Infrared Thermography (SSIR)

##### E.71.5.1 Partner: NGIS

##### E.71.5.2 Technique Applicability: ★★☆☆

The thermal response produced by single-sided thermographic inspection has been determined to be dominated by factors other than porosity. It was found that slight variations in thickness and localized thermal property variation dominated the surface temperature compared to material's

porosity. For this reason, single-sided inspection is not recommend as a technique for discriminating porosity.

### E.71.5.3 Laboratory Setup:

Single-sided thermography images were acquired using a FLIR SC6000 IR camera setup. The thermal camera is mounted to the back of the flash hood and mounted in a fixed location on an optical table. The panel is held vertically within a fixture that slides across a linear track between captures in order to ensure total coverage. Paper light shields were constructed for the fixture to block flash spillover around the edges of the panel.

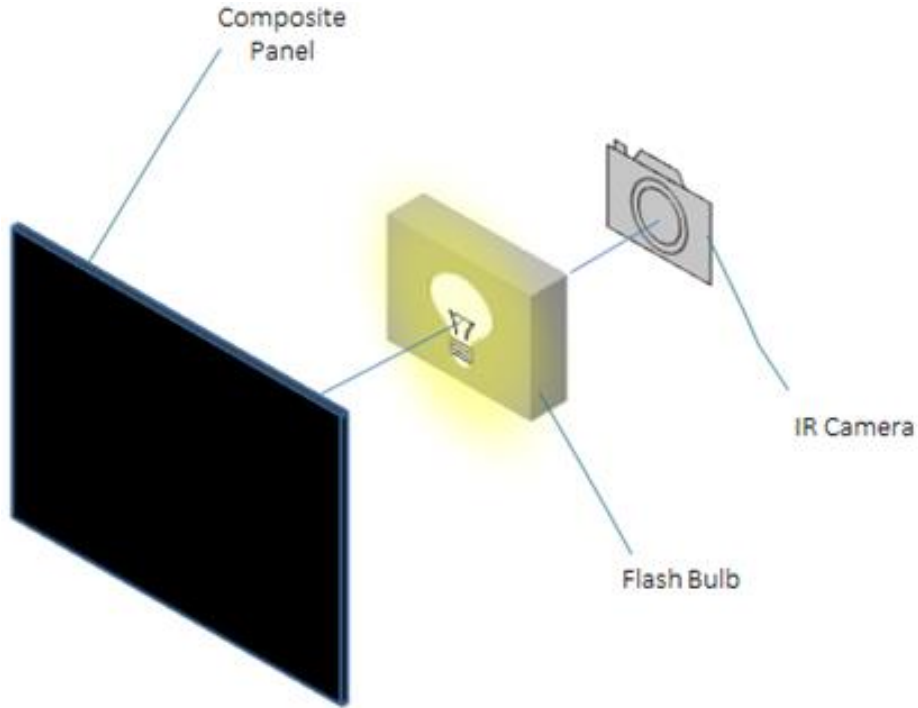


*Figure E.71-17. SSIR schematic.*



*Figure E.71-18. Photo of SSIR setup.*

**E.71.5.4 Equipment List and Specifications:**

- FLIR SC6000 IR camera, mid wavelength IR sensor (3.0- to 5.0- $\mu\text{m}$ )
- Flash power supplies, hood, and lamps
- EchoTherm® V8 Software

**E.71.5.5 Settings**

*Table E.71-8. Equipment settings for SSIR scan.*

Flash Duration (ms)	30
Capture Elapsed Time (s)	20.08
Camera Frequency (Hz)	37.86
Integration Time (s)	2

### E.71.5.6 Inspection Results



Figure E.71-19. SSIR image of Specimen #71.

### Porosity Panel #3

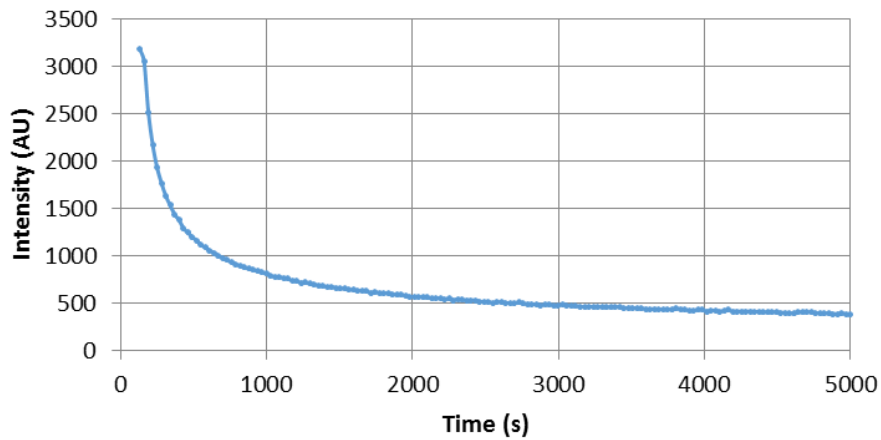


Figure E.71-20. Intensity curve showing heat dispersion over time for Specimen #71.

### E.71.5.7 References

- [1] Parker, W. J.; Jenkins, R. J.; Butler, C. P.; and Abbott, G. L.: "Method of Determining Thermal Diffusivity, Heat Capacity and Thermal Conductivity," *Journal of Applied Physics*, 32 (9): 1679, Bibcode:1961JAP....32.1679P. doi:10.1063/1.1728417, 1961.



**E.71.6 Method: Through-Transmission Infrared Thermography (TTIR)**

**E.71.6.1 Partner: NGIS**

**E.71.6.2 Technique Applicability: ★★★**

**E.71.6.3 Laboratory Setup:**

TT thermography images were acquired using a FLIR SC6000 IR camera setup. The flash hood is mounted in a fixed location on an optical table. The thermal camera is mounted on a tripod with the panel between it and the flash hood. The panel is held vertically within a fixture that slides across a linear track between captures in order to ensure total coverage. Paper light shields were constructed for the fixture to block flash spillover around the edges of the panel.

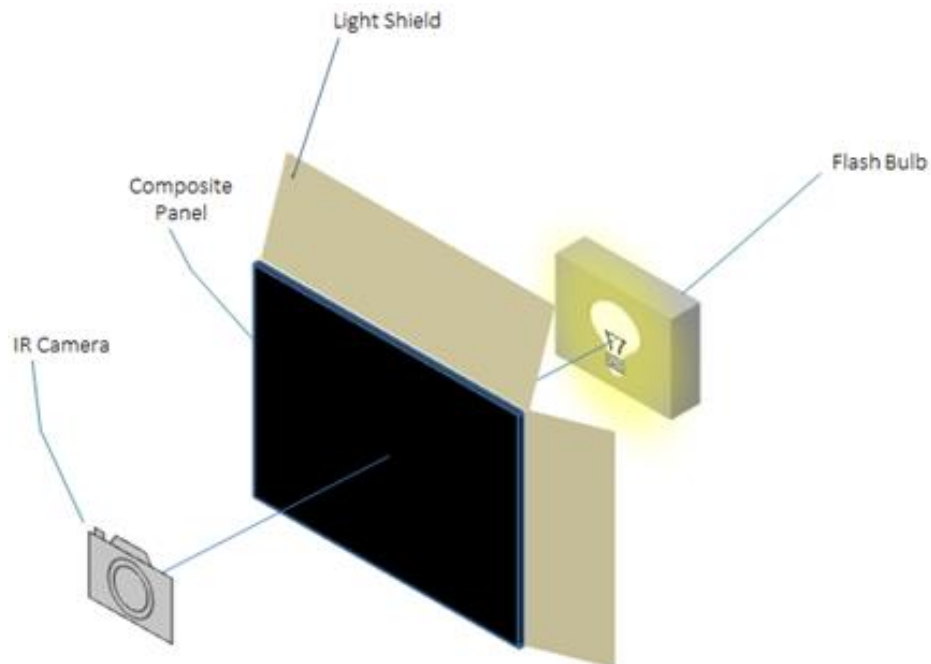


*Figure E.71-21. TTIR schematic.*



*Figure E.71-22. Photo of TTIR setup.*

**E.71.6.4 Equipment List and Specifications:**

- FLIR SC6000 IR camera, mid wavelength IR sensor (3.0- to 5.0- $\mu\text{m}$ )
- Flash power supplies, hood, and lamps
- EchoTherm® V8 Software

**E.71.6.5 Settings**

*Table E.71-9. Equipment settings for TTIR scan.*

Panel Thickness (mm)	3.63
Flash Duration (ms)	30
Capture Elapsed Time (s)	21.19
Camera Frequency (Hz)	8.79
Integration Time (s)	2

**E.71.6.6 Inspection Results**

Images were captured and the thermal diffusivity data was processed. Lower thermal diffusivity correlates to higher levels of porosity. Less variation in the histogram of thermal diffusivity shows consistent porosity across the total area.

### Specimen #71

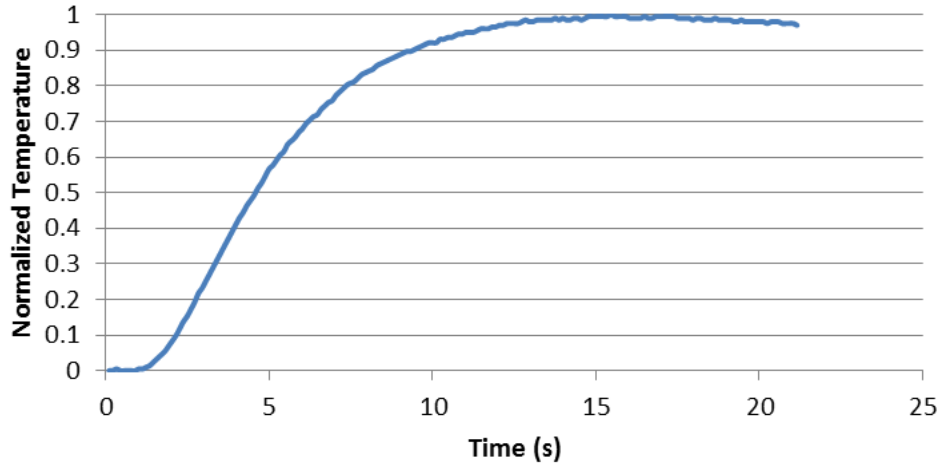


Figure E.71-23. Temperature curve showing the dispersion of heat over time during image capture.

### Specimen #71

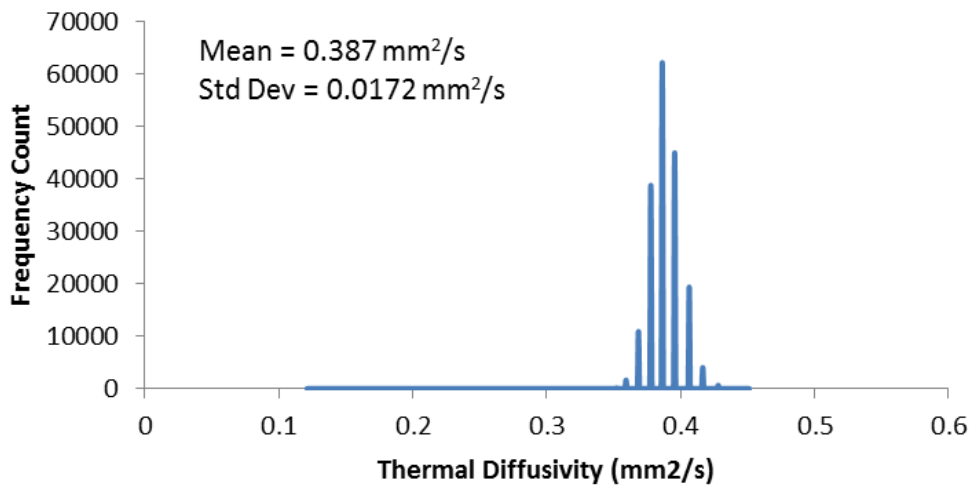
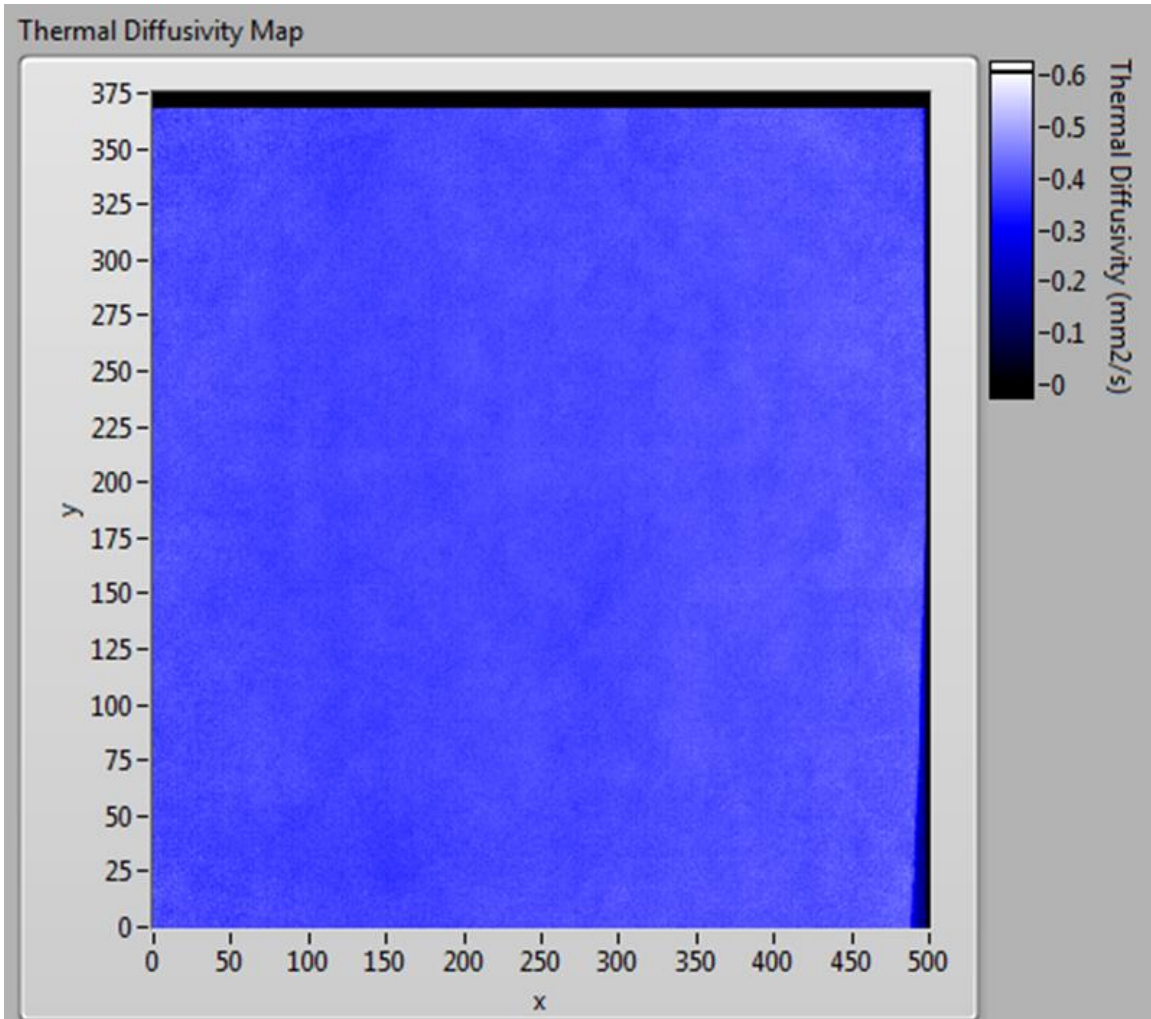


Figure E.71-24. Histogram showing frequency of thermal diffusivity values. Tighter point spread shows consistent porosity throughout panel and a larger standard deviation could indicate porosity.



*Figure E.71-25. Image of thermal diffusivity post processing.  
Low thermal diffusivity shows indications of porosity.*

**E.71.6.7 References**

- [1] Parker, W. J.; Jenkins, R. J.; Butler, C. P.; and Abbott, G. L.: "Method of Determining Thermal Diffusivity, Heat Capacity and Thermal Conductivity," *Journal of Applied Physics*, 32 (9): 1679, Bibcode:1961JAP....32.1679P. doi:10.1063/1.1728417, 1961.

**E.72 Specimen #72A&B: NASA-03-Porosity-Panel-004**

Structure	Material	Details	Dimensions (inches)	Partner Methods	
Fiber Placed Panel	IM7/8552-1 Slit Tape w/ IM7/8552 Fabric OML	Flat Panel with high porosity	15 × 17.5 × 0.15	NASA	E.72.1 PEUT E.72.2 XCT
				NGIS	E.72.3 PEUT E.72.4 TTUT E.72.5 SSIR E.72.6 TTIR



*Figure E.72-1. Photographs of Specimen #72: NASA-03-Porosity-Panel-004.*

**E.72.1 Method: Pulse-Echo Ultrasound Testing (PEUT)**

**E.72.1.1 Partner: NASA**

**E.72.1.2 Technique Applicability: ★★★**

PEUT detected the porosity in this specimen.

**E.72.1.3 Laboratory Setup**

Immersion Ultrasonic Testing: NASA LaRC uses a custom-designed single-probe ultrasonic scanning system. The system has an 8-axis motion controller, a multi-axis gantry robot mounted above a medium-size water tank, a dual-channel, 16-bit, high-speed digitizer, and an off-the-shelf ultrasonic pulser receiver. The system can perform TTUT and PEUT inspections. TT inspection employs two aligned ultrasonic probes, one transmitter, and one receiver, placed on either side of a test specimen. Pulse-echo inspection is a single-sided method where a single ultrasonic probe is both transmitter and receiver. In each method, data are acquired while raster scanning the ultrasonic probe(s) in relation to a part. Figure E.72-2 shows a simplified block diagram of a scanning Pulse-echo inspection.

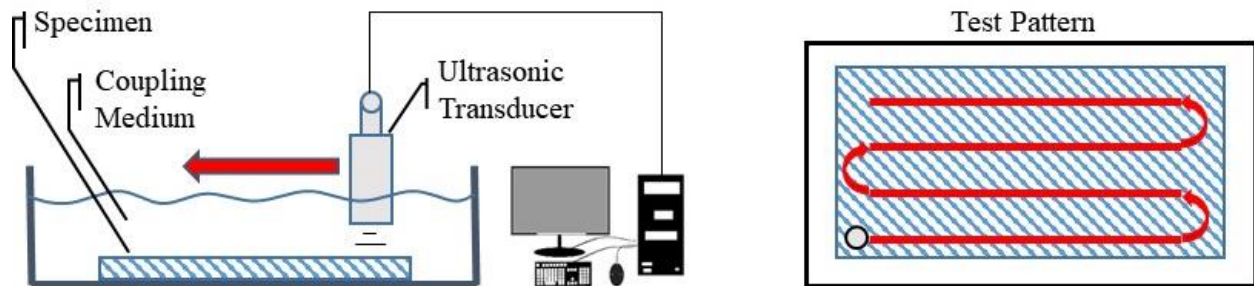


*Figure E.72-2. Ultrasonic system components.*

**E.72.1.4 Equipment List and Specifications:**

- Pulser/Receiver: Olympus 5073PR
- Digitizer: AlazarTech ATS9462, dual channel, 16 bit, 180 MS/s
- Sensor: Olympus 2-inch spherical focus immersion ultrasonic transducer
- Motion system: open looped stepper motor based X-YY-Z gantry robot
- Motion Controller: Galil DMC-4183
- Acquisition Software: FastScan, custom developed at NASA LaRC
- Signal Processing Software: DataViewer, custom developed at NASA LaRC



### E.72.1.5 Settings

*Table E.72-1. Data collection settings.*

Resolution (horizontal) [in/pixel]	0.01
Resolution (vertical) [in/pixel]	0.01
Probe frequency [MHz]	10
Focal Length [in]	2
Array Dimensions [pixels]	676 × 581

The specimen is placed flat against the zero position of the tank raised above the glass bottom by several metal washers. The test probe is computer-controlled and correlated to the position on the sample. It is also focused to a point 1 mm below the surface of the test material. The specimen remains in place while the transducer follows a preprogrammed test grid across the surface as indicated in Figure E.72-2. At each point, ultrasonic data is collected from individual pulses. Larger step sizes between data collection result in lower image resolution. These data points are reconstructed into a data cube displaying spatial coordinates as time progresses. 2D reconstruction of the collection of ultrasonic responses create flattened slices at varying depths within the material.

### E.72.1.6 Inspection Results

Specimen #72 is a fiber placed flat panel fabricated from IM7/8552-1 Slit Tape with the objective of achieving porosity throughout the sample. PEUT was performed on this specimen in NASA's immersion tank specified above.

Figure E.72-3 is at a depth of .029in and shows multiple instances of porosity as indicated. The larger porosity appears white initially as the air pockets reflect acoustic waves creating a strong early response. Visually this is demonstrated by the peppered dark regions in Figure E.72-4. Porosity is found throughout the bulk of the specimen concentrated at a depth halfway through the specimen. The striations seen in Figures E.72-3 and Figure E.72-4 are the fiber directions of the individual plies.

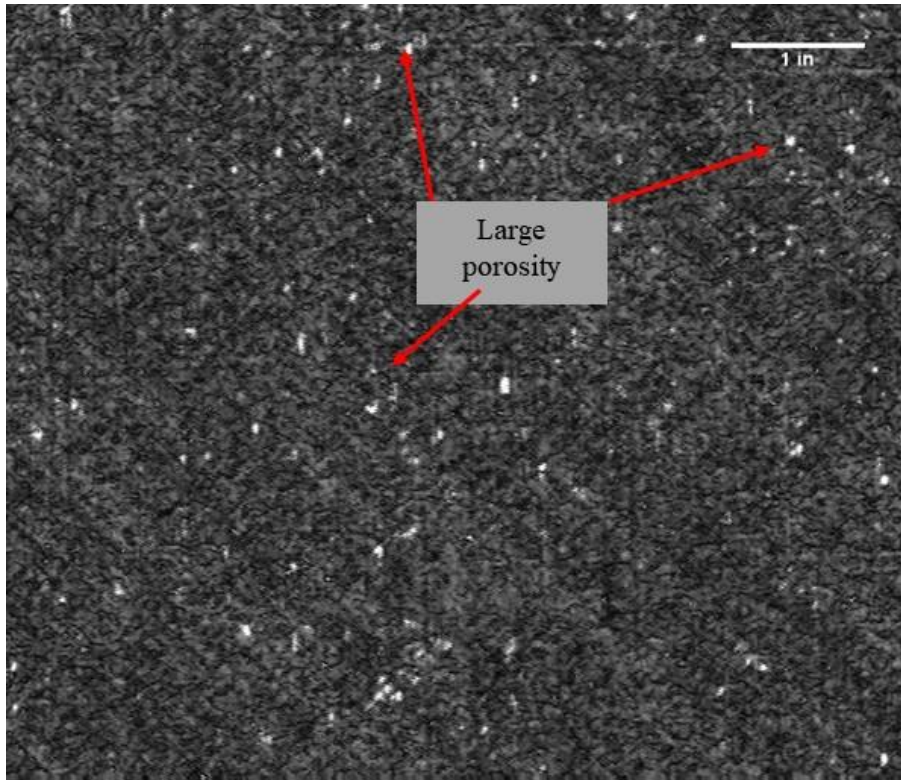


*Figure E.72-3. UT image of porosity within the sample.*

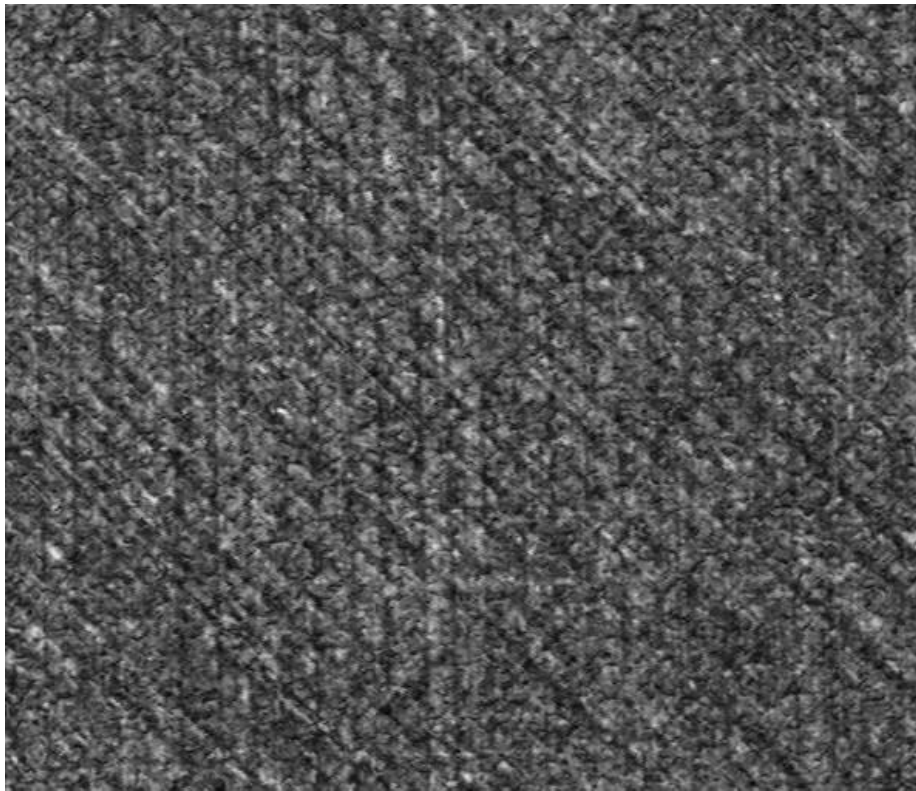


*Figure E.72-4. UT image of porosity at a greater depth within the sample.*

## E.72.2 Method: X-ray Computed Tomography (XCT)

### E.72.2.1 Partner: NASA

### E.72.2.2 Technique Applicability: ★★★

XCT is capable of imaging the high porosity in this specimen.

### E.72.2.3 Laboratory Setup

The microfocus XCT system at NASA LaRC is a commercially available Avonix (Nikon C2) Metrology System designed for high-resolution NDE inspections. The system is an advanced microfocus X-ray system, capable of resolving details down to 5  $\mu\text{m}$ , and with magnifications up to 60X. Supplied as complete, the system is a large-dimension radiation enclosure with X-ray source, specimen manipulator, and an amorphous silica detector, as shown in Figure E.72-5. The imaging controls are housed in a separate control console. The detector is a Perkin-Elmer, 16-bit, amorphous-silicon digital detector with a  $2000 \times 2000$ -pixel array.

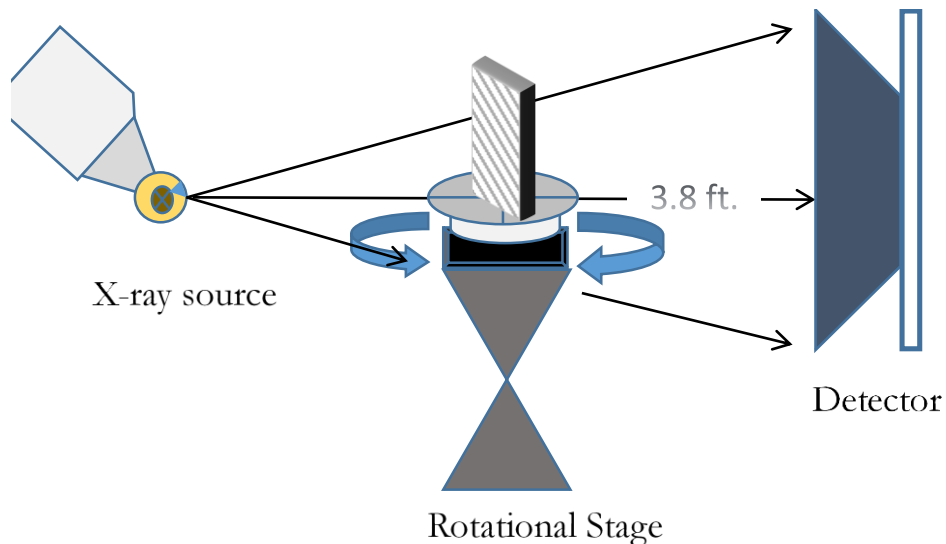


*Figure E.72-5. XCT system components.*

A consistent Cartesian coordinate system is used to define slice direction as illustrated in Figure E.72-6. Slices normal to the X-, Y-, and Z-directions are shown in Figure E.72-6a, b, and c, respectively.

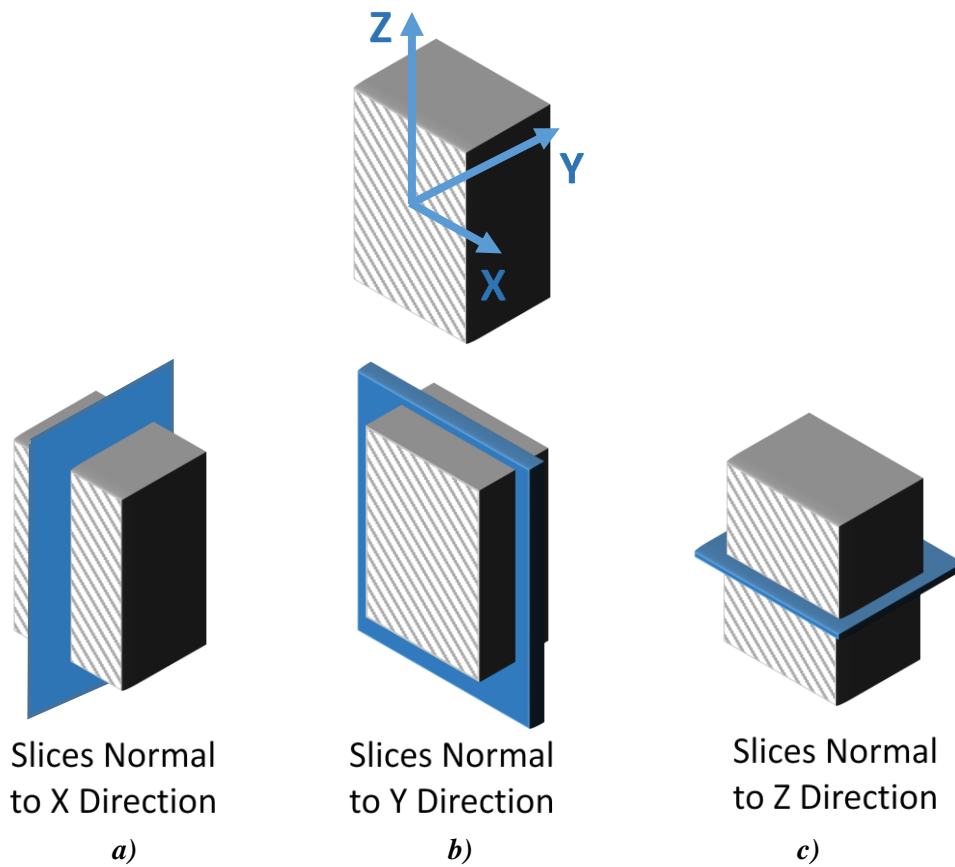


*Figure E.72-6. Slice direction nomenclature.*

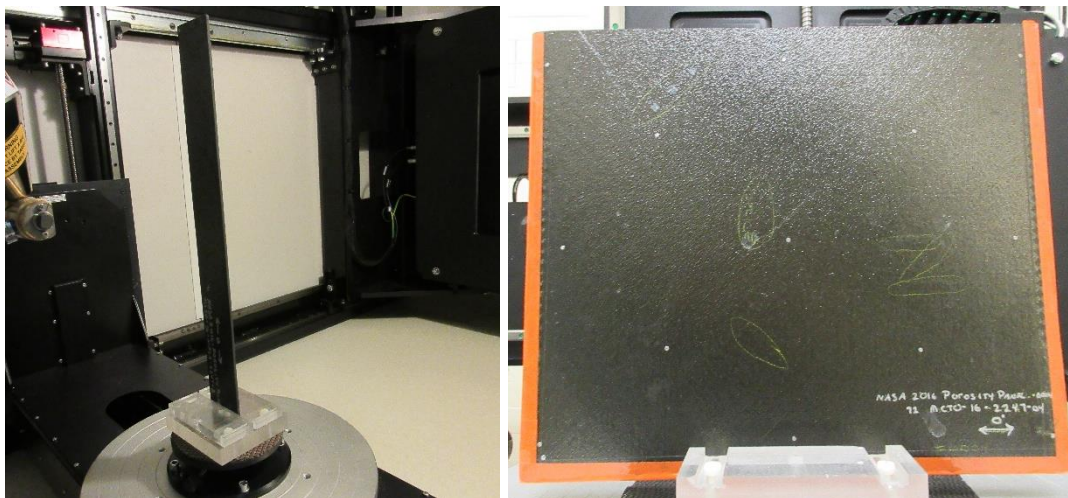


*Figure E.72-7. Test setup showing specimen orientation.*

#### E.72.2.4 Equipment List and Specifications:

- Avonix 225 CT System
- 225 kV microfocus X-ray source with 5  $\mu\text{m}$  focal spot size
- 15 or 30kg Capacity 5 axis fully programmable manipulator.
- Detector: Perkin Elmer XRD 1621 – 2000  $\times$  2000 pixels with 200  $\mu\text{m}$  pitch

- 10  $\mu\text{m}$  spatial resolution for specimens 1.5 cm wide
- Thin panels 10-inch  $\times$  10-inch – full volume 200  $\mu\text{m}$  spatial resolution

#### E.72.2.5 Settings

*Table E.72-2. Data collection settings.*

Source Energy	120 kV
Current	100 $\mu\text{A}$
Magnification	1.30 X
Filter	NF
# Rotational angles	3142
Exposure time / frame	1.0 sec
Max Histogram Grey Level	22 K
# Averages	8
Resolution ( $\mu\text{m}$ )	154.162 $\mu\text{m}$
Array Dimensions (pixels)	Set 1: 1999 $\times$ 362 $\times$ 1998 Set 2: 1998 $\times$ 686 $\times$ 1997

The specimen is placed vertically (rotated about the smallest dimension) on the rotational stage located between the radiation source and the detector. The rotational stage is computer-controlled and correlated to the position of the sample. As the sample is rotated the full  $360^\circ$  ( $\sim 0.11^\circ$  increments), the detector collects radiographs at each rotated angle as the X-ray path intersects the sample. 3D reconstruction of the collection of radiographs produces a volume of data that can then be viewed along any plane in the volume. The closer the sample can be placed to the X-ray source, the higher the spatial resolution that can be obtained.

#### E.72.2.6 Inspection Results

Specimen #72 had two components labeled A and B, A being the large bulk section of the material and B a 2 by 16-inch piece cut from the top. These were imaged separately at different distances from the source to produce scans of differing resolution. Figure E.72-8 shows scans from the same direction of the large specimen A and several scans from B stitched together using image registration techniques. Gross porosity and some delaminations are evident in both scans, but some of the smaller defects are lost on the large-scale specimen.

The porosity in Figure E.72-8 and Figure E.72-9 is represented by the small darker areas within the sample. While the large delaminations seen in Figure E.72-9 draw the most attention, the smaller bubbles of porosity peppered throughout the rest of the bulk material is still easily identifiable even on the lower resolution image. The cross-stitched pattern on the y-view image is a result of the viewing angle not being perfectly normal with the specimen layers. A perfectly normal view is near impossible to achieve in this specimen as the amount of defects cause severe bowing.



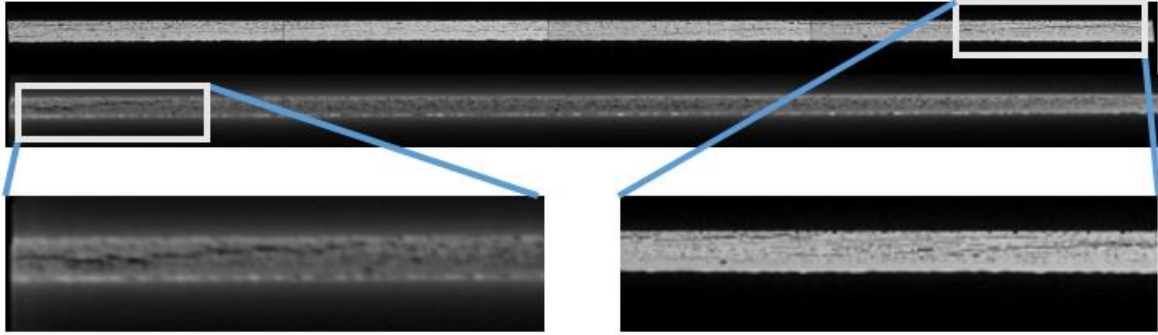


*Figure E.72-8. XCT of specimen #72 A (top) and B (bottom) showing porosity at different resolutions.*

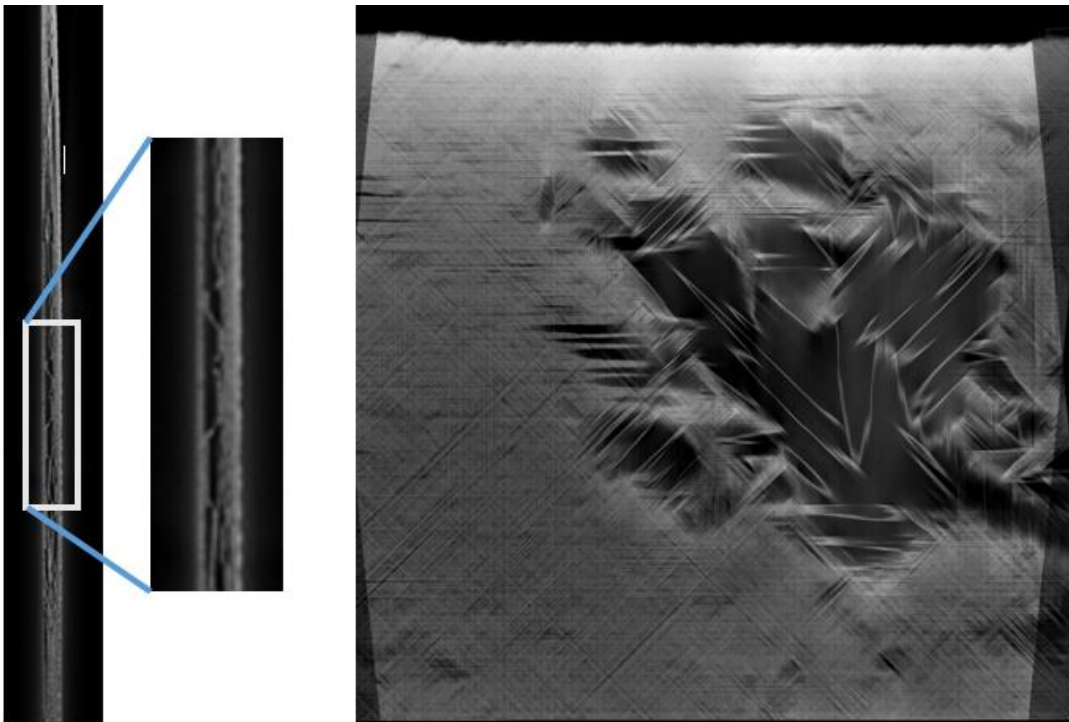


*Figure E.72-9. XCT of Specimen #72 from the z-view (left) and y-view (right).*

**E.72.3 Method: Pulse-Echo Ultrasound Testing (PEUT)**

**E.72.3.1 Partner: NGIS**

**E.72.3.2 Technique Applicability: ★★★**

PEUT scans were performed on the flat tool side of the panel in order to detect defects.

**E.72.3.3 Laboratory Setup**

PEUT scans performed in the Test-Tech 3-axis scanning tank used the water-squirter method. For each panel, use of optimum water nozzle and column diameter achieved optimal SNR and defect detection (if defects existed).

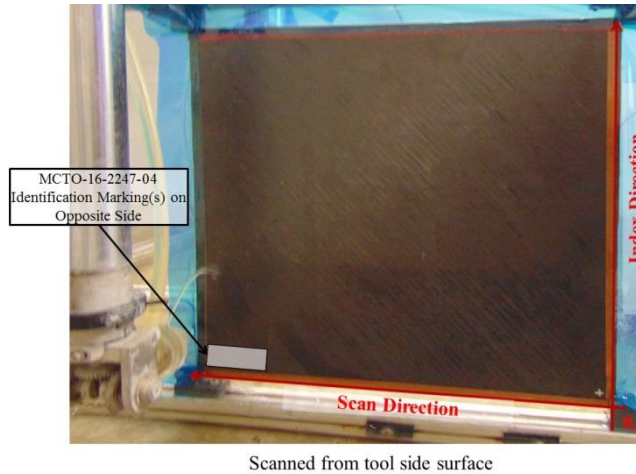


Figure E.72-10. PEUT setup in Test-Tech scanning tank.

#### E.72.3.4 Equipment List and Specifications:

- Test-Tech 3-axis scanning tank
- Olympus 5077PR Square Wave Pulsar/Receiver
- Transducer Frequencies: (1, 2.25, and 5 MHz)

#### E.72.3.5 Settings

Table E.72-3. Equipment settings for 1.0 MHz scan.

Transducer	Brand	Model	Freq. (MHz)	Element Dia. (in.)	Water Column Dia. (in.)			Outer Dia. (in)		
Transmitter	Krautkramer	Benchmark	1	0.25	0.25			0.5		
Pulsar/Receiver	PRF	Voltage	Freq. (MHz)		HPF	LPF (MHz)	Rtune	Ttune	Attn	Range
Olympus	Ext	100	1.0		Out	Full BW	N/A	N/A	N/A	N/A
	Gain (dB)		1							

Table E.72-4. Equipment settings for 2.25 MHz scan.

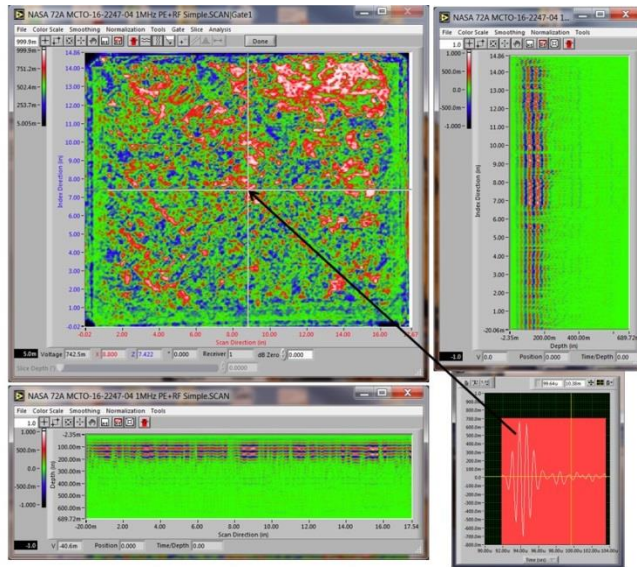
Transducer	Brand	Model	Freq. (MHz)	Element Dia. (in.)	Water Column Dia. (in.)			Outer Dia. (in)		
Transmitter	KB-Aerotech	Alpha	2.25	0.25	0.25			0.5		
Pulsar/Receiver	PRF	Voltage	Freq. (MHz)		HPF (MHz)	LPF (MHz)	Rtune	Ttune	Attn	Range
Olympus	Ext	100	2-2.25		Out	Full BW	N/A	N/A	N/A	N/A

Table E.72-5. Equipment settings for 5.0 MHz scan.

Transducer	Brand	Model	Freq. (MHz)	Element Dia. (in.)	Water Column Dia. (in.)			Outer Dia. (in)		
Transmitter	Krautkramer	Benchmark	5	0.25	0.25			0.5		
Pulsar/Receiver	PRF	Voltage	Freq. (MHz)		HPF	LPF (MHz)	Rtune	Ttune	Attn	Range
Olympus	Ext	100	5-6		Out	Full BW	N/A	N/A	N/A	N/A
	Gain (dB)		-6							

#### E.72.3.6 Inspection Results

Scans were performed and data quality was verified by producing C-scans for the different panels. Back-wall signals were not resolved or detected at any frequency due to high attenuation.



**Figure E.72-11. PEUT C-scans at 1.0 MHz.**

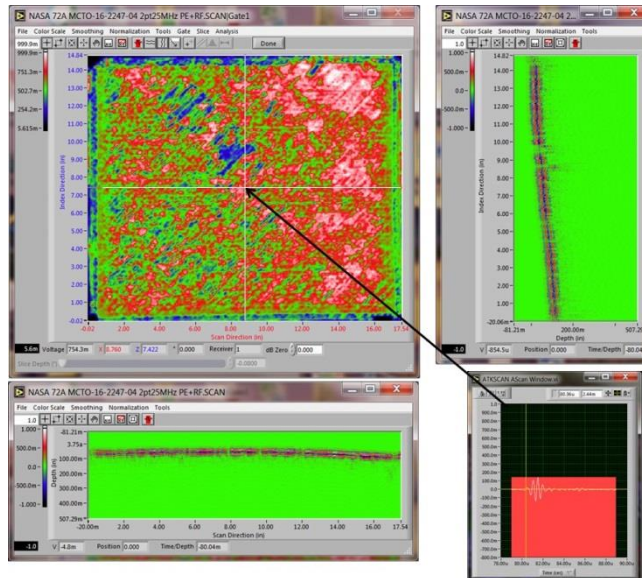


**Figure E.72-12. PEUT C-scans at 2.25 MHz.**

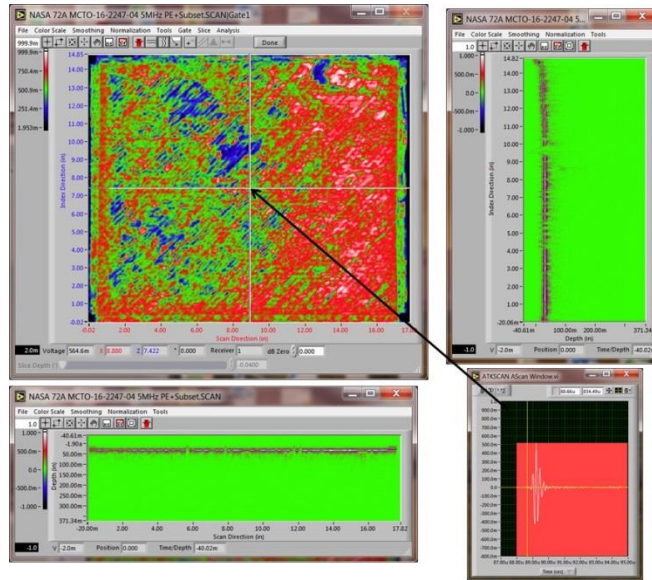


Figure E.72-13. PEUT C-scans at 5.0 MHz.

### E.72.3.7 References

- [1] Workman, Gary L; and Kishoni, Doron: *Nondestructive Testing Handbook*, Third. Edited by Patrick O Moore. Vol. 7. American Society for Nondestructive Testing (ANST), 2007.

### E.72.4 Method: Through-Transmission Ultrasound Testing (TTUT)

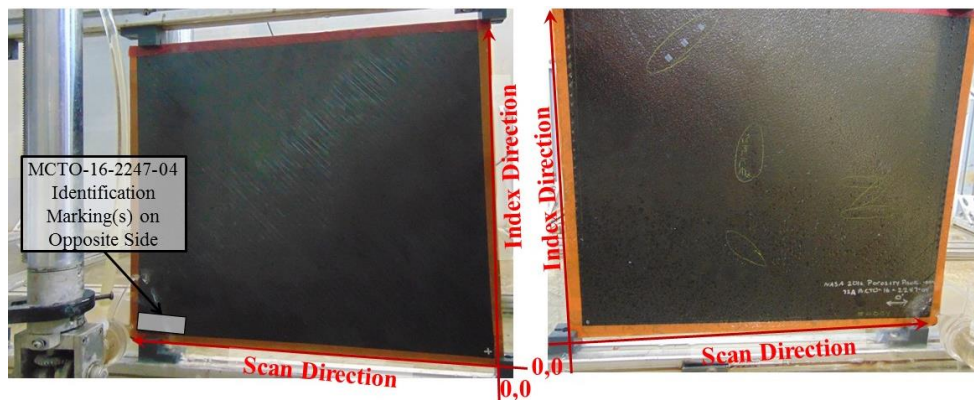
#### E.72.4.1 Partner: NGIS

#### E.72.4.2 Technique Applicability: ★★★

TTUT scans were performed on the stepped panel in order to detect defects. Depth of defect cannot be determined with this method.

#### E.72.4.3 Laboratory Setup

TTUT scans were performed in the Test-Tech 3-axis scanning tank using a water-squirter method. Transmission was performed on the flat tool side of the panel and received from the bagged stepped side of the panel. For each panel, water nozzle and column diameter was optimized to achieve optimal SNR and defect detection (if defects existed).



Transmitted from tool side surface

Received from bag side surface

Figure E.72-14. TTUT setup in Test-Tech scanning tank.



#### E.72.4.4 Equipment List and Specifications:

- Test-Tech 3-axis scanning tank
- Olympus 5077PR Square Wave Pulsar/Receiver
- Transducer Pairs (1.0, 2.25 MHz)

#### E.72.4.5 Settings

*Table E.72-6. Equipment settings for 1.0 MHz scan.*

Transducer	Brand	Model	Freq. (MHz)	Element Dia. (in.)	Water Column Dia. (in.)			Outer Dia. (in.)		
Transmitter	Sonic	IBK I-2	1	0.5	0.25			0.5		
Receiver	Sonic	IBK I-2	1	0.5	0.25			0.5		
Pulsar/Receiver	PRF	Voltage	Freq. (MHz)		HPF	LPF (MHz)	Rtune	Ttune	Attn	Range
Olympus	Ext	100	1.0		Out	Full BW	N/A	N/A	N/A	N/A
	Gain (dB)	31								

*Table E.72-7. Equipment settings for 2.25 MHz scan.*

Transducer	Brand	Model	Freq. (MHz)	Element Dia. (in.)	Water Column Dia. (in.)			Outer Dia. (in.)		
Transmitter	KB-Aerotech	Alpha	2.25	0.25	0.25			0.5		
Receiver	KB-Aerotech	Alpha	2.25	0.25	0.25			0.5		
Pulsar/Receiver	PRF	Voltage	Freq. (MHz)		HPF (MHz)	LPF (MHz)	Rtune	Ttune	Attn	Range
Olympus	Ext	100	2-2.25		Out	Full BW	N/A	N/A	N/A	N/A
	Gain (dB)	23								

#### E.72.4.6 Inspection Results

Transmitted signals were not reliably detected due to extremely high attenuation at 1 MHz and 2.25 MHz.

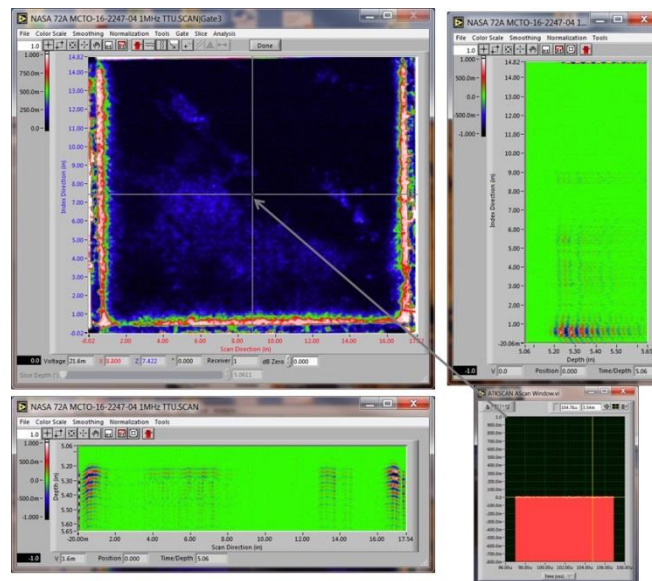


*Figure E.72-15. TTUT C-scans at 1 MHz.*



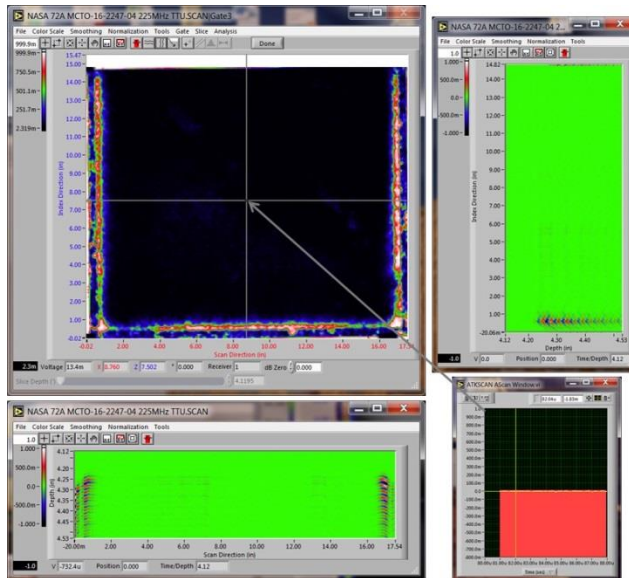


Figure E.72-16. TTUT C-scans at 2.25 MHz.

#### E.72.4.7 References

- [1] Workman, Gary L; and Kishoni, Doron: *Nondestructive Testing Handbook*, Third. Edited by Patrick O Moore. Vol. 7. American Society for Nondestructive Testing (ANST), 2007.

#### E.72.5 Method: Single-Side Infrared Thermography (SSIR)

##### E.72.5.1 Partner: NGIS

##### E.72.5.2 Technique Applicability: ★☆☆

The thermal response produced by single-sided thermographic inspection has been determined to be dominated by factors other than porosity. It was found that slight variations in thickness and localized thermal property variation dominated the surface temperature compared to material's porosity. For this reason, single-sided inspection is not recommend as a technique for discriminating porosity.

##### E.72.5.3 Laboratory Setup

Single-sided thermography images were acquired using a FLIR SC6000 IR camera setup. The thermal camera is mounted to the back of the flash hood and mounted in a fixed location on an optical table. The panel is held vertically within a fixture that slides across a linear track between captures in order to ensure total coverage. Paper light shields were constructed for the fixture to block flash spillover around the edges of the panel.

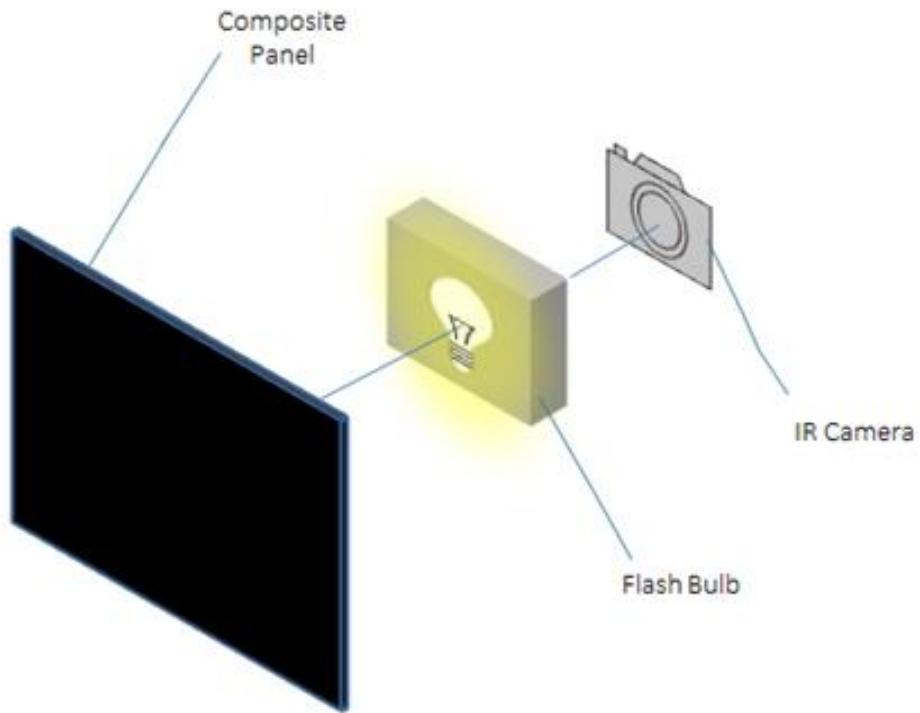


*Figure E.72-17. SSIR schematic.*



*Figure E.72-18. Photo of SSIR setup.*

**E.72.5.4 Equipment List and Specifications:**

- FLIR SC6000 IR camera, mid wavelength IR sensor (3.0- to 5.0- $\mu\text{m}$ )
- Flash power supplies, hood, and lamps
- EchoTherm® V8 Software

**E.72.5.5 Settings**

*Table E.72-8. Equipment settings for SSIR scan.*

Flash Duration (ms)	30
Capture Elapsed Time (s)	43.34
Camera Frequency (Hz)	37.94
Integration Time (s)	2

**E.72.5.6 Inspection Results**

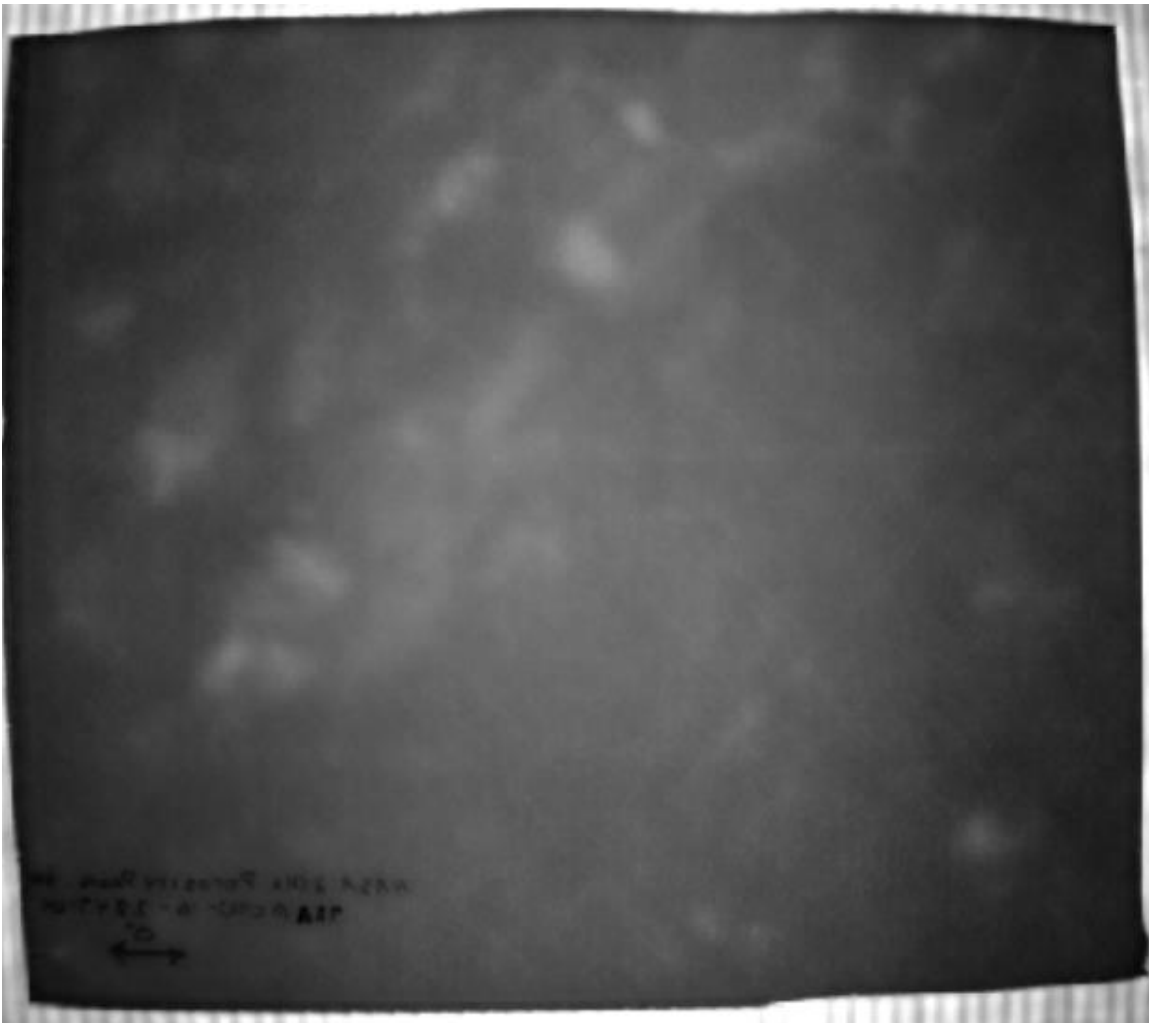


*Figure E.72-19. SSIR image of Specimen #72.*

## Porosity Panel #4

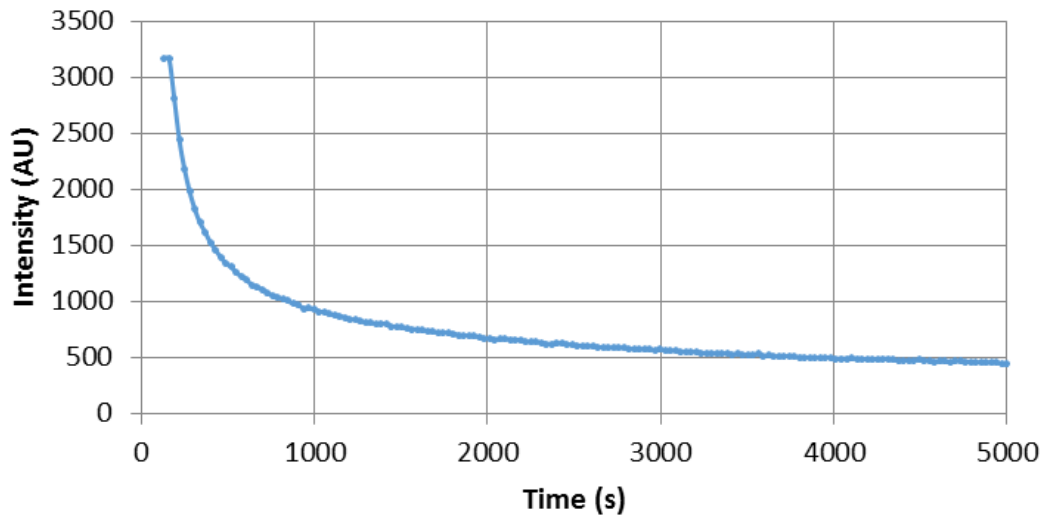


Figure E.72-20. Intensity curve showing heat dispersion over time for Specimen #72.

### E.72.5.7 References

- [1] Parker, W. J.; Jenkins, R. J.; Butler, C. P.; and Abbott, G. L.: "Method of Determining Thermal Diffusivity, Heat Capacity and Thermal Conductivity," *Journal of Applied Physics*, 32 (9): 1679, Bibcode:1961JAP....32.1679P. doi:10.1063/1.1728417, 1961.

### E.72.6 Method: Through-Transmission Infrared Thermography (TTIR)

#### E.72.6.1 Partner: NGIS

#### E.72.6.2 Technique Applicability: ★★★

#### E.72.6.3 Laboratory Setup

TT thermography images were acquired using a FLIR SC6000 IR camera setup. The flash hood is mounted in a fixed location on an optical table. The thermal camera is mounted on a tripod with the panel between it and the flash hood. The panel is held vertically within a fixture that slides across a linear track between captures in order to ensure total coverage. Paper light shields were constructed for the fixture to block flash spillover around the edges of the panel.

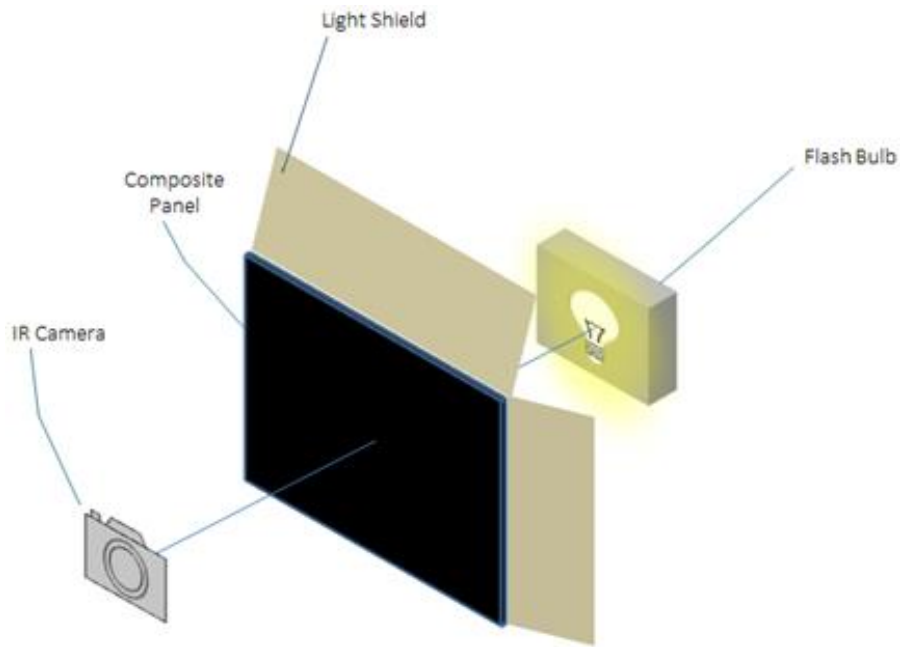


*Figure E.72-21. TTIR schematic.*

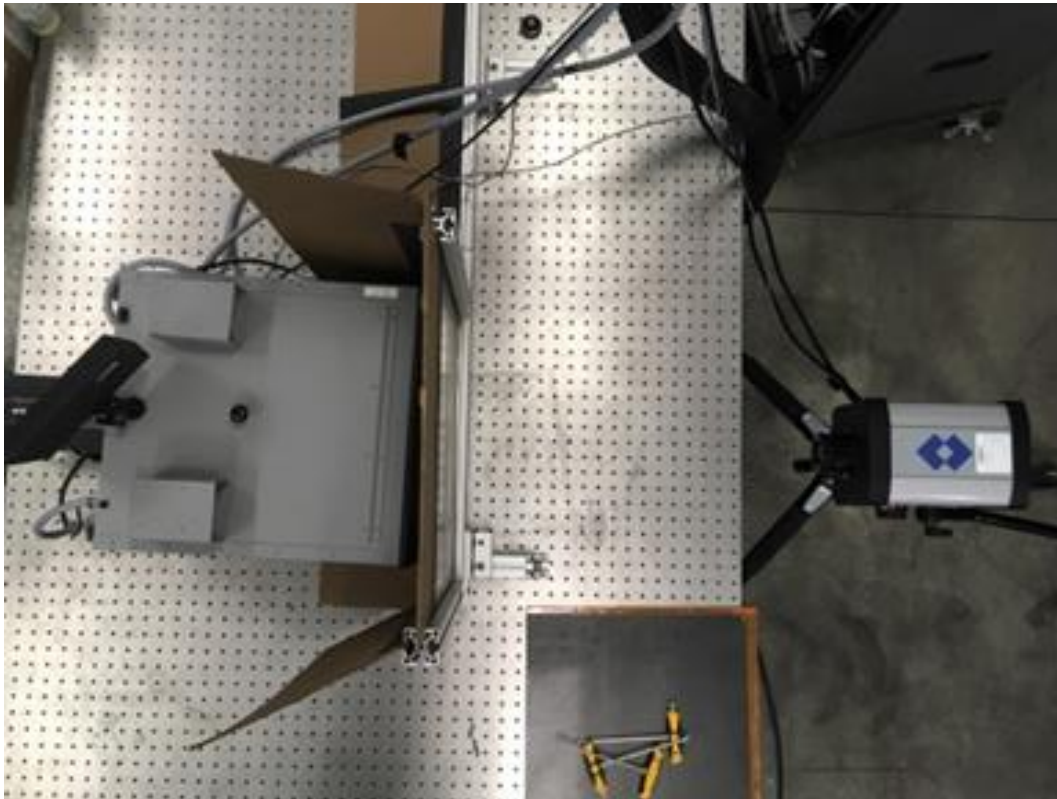


*Figure E.72-22. Photo of TTIR setup.*

**E.72.6.4 Equipment List and Specifications:**

- FLIR SC6000 IR camera, mid wavelength IR sensor (3.0- to 5.0- $\mu\text{m}$ )
- Flash power supplies, hood, and lamps
- EchoTherm® V8 Software



### E.72.6.5 Settings

Table E.72-9. Equipment settings for TTIR scan.

Panel Thickness (mm)	3.66
Flash Duration (ms)	30
Capture Elapsed Time (s)	43.34
Camera Frequency (Hz)	4.18
Integration Time (s)	2

### E.72.6.6 Inspection Results

## Specimen #72

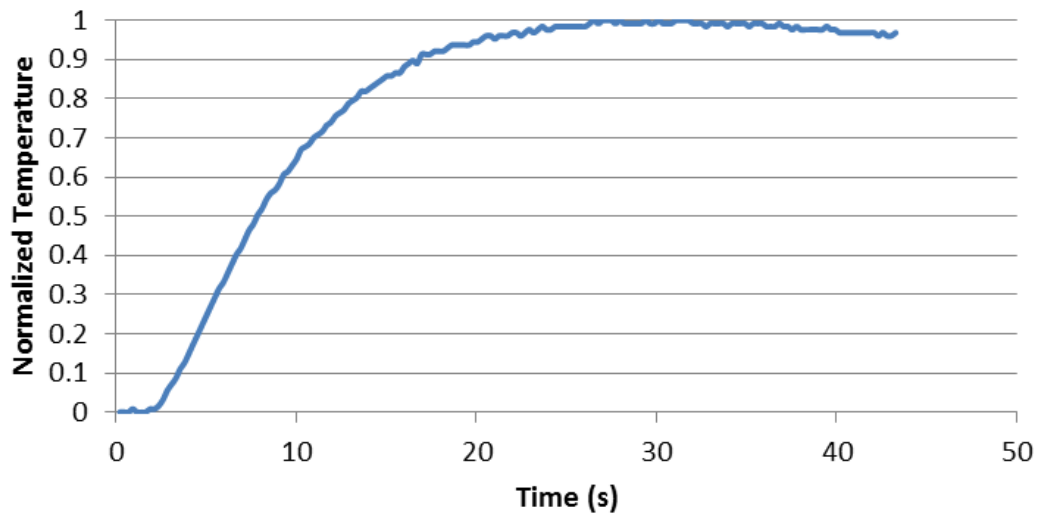


Figure E.72-23. Temperature curve showing the dispersion of heat over time during image capture.

## Specimen #72

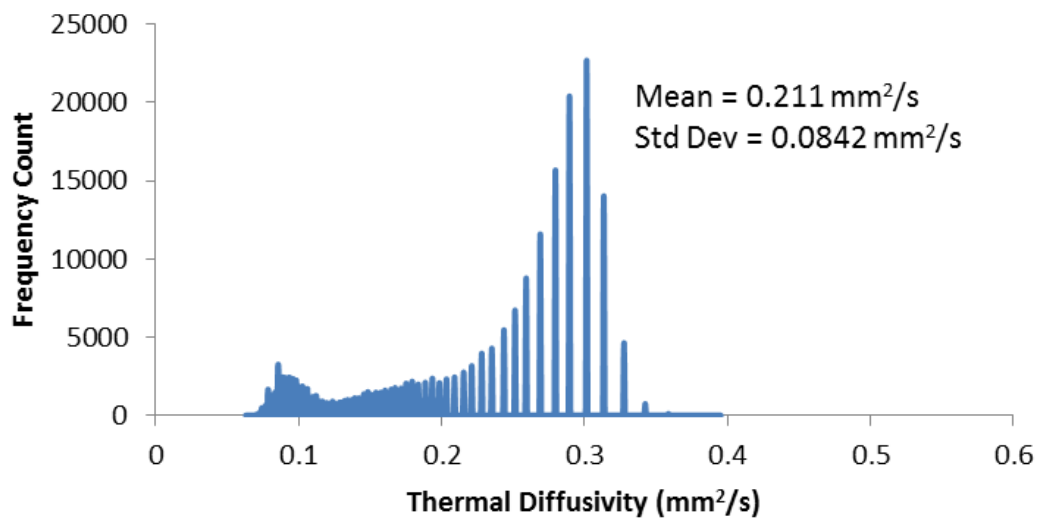


Figure E.72-24. Histogram showing frequency of thermal diffusivity values. Expansive point spread shows inconsistent levels of porosity throughout panel and a high standard deviation shows high porosity levels.

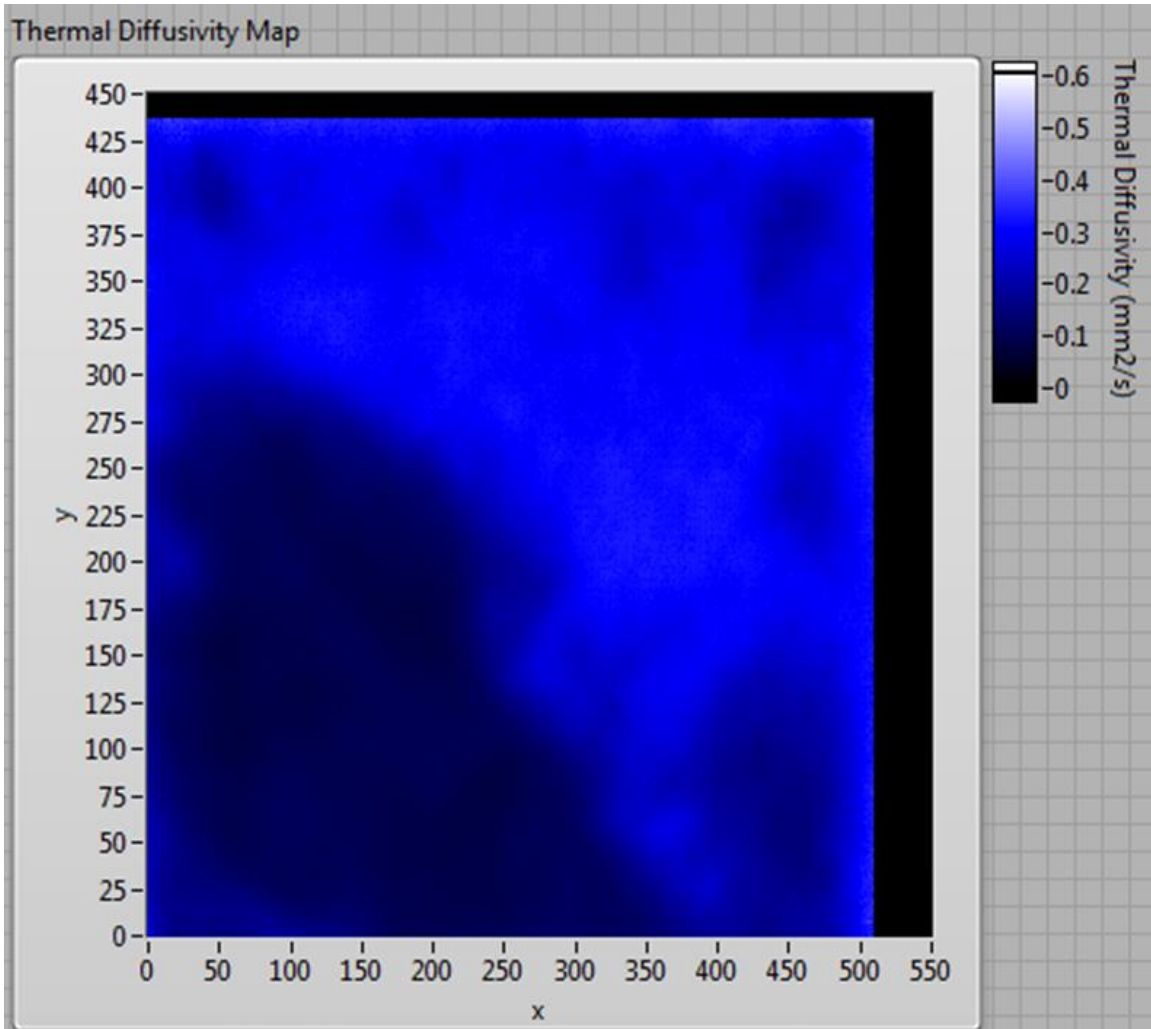


Figure E.72-25. Image of thermal diffusivity post processing.  
Dark patches show areas of high porosity.

#### E.72.6.7 References

- [2] Parker, W. J.; Jenkins, R. J.; Butler, C. P.; and Abbott, G. L.: “Method of Determining Thermal Diffusivity, Heat Capacity and Thermal Conductivity,” *Journal of Applied Physics*, 32 (9): 1679, Bibcode:1961JAP....32.1679P. doi:10.1063/1.1728417, 1961.

#### E.73 Specimen #73 – NASA-005-STANDARD-001 – Not Tested

Structure	Material	Details	Dimensions (inches)	Partner Methods
Quasi-isotropic	IM7/8552 satin weave fabric	Rotocraft blade spar tube – pristine	11.5 × 8.5 × 2.8	Not Tested

#### E.74 Specimen #74 – NASA-005-STANDARD-002 – Not Tested

Structure	Material	Details	Dimensions (inches)	Partner Methods
Quasi-isotropic	IM7/8552 satin weave fabric	Rotocraft blade spar tube – pristine	11.5 × 8.5 × 2.8	Not Tested

**E.75 Specimen #75 – NASA-005-Wrinkle-001 – Not Tested**

Structure	Material	Details	Dimensions (inches)	Partner Methods
Quasi-isotropic	IM7/8552 satin weave fabric	Rotocraft blade spar tube – out of plane wrinkle	11.5 × 8.5 × 2.8	Not Tested

**E.76 Specimen #76 – NASA-05-Wrinkle-002 – Not Tested**

Structure	Material	Details	Dimensions (inches)	Partner Methods
Quasi-isotropic	IM7/8552 satin weave fabric	Rotocraft blade spar tube – out of plane wrinkle	11.5 × 8.5 × 2.8	Not Tested

**E.77 Specimen #77 – NASA-005-Porosity-001 – Not Tested**

Structure	Material	Details	Dimensions (inches)	Partner Methods
Quasi-isotropic	IM7/8552 satin weave fabric	Rotocraft blade spar tube – porosity	11.5 × 8.5 × 2.8	Not Tested

**E.78 Specimen #78 – NASA-005-Porosity-002 – Not Tested**

Structure	Material	Details	Dimensions (inches)	Partner Methods
Quasi-isotropic	IM7/8552 satin weave fabric	Rotocraft blade spar tube – porosity	11.5 × 8.5 × 2.8	Not Tested

**E.79 Specimen #79: NASA-005-Porosity-003**

Structure	Material	Details	Dimensions (inches)	Partner Methods	
Quasi Isotropic	IM7/8552 satin weave fabric and unidirectional	Rotocraft blade spar tube with porosity	11.5 × 8.5 × 2.8	NASA	E.79.1 PEUT



*Figure E.79-1. Photographs of Specimen #79: NASA 005 Porosity 003.*

**E.79.1 Method: Pulse-Echo Ultrasound Testing (PEUT)**

**E.79.1.1 Partner: NASA**

**E.79.1.2 Technique Applicability: ★★★**

PEUT is capable of detecting the porosity within this specimen.

### E.79.1.3 Laboratory Setup

Immersion Ultrasonic Testing: NASA LaRC uses a custom-designed single-probe ultrasonic scanning system. The system has an 8-axis motion controller, a multi-axis gantry robot mounted above a medium-size water tank, a dual-channel, 16-bit, high-speed digitizer, and an off-the-shelf ultrasonic pulser receiver. The system can perform TTUT and PEUT inspections. TT inspection employs two aligned ultrasonic probes, one transmitter, and one receiver, placed on either side of a test specimen. Pulse-echo inspection is a single-sided method where a single ultrasonic probe is both transmitter and receiver. In each method, data are acquired while raster scanning the ultrasonic probe(s) in relation to a part. Figure E.79-2 shows a simplified block diagram of a scanning Pulse-echo inspection.

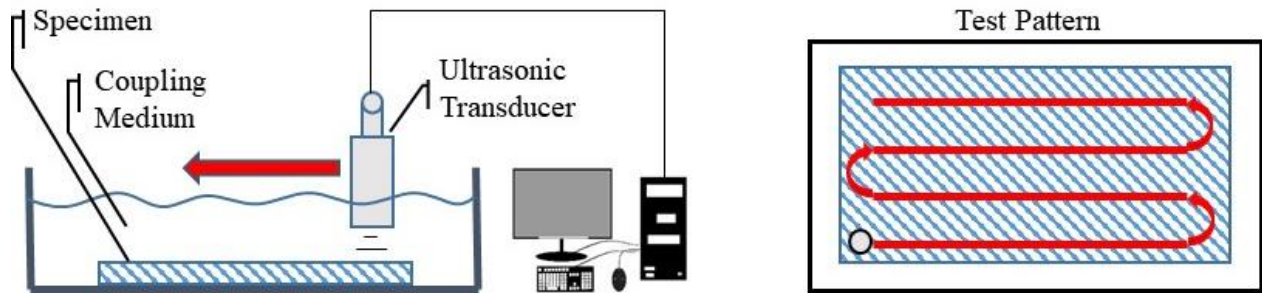


Figure E.79-2. Ultrasonic system components.

### E.79.1.4 Equipment List and Specifications:

- Pulser/Receiver: Olympus 5073PR
- Digitizer: AlazarTech ATS9462, dual channel, 16 bit, 180 MS/s
- Sensor: Olympus 2-inch spherical focus immersion ultrasonic transducer
- Motion system: open looped stepper motor based X-YY-Z gantry robot
- Motion Controller: Galil DMC-4183
- Acquisition Software: FastScan, custom developed at NASA LaRC
- Signal Processing Software: DataViewer, custom developed at NASA LaRC

### E.79.1.5 Settings

Table E.79-1. Data collection settings.

Resolution (horizontal) [in/pixel]	0.05
Resolution (vertical) [in/pixel]	0.05
Probe frequency [MHz]	10
Focal Length [in]	2
Array Dimensions [pixels]	211 × 181

The specimen is placed flat against the zero position of the tank raised above the glass bottom by several metal washers. The test probe is computer-controlled and correlated to the position on the sample. It is also focused to a point one mm below the surface of the test material. The specimen remains in place while the transducer follows a preprogrammed test grid across the surface as indicated in Figure E.79-2. At each point, ultrasonic data are collected from individual pulses. Larger step sizes between data collection result in lower image resolution. These data points are reconstructed into a data cube displaying spatial coordinates as time progresses. 2D reconstruction

of the collection of ultrasonic responses create flattened slices at varying depths within the material.

### E.79.1.6 Inspection Results

Specimen #79 is a rotocraft blade tube spar fabricated from IM7/8552 with the objective of achieving porosity in the tube walls. PEUT was performed on this specimen in NASA’s immersion tank specified above.

Figure E.79-3 shows three large instances of large porosity at depths of 0.054, 0.073 and 0.096 inches. The larger porosity appears white initially as the air pocket reflects acoustic waves creating a strong early response. Smaller porosity exists throughout the bulk of the specimen as indicated by the scattered white specs. The dark band is a consequence of surface tape on the specimen blocking acoustic waves.

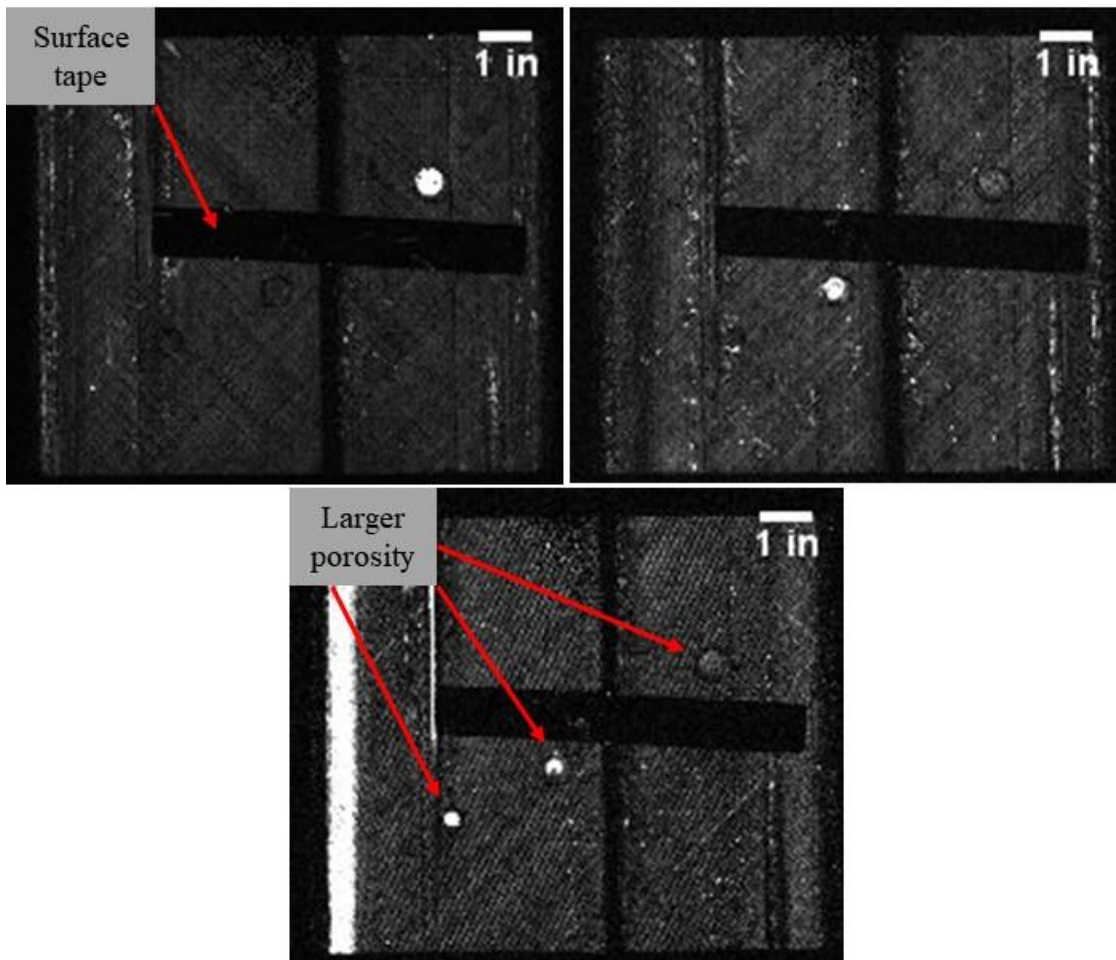


Figure E.79-3. PEUT image of large porosity throughout the side wall of the specimen.

### E.80 Specimen #80 – NASA-005-Porosity-004 – Not Tested

Structure	Material	Details	Dimensions (inches)	Partner Methods
Quasi-isotropic	IM7/8552 satin weave fabric	Rotocraft blade spar tube – porosity	11.5 × 8.5 × 2.8	Not Tested



**E.81 Specimen #81: Boeing Impact QI 45 8ply 6x5 Impact 1**

Structure	Material	Details	Dimensions (inches)	Partner Methods	
8 plies	IM7/8552	Single Impact Location	6 × 5 6 × 3	Boeing	E.81.1 XCT E.81.2 X-ray CR
				NASA	E.81.3 PEUT

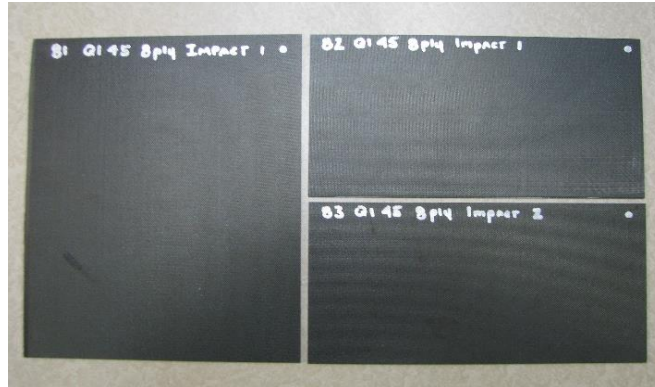


*Figure E.81-1. Photographs of radii delamination standard.*

**E.81.1 Method: X-ray Computed Tomography (XCT)**

**E.81.1.1 Partner: Boeing**

**E.81.1.2 Technique Applicability: ★★☆☆**

XCT is able to detect impact damage on some of the panels.

**E.81.1.3 Equipment List and Specifications:**

- YXLON Modular CT System
- 225 kV microfocus X-ray source with variable focal spot size
- 100 kg capacity 7 axis granite based manipulator
- XRD 1621 Detector- 2048 × 2048 pixels with 200-μm pitch, 400 × 400-mm active area
- 111-μm spatial resolution for impact panel scan
- Volume Graphics 3.0 visualizing software
- Reconstruction Computer

**E.81.1.4 Settings**

*Table E.81-1. Data collection settings.*

Source Energy	120 kV
Current	0.60 mA
Magnification	1.80 X
Filter	Copper
# Rotational angles	1410
Exposure time / frame	500 ms
Frame Binning	2
Spatial Resolution (μm)	111 μm
Array Dimensions (pixels)	Set 1: 1999 × 362 × 1998 Set 2: 1998 × 686 × 1997

### E.81.1.5 Laboratory Setup

The Digital Radiography Center (DRC) utilizes an YXLON Modular CT System. This system has the capability to utilize various X-ray sources for varying applications, including a 450-kV source, a microfocus source, and a nanofocus source. The microfocus source used has a variable focal spot size of less than 4  $\mu\text{m}$  and is suitable for magnifications up to 10X, with the nanofocus ranging up to 187X. The detector has 3 degrees of freedom (DOFs), allowing the effective detector area to be increased through combined scans. The manipulator controls the position of the detector, object, and source. It has 7 DOFs including a rotating stage to rotate the object during the scan. The entire system includes the source, detector, manipulator, control and reconstruction computers, and user control station. The computers and control station are outside of the radiation enclosure (vault) and utilize a safety interlock system to operate. Cameras are located in the vault to allow the operator to monitor the part from outside the enclosure.

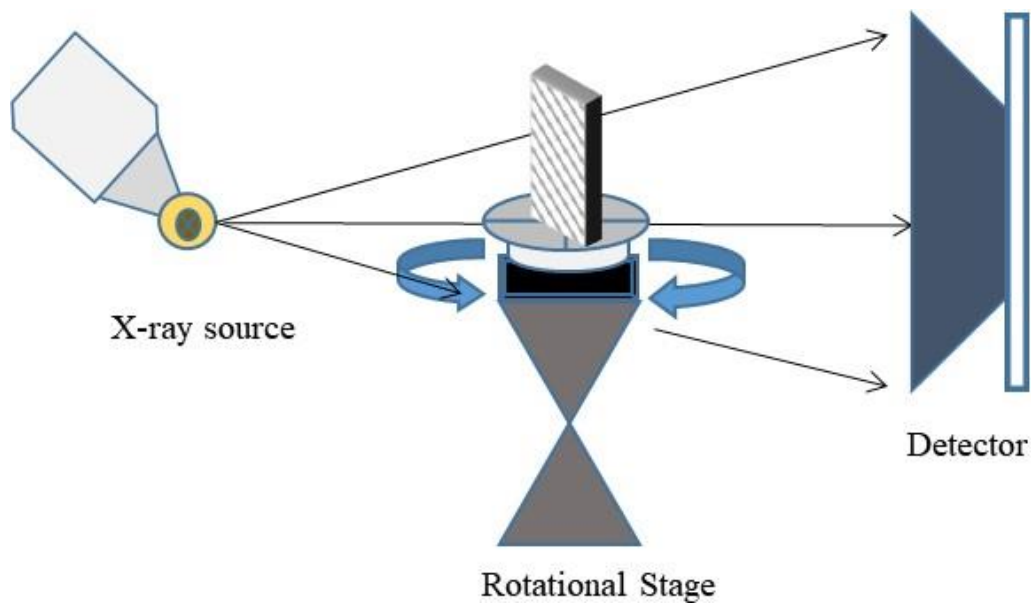


*Figure E.81-2. XCT system components.*

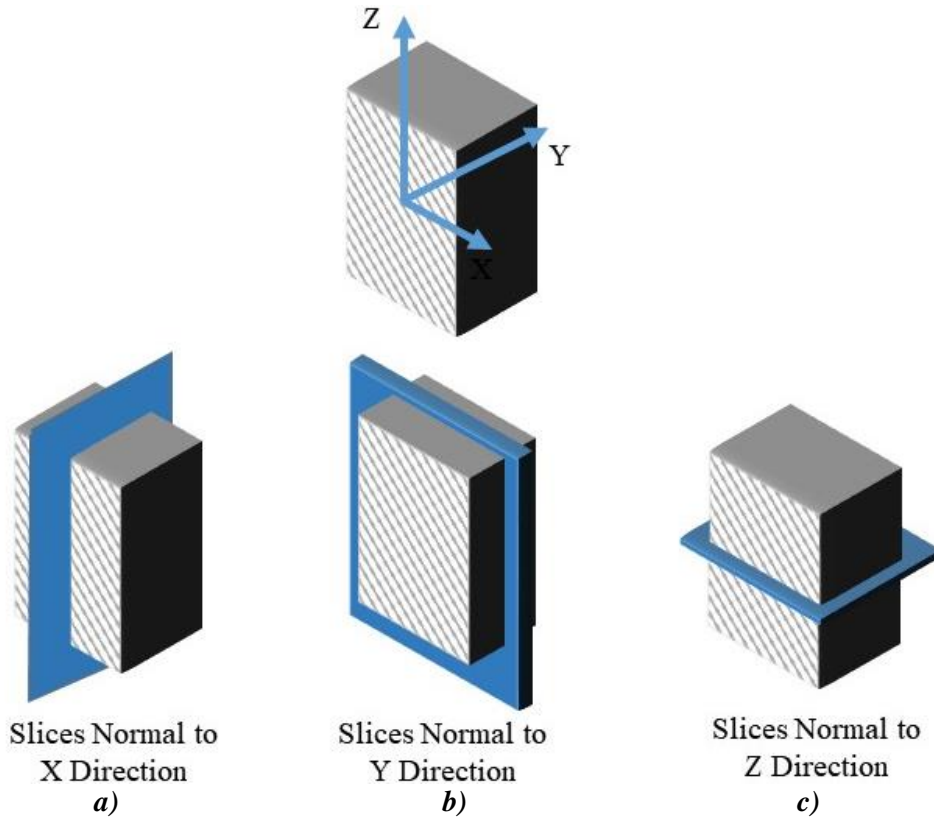


**Figure E.81-3. Slice direction nomenclature.**

To reduce overall scan time, the standard panels of the same thickness were stacked together, separated by light foam sheets and held together with tape. This allowed three parts to be scanned at once and analyzed separately in post-processing. The panel bundle was then secured in a foam fixture. The position of the specimen, source, and detector are controlled to produce geometric magnification of the image and increase the spatial resolution. The image data are gathered as X-rays penetrate the part and expose the detector for a set amount of time. For each scan, these image data are collected at 1410 different angles throughout a 360° rotation. These images are then reconstructed to create the 3D volume dataset. This dataset is viewed and analyzed in Volume Graphics, a volume rendering software, to identify the relevant components.

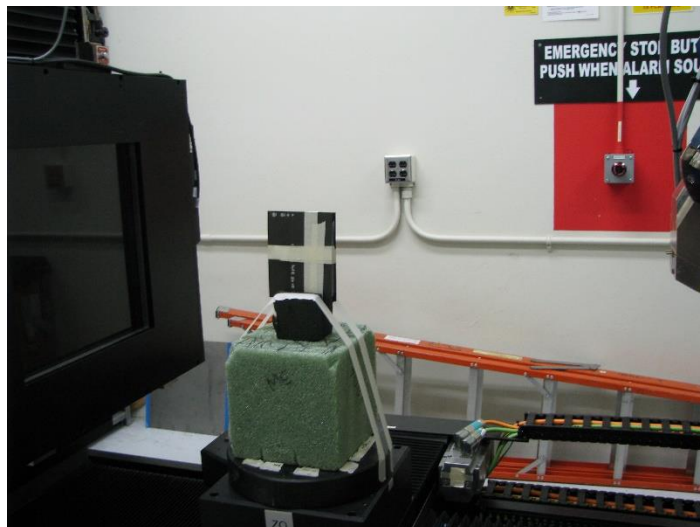


*Figure E.81-4. Microfocus XCT setup for impact damage standards.*

#### **E.81.1.6 Inspection Results**

Unlike 2D X-ray imaging, CT shows slice views of the object that are not superimposed. This allows for improved detection of flaws. In the case of the impact panels, the damage would show as a slightly dented region at the near surface. Figure E.81-5 shows a slice view at the near surface of each panel. The dark spot in the center of Figure E.81-5b and c indicates less dense or lack of material, caused by the indentation of the impact on Panels 82 and 83. The tape used to hold the panels together for the scan is visible in Figure E.81-5a, however there is no detected impact damage for Panel 81.

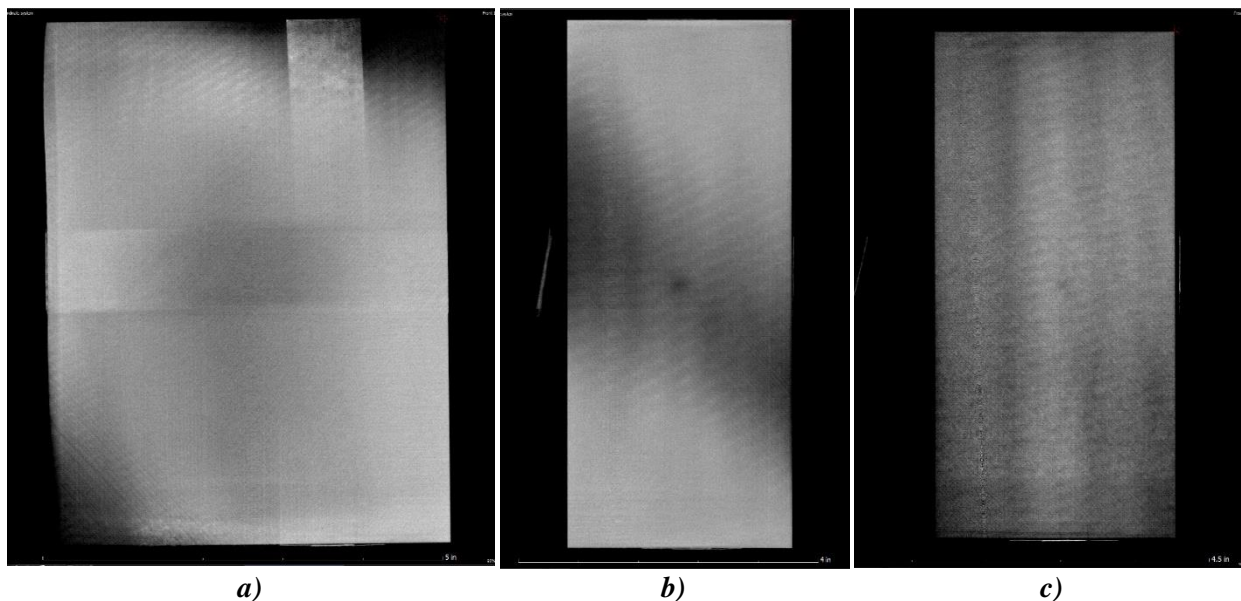


*Figure E.81-5. CT slice view of 8-ply impact damage panels 81 (a), 82 (b), and 83 (c).*

## E.81.2 Method: X-ray Computed Radiography (CR)

### E.81.2.1 Partner: Boeing

### E.81.2.2 Technique Applicability: ☆☆☆

X-ray CR is unable to reliably detect the impact damage.

### E.81.2.3 Equipment List and Specifications:

- Philips 160 kV X-Ray source, 0.4 mm focal spot size
- IPS Phosphorus Imaging Plate
- GE CRxFlex Scanner, 50  $\mu\text{m}$  resolution
- GE Rhythm Review 5.0 visualizing software

### E.81.2.4 Settings

*Table E.81-2. Imaging and exposure parameters.*

Source Energy	40 kV
Current	2 mA
Source-Detector Distance	60 in
Magnification	1X
Exposure time	20 s
Resolution ( $\mu\text{m}$ )	50 $\mu\text{m}$
Imaging Area (in)	14 $\times$ 17

### E.81.2.5 Laboratory Setup:

The DRC has a small X-ray enclosure (vault) for the primary purpose of 2D X-ray imaging. It includes a Philips 160-kV X-ray source and the ability to use film, CR, and digital detector arrays. The CR imaging plates are placed on a table and the source, suspended from the ceiling by a 3-axis crane, can be positioned to control the Source to Object Distance. Outside of the enclosure are the controls for the source, utilizing a safety interlock system. These controls allow the user to set the energy, current, and exposure time for the source. In addition to the vault, the DRC utilizes a CRxFlex system to scan and erase the CR imaging plates, storing the images on a computer. The phosphorus imaging plates, after exposure to X-rays, will luminesce the images when exposed to red light, allowing the 50- $\mu\text{m}$  scanner to create digital versions and “erase” the plates using bright white light to be used again. The CR digital images are then reviewed using Rhythm Review.



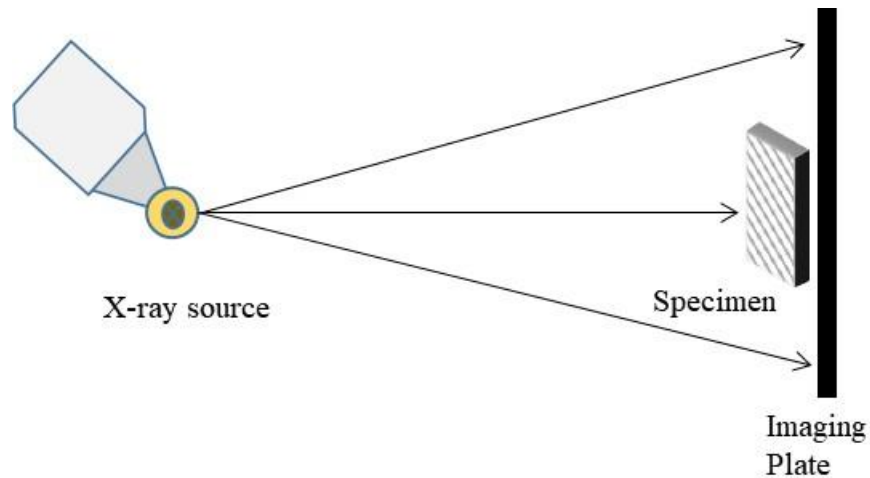


*Figure E.81-6. X-ray CR imaging.*

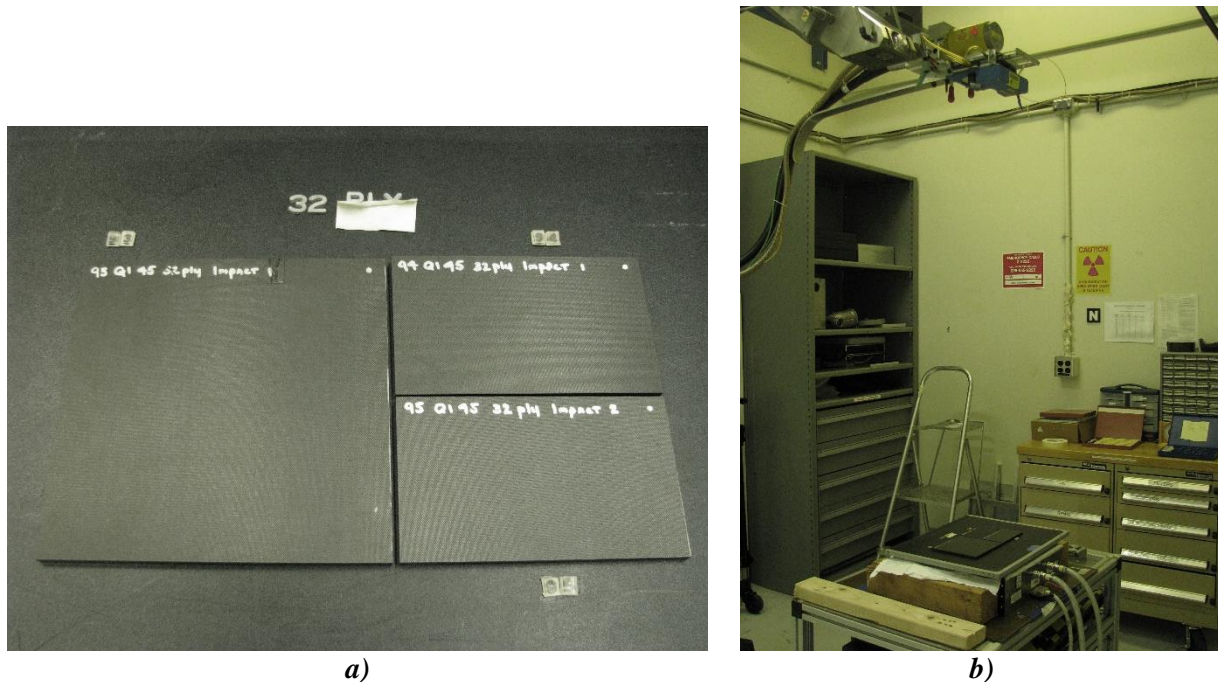


*Figure E.81-7. Laboratory setup of impact plate standards for CR imaging.*

### E.81.2.6 Inspection Results

CR imaging is dependent on the superimposed density of the part being imaged. In the case of the impact damage, the damaged portion tends to get indented, slightly compressing the material underneath the indent. Therefore, the superimposed density remains approximately the same. This makes the detection of impact damage by an operator using 2D radiography such as CR very difficult. As seen in Figure E.81-8, the impact damage is not easily visible. Given knowledge of the locations, an operator may be able to discern damage but contrast from the damage is not enough to be detected in a general case.

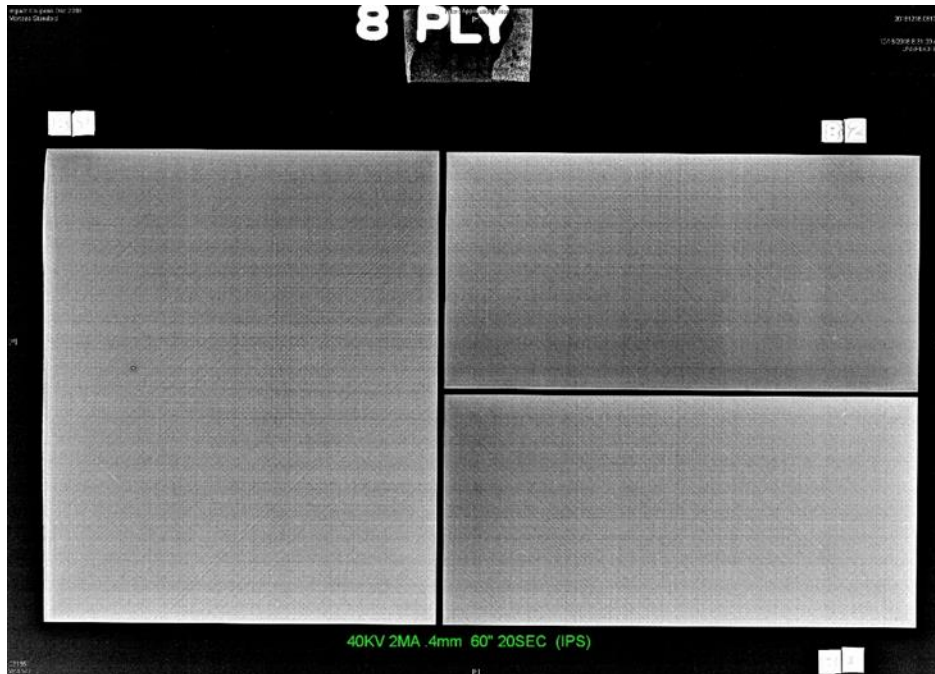


Figure E.81-8. Flash filtered CR image of 8-ply impact panels.

**E.81.3 Method: Pulse-Echo Ultrasound Testing (PEUT)**

**E.81.3.1 Partner: NASA**

**E.81.3.2 Technique Applicability: ★★ ★**

PEUT detected the impact damage in this sample.

**E.81.3.3 Laboratory Setup**

Immersion Ultrasonic Testing: NASA LaRC uses a custom-designed single-probe ultrasonic scanning system. The system has an 8-axis motion controller, a multi-axis gantry robot mounted above a medium-size water tank, a dual-channel, 16-bit, high-speed digitizer, and an off-the-shelf ultrasonic pulser receiver. The system can perform TTUT and PEUT inspections. TT inspection employs two aligned ultrasonic probes, one transmitter, and one receiver, placed on either side of a test specimen. Pulse-echo inspection is a single-sided method where a single ultrasonic probe is both transmitter and receiver. In each method, data are acquired while raster scanning the ultrasonic probe(s) in relation to a part. Figure E.81-9 shows a simplified block diagram of a scanning Pulse-echo inspection

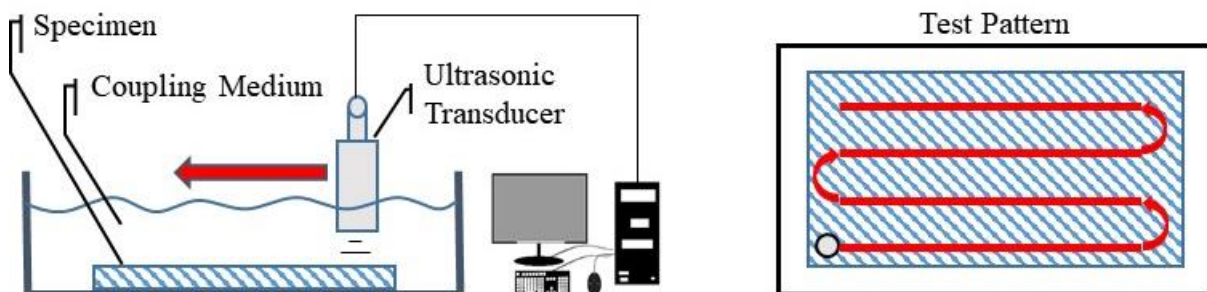


Figure E.81-9. Ultrasonic system components.



*Figure E.81-10. Specimen baseline inspection orientation.*

#### **E.81.3.4 Equipment List and Specifications:**

- Pulsar/Receiver: Olympus 5073PR
- Digitizer: AlazarTech ATS9462, dual channel, 16 bit, 180 MS/s
- Sensor: Olympus 2-inch spherical focus immersion ultrasonic transducer
- Motion system: open looped stepper motor based X-YY-Z gantry robot
- Motion Controller: Galil DMC-4183
- Acquisition Software: FastScan, custom developed at NASA LaRC
- Signal Processing Software: DataViewer, custom developed at NASA LaRC

#### **E.81.3.5 Settings**

*Table E.81-3. Post-impact inspection settings.*

Resolution (horz) [in/pixel]	0.01
Resolution (ver) [in/pixel]	0.01
Probe frequency [MHz]	10
Focal Length [in]	2
Array Dimensions [pixels]	501 × 601

The specimen is placed flat against the zero position of the tank raised above the glass bottom by several metal washers. The test probe is computer-controlled and correlated to the position on the sample. It is also focused to a point 1 mm below the surface of the test material. The specimen remains in place while the transducer follows a preprogrammed test grid across the surface as indicated in Figure E.81-9. At each point, ultrasonic data are collected from individual pulses. Larger step sizes between data collection result in lower image resolution. These data points are reconstructed into a data cube displaying spatial coordinates as time progresses. 2D reconstruction of the collection of ultrasonic responses create flattened slices at varying depths within the material.

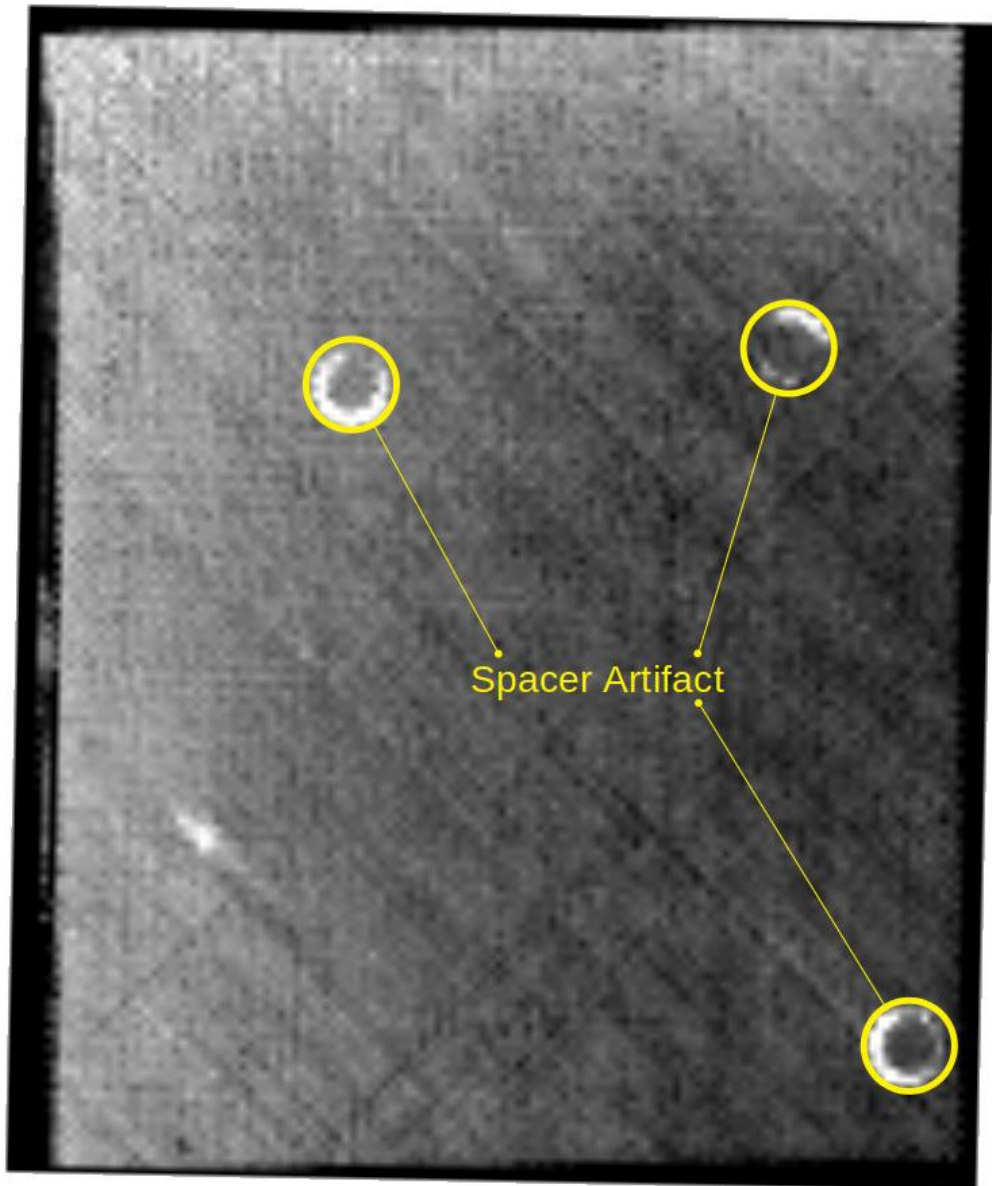
#### **E.81.3.6 Inspection Results**

Specimen #81 is a 6 by 5-inch, 8-ply flat panel with an 0.34-inch impact. PEUT was performed on this specimen in NASA's immersion tank specified above.

Figure E.81-11 shows a back side surface amplitude image of the sample in its pre-impacted state. No significant internal flaws were noted. The highlighted areas above are high-amplitude

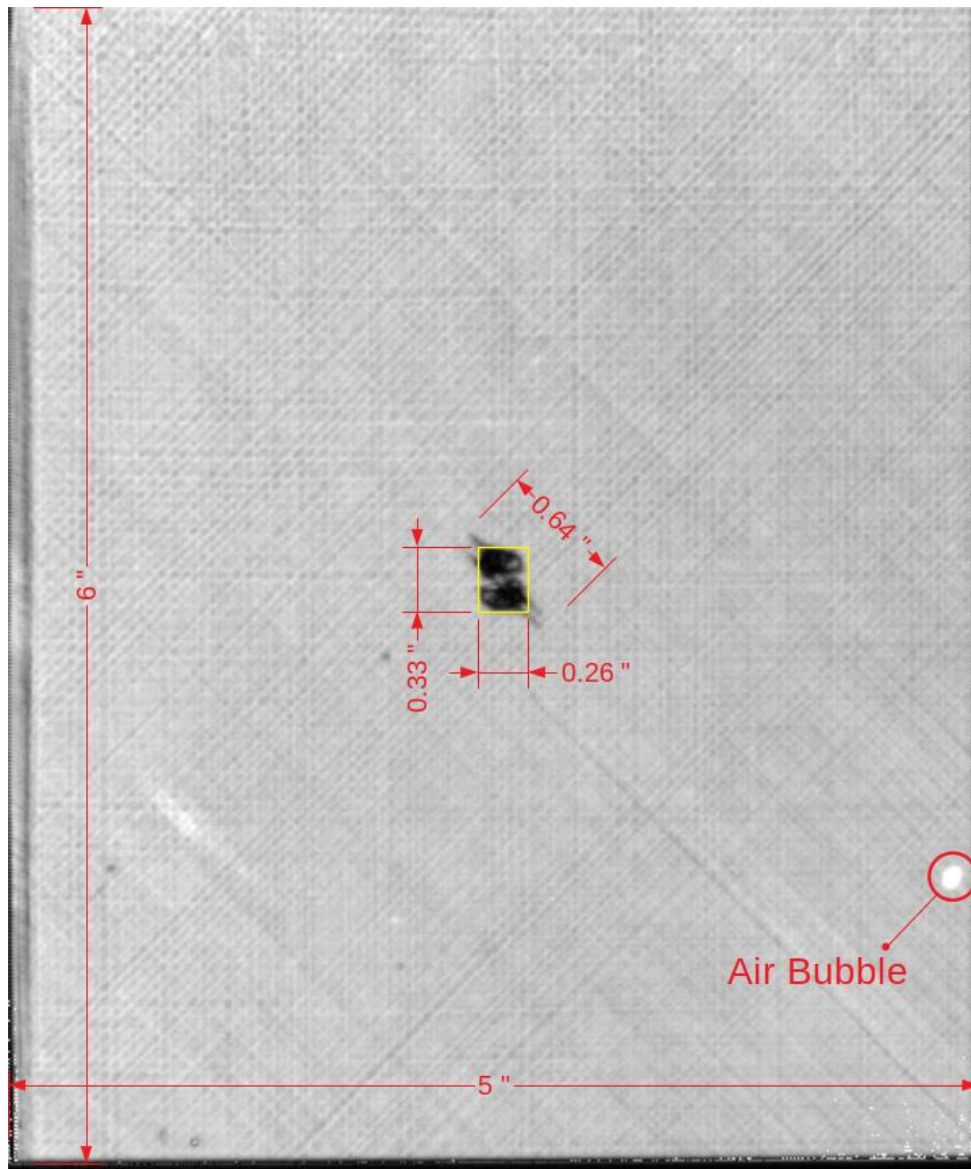
reflections from the three spacers used to position the sample above the bottom of the immersion tank.

Figure E.81-12a shows a back side surface amplitude image of the sample in its post-impacted state. The impact damage region is identified with measurements. An air bubble on the under side of the sample in the immersion tank is also noted. Figure E.81-12b is an internal reflection amplitude image. The gate region is selected to highlight reflections from the delaminations caused by the impact.



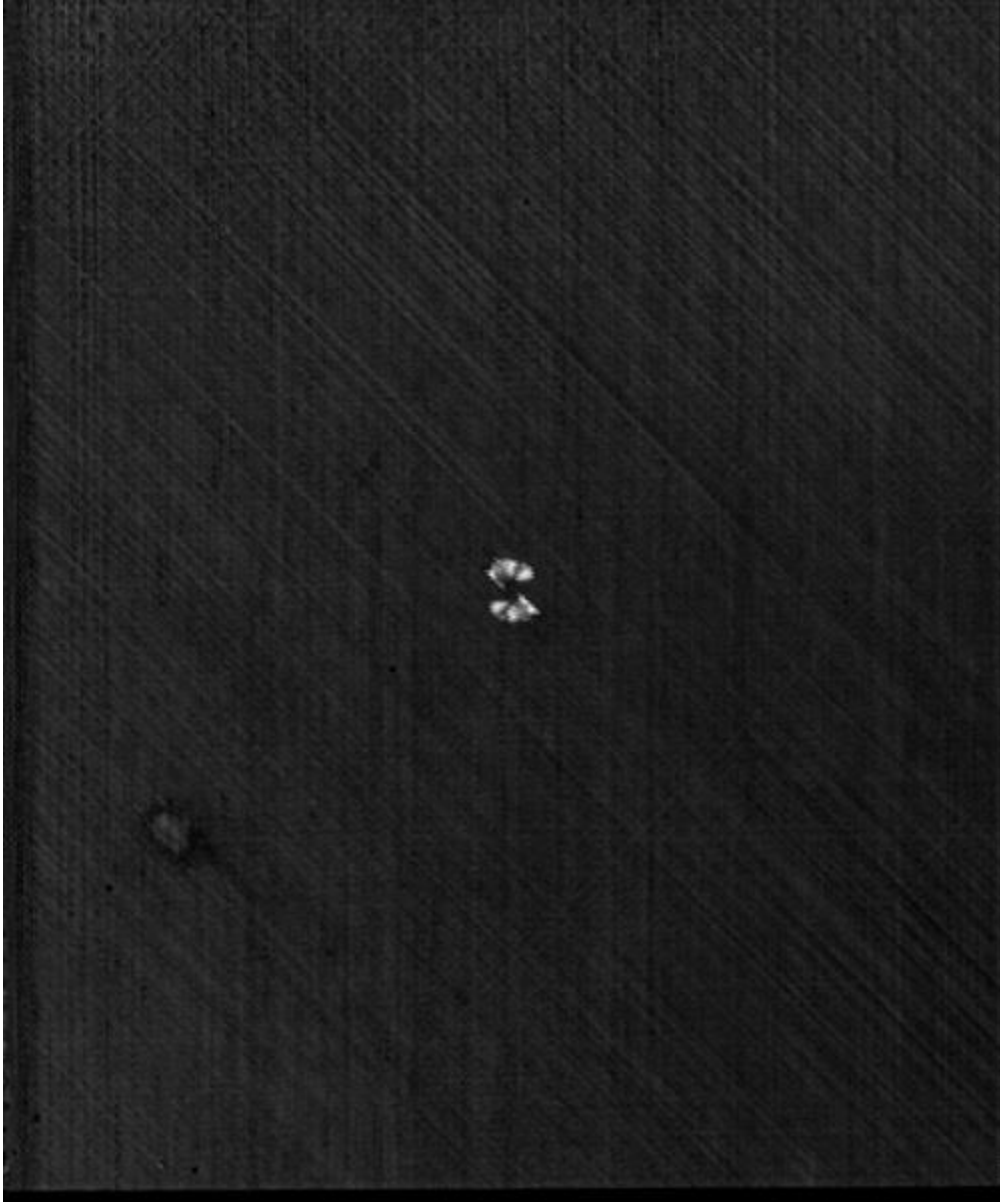
*Figure E.81-11. 10-MHz baseline image.*





*a) Back side surface amplitude image.*





*b) Internal reflection amplitude image.  
Figure E.81-12. 10-MHz post-impact image.*

**E.82 Specimen #82: Boeing Impact QI\_45 8ply 3x6 Impact 1**

Structure	Material	Details	Dimensions (inches)	Partner Methods	
8 plies	IM7/8552	Single Impact Location	6 × 5 6 × 3	Boeing	E.82.1 XCT E.82.2 X-ray CR
				NASA	E.82.3 PEUT E.82.4 SSIR E.82.5 XCT

**E.82.1 Method: X-ray Computed Tomography**

**E.82.1.1 Partner: Boeing**

**E.82.1.2 Technique Applicability: ★★☆☆**

XCT is able to detect impact damage on some of the panels.

**E.82.2 Method: X-ray Computed Radiography (CR)**

**E.82.2.1 Partner: Boeing**

**E.82.2.2 Technique Applicability: ☆☆☆**

X-ray CR is unable to reliably detect the impact damage. Refer back to Specimen #81.

**E.82.3 Method: Pulse-Echo Ultrasound Testing (PEUT)**

**E.82.3.1 Partner: NASA**

**E.82.3.2 Technique Applicability: ★★☆☆**

PEUT detected the impact damage in this sample.

**E.82.3.3 Laboratory Setup**

Immersion Ultrasonic Testing: NASA LaRC uses a custom-designed single-probe ultrasonic scanning system. The system has an 8-axis motion controller, a multi-axis gantry robot mounted above a medium-size water tank, a dual-channel, 16-bit, high-speed digitizer, and an off-the-shelf ultrasonic pulser receiver. The system can perform TTUT and PEUT inspections. TT inspection employs two aligned ultrasonic probes, one transmitter, and one receiver, placed on either side of a test specimen. Pulse-echo inspection is a single-sided method where a single ultrasonic probe is both transmitter and receiver. In each method, data are acquired while raster scanning the ultrasonic probe(s) in relation to a part. Figure E.82-1 shows a simplified block diagram of a scanning Pulse-echo inspection.

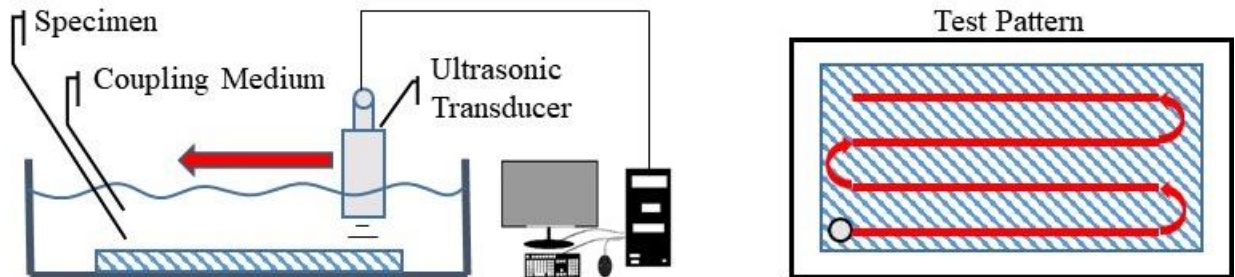


*Figure E.82-1. Ultrasonic system components.*

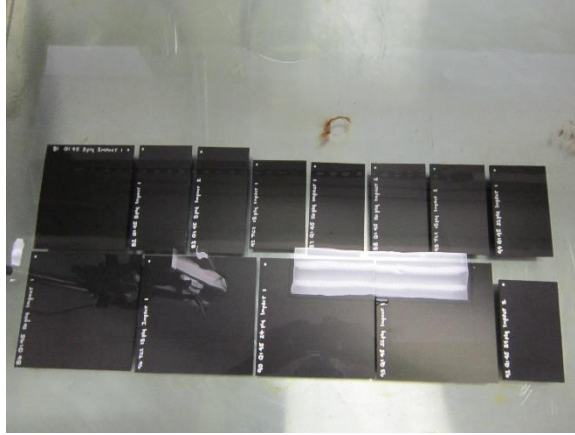


*Figure E.82-2. Specimen baseline inspection orientation.*

#### **E.82.3.4 Equipment List and Specifications:**

- Pulsar/Receiver: Olympus 5073PR
- Digitizer: AlazarTech ATS9462, dual channel, 16-bit, 180 MS/s
- Sensor: Olympus 2-inch spherical focus immersion ultrasonic transducer
- Motion system: open looped stepper motor based X-YY-Z gantry robot
- Motion Controller: Galil DMC-4183
- Acquisition Software: FastScan, custom developed at NASA LaRC
- Signal Processing Software: DataViewer, custom developed at NASA LaRC

#### **E.82.3.5 Settings**

*Table E.82-1. Post-impact inspection settings.*

Resolution (horz) [in/pixel]	0.01
Resolution (ver) [in/pixel]	0.01
Probe frequency [MHz]	10
Focal Length [in]	2
Array Dimensions [pixels]	601 × 311

The specimen is placed flat against the zero position of the tank raised above the glass bottom by several metal washers. The test probe is computer-controlled and correlated to the position on the sample. It is also focused to a point one mm below the surface of the test material. The specimen remains in place while the transducer follows a preprogrammed test grid across the surface as indicated in Figure E.82-1. At each point, ultrasonic data are collected from individual pulses. Larger step sizes between data collection result in lower image resolution. These data points are reconstructed into a data cube displaying spatial coordinates as time progresses. 2D reconstruction of the collection of ultrasonic responses create flattened slices at varying depths within the material.

#### **E.82.3.6 Inspection Results**

Specimen #82 is a 3 by 6-inch, 8-ply flat panel with a 0.82-inch impact. PEUT was performed on this specimen in NASA's immersion tank specified above.

Figure E.82-3 shows a back side surface amplitude image of the sample in its pre-impacted state. No significant internal flaws were noted. The highlighted areas above are high-amplitude

reflections from the three spacers used to position the sample above the bottom of the immersion tank.

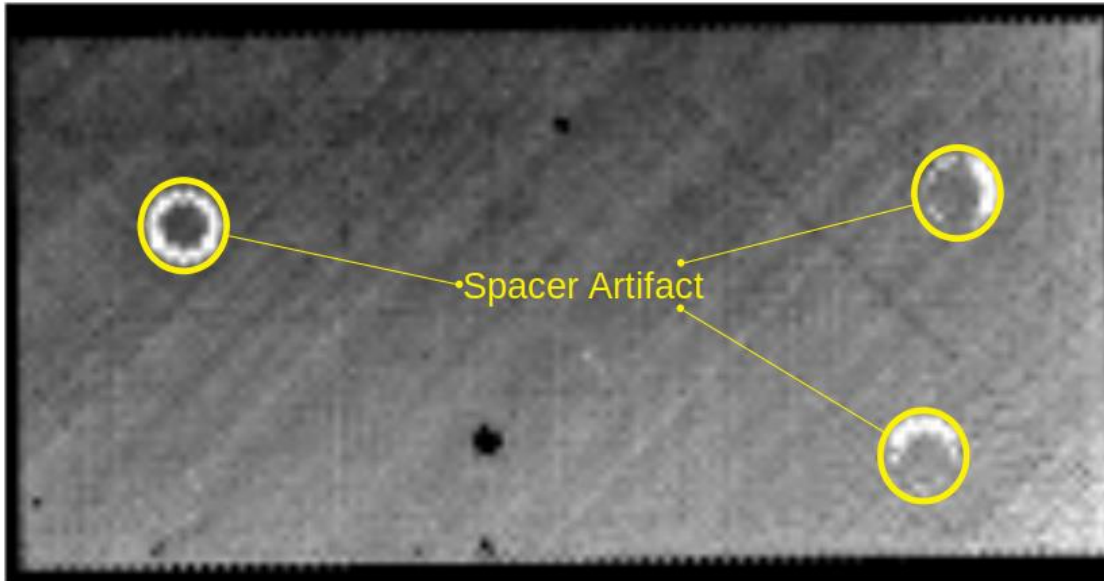
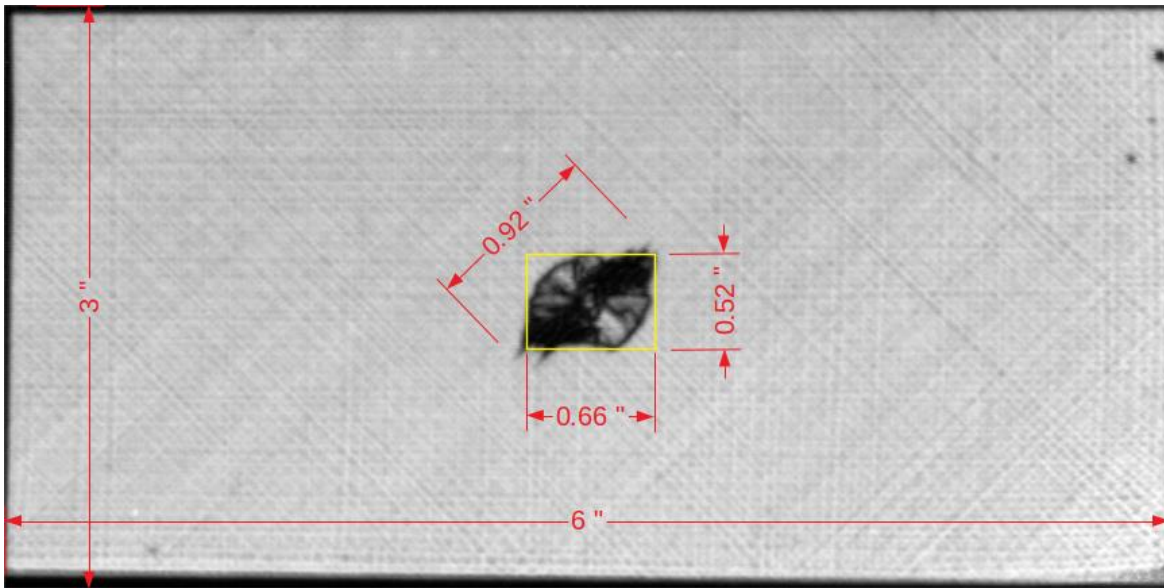
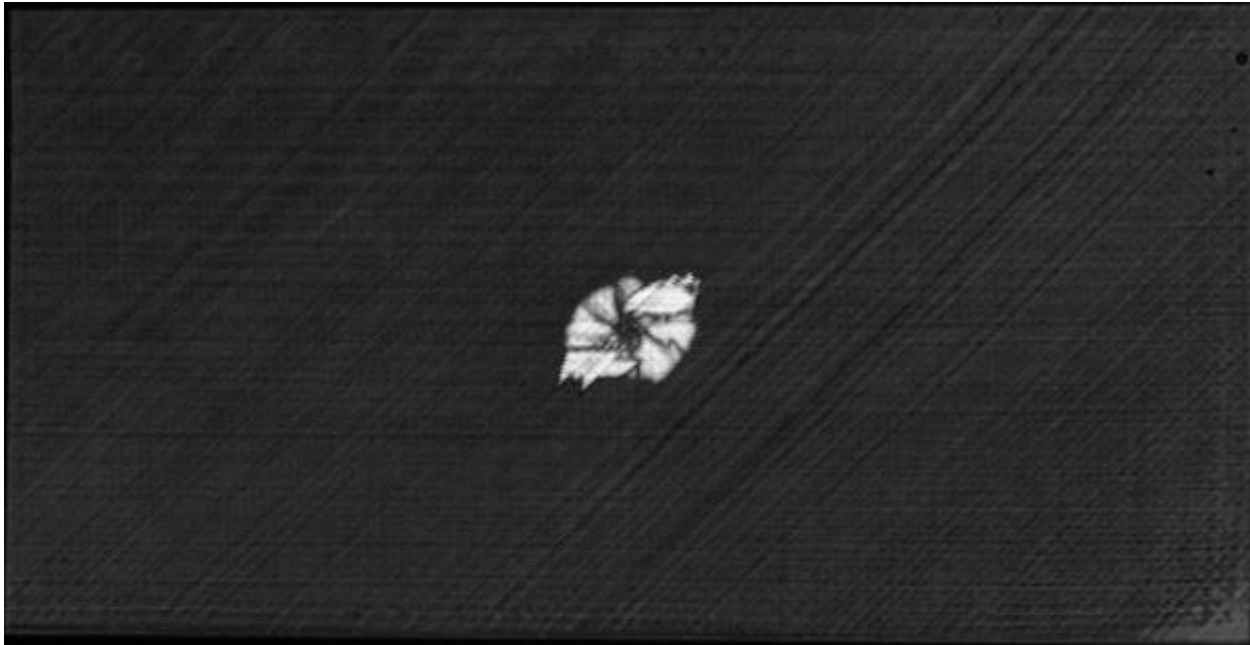


*Figure E.82-3. 10-MHz baseline image.*

Figure E.82-4a shows a back side surface amplitude image of the sample in its post-impacted state. The impact damage region is identified with measurements. Figure E.82-4b is an internal reflection amplitude image. The gate region is selected to highlight reflections from the delaminations caused by the impact.



*a) Back side surface amplitude image.*



*b) Internal reflection amplitude image.*

*Figure E.82-4. 10-MHz post-impact image.*

**E.82.4 Method: X-ray Computed Tomography (XCT)**

**E.82.4.1 Partner: NASA**

**E.82.4.2 Technique Applicability: ★★★**

XCT is capable of imaging and quantifying the damage due to low-impact energy in this specimen.

**E.82.4.3 Laboratory Setup**

The microfocus XCT system at NASA LaRC is a commercially available Avonix (Nikon C2) Metrology System designed for high-resolution NDE inspections. The system is an advanced



microfocus X-ray system, capable of resolving details down to 5  $\mu\text{m}$ , and with magnifications up to 60X. The system is supplied as a complete, large-dimension radiation enclosure, with X-ray source, specimen manipulator, and an amorphous silica detector as shown in Figure E.82-5. The imaging controls are housed in a separate control console. The detector is a Perkin-Elmer 16-bit amorphous silicon digital detector with a  $2000 \times 2000$ -pixel array.

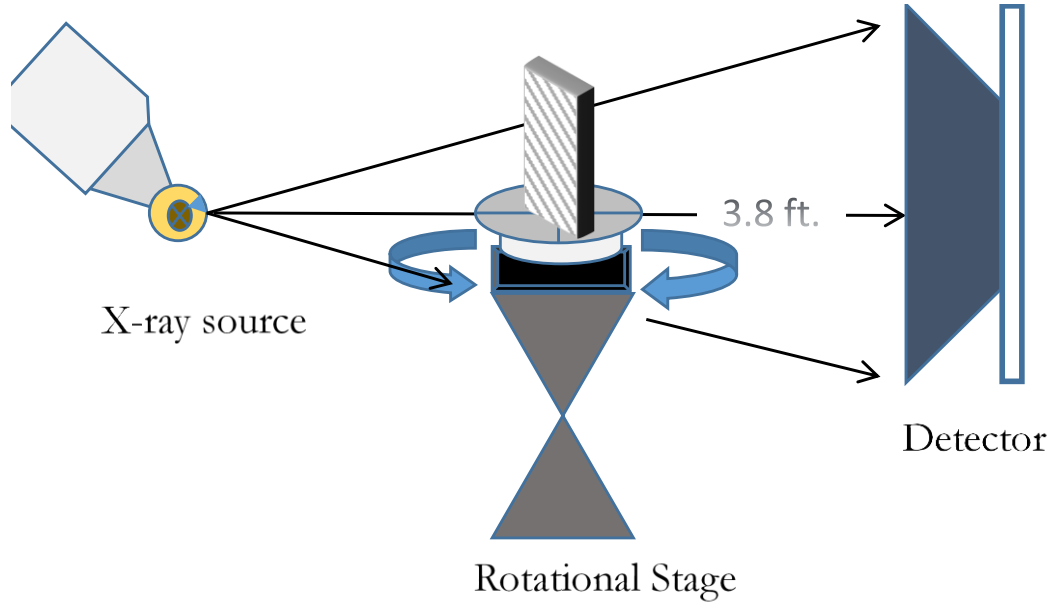


*Figure E.82-5. XCT system components.*

A consistent Cartesian coordinate system is used to define slice direction as illustrated in Figure E.82-6. Slices normal to the X, Y, and Z-directions are shown in Figure E.82-6a, b, and c, respectively.

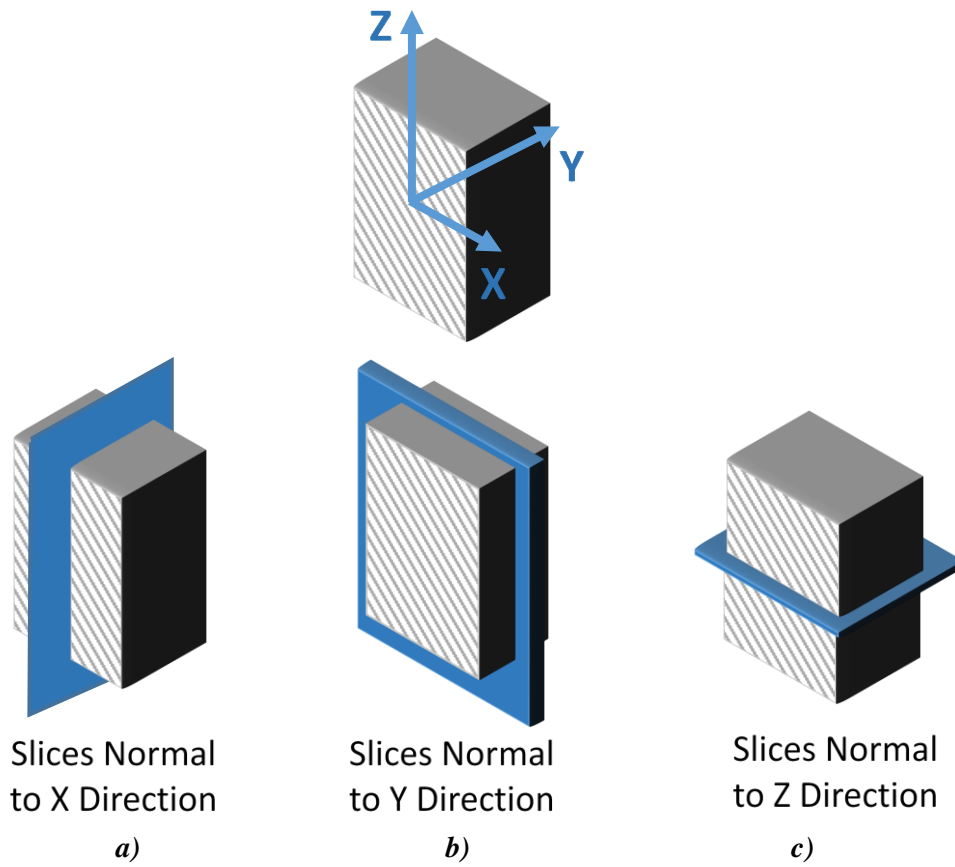


*Figure E.82-6. Slice direction nomenclature.*

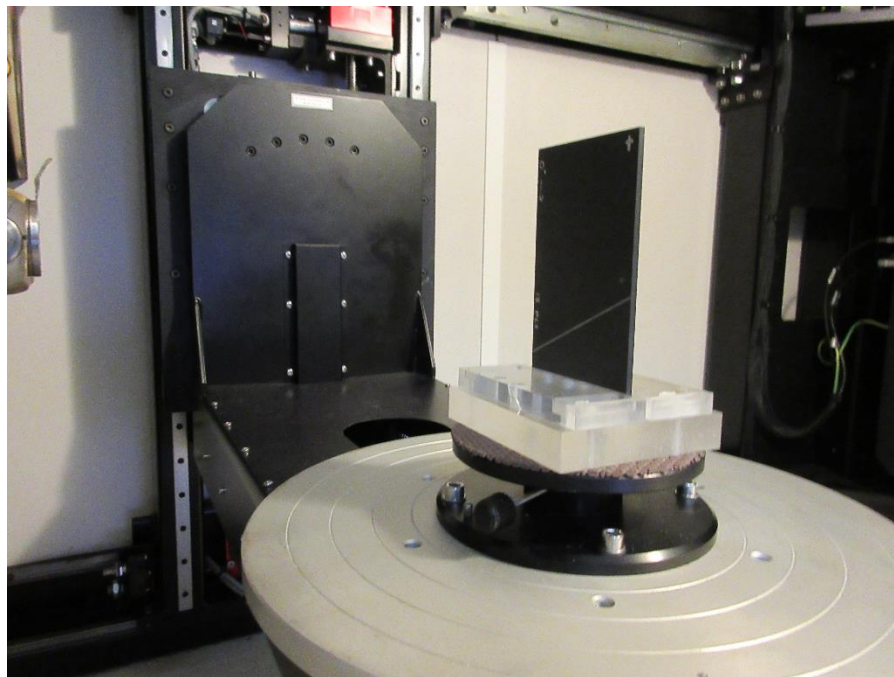


*Figure E.82-7. Impact specimen test stand setup.*

#### E.82.4.4 Equipment List and Specifications:

- Avonix 225 CT System
- 225 kV microfocus X-ray source with 5  $\mu\text{m}$  focal spot size
- 15 or 30kg Capacity 5 axis fully programmable manipulator.
- Detector: Perkin Elmer XRD 1621 – 2000  $\times$  2000 pixels with 200  $\mu\text{m}$  pitch
- 10  $\mu\text{m}$  spatial resolution for specimens 1.5 cm wide
- Thin panels 10-inch  $\times$  10-inch – full volume 200  $\mu\text{m}$  spatial resolution

#### E.82.4.5 Settings

*Table E.82-2. Data collection settings.*

Source Energy	160 kV
Current	37 $\mu\text{A}$
Magnification	5.0 X
Filter	0.125 Sn
# Rotational angles	3142
Exposure time / frame	1.0 sec
Max Histogram Grey Level	51 K
# Averages	8
Resolution ( $\mu\text{m}$ )	40.04 $\mu\text{m}$
Array Dimensions (pixels)	Set 1: 1999 $\times$ 362 $\times$ 1998 Set 2: 1998 $\times$ 686 $\times$ 1997

The specimen is placed vertically (rotated about the smallest dimension) on the rotational stage located between the radiation source and the detector. The rotational stage is computer-controlled and correlated to the position of the sample. As the sample is rotated the full 360° (~0.11° increments), the detector collects radiographs at each rotated angle as the X-ray path intersects the sample. 3D reconstruction of the collection of radiographs produces a volume of data that can then be viewed along any plane in the volume. The closer the sample can be placed to the X-ray source, the higher the spatial resolution that can be obtained.

#### E.82.4.6 Data and Results

Specimen #82, is a 3 by 6-inch 8-ply flat panel with a Barely Visible Impact Damage (BVID) impact. XCT was performed on this specimen in NASA LaRC's CT system with the settings defined in Table E-82.2.

The damage caused by the impact is clearly seen from all viewing directions as shown in Figure E.82-8. There is no surface indication of an impact. Damage extends approximately halfway through the thickness of the specimen.



*Figure E.82-8. CT slice normal to the thickness direction show delaminations and matrix cracking (left). CT slice normal to the front surface shows delaminations between plies (right).*

**E.83 Specimen #83: Boeing Impact QI\_45 8ply 3x6 Impact 2**

Structure	Material	Details	Dimensions (inches)	Partner Methods	
8 plies	IM7/8552	Single Impact Location	6 × 5 6 × 3	Boeing	E.81.1 XCT E.81.2 X-ray CR
				NASA	E.81.3 PEUT E.81.4 XCT

**E.83.1 Method: X-ray Computed Tomography (XCT)**

**E.83.1.1 Partner: Boeing**

**E.83.1.2 Technique Applicability: ★★★**

XCT is able to detect impact damage on some of the panels. Refer to Specimen #81.

**E.83.2 Method: X-ray Computed Radiography (CR)**

**E.83.2.1 Partner: Boeing**

**E.83.2.2 Technique Applicability: ☆☆☆**

X-ray CR is able to detect impact damage on some of the panels. Refer to Specimen #81.

**E.83.3 Method: Pulse-Echo Ultrasound Testing (PEUT)**

**E.83.3.1 Partner: NASA**

**E.83.3.2 Technique Applicability: ★★★**

PEUT detected the impact damage in this sample.

### E.83.3.3 Laboratory Setup

Immersion Ultrasonic Testing: NASA LaRC uses a custom-designed single-probe ultrasonic scanning system. The system has an 8-axis motion controller, a multi-axis gantry robot mounted above a medium-size water tank, a dual-channel, 16-bit, high-speed digitizer, and an off-the-shelf ultrasonic pulser receiver. The system can perform TTUT and PEUT inspections. TT inspection employs two aligned ultrasonic probes, one transmitter, and one receiver, placed on either side of a test specimen. Pulse-echo inspection is a single-sided method where a single ultrasonic probe is both transmitter and receiver. In each method, data are acquired while raster scanning the ultrasonic probe(s) in relation to a part. Figure E.83-1 shows a simplified block diagram of a scanning Pulse-echo inspection

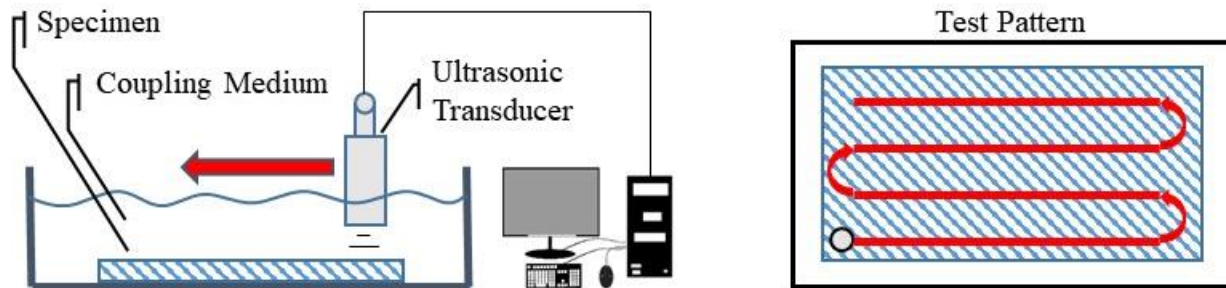


Figure E.83-1. Ultrasonic system components.

### E.83.3.4 Equipment List and Specifications:

- Pulser/Receiver: Olympus 5073PR
- Digitizer: AlazarTech ATS9462, dual channel, 16 bit, 180 MS/s
- Sensor: Olympus 2-inch spherical focus immersion ultrasonic transducer
- Motion system: open looped stepper motor based X-YY-Z gantry robot
- Motion Controller: Galil DMC-4183
- Acquisition Software: FastScan, custom developed at NASA LaRC
- Signal Processing Software: DataViewr, custom developed at NASA LaRC

### E.83.3.5 Settings

Table E.83-1. Post-impact inspection settings.

Resolution (horz) [in/pixel]	0.01
Resolution (ver) [in/pixel]	0.01
Probe frequency [MHz]	10
Focal Length [in]	2
Array Dimensions [pixels]	601 × 311

The specimen is placed flat against the zero position of the tank raised above the glass bottom by several metal washers. The test probe is computer-controlled and correlated to the position on the sample. It is also focused to a point 1 mm below the surface of the test material. The specimen remains in place while the transducer follows a preprogrammed test grid across the surface as indicated in Figure E.83-2. At each point, ultrasonic data are collected from individual pulses. Larger step sizes between data collection result in lower image resolution. These data points are reconstructed into a data cube displaying spatial coordinates as time progresses. 2D reconstruction



of the collection of ultrasonic responses create flattened slices at varying depths within the material.

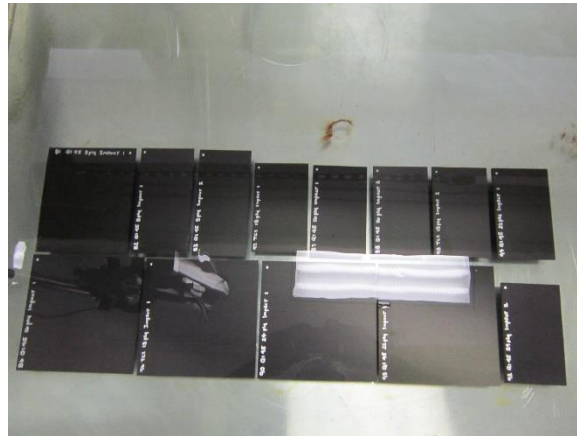
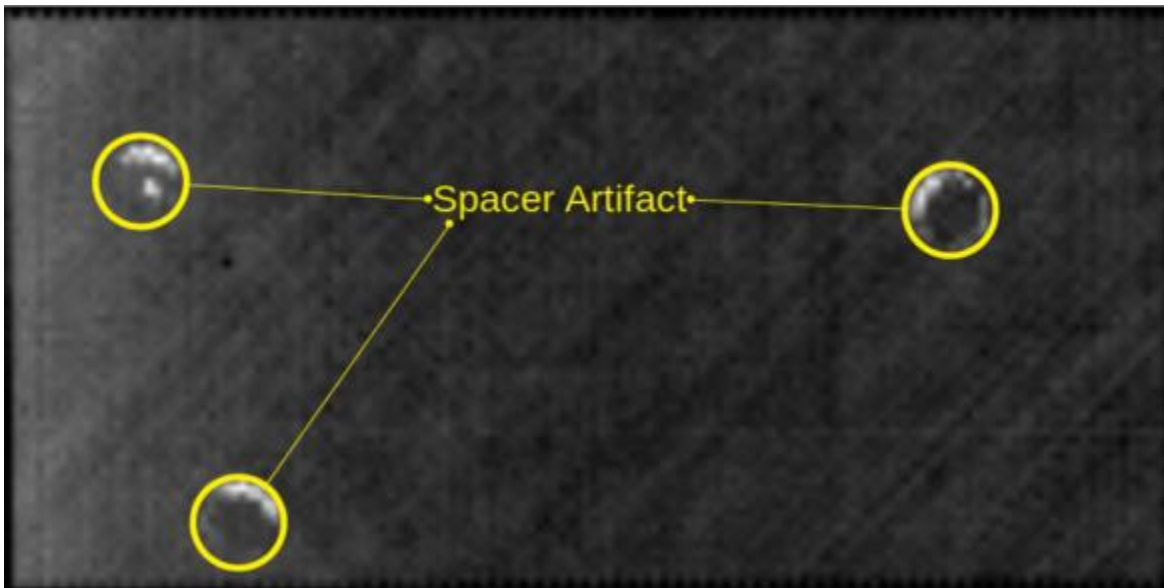


*Figure E.83-2. Specimen baseline inspection orientation.*

### **E.83.3.6 Inspection Results**

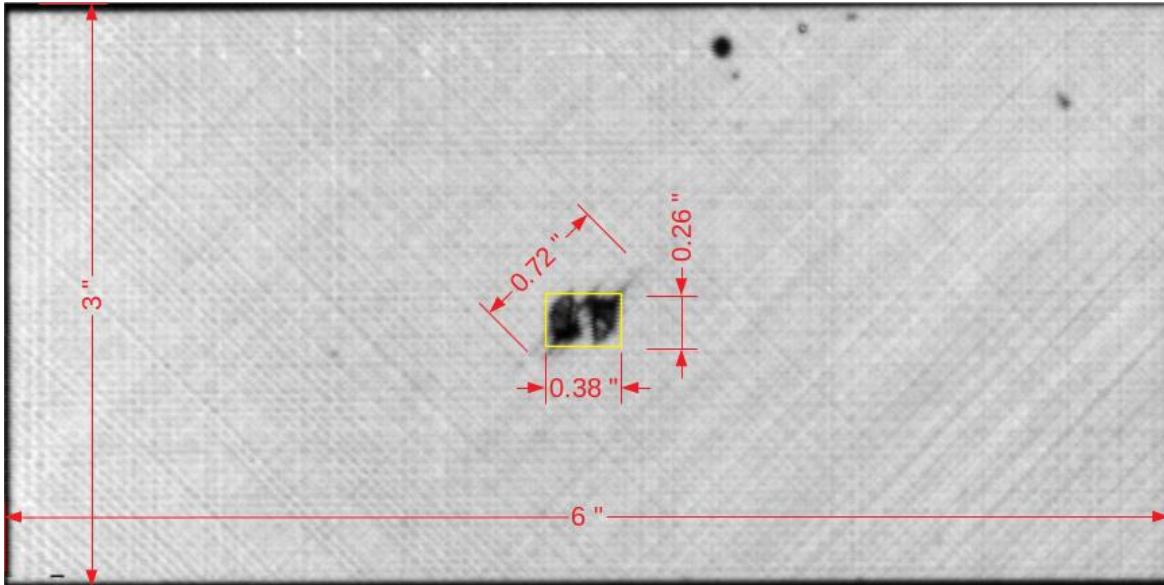
Specimen #83 is a 3 by 6-inch, 8-ply flat panel with a 0.37-inch impact. PEUT was performed on this specimen in NASA's immersion tank specified above.

Figure E.83-3 shows a back side surface amplitude image of the sample in its pre-impacted state. No significant internal flaws were noted. The highlighted areas above are high-amplitude reflections from the three spacers used to position the sample above the bottom of the immersion tank.

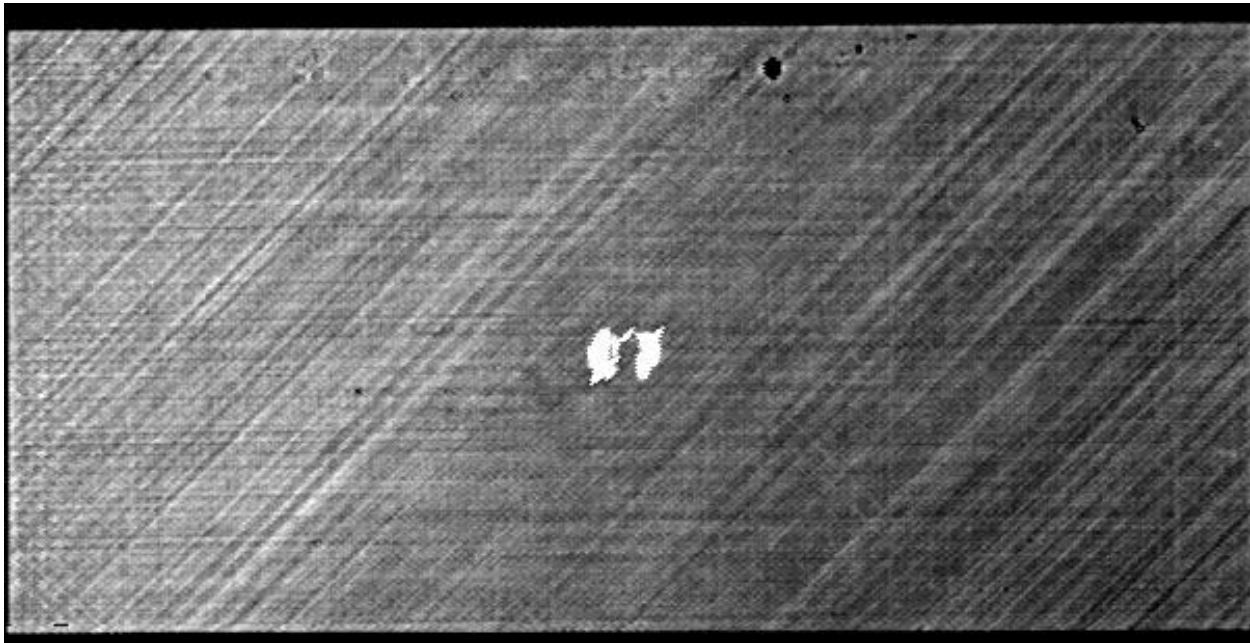


*Figure E.83-3. 10-MHz baseline image.*

Figure E.83-4a shows a back side surface amplitude image of the sample in its post-impacted state. The impact damage region is identified with measurements. Figure E.83-4b is an internal reflection amplitude image. The gate region is selected to highlight reflections from the delaminations caused by the impact. The large dark indication top-middle of both images is from a large air bubble on top of the sample overlooked during inspection.



*a) Back side surface amplitude image.*



*b) Internal reflection amplitude image.*

*Figure E.83-4. 10-MHz post-impact image.*

**E.83.4 Method: X-ray Computed Tomography (XCT)**

**E.83.4.1 Partner: NASA**

**E.83.4.2 Technique Applicability: ★★★**

XCT is capable of imaging and quantifying the damage due to low-impact energy in this specimen.

**E.83.4.3 Laboratory Setup**

The microfocus XCT system at NASA LaRC is a commercially available Avonix (Nikon C2) Metrology System designed for high-resolution NDE inspections. The system is an advanced

microfocus X-ray system, capable of resolving details down to 5  $\mu\text{m}$ , and with magnifications up to 60X. The system is supplied as a complete, large-dimension radiation enclosure, with X-ray source, specimen manipulator, and an amorphous silica detector as shown in Figure E.83-5. The imaging controls are housed in a separate control console. The detector is a Perkin-Elmer 16-bit amorphous silicon digital detector with a  $2000 \times 2000$ -pixel array.

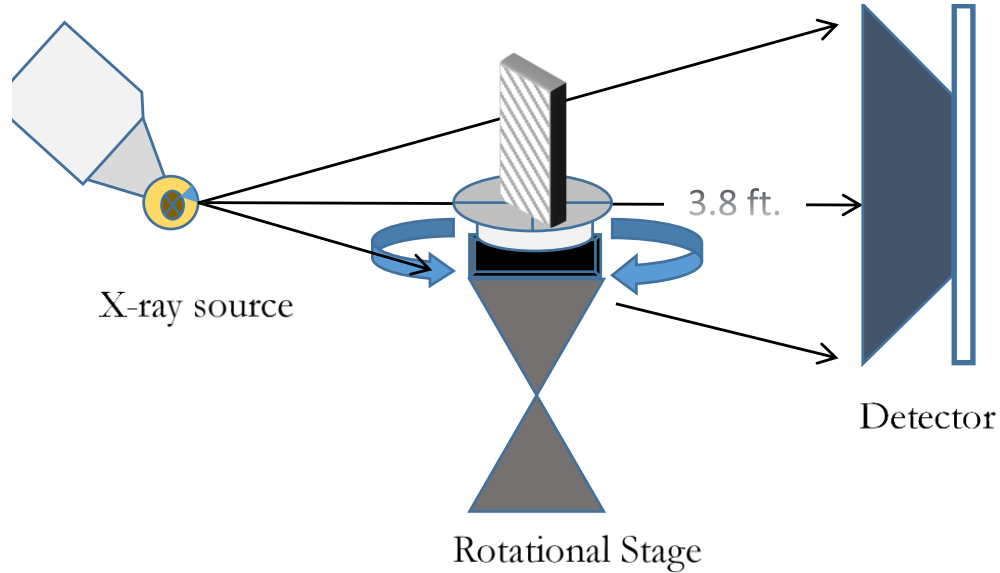


**Figure E.83-5. XCT system components.**

A consistent Cartesian coordinate system is used to define slice direction as illustrated in Figure E.83-6. Slices normal to the X, Y, and Z-directions are shown in Figure E.83-6a, b, and c, respectively.

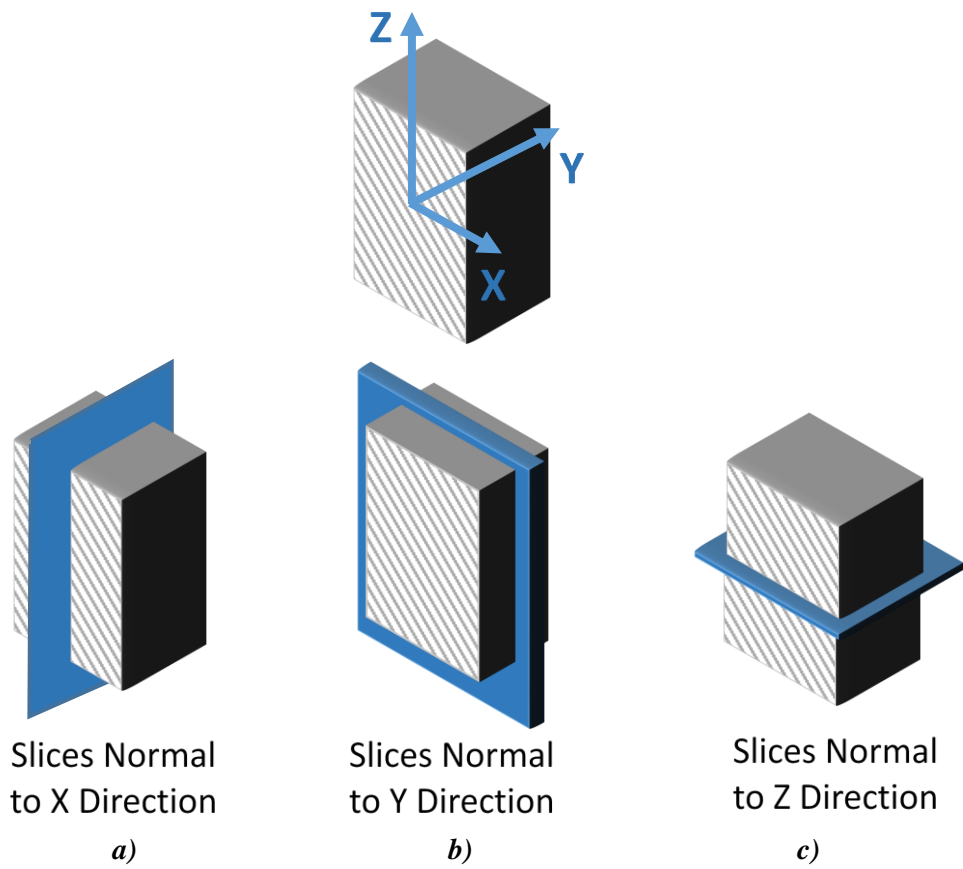


*Figure E.83-6. Slice direction nomenclature.*

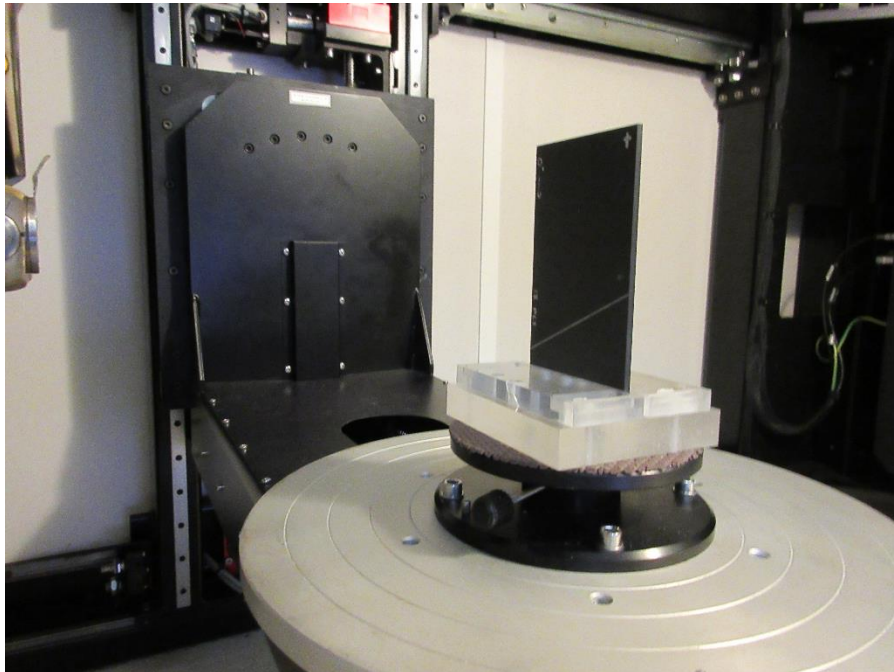


*Figure E.83-7. Impact specimen test stand setup.*

#### E.83.4.4 Equipment List and Specifications:

- Avonix 225 CT System
- 225 kV microfocus X-ray source with 5  $\mu\text{m}$  focal spot size
- 15 or 30kg Capacity 5 axis fully programmable manipulator.
- Detector: Perkin Elmer XRD 1621 – 2000  $\times$  2000 pixels with 200  $\mu\text{m}$  pitch
- 10  $\mu\text{m}$  spatial resolution for specimens 1.5 cm wide
- Thin panels 10-inch  $\times$  10-inch – full volume 200  $\mu\text{m}$  spatial resolution

#### E.83.4.5 Settings

*Table E-83-2. Data collection settings.*

Source Energy	160 kV
Current	37 $\mu\text{A}$
Magnification	5.0 X
Filter	0.125 Sn
# Rotational angles	3142
Exposure time / frame	1.0 sec
Max Histogram Grey Level	54.7 K
# Averages	8
Resolution ( $\mu\text{m}$ )	40.04 $\mu\text{m}$
Array Dimensions (pixels)	Set 1: 1999 $\times$ 362 $\times$ 1998 Set 2: 1998 $\times$ 686 $\times$ 1997

The specimen is placed vertically (rotated about the smallest dimension) on the rotational stage located between the radiation source and the detector. The rotational stage is computer-controlled and correlated to the position of the sample. As the sample is rotated the full 360° (~0.11° increments), the detector collects radiographs at each rotated angle as the X-ray path intersects the sample. 3D reconstruction of the collection of radiographs produces a volume of data that can then be viewed along any plane in the volume. The closer the sample can be placed to the X-ray source, the higher the spatial resolution that can be obtained.

#### E.83.4.6 Data and Results

Specimen #83, is a 3 by 6-inch 8-ply flat panel with a BVID impact. XCT was performed on this specimen in NASA LaRC's CT system with the settings defined in Table E-83.2.

The damage caused by the impact can be clearly seen from all viewing directions as shown in Figure E.83-8. There is no surface indication of an impact. Damage extends approximately one-third of the way through the thickness of the specimen. Very minimal damage from the impact exists.



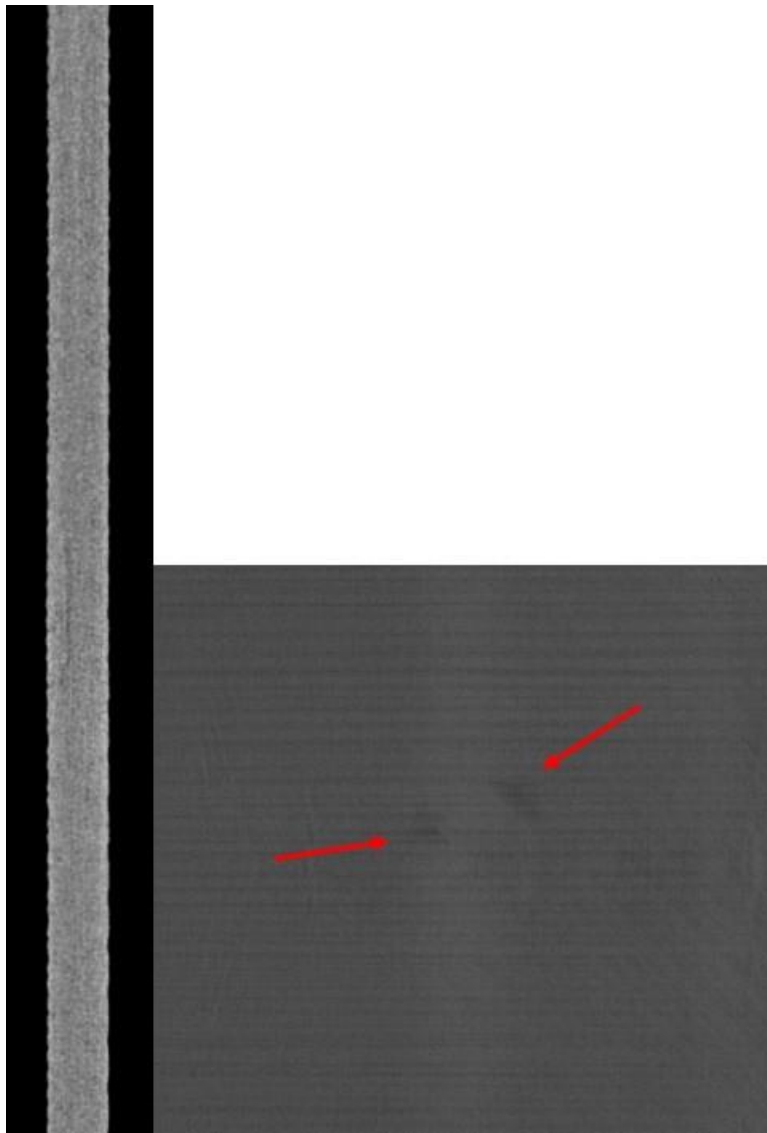


*Figure E.83-8. CT slice normal to the thickness direction shows 1 delamination approximately 30% through the thickness from the impact surface (left). CT slice normal to the front surface shows small delaminations between plies (right).*

**E.84 Specimen #84 – QI\_45 8ply Impact 1 – Not Tested**

Structure	Material	Details	Dimensions (inches)	Partner Methods
Laminate	IM7/8552	Flat panel – spare – no impact	11 × 11 × 8 ply	Not Tested

**E.85 Specimen #85: Boeing Impact QI\_45 8ply 22x22 Impact 1**

Structure	Material	Details	Dimensions (inches)	Partner Methods
8 ply (45/90/-45/0)s	IM7/8552	4 impact-damaged points	N/A	Boeing E.85.1 XCT E.85.2 X-ray CR E.85.3 Shearography E.85.4 Backscatter



**Figure E.85-1. Photographs of impact panel reference standards 8-ply (a) and 16-ply (b).**

**E.85.1 Method: X-ray Computed Tomography (XCT)**

**E.85.1.1 Partner: Boeing**

**E.85.1.2 Technique Applicability: ★★★**

XCT is capable of identifying the impact damage.

**E.85.1.3 Equipment List and Specifications:**

- YXLON Modular CT System
- 225 kV microfocus X-ray source with variable focal spot size
- 100 kg capacity 7-axis granite based manipulator
- XRD 1621 Detector- 2048 × 2048 pixels with 200- $\mu$ m pitch, 400 × 400-mm active area
- 126- $\mu$ m spatial resolution for half volume scan
- Volume Graphics 3.0 visualizing software
- Reconstruction Computer

**E.85.1.4 Settings**

*Table E.85-1. Data collection settings.*

Source Energy	140 kV
Current	0.3 mA
Magnification	1.48 X
Filter	Copper
# Rotational angles	1800
Exposure time / frame	1000 ms
Spatial Resolution	0.0053"
Array Dimensions (pixels)	2048 × 2048

**E.85.1.5 Laboratory Setup**

The DRC utilizes an YXLON Modular CT System. This system has the capability to utilize various X-ray sources for varying applications, including a 450-kV source, a microfocus source, and a nanofocus source. The microfocus source used has a variable focal spot size of less than 4  $\mu$ m and is suitable for magnifications up to 10X, with the nanofocus ranging up to 187X. The detector has

3 DOFs, allowing the effective detector area to be increased through combined scans. The manipulator controls the position of the detector, object, and source. It has 7 DOFs including a rotating stage to rotate the object during the scan. The entire system includes the source, detector, manipulator, control and reconstruction computers, and user control station. The computers and control station are outside of the radiation enclosure (vault) and utilize a safety interlock system to operate. Cameras are located in the vault to allow the operator to monitor the part from outside the enclosure.

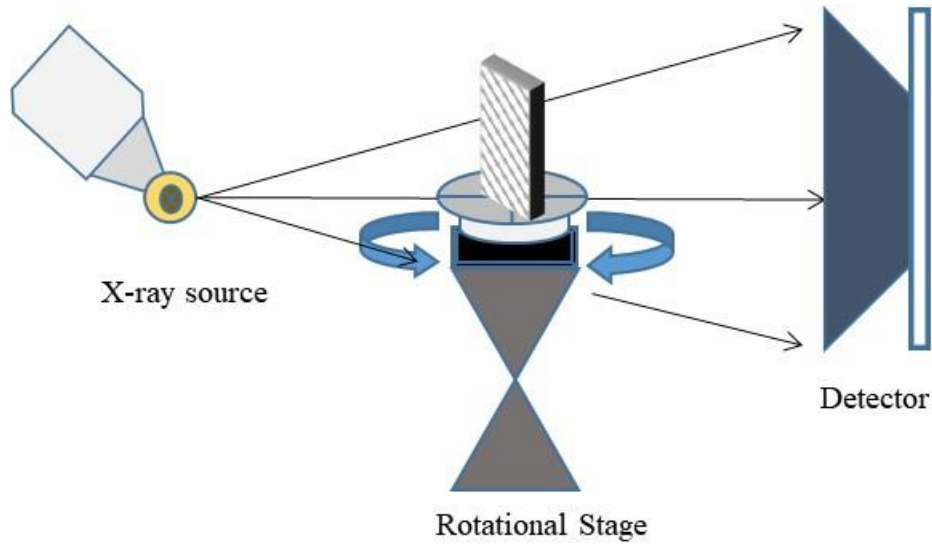


*Figure E.85-2. XCT system components.*

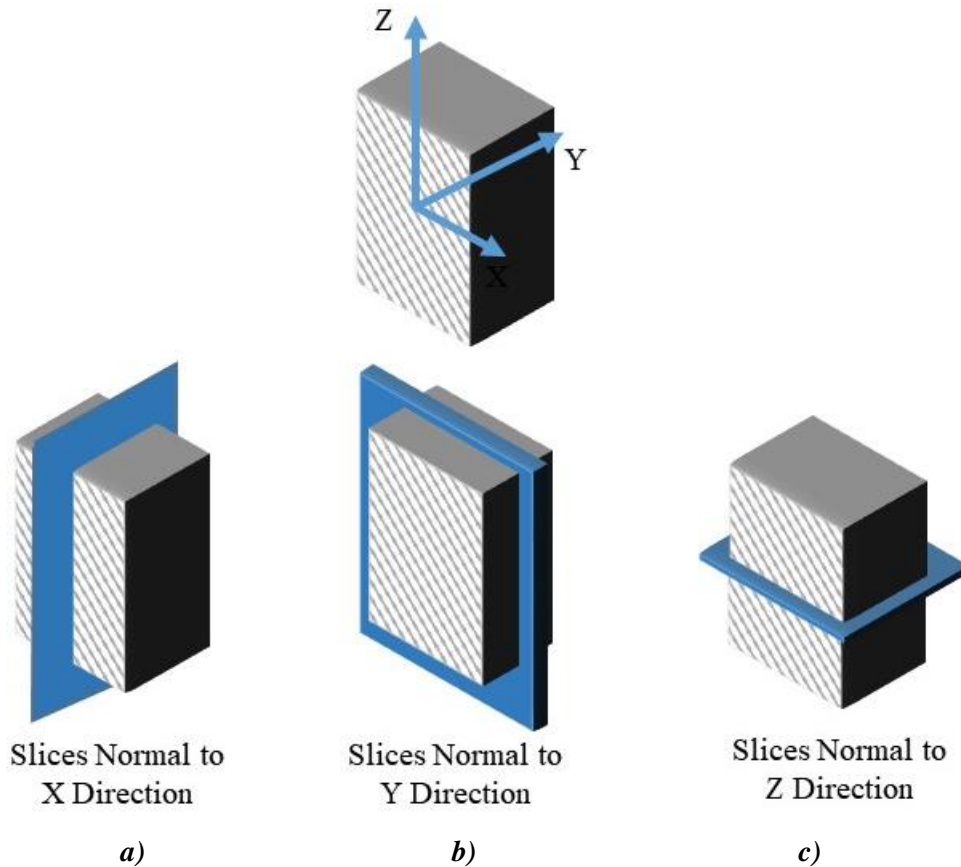


*Figure E.85-3. Slice direction nomenclature.*

The panels were individually placed in a clamp of the rotating stage of the CT system (Figure E.85-4). Plastic markers, which show up in 3D reconstruction, were placed to show the area of interest at the center of the panel. The position of the specimen, source, and detector are controlled to produce geometric magnification of the image and increase the spatial resolution. The image data are gathered as X-rays penetrate the part and expose the detector for a set amount of time. For each scan, these image data are collected at 1800 different angles throughout a 360° rotation. This high projection count helps to compensate for the few non-optimal angles in which the X-rays had to penetrate the full chord length of the panel. These images are then reconstructed to create the 3D volume dataset. This dataset is viewed and analyzed in Volume Graphics, a volume rendering software, to identify the relevant components.

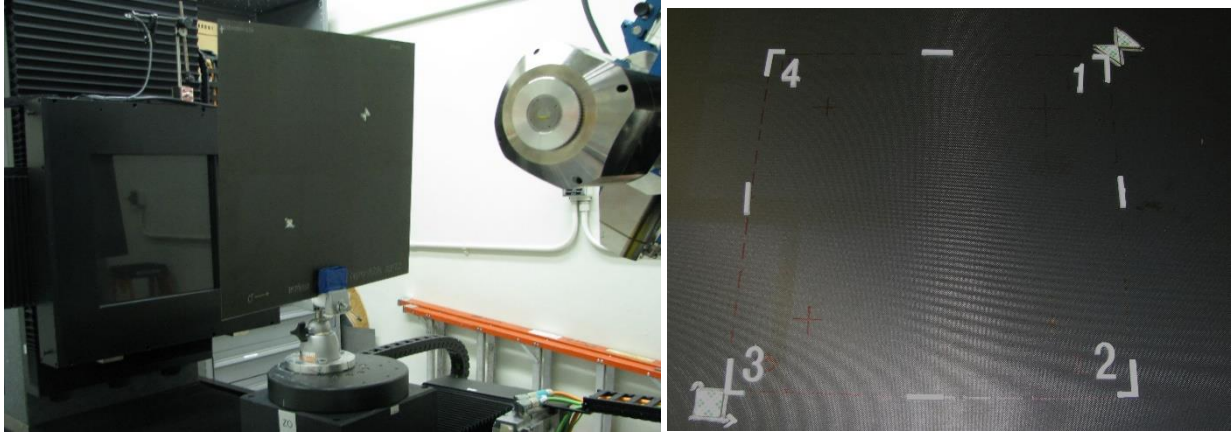


*Figure E.85-4. Microfocus XCT setup for impact panel standard.*

### E.85.1.6 Inspection Results

While the CT reconstructed data set includes the ability to view the part in 3D and 3-orthogonal slice views, for the flat panel only the slice view oriented with the laminate is particularly helpful for viewing (Figures E.85-5 and E.85-6). The brightness and contrast settings are also adjusted to make defects clear, but retain the visible noise at a reasonable level. As shown in the figures of the slices near the surface, one can identify the slight indent of the impact damage in two locations and three locations for the 8- and 16-ply panels, respectively. These are seen as small, dark circular areas meant to be located in four corner locations.

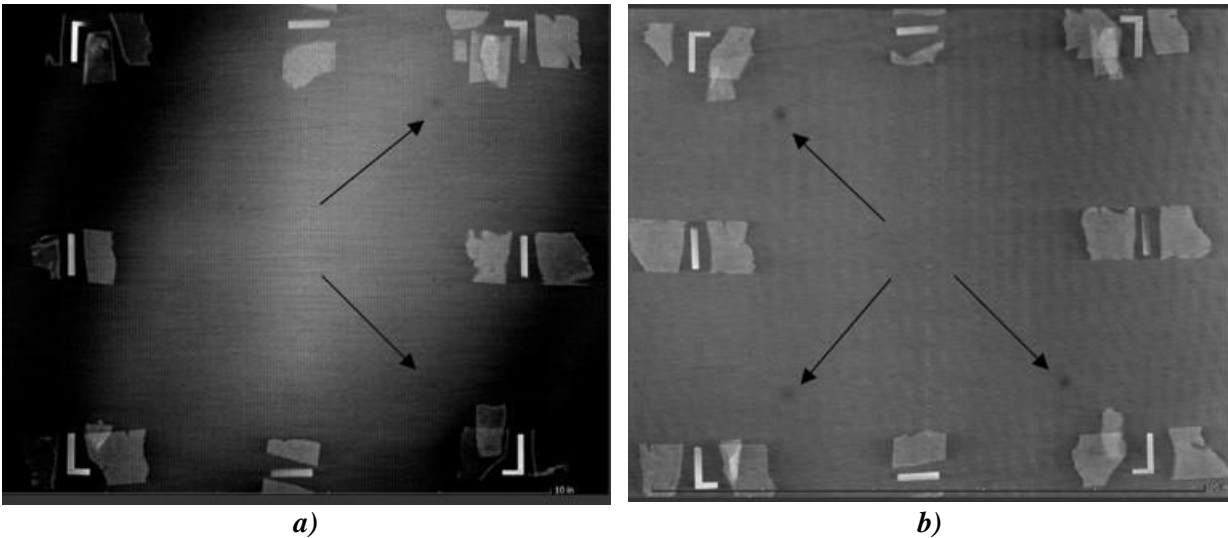


*Figure E.85-5. Slice view of impact standards showing top surface indent on 8-ply (a) and 16-ply (b).*

Moving the slice view deeper into the panel, nearing the back surface, indications of higher density appear at the damage locations as whiter marks. These are seen at 4 and 3 locations for the 8 and 16-ply panels, respectively. This indicates that the impact damage created a small area in the panel with an increased density from compression. For both the indent and compression, the damage appears more intense on the 16-ply than the 8-ply panel, noted by the higher contrast of the damage to the surrounding panel. This may be due to the thinner panel's ability to flex and disperse the energy of the impact more than the thicker panel.



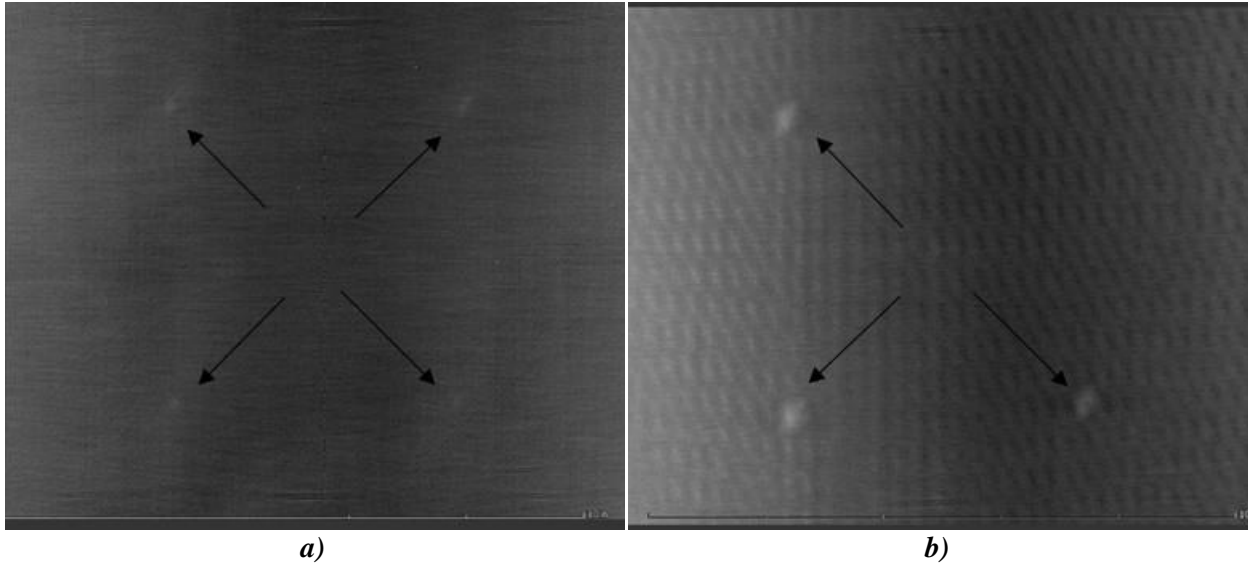


Figure E.85-6. Slice view of impact standards showing bottom surface compression damage on 8-ply (a) and 16-ply (b).

**E.85.2 Method: X-ray Computed Radiography (CR)**

**E.85.2.1 Partner: Boeing**

**E.85.2.2 Technique Applicability: ☆☆☆**

X-ray CR is unable to reliably detect the impact damage.

**E.85.2.3 Equipment List and Specifications:**

- Philips 160 kV X-Ray source, 0.4-mm focal spot size
- IPS Phosphorus Imaging Plate
- GE CRxFlex Scanner, 50- $\mu$ m resolution
- GE Rhythm Review 5.0 visualizing software

**E.85.2.4 Settings**

*Table E.85-2. Imaging and exposure parameters.*

Source Energy	40, 20 kV (8-ply, 16-ply)
Current	4, 6.65 mA (8-ply, 16-ply)
Source-Detector Distance	60 in
Magnification	1X
Exposure time	15, 60 s
Resolution ( $\mu$ m)	50 $\mu$ m
Imaging Area (in)	14 $\times$ 17

**E.85.2.5 Laboratory Setup**

The DRC has a small X-ray enclosure (vault) for the primary purpose of 2D X-ray imaging. It includes a Philips 160-kV X-ray source and the ability to use film, CR, and digital detector arrays. The CR imaging plates are placed on a table and the source, suspended from the ceiling by a 3-axis crane, can be positioned to control the Source to Object Distance. Outside of the enclosure are the controls for the source, utilizing a safety interlock system. These controls allow the user to

set the energy, current, and exposure time for the source. In addition to the vault, the DRC utilizes a CRxFlex system to scan and erase the CR imaging plates, storing the images on a computer. The phosphorus imaging plates, after exposure to X-rays, will luminesce the images when exposed to red light, allowing the 50- $\mu\text{m}$  scanner to create digital versions and “erase” the plates using bright white light to be used again. The CR digital images are then reviewed using Rhythm Review.

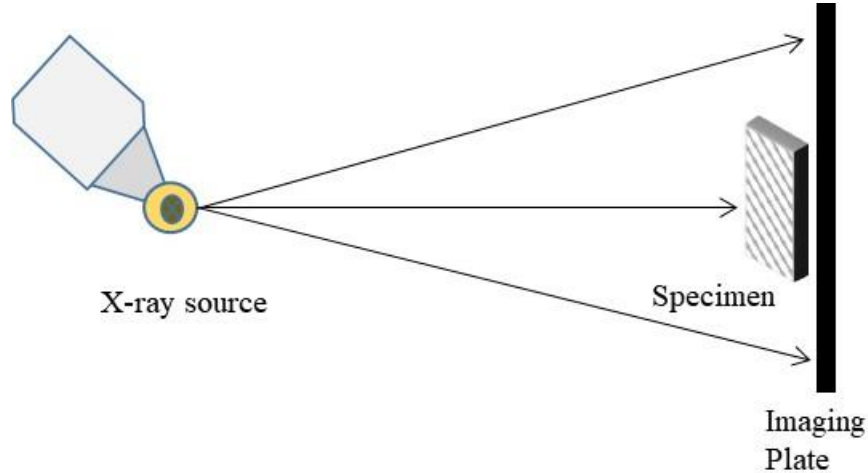


*Figure E.85-7. X-ray CR imaging.*

The standards have a marked area containing the damage which was placed directly on the plastic cassette containing the imaging plate with the X-ray source directly overhead (Figure E.85-8). The source was located 60 inches from the specimen and imaging plate to reduce geometric distortion. Plastic markers were used to show the area boundaries and label the images, showing up in the results as brighter white. Because of the difference in laminate thicknesses between the standards, two separate source energies, currents, and exposure times were used.

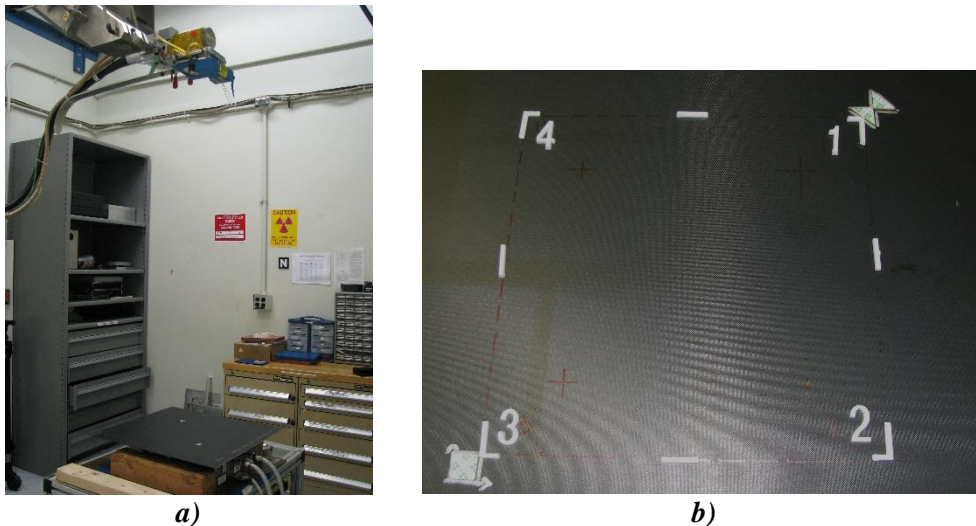


*Figure E.85-8. Laboratory setup of impact plate standards for CR imaging.*

### E.85.2.6 Inspection Results

CR imaging is dependent on the superimposed density of the part being imaged. In the case of the impact damage, the damaged portion tends to get indented, slightly compressing the material underneath the indent. Thus, the superimposed density remains approximately the same. This

makes the detection of impact damage by an operator using 2D radiography such as CR very difficult. As seen in Figure E.85-9, the impact damage is not easily visible. The damage is located within the bounds of the plastic markers in a 4-corner pattern. Given knowledge of the locations, an operator may be able to discern damage but contrast from the damage is not enough to reliably be detected.

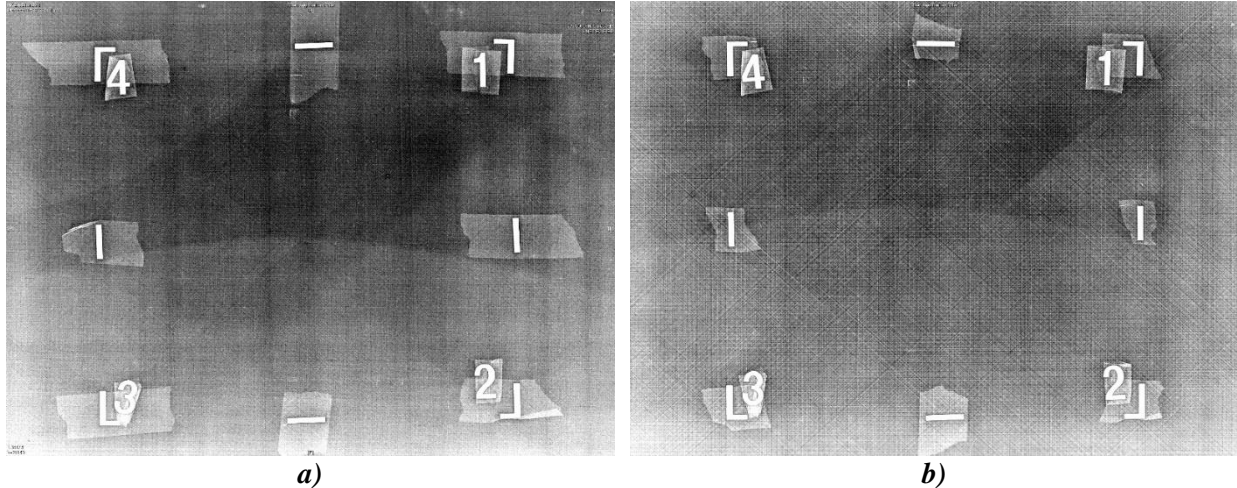


*Figure E.85-9. Flash filtered CR images of 8-ply (a) and 16-ply (b) impact panels.*

### E.85.3 Method: Electronics Shearography with Vacuum Excitation

#### E.85.3.1 Partner: Boeing

#### E.85.3.2 Technique Applicability: ★☆☆

Shearography could not see any of the impact damage in the standards.

#### E.85.3.3 Equipment List and Specifications:

- Model LT5200 by Laser Technology Inc.

#### E.85.3.4 Settings

*Table E.85-3. Inspection time and vacuum.*

Vacuum	Up to 100 inches of water	
Inspection Time	10 sec	
Frame Rate	30 frames/sec	
Surface	Glossy and Brown	

#### E.85.3.5 Laboratory Setup

A shearography nondestructive inspection system with vacuum excitation was used in order to detect subsurface impact damage defects. Shearography is a laser interferometry technique that measures out of plane displacement see Figure E.85-10. Shearography inspection is a noncontact, full-field, single-sided, and real-time inspection technique. By using vacuum excitation above the part's surface, any air entrapped beneath the surface will expand and cause surface deformation, as shown in Figures E.85-11a and E.85-11b. The resulting deformation can be depicted as a series of optical fringe patterns.

Figure E.85-12 shows a shearography detection setup. In electronics shearography, the shearing images are generated by subtracting the initial image (Pre Vacuum Excitation) from consecutive post excitation images where the fringe density is proportional to the surface displacement.

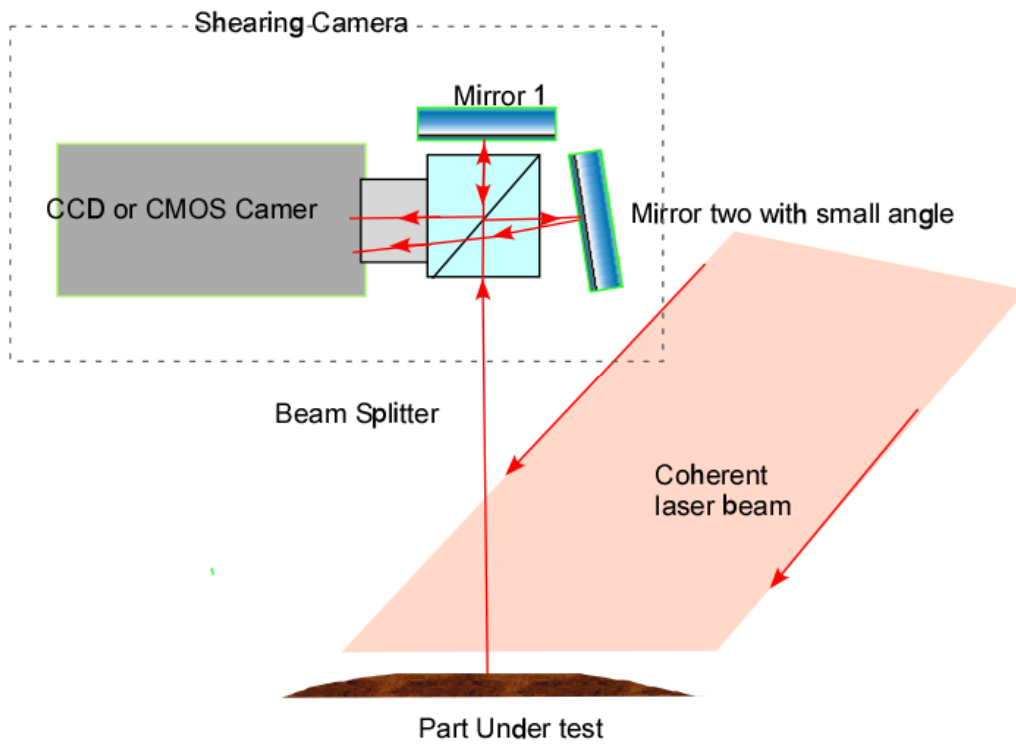


*Figure E.85-10. Shearography camera and speckle laser patterns.*

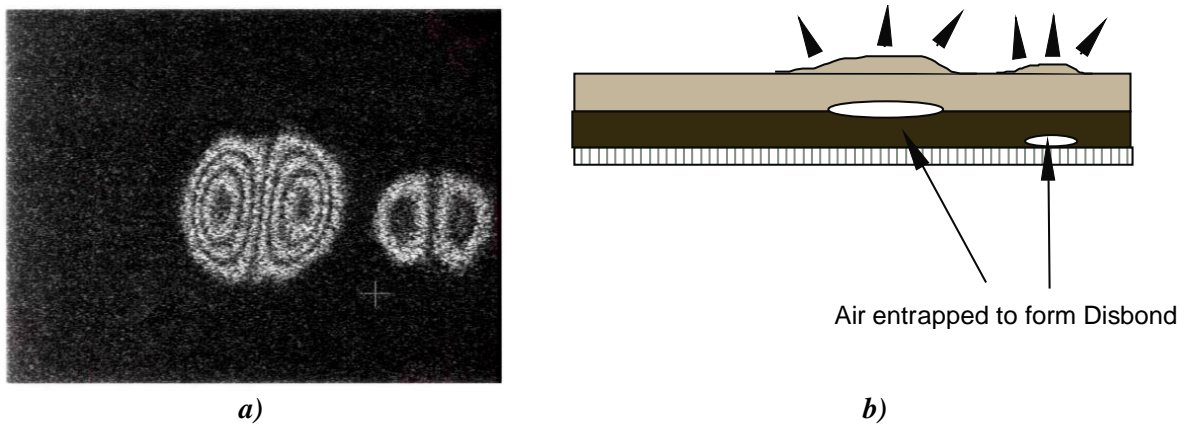


*Figure E.85-11. a) shearography image of subsurface disbands and b) surface deformation caused from vacuum excitation.*



*Figure E.85-12. Shearography inspection system with vacuum excitation.*

### **E.85.3.6 Inspection Results**

The Standards were carbon fiber composite panels with four defined impact damage areas. The Impact damaged areas were verified using 10 MHz ultrasonic inspection. The impact-damaged areas were created by dropping a steel ball from a fixed height on the four corners of the panel. The standards were made of 8- and 16-ply unidirectional carbon fiber epoxy.

Shearography inspection was not able to detect any of the subsurface impact damage due to excessive flexing of the panels from the vacuum excitation. Surface flexing can cause de-correlation noise across the part and therefore it became extremely difficult to isolate the defects. In such cases, other excitation techniques for shearography inspection may be necessary.

### **E.85.4 Method: X-Ray Backscatter**

#### **E.85.4.1 Partner: Boeing**

#### **E.85.4.2 Technique Applicability: ☆☆☆**

X-ray Backscatter is not capable of detecting impact damage.

#### **E.85.4.3 Equipment List and Specifications:**

- NuSAFE Portable X-ray Backscatter imaging system

#### **E.85.4.4 Settings**

*Table E.85-4. Imaging and exposure parameters.*

Source Energy	60 kV
Current	28.5 mA
Scan Velocity	36 mm/min
Collimator Speed	4.5 RPM
Exposure per pixel	7.407 ms
Image width and height	305 × 200 pixels
Pixel Size	1 mm × 0.2°
Imaging Sweep Area	40°



#### E.85.4.5 Laboratory Setup

The DRC has a large X-ray enclosure (vault) which is utilized for high-energy CT scanning, large 2D X-ray imaging, and X-ray backscatter scanning. A custom NuSAFE portable backscatter system is set up in this enclosure. Because of the relatively low radiation output, it can be safely operated with the operator in the vault, outside of a boundary established by the controlling Radiation Health and Safety organization. Figure E.85-13 shows the backscatter unit facing the impact panel (left), while the high voltage, generator, cooling system, and control computer are housed in a portable cart (right), which can also hold the unit for transportation.



*Figure E.85-13. NuSAFE portable X-ray Backscatter system.*

Unlike most other X-ray methods, which are TT, Backscatter X-ray is a method of 2D imaging that only requires one-sided access. When X-rays interact with a material, most pass through with some attenuation; however, a small fraction scatters back and can be detected (Compton Scattering). Backscatter uses this by exposing a small area of a specimen to a rotating collimated X-ray beam (Figure E.85-14). The scattered X-rays are collected with detectors and used along with the swept area of the beam to construct a column of an image. By translating the whole source, another column is made and sequentially a full 2D image is created as seen from the source side. In this test, the part was simply placed a short distance from the unit with the X-rays initially aligned to one side. During scanning the unit then translated across the part to build the image.

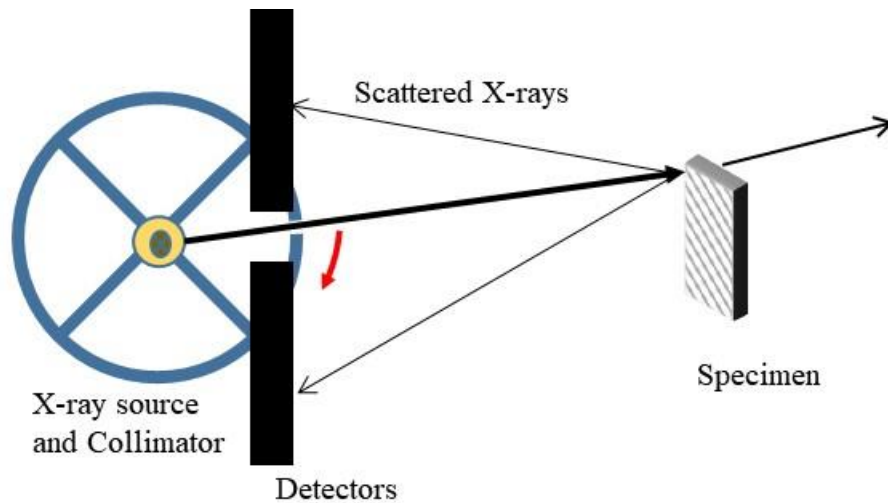


*Figure E.85-14. X-ray Backscatter imaging.*

#### **E.85.4.6 Inspection Results**

Backscatter X-ray is particularly sensitive to material differences that cause large variations in scatter. Metallic foreign material or water in honeycomb panels are examples of detectable phenomena. Changes in surface orientation such as the indents from impact damage are theoretically detectable, if they cause a large enough change in scatter. Figure E.85-15 shows no indent indications however. The lack of detectability in this case may be caused by the limited resolution of this imaging method or an insufficient difference in X-ray scatter that cannot be effectively detected. In this case, X-ray backscatter imaging is not able to detect the small impact damage that is present in this panel.

The faint horizontal lines in this image are the metal pipes along the wall that was behind the panel (about +10 ft.). This showcases backscatter X-ray's ability to detect concealed foreign material, which is applied in law enforcement due to backscatter's relatively low radiation exposure. The black rectangle at the bottom of the image is the clamp holding the panel in place.

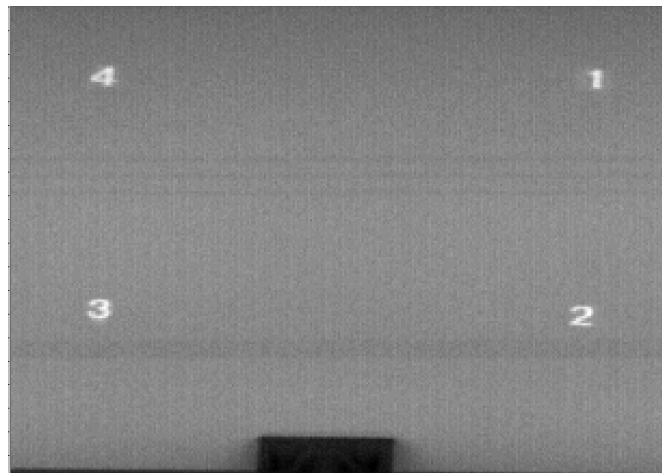


*Figure E.85-15. X-ray Backscatter image of 8-ply impact damage panel.*

**E.86 Specimen #86: Boeing Impact QI 45 16ply 6x6 Impact 1**

Structure	Material	Details	Dimensions (inches)	Partner Methods	
16 plies	IM7/8552	Single Impact Location	6 × 6	Boeing	E.86.1 X-ray CR E.86.2 XCT
				NASA	E.86.3 PEUT

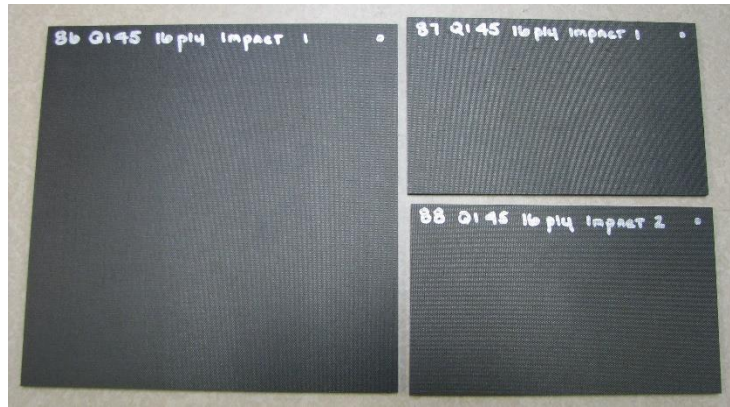


*Figure E-86.1. Photographs of radii delamination standard.*

**E.86.1 Method: X-ray Computed Tomography (XCT)**

**E.86.1.1 Partner: Boeing**

**E.86.1.2 Technique Applicability: ★★☆☆**

XCT is able to detect impact damage on some of the panels.

**E.86.1.3 Equipment List and Specifications:**

- YXLON Modular CT System
- 225 kV microfocus X-ray source with variable focal spot size
- 100kg capacity 7-axis granite based manipulator
- XRD 1621 Detector- 2048 × 2048 pixels with 200- $\mu$ m pitch, 400 × 400-mm active area
- 111- $\mu$ m spatial resolution for impact panel scan
- Volume Graphics 3.0 visualizing software
- Reconstruction Computer

**E.86.1.4 Settings**

*Table E.86-1. Data collection settings.*

Source Energy	120 kV
Current	0.60 mA
Magnification	1.80 X
Filter	Copper
# Rotational angles	1410
Exposure time / frame	500 ms
Frame Binning	2
Spatial Resolution ( $\mu$ m)	111 $\mu$ m
Array Dimensions (pixels)	2048 × 2048

### E.86.1.5 Laboratory Setup

The DRC utilizes an YXLON Modular CT System. This system has the capability to utilize various X-ray sources for varying applications, including a 450-kV source, a microfocus source, and a nanofocus source. The microfocus source used has a variable focal spot size of less than 4  $\mu\text{m}$  and is suitable for magnifications up to 10X, with the nanofocus ranging up to 187X. The detector has 3 DOFs, allowing the effective detector area to be increased through combined scans. The manipulator controls the position of the detector, object, and source. It has 7 DOFs including a rotating stage to rotate the object during the scan. The entire system includes the source, detector, manipulator, control and reconstruction computers, and user control station. The computers and control station are outside of the radiation enclosure (vault) and utilize a safety interlock system to operate. Cameras are located in the vault to allow the operator to monitor the part from outside the enclosure.

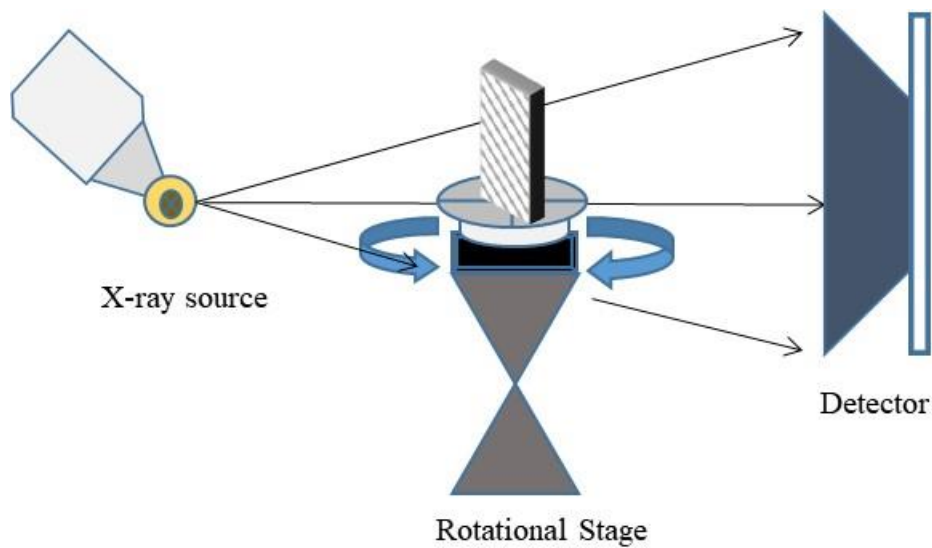


*Figure E.86-2. XCT system components.*

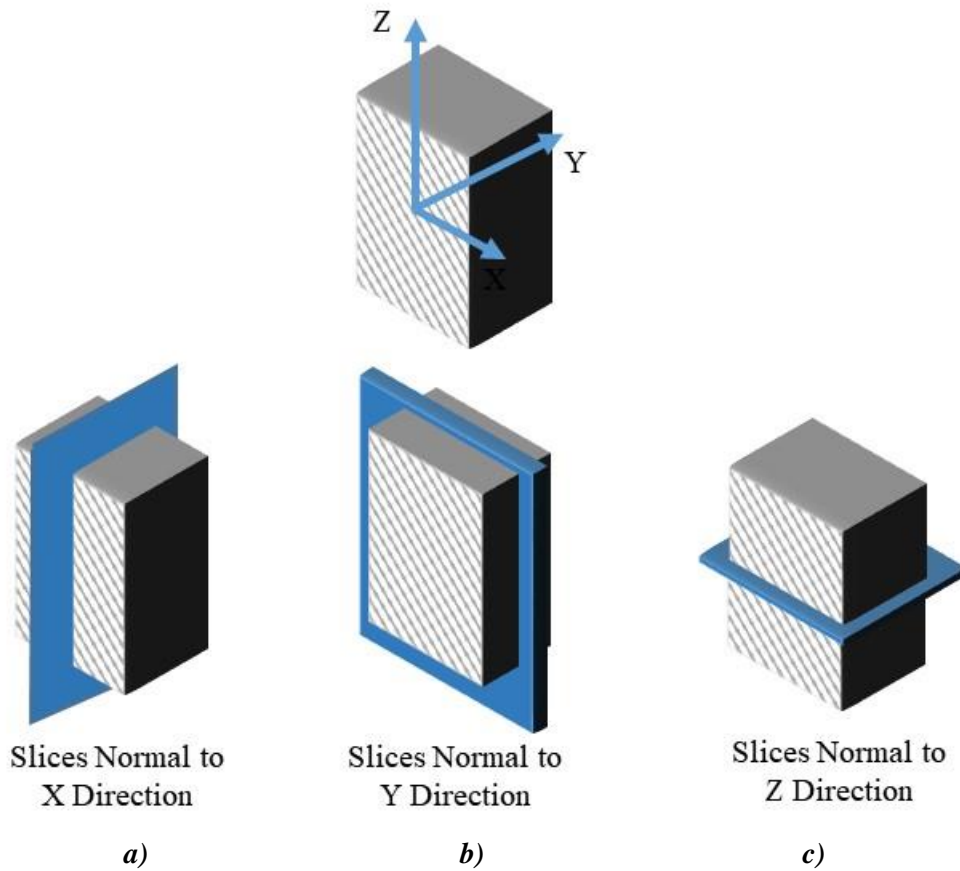


*Figure E.86-3. Slice direction nomenclature.*

To reduce overall scan time, the standard panels of the same thickness were stacked together, separated by light foam sheets and held together with tape. This allowed three parts to be scanned at once and analyzed separately in post-processing. The panel bundle was then secured in a foam fixture. The position of the specimen, source, and detector are controlled to produce geometric magnification of the image and increase the spatial resolution. The image data are gathered as X-rays penetrate the part and expose the detector for a set amount of time. For each scan, these image data are collected at 1410 different angles throughout a 360° rotation. These images are then reconstructed to create the 3D volume dataset. This dataset is viewed and analyzed in Volume Graphics, a volume rendering software, to identify the relevant components.



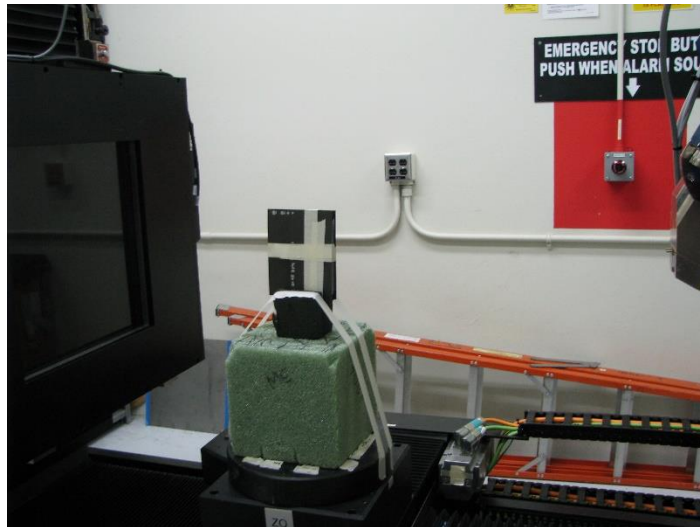


*Figure E.86-4. Microfocus XCT setup for impact damage standards.*

### **E.86.1.6 Inspection Results**

Unlike 2D X-ray imaging, CT shows slice views of the object that are not superimposed. This allows for improved detection of flaws. In the case of the impact panels, the damage would show as a slightly dented region at the near surface. Figure E.86-5 shows a slice view at the near surface of each panel. The dark spot in the center of Figure E.86-5b and c indicates less dense or lack of material, caused by the indentation of the impact on Panels 87 and 88. Figure E.86-5a shows no detectable evidence of impact damage on Panel 86.

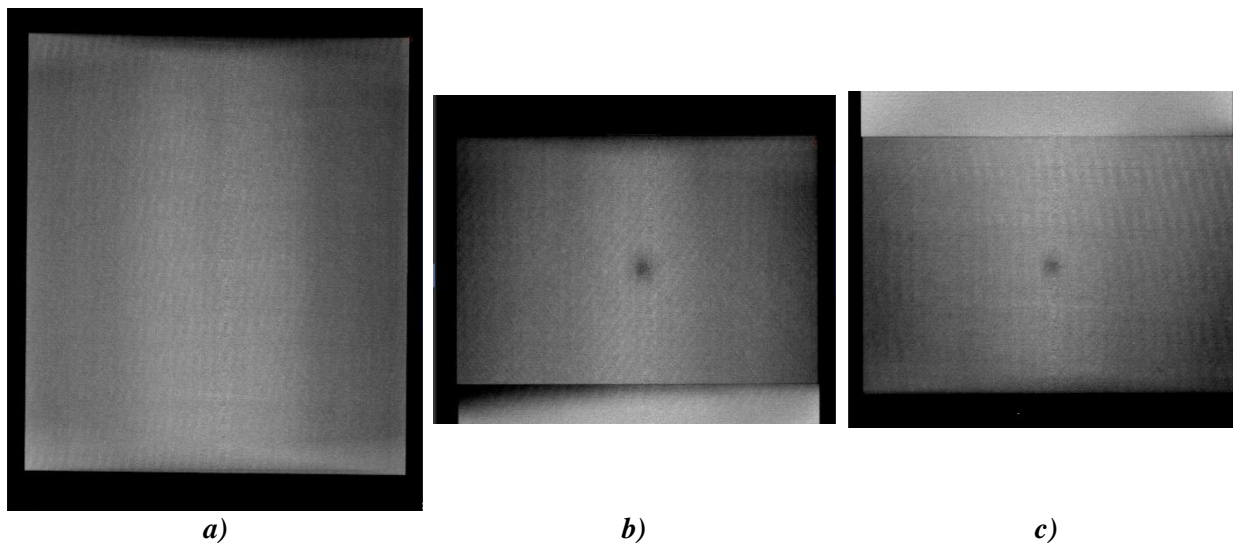


*Figure E-86.5. CT slice view of 16-ply impact damage panels 86 (a), 87 (b), and 88 (c).*

### **E.86.2 Method: X-ray Computed Radiography (CR)**

#### **E.86.2.1 Partner: Boeing**

#### **E.86.2.2 Technique Applicability: ☆☆☆**

X-ray CR is unable to reliably detect the impact damage.

### E.86.2.3 Equipment List and Specifications:

- Philips 160 kV X-Ray source, 0.4-mm focal spot size
- IPS Phosphorus Imaging Plate
- GE CRxFlex Scanner, 50- $\mu$ m resolution
- GE Rhythm Review 5.0 visualizing software

### E.86.2.4 Settings

*Table E.86-2. Imaging and exposure parameters.*

Source Energy	40 kV
Current	2 mA
Source-Detector Distance	60 in
Magnification	1X
Exposure time	30 s
Resolution ( $\mu$ m)	50 $\mu$ m
Imaging Area (in)	14 $\times$ 17

### E.86.2.5 Laboratory Setup

The Digital Radiography Center (DRC) has a small X-ray enclosure (vault) for the primary purpose of 2D X-ray imaging. It includes a Philips 160-kV X-ray source and the ability to use film, CR, and digital detector arrays. The CR imaging plates are placed on a table and the source, suspended from the ceiling by a 3-axis crane, can be positioned to control the Source to Object Distance. Outside of the enclosure are the controls for the source, utilizing a safety interlock system. These controls allow the user to set the energy, current, and exposure time for the source. In addition to the vault, the DRC utilizes a CRxFlex system to scan and erase the CR imaging plates, storing the images on a computer. The phosphorus imaging plates, after exposure to X-rays, will luminesce the images when exposed to red light, allowing the 50- $\mu$ m scanner to create digital versions and “erase” the plates using bright white light to be used again. The CR digital images are then reviewed using Rhythm Review.

The three panels of the same thickness, each containing an impact damaged point, were placed directly on the plastic cassette containing the imaging plate with the X-ray source directly overhead (Figure E.86-6). The source was located 60-inches from the specimen and imaging plate to reduce geometric distortion. Lead markers were used to label the image, showing up in the results as bright white.

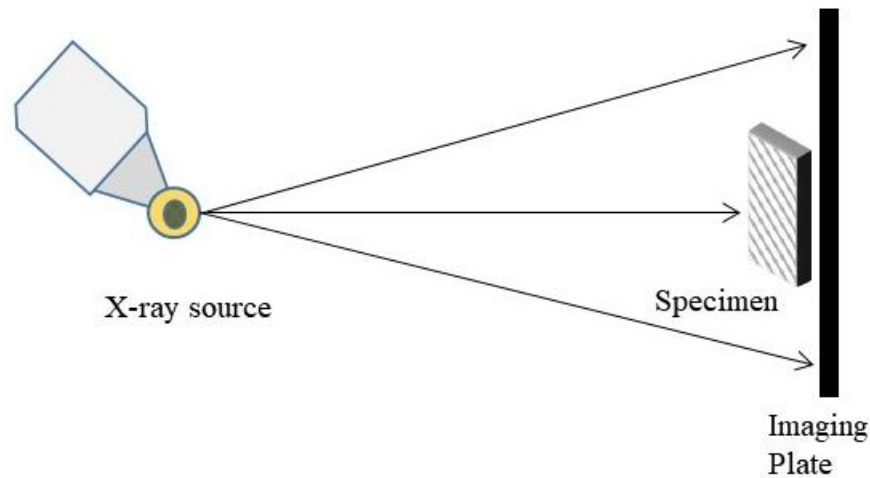


*Figure E.86-6. X-ray CR imaging.*

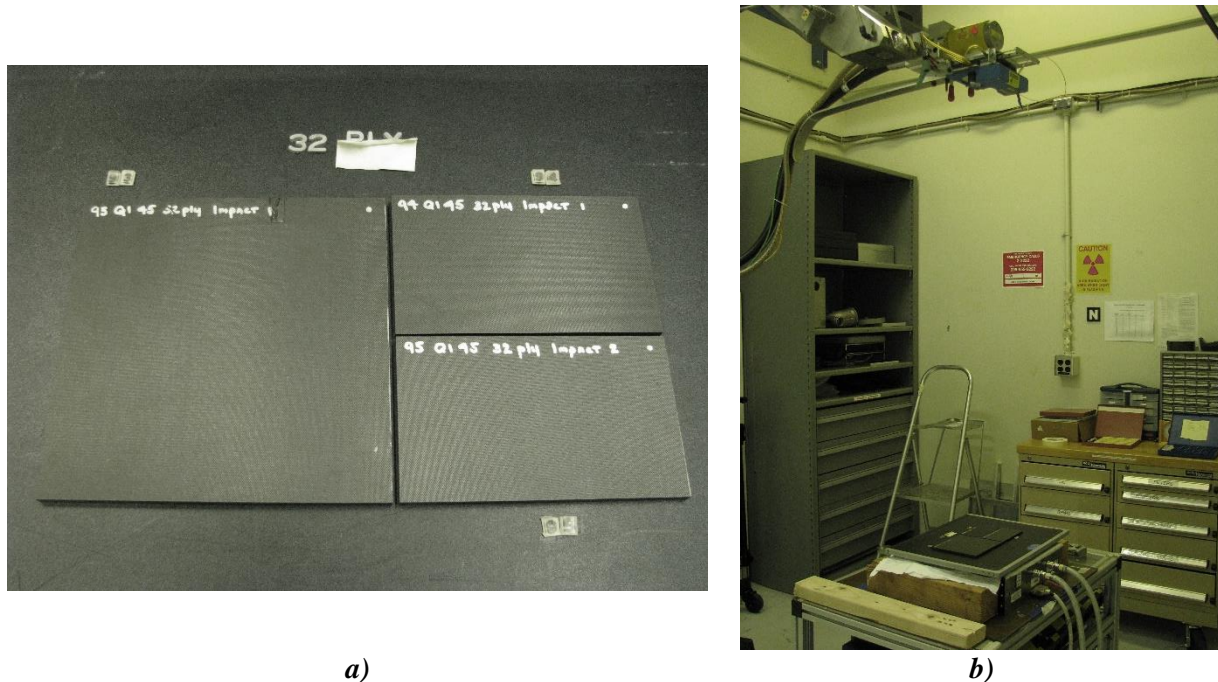


*Figure E.86-7. Laboratory setup of impact plate standards for CR imaging.*

### E.86.2.6 Inspection Results

CR imaging is dependent on the superimposed density of the part being imaged. In the case of the impact damage, the damaged portion tends to get indented, slightly compressing the material underneath the indent. Therefore, the superimposed density remains approximately the same. This makes the detection of impact damage by an operator using 2D radiography such as CR very difficult. As seen in Figure E.86-8, the impact damage is not easily visible. Given knowledge of the locations, an operator may be able to discern damage but contrast from the damage is not enough for detection in a general case.

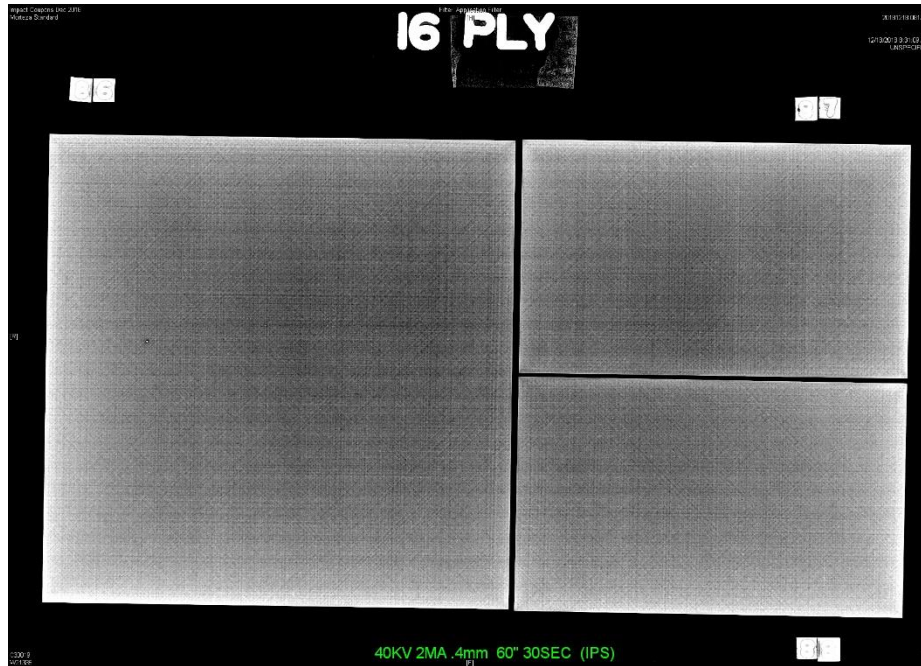


*Figure E.86-8. Flash filtered CR image of 16-ply impact panels.*

**E.86.3 Method: Pulse-Echo Ultrasound Testing (PEUT)**

**E.86.3.1 Partner: NASA**

**E.86.3.2 Technique Applicability: ★★ ★**

PEUT detected the impact damage in this sample.

**E.86.3.3 Laboratory Setup**

Immersion Ultrasonic Testing: NASA LaRC uses a custom-designed single-probe ultrasonic scanning system. The system has an 8-axis motion controller, a multi-axis gantry robot mounted above a medium-size water tank, a dual-channel, 16-bit, high-speed digitizer, and an off-the-shelf ultrasonic pulser receiver. The system can perform TTUT and PEUT inspections. TT inspection employs two aligned ultrasonic probes, one transmitter, and one receiver, placed on either side of a test specimen. Pulse-echo inspection is a single-sided method where a single ultrasonic probe is both transmitter and receiver. In each method, data are acquired while raster scanning the ultrasonic probe(s) in relation to a part. Figure E.86-9 shows a simplified block diagram of a scanning Pulse-echo inspection.

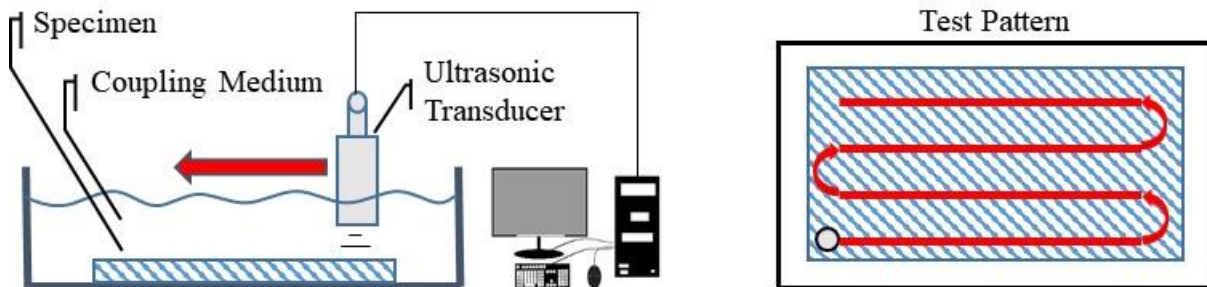


*Figure E.86-9. Ultrasonic system components.*



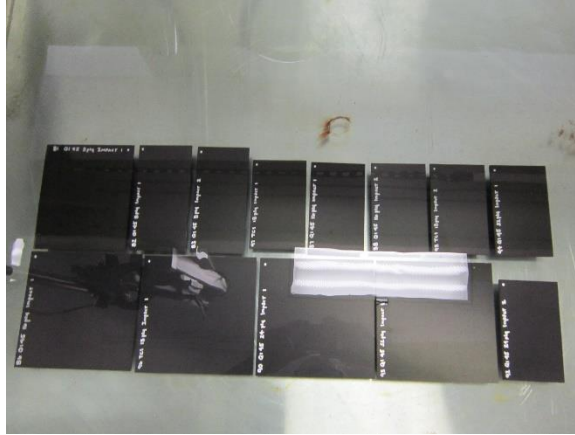


*Figure E.86-10. Specimen baseline inspection orientation.*

#### **E.86.3.4 Equipment List and Specifications:**

- Pulsar/Receiver: Olympus 5073PR
- Digitizer: AlazarTech ATS9462, dual channel, 16 bit, 180 MS/s
- Sensor: Olympus 2-inch spherical focus immersion ultrasonic transducer
- Motion system: open looped stepper motor based X-YY-Z gantry robot
- Motion Controller: Galil DMC-4183
- Acquisition Software: FastScan, custom developed at NASA LaRC
- Signal Processing Software: DataViewer, custom developed at NASA LaRC

#### **E.86.3.5 Settings**

*Table E.86-3. Post-impact inspection settings.*

Resolution (horz) [in/pixel]	0.01
Resolution (ver) [in/pixel]	0.01
Probe frequency [MHz]	10
Focal Length [in]	2
Array Dimensions [pixels]	601 × 601

The specimen is placed flat against the zero position of the tank raised above the glass bottom by several metal washers. The test probe is computer-controlled and correlated to the position on the sample. It is also focused to a point 1 mm below the surface of the test material. The specimen remains in place while the transducer follows a preprogrammed test grid across the surface as indicated in Figure E.86-9. At each point, ultrasonic data are collected from individual pulses. Larger step sizes between data collection result in lower image resolution. These data points are reconstructed into a data cube displaying spatial coordinates as time progresses. 2D reconstruction of the collection of ultrasonic responses create flattened slices at varying depths within the material.

#### **E.86.3.6 Inspection Results**

Specimen #86 is a 6 by 6-inch, 16-ply flat panel with a 2.0-inch impact. PEUT was performed on this specimen in NASA's immersion tank specified above.

Figure E.86-11 shows a back side surface amplitude image of the sample in its pre-impacted state. No significant internal flaws were noted. The highlighted areas above are high-amplitude



reflections from the four spacers used to position the sample above the bottom of the immersion tank.

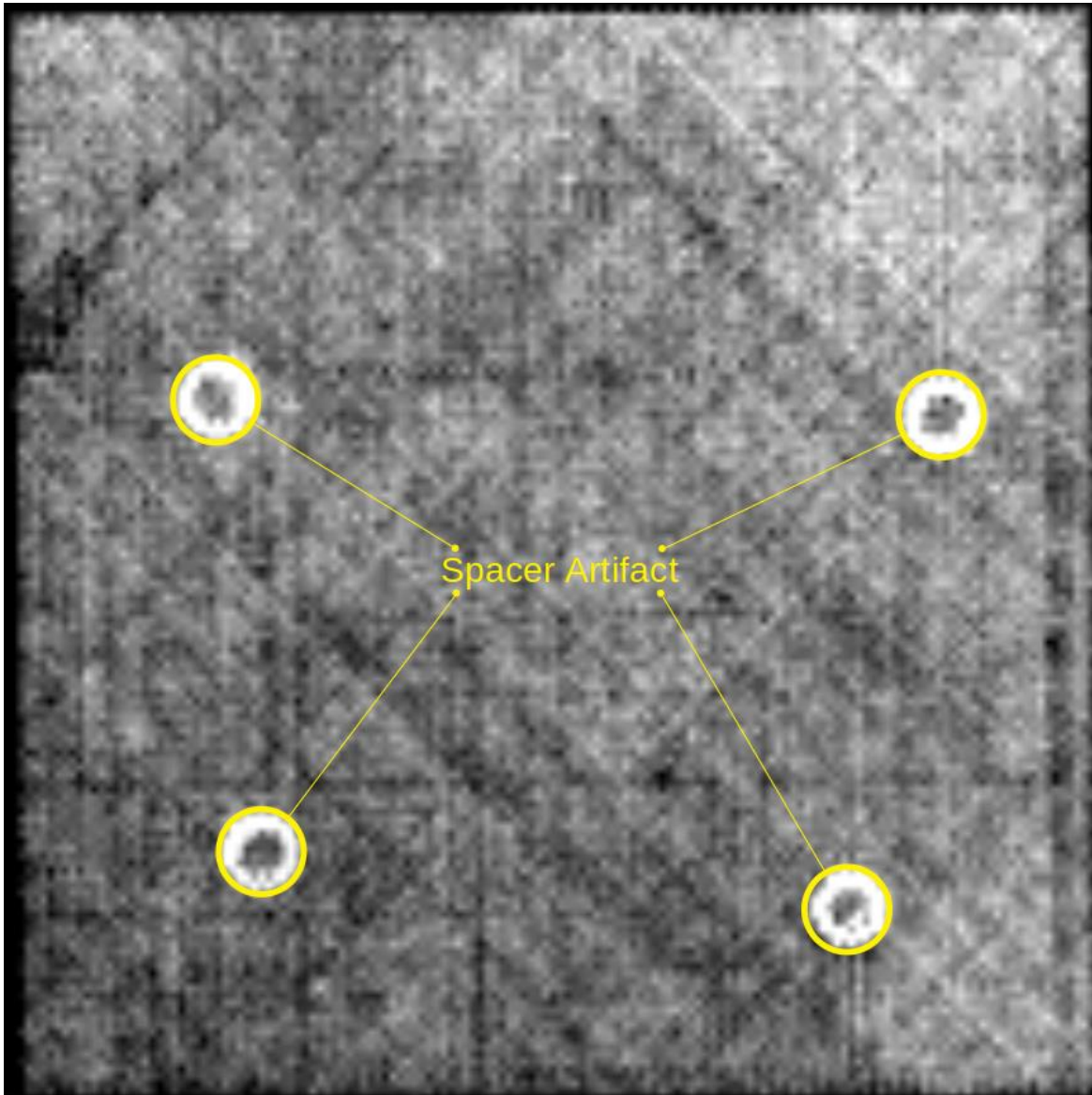
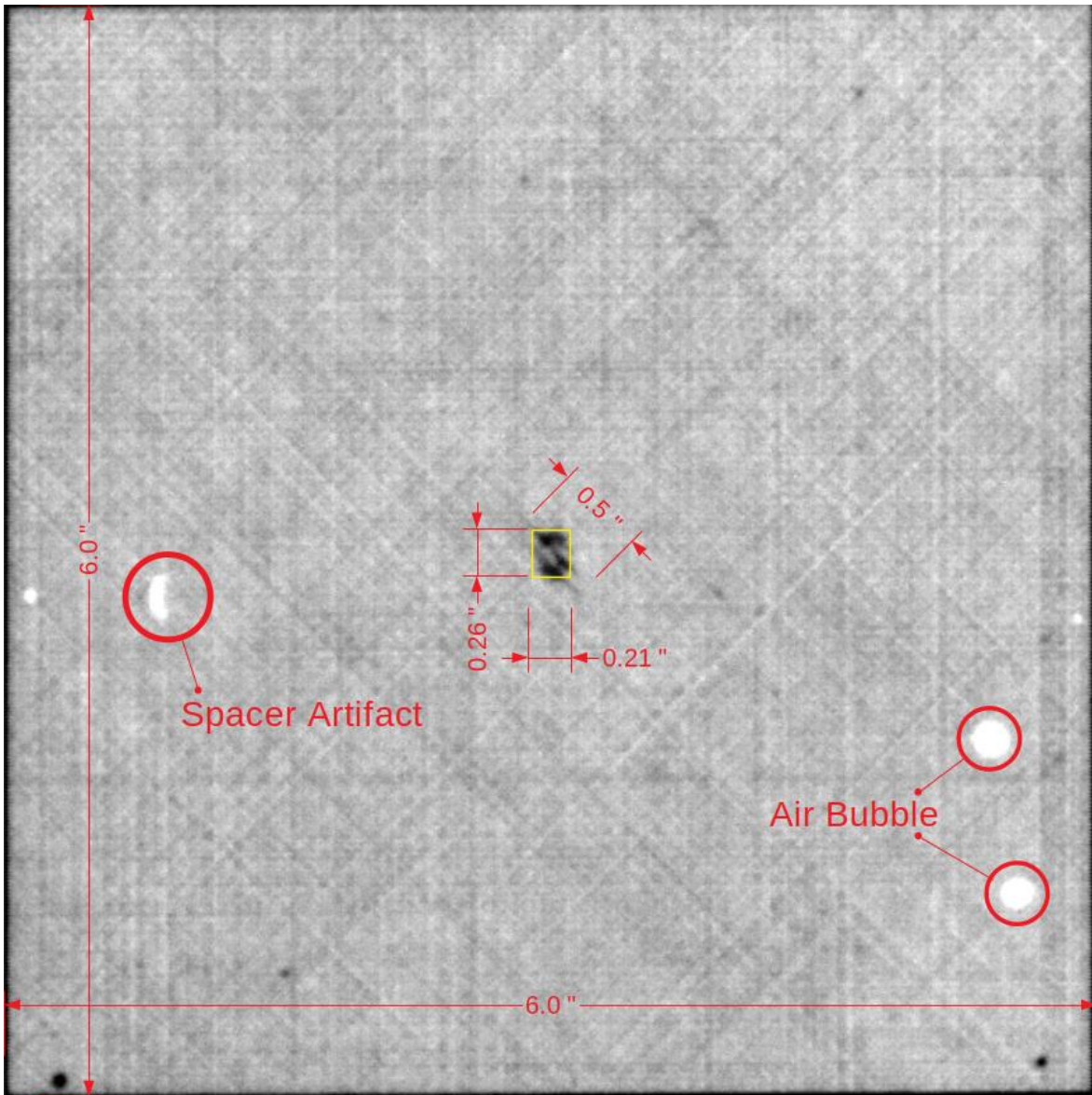
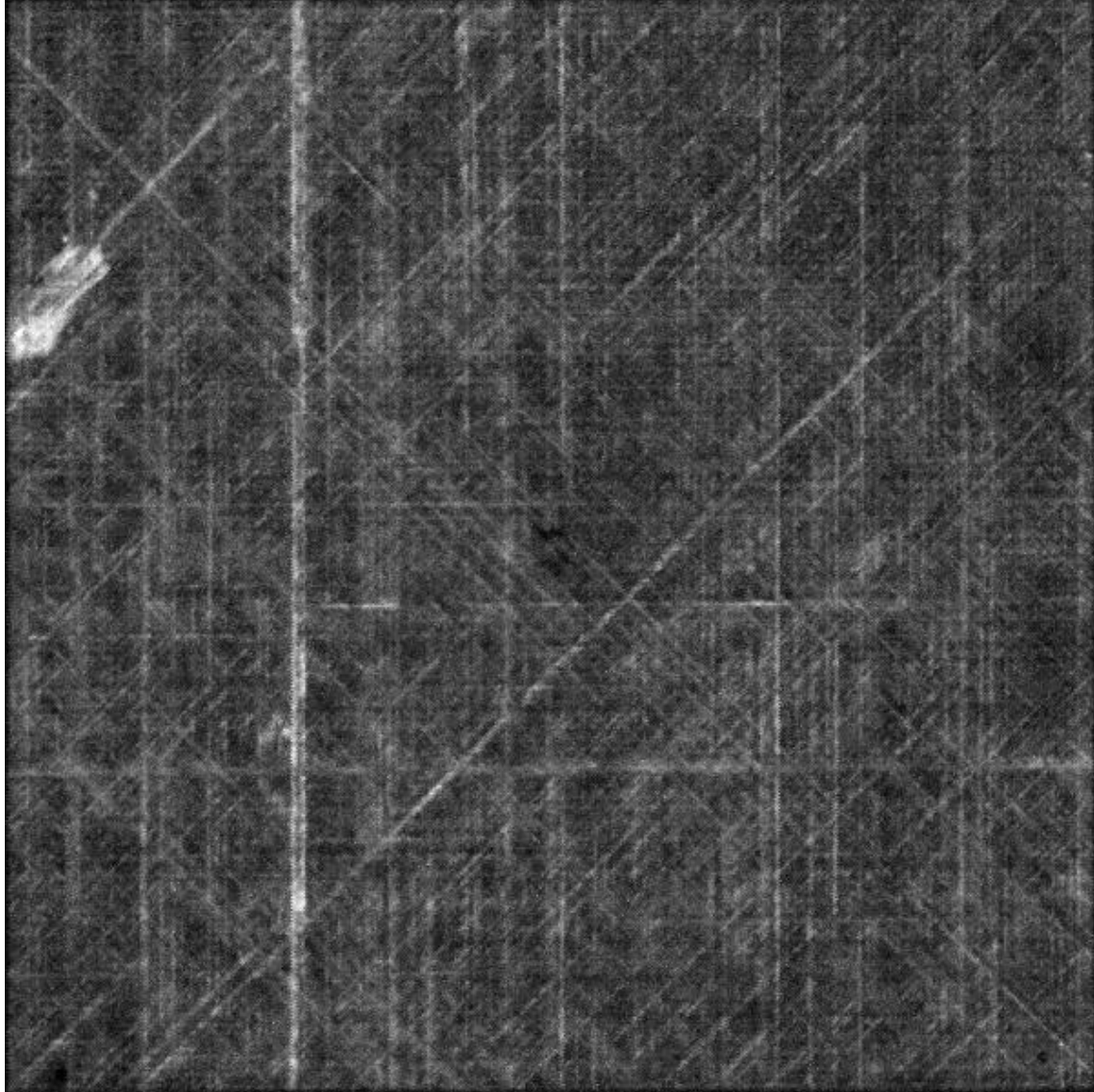


*Figure E.86-11. 10-MHz baseline image.*

Figure E.86-12a shows a back side surface amplitude image of the sample in its post-impacted state. The impact damage region is identified with measurements. Air bubbles and a spacer under the sample are also noted. Figure E.86-12b is an internal reflection amplitude image. The gate region is selected to highlight reflections from the delaminations caused by the impact.



*a) Back side surface amplitude image.*



*b) Internal reflection amplitude image.*

*Figure E.86-12. 10-MHz post-impact image.*

**E.87 Specimen #87: Boeing Impact QI 45 16ply 3x5 Impact 1**

Structure	Material	Details	Dimensions (inches)	Partner Methods	
16 plies	IM7/8552	Single Impact Location	6 × 5 5 × 3	NASA	E.87.1 SSIR E.87.2 X- Ray CT

**E.87.1 Method: Pulse-Echo Ultrasound Testing (PEUT)**

**E.87.1.1 Partner: NASA**

**E.87.1.2 Technique Applicability: ★★★**

PEUT detected the impact damage in this sample.

### E.87.1.3 Laboratory Setup

Immersion Ultrasonic Testing: NASA LaRC uses a custom-designed single-probe ultrasonic scanning system. The system has an 8-axis motion controller, a multi-axis gantry robot mounted above a medium-size water tank, a dual-channel, 16-bit, high-speed digitizer, and an off-the-shelf ultrasonic pulser receiver. The system can perform TTUT and PEUT inspections. TT inspection employs two aligned ultrasonic probes, one transmitter, and one receiver, placed on either side of a test specimen. Pulse-echo inspection is a single-sided method where a single ultrasonic probe is both transmitter and receiver. In each method, data are acquired while raster scanning the ultrasonic probe(s) in relation to a part. Figure E.87-1 shows a simplified block diagram of a scanning Pulse-echo inspection.

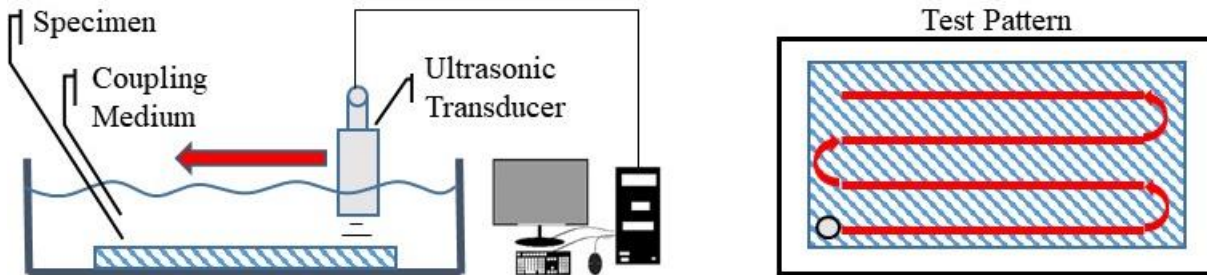


Figure E.87-1. Ultrasonic system components.

### E.87.1.4 Equipment List and Specifications:

- Pulser/Receiver: Olympus 5073PR
- Digitizer: AlazarTech ATS9462, dual channel, 16 bit, 180 MS/s
- Sensor: Olympus 2-inch spherical focus immersion ultrasonic transducer
- Motion system: open looped stepper motor based X-YY-Z gantry robot
- Motion Controller: Galil DMC-4183
- Acquisition Software: FastScan, custom developed at NASA LaRC
- Signal Processing Software: DataViewer, custom developed at NASA LaRC

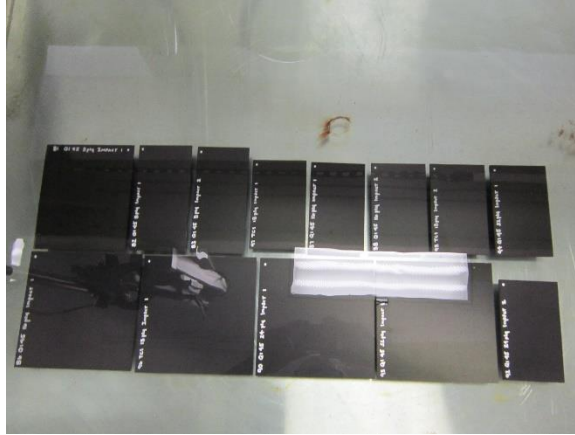
### E.87.1.5 Settings

Table E.87-1. Post-impact inspection settings.

Resolution (horz) [in/pixel]	0.01
Resolution (ver) [in/pixel]	0.01
Probe frequency [MHz]	10
Focal Length [in]	2
Array Dimensions [pixels]	501 × 299

The specimen is placed flat against the zero position of the tank raised above the glass bottom by several metal washers. The test probe is computer-controlled and correlated to the position on the sample. It is also focused to a point 1 mm below the surface of the test material. The specimen remains in place while the transducer follows a preprogrammed test grid across the surface as indicated in Figure E.87-2. At each point, ultrasonic data are collected from individual pulses. Larger step sizes between data collection result in lower image resolution. These data points are reconstructed into a data cube displaying spatial coordinates as time progresses. 2D reconstruction of the collection of ultrasonic responses create flattened slices at varying depths within the material.





*Figure E.87-2. Specimen baseline inspection orientation.*

### **E.87.1.6 Inspection Results**

Specimen #87 is a 3 by 5-inch, 16-ply flat panel with a 1.28-inch impact. PEUT was performed on this specimen in NASA's immersion tank specified above.

Figure E.87-3 shows a back side surface amplitude image of the sample in its pre-impacted state. No significant internal flaws were noted. The highlighted areas above are high-amplitude reflections from the three spacers used to position the sample above the bottom of the immersion tank. A small internal flaw can be seen on the left side of the sample. The small indication is also visible in the post-impact image below.

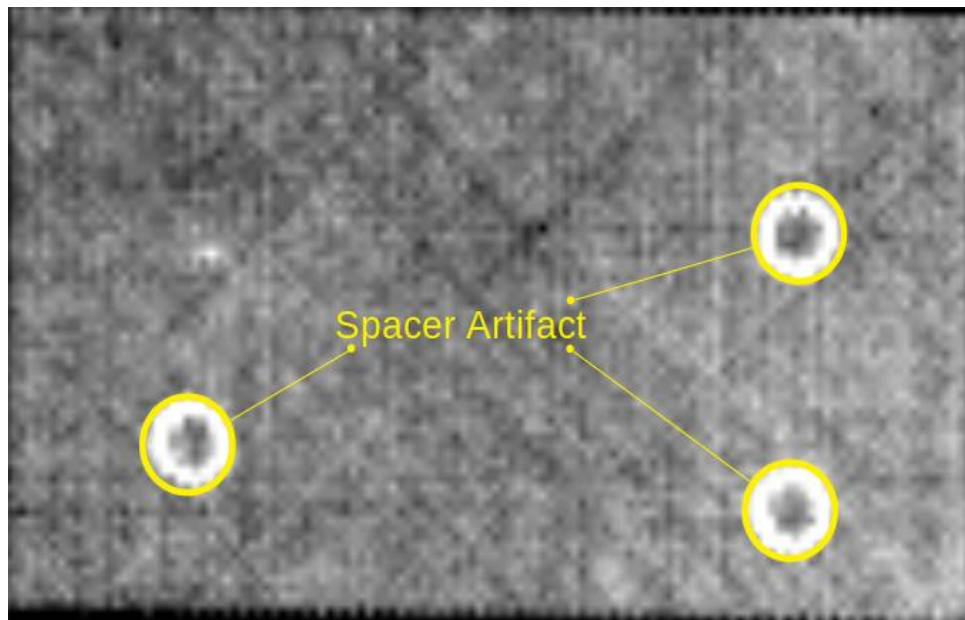


*Figure E.87-3. 10-MHz baseline image.*

Figure E.87-4 shows an internal reflection amplitude image of the sample in its post-impacted state. The gate region is selected to highlight reflections from the delaminations caused by the impact. The impact damage region is identified with measurements.



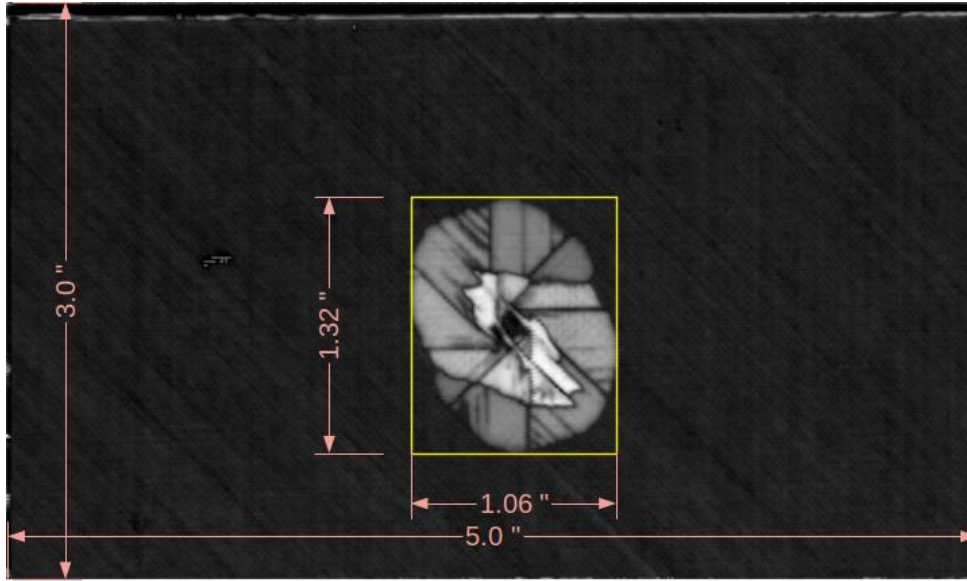


*Figure E.87-4. 10-MHz post-impact image.*

**E.87.1.7 Method: X-ray Computed Tomography (XCT)**

**E.87.1.8 Partner: NASA**

**E.87.1.9 Technique Applicability: ★★ ★**

XCT is capable of imaging and quantifying the damage due to low-impact energy in this specimen.

**E.87.1.10 Laboratory Setup**

The microfocus XCT system at NASA LaRC is a commercially available Avonix (Nikon C2) Metrology System designed for high-resolution NDE inspections. The system is an advanced microfocus X-ray system, capable of resolving details down to 5  $\mu\text{m}$ , and with magnifications up to 60X. The system is supplied as a complete, large-dimension radiation enclosure, with X-ray source, specimen manipulator, and an amorphous silica detector as shown in Figure E.87-5. The imaging controls are housed in a separate control console. The detector is a Perkin-Elmer 16-bit amorphous silicon digital detector with a  $2000 \times 2000$ -pixel array.

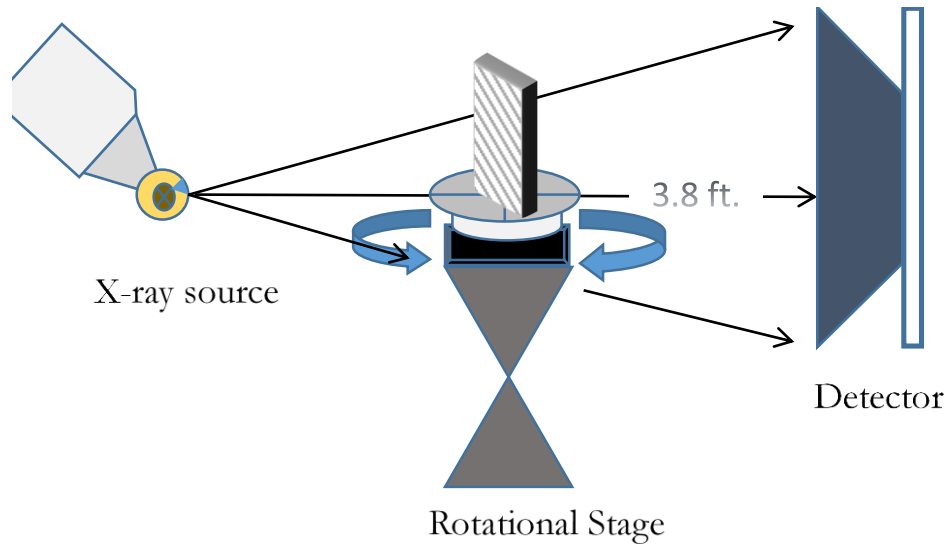


**Figure E.87-5. XCT system components.**

A consistent Cartesian coordinate system is used to define slice direction as illustrated in Figure E.87-6. Slices normal to the X, Y, and Z-directions are shown in Figure E.87-6a, b, and c, respectively.

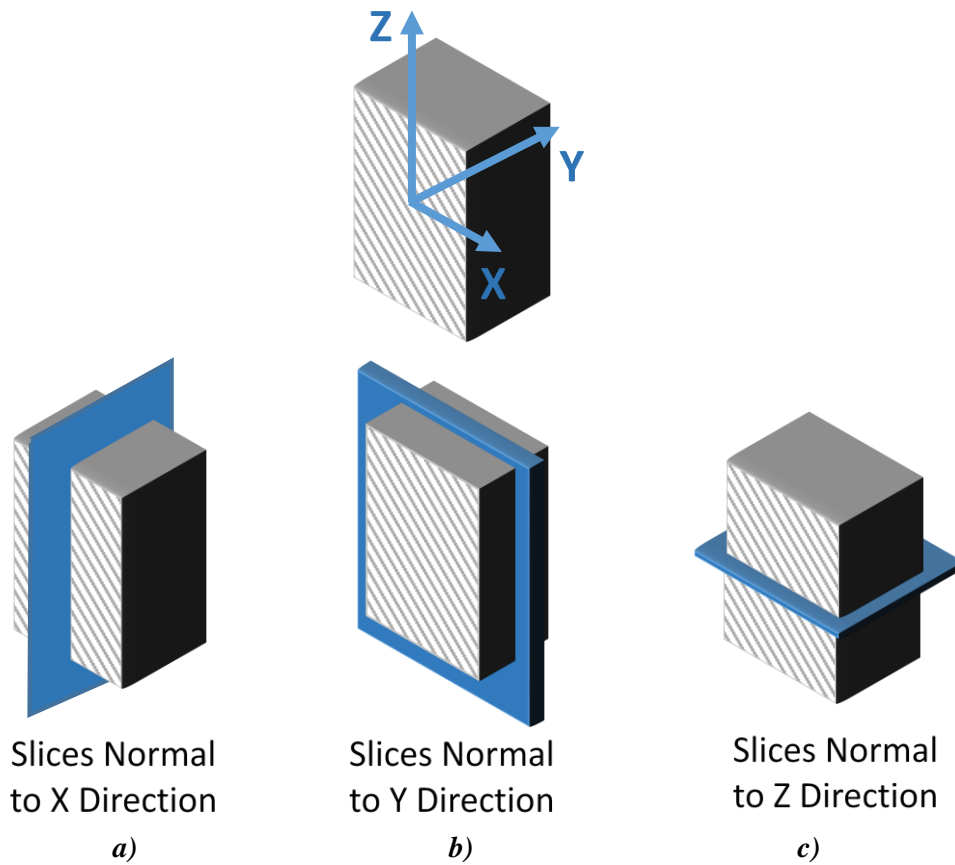


**Figure E.82-6. Slice direction nomenclature.**

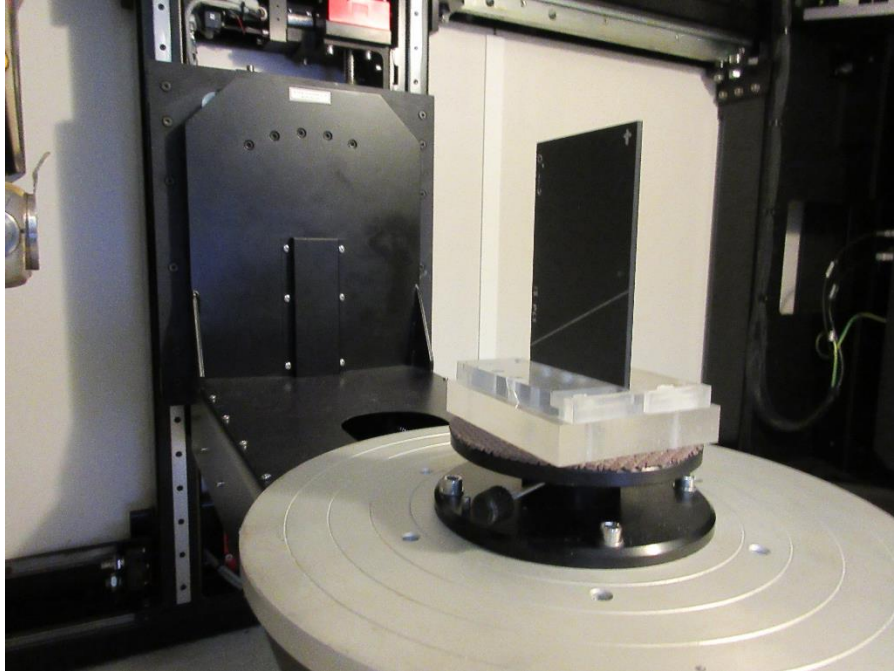


*Figure E.87-7. Impact specimen test stand setup.*

#### **E.87.1.11 Equipment List and Specifications:**

- Avonix 225 CT System
- 225 kV microfocus X-ray source with 5  $\mu\text{m}$  focal spot size
- 15 or 30kg Capacity 5 axis fully programmable manipulator.
- Detector: Perkin Elmer XRD 1621 – 2000  $\times$  2000 pixels with 200  $\mu\text{m}$  pitch
- 10  $\mu\text{m}$  spatial resolution for specimens 1.5 cm wide
- Thin panels 10-inch  $\times$  10-inch – full volume 200  $\mu\text{m}$  spatial resolution

#### **E.87.1.12 Settings**

*Table E.87-2. Data collection settings.*

Source Energy	160 kV
Current	37 $\mu\text{A}$
Magnification	5.0 X
Filter	0.125 Sn
# Rotational angles	3142
Exposure time / frame	1.0 sec
Max Histogram Grey Level	53 K
# Averages	8
Resolution ( $\mu\text{m}$ )	40.04 $\mu\text{m}$
Array Dimensions (pixels)	1999 $\times$ 207 $\times$ 1998

The specimen is placed vertically (rotated about the smallest dimension) on the rotational stage located between the radiation source and the detector. The rotational stage is computer-controlled and correlated to the position of the sample. As the sample is rotated the full 360° (~0.11° increments), the detector collects radiographs at each rotated angle as the X-ray path intersects the sample. 3D reconstruction of the collection of radiographs produces a volume of data that can then

be viewed along any plane in the volume. The closer the sample can be placed to the X-ray source, the higher the spatial resolution that can be obtained.

**E.87.1.13 Data and Results**

Specimen #87, is a 3 by 5-inch 16-ply flat panel with a BVID impact. XCT was performed on this specimen in NASA LaRC’s CT system with the settings defined in Table E-87.2.

The damage caused by the impact can be clearly seen from all viewing directions as shown in Figure E.87-8. There is a very small surface indication of an impact. Damage extends almost completely through the thickness of the specimen.

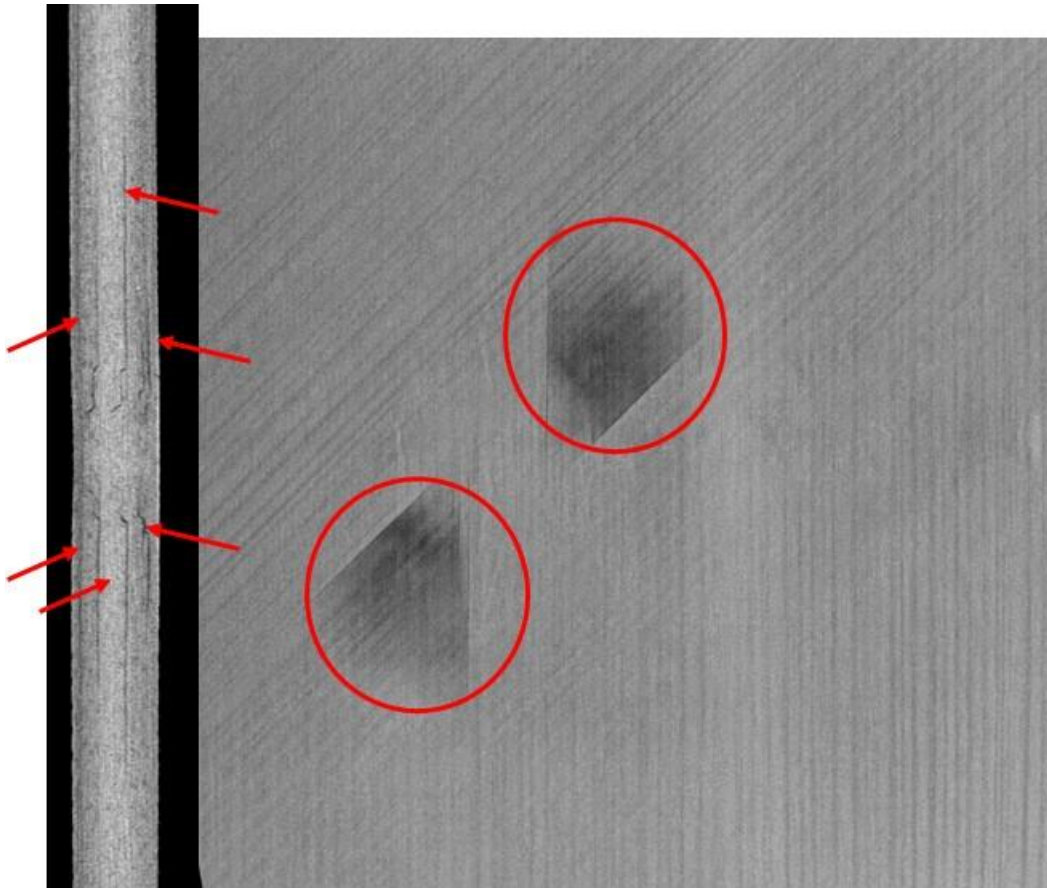


*Figure E.87-8. CT slice normal to the thickness direction show delaminations and matrix cracking (left). CT slice normal to the front surface shows delaminations between plies (right).*

**E.88 Specimen #88: Boeing Impact QI 45 16ply 3x5 Impact 2**

Structure	Material	Details	Dimensions (inches)	Partner Methods	
16 plies	IM7/8552	Single Impact Location	6 × 6 5 × 3	NASA	E.88.1 PEUT E.88.2 XCT

**E.88.1 Method: Pulse-Echo Ultrasound Testing (PEUT)**

**E.88.1.1 Partner: NASA**

**E.88.1.2 Technique Applicability: ★★★**

PEUT detected the impact damage in this sample.

### E.88.1.3 Laboratory Setup

Immersion Ultrasonic Testing: NASA LaRC uses a custom-designed single-probe ultrasonic scanning system. The system has an 8-axis motion controller, a multi-axis gantry robot mounted above a medium-size water tank, a dual-channel, 16-bit, high-speed digitizer, and an off-the-shelf ultrasonic pulser receiver. The system can perform TTUT and PEUT inspections. TT inspection employs two aligned ultrasonic probes, one transmitter, and one receiver, placed on either side of a test specimen. Pulse-echo inspection is a single-sided method where a single ultrasonic probe is both transmitter and receiver. In each method, data are acquired while raster scanning the ultrasonic probe(s) in relation to a part. Figure E.88-1 shows a simplified block diagram of a scanning Pulse-echo inspection.

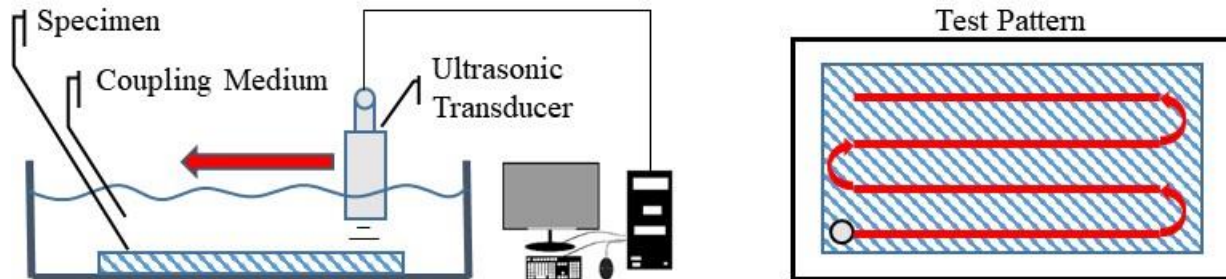


Figure E.88-1. Ultrasonic system components.

### E.88.1.4 Equipment List and Specifications:

- Pulser/Receiver: Olympus 5073PR
- Digitizer: AlazarTech ATS9462, dual channel, 16 bit, 180 MS/s
- Sensor: Olympus 2-inch spherical focus immersion ultrasonic transducer
- Motion system: open looped stepper motor based X-YY-Z gantry robot
- Motion Controller: Galil DMC-4183
- Acquisition Software: FastScan, custom developed at NASA LaRC
- Signal Processing Software: DataViewer, custom developed at NASA LaRC

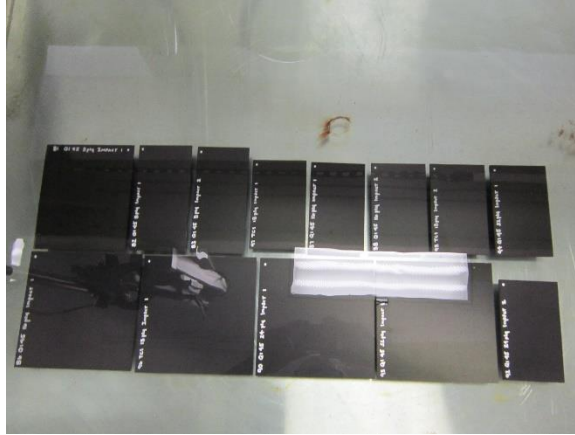
### E.88.1.5 Settings

Table E.88-1. Post-impact inspection settings.

Resolution (horz) [in/pixel]	0.01
Resolution (ver) [in/pixel]	0.01
Probe frequency [MHz]	10
Focal Length [in]	2
Array Dimensions [pixels]	498 × 298

The specimen is placed flat against the zero position of the tank raised above the glass bottom by several metal washers. The test probe is computer-controlled and correlated to the position on the sample. It is also focused to a point one mm below the surface of the test material. The specimen remains in place while the transducer follows a preprogrammed test grid across the surface as indicated in Figure E.88-2. At each point, ultrasonic data are collected from individual pulses. Larger step sizes between data collection result in lower image resolution. These data points are reconstructed into a data cube displaying spatial coordinates as time progresses. 2D reconstruction of the collection of ultrasonic responses create flattened slices at varying depths within the material.



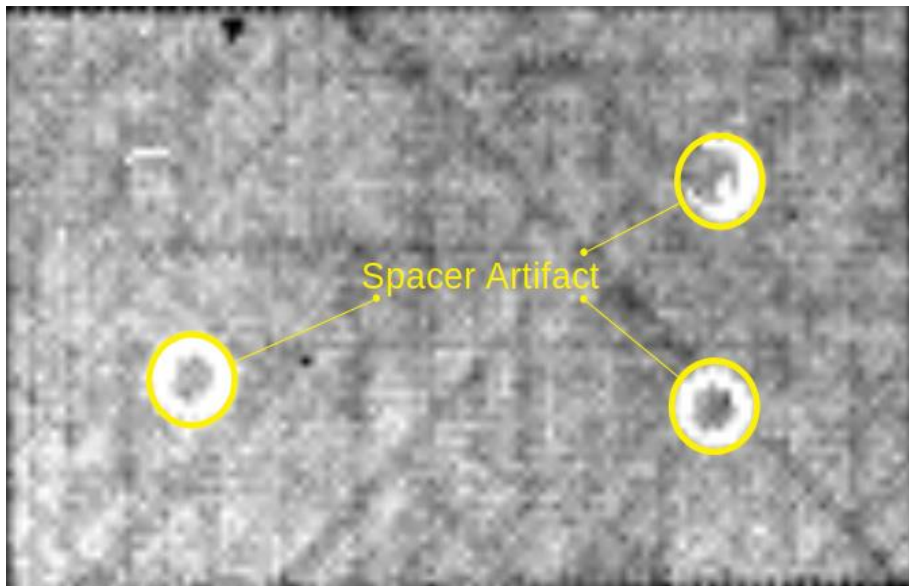


*Figure E.88-2. Specimen baseline inspection orientation.*

### **E.88.1.6 Inspection Results**

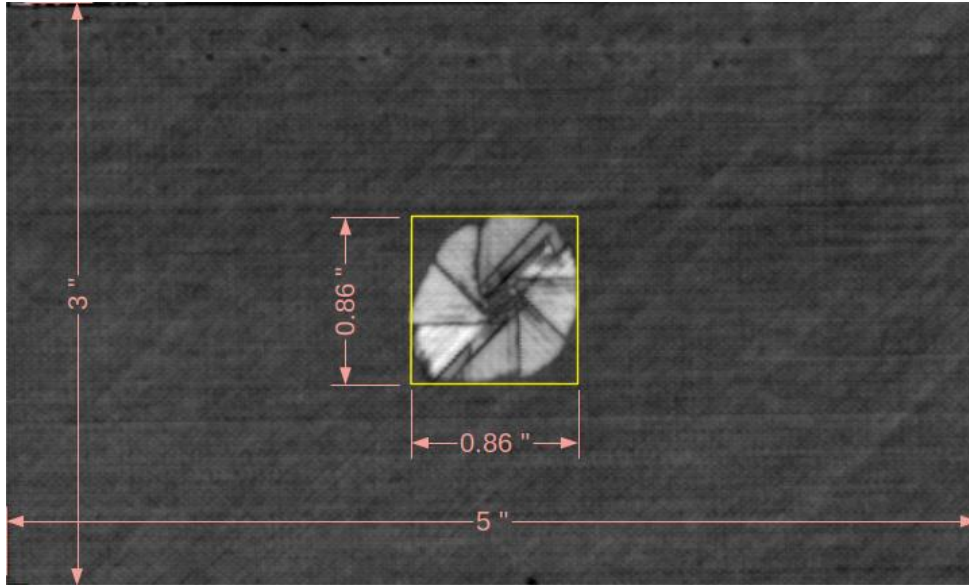
Specimen #88 is a 3 by 5-inch, 16-ply flat panel with a 0.88-inch impact. PEUT was performed on this specimen in NASA's immersion tank specified above.

Figure E.81-3 shows a back side surface amplitude image of the sample in its pre-impacted state. No significant internal flaws were noted. The highlighted areas above are high-amplitude reflections from the three spacers used to position the sample above the bottom of the immersion tank.



*Figure E.88-3. 10-MHz baseline image.*

Figure E.88-4 shows an internal reflection amplitude image of the sample in its post-impacted state. The gate region is selected to highlight reflections from the delaminations caused by the impact. The impact damage region is identified with measurements.



*Figure E.88-4. 10-MHz post-impact image.*

**E.88.2 Method: X-ray Computed Tomography (XCT)**

**E.88.2.1 Partner: NASA**

**E.88.2.2 Technique Applicability: ★★ ★**

XCT is capable of imaging and quantifying the damage due to low-impact energy in this specimen

**E.88.2.3 Laboratory Setup**

The microfocus XCT system at NASA LaRC is a commercially available Avonix (Nikon C2) Metrology System designed for high-resolution NDE inspections. The system is an advanced microfocus X-ray system, capable of resolving details down to 5  $\mu\text{m}$ , and with magnifications up to 60X. The system is supplied as a complete, large-dimension radiation enclosure, with X-ray source, specimen manipulator, and an amorphous silica detector as shown in Figure E.88-5. The imaging controls are housed in a separate control console. The detector is a Perkin-Elmer 16 bit amorphous silicon digital detector with a 2000  $\times$  2000-pixel array.

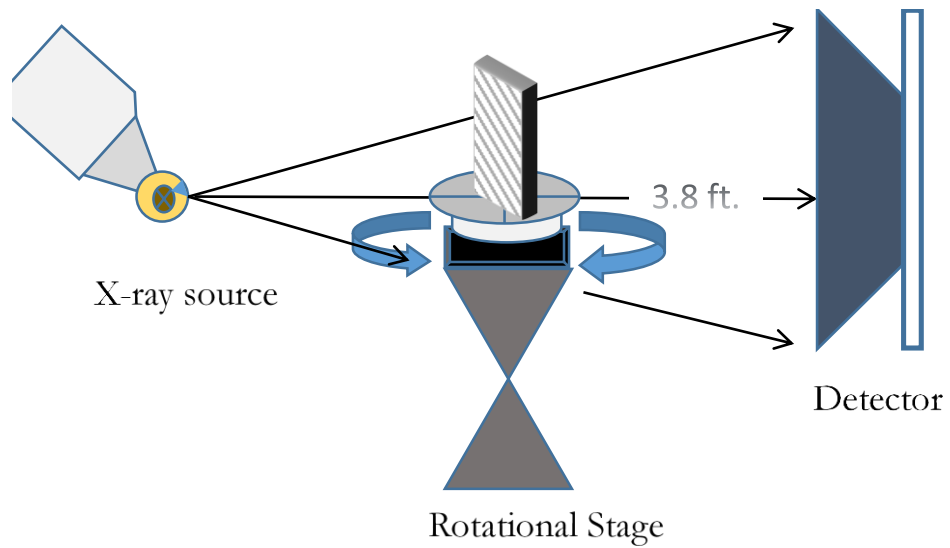


**Figure E.88-5. XCT system components**

A consistent Cartesian coordinate system is used to define slice direction as illustrated in Figure E.88-6. Slices normal to the X, Y, and Z-directions are shown in Figure E.88-6a, b, and c, respectively.

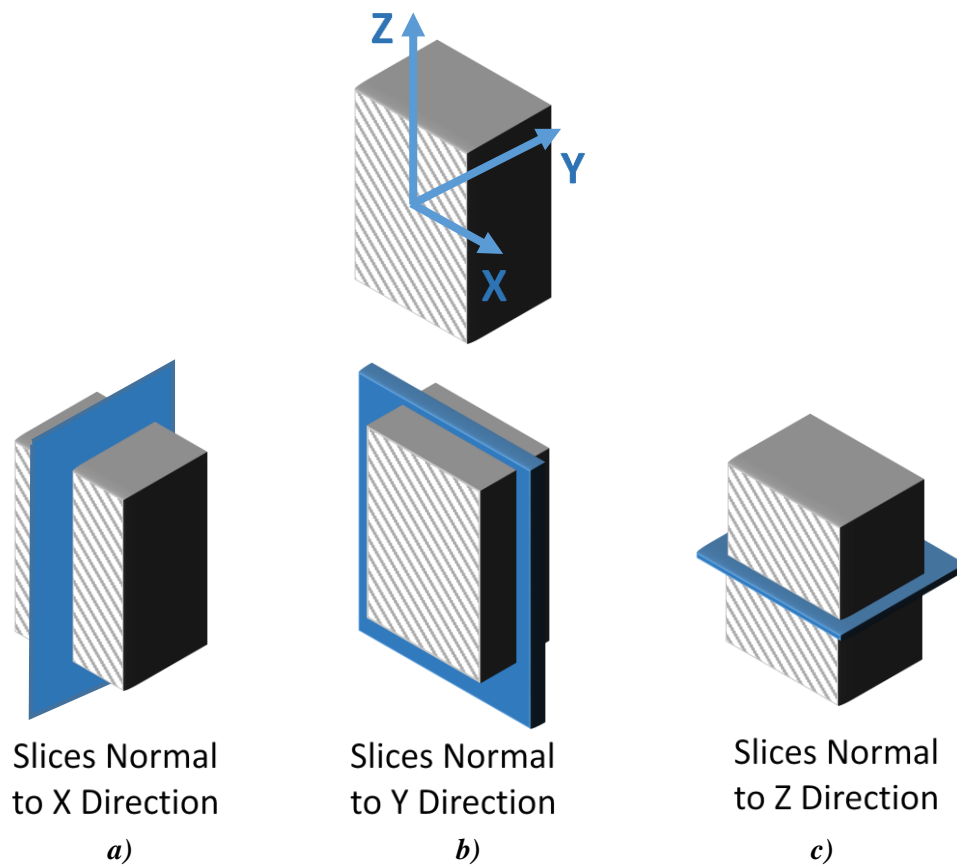


**Figure E.88-6. Slice direction nomenclature.**

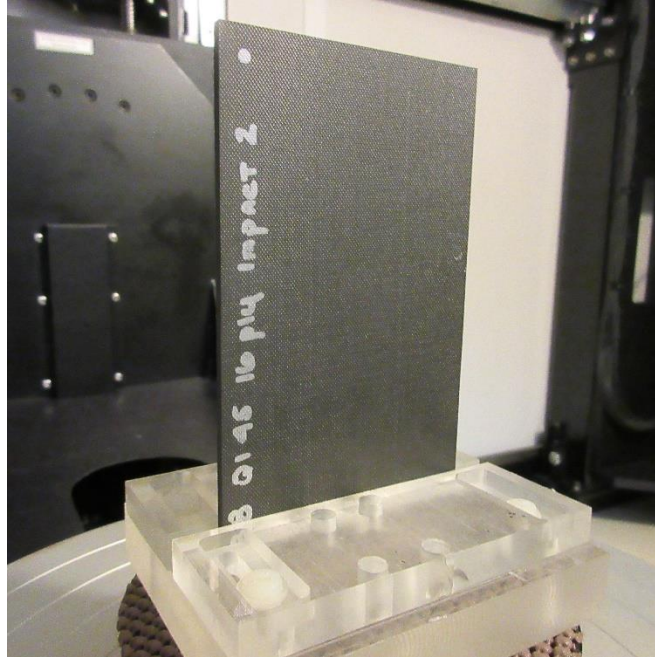


*Figure E.88-7. Impact specimen test stand setup.*

#### **E.88.2.4 Equipment List and Specifications:**

- Avonix 225 CT System
- 225 kV microfocus X-ray source with 5  $\mu\text{m}$  focal spot size
- 15 or 30kg Capacity 5 axis fully programmable manipulator.
- Detector: Perkin Elmer XRD 1621 – 2000  $\times$  2000 pixels with 200  $\mu\text{m}$  pitch
- 10  $\mu\text{m}$  spatial resolution for specimens 1.5 cm wide
- Thin panels 10-inch  $\times$  10-inch – full volume 200  $\mu\text{m}$  spatial resolution

#### **E.88.2.5 Settings**

*Table E.88-2. Data collection settings.*

Source Energy	160 kV
Current	37 $\mu\text{A}$
Magnification	5.0 X
Filter	0.125 Sn
# Rotational angles	3142
Exposure time / frame	1.0 sec
Max Histogram Grey Level	55 K
# Averages	8
Resolution ( $\mu\text{m}$ )	40.04 $\mu\text{m}$
Array Dimensions (pixels)	1999 $\times$ 204 $\times$ 1998

The specimen is placed vertically (rotated about the smallest dimension) on the rotational stage located between the radiation source and the detector. The rotational stage is computer-controlled and correlated to the position of the sample. As the sample is rotated the full 360° (~0.11° increments), the detector collects radiographs at each rotated angle as the X-ray path intersects the sample. 3D reconstruction of the collection of radiographs produces a volume of data that can then

be viewed along any plane in the volume. The closer the sample can be placed to the X-ray source, the higher the spatial resolution that can be obtained.

### E.88.2.6 Data and Results

Specimen #88, is a 3 by 5-inch 16-ply flat panel with a BVID impact. XCT was performed on this specimen in NASA LaRC’s CT system with the settings defined in Table E-88.2.

The damage caused by the impact can be clearly seen from all viewing directions as shown in Figure E.88-8. There is a small surface indication of an impact. Damage extends approximately three-fourths of the way through the thickness of the specimen. Delaminations and matrix cracking are detectable.

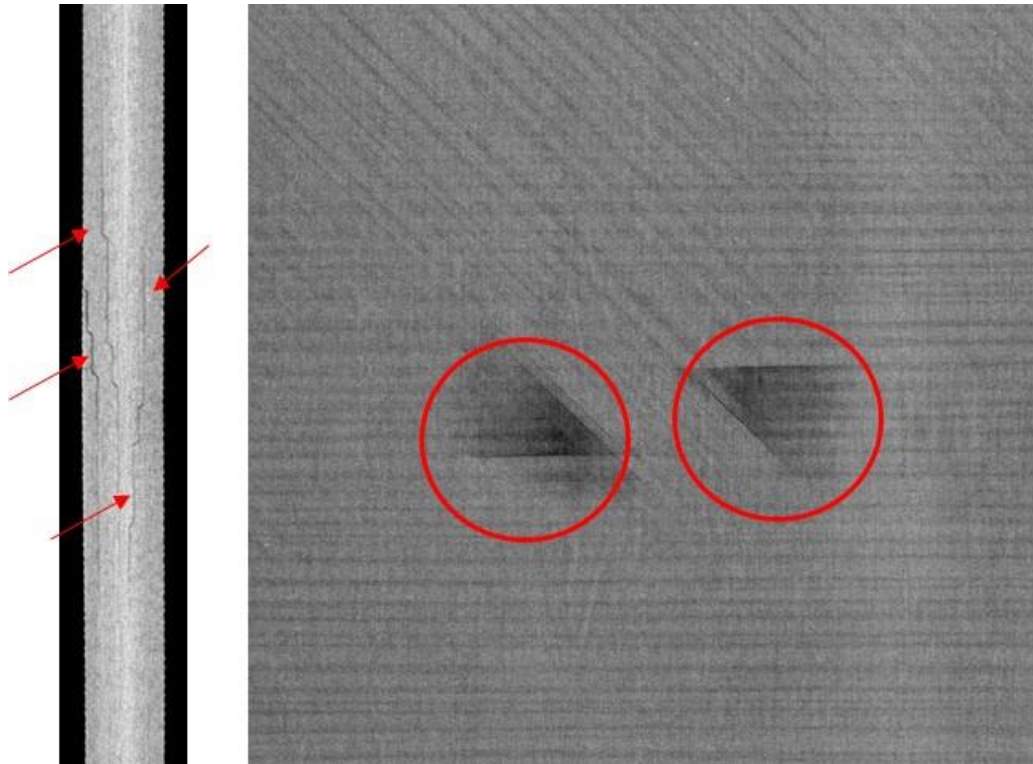


*Figure E.88-8. CT slice normal to the thickness direction show delaminations and matrix cracking (left). CT slice normal to the front surface shows delaminations between plies (right).*

### E.89 Specimen #89: Boeing Impact QI 45 16ply 22x22 Impact 1

Structure	Material	Details	Dimensions (inches)	Partner Methods	
16 plies	IM7/8552	Single Impact Location	22 × 22	Boeing	E.89.1 X-ray CR E.89.2 XCT E.89.3 Shearography
				NASA	E.89.4 SSIR

### E.90 Specimen #90: Boeing Impact QI 45 24ply 6x6 Impact 1

Structure	Material	Details	Dimensions (inches)	Partner Methods	
24 plies	IM7/8552	Single Impact Location	6 × 6 5 × 3	Boeing	E.90.1 XCT E.90.1 X-ray CR
				NASA	E.90.3 PEUT



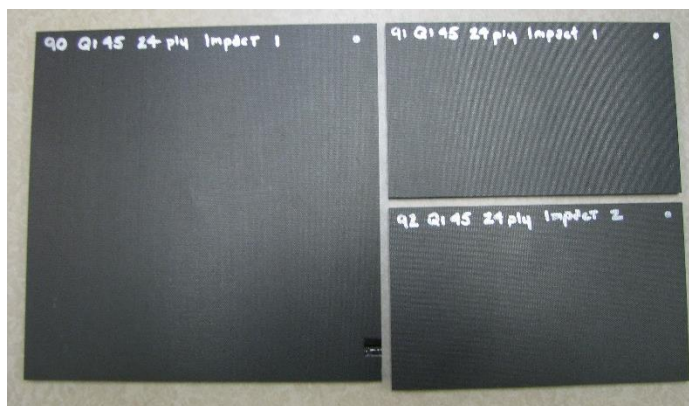


Figure E.90-1. Photographs of radii delamination standard.

### E.90.1 Method: X-ray Computed Tomography (XCT)

#### E.90.1.1 Partner: Boeing

#### E.90.1.2 Technique Applicability: ★★★

XCT is able to detect impact damage on some of the panels.

#### E.90.1.3 Equipment List and Specifications:

- YXLON Modular CT System
- 225 kV microfocus X-ray source with variable focal spot size
- 100 kg capacity 7-axis granite based manipulator
- XRD 1621 Detector- 2048 × 2048 pixels with 200- $\mu\text{m}$  pitch, 400 × 400-mm active area
- 111- $\mu\text{m}$  spatial resolution for impact panel scan
- Volume Graphics 3.0 visualizing software
- Reconstruction Computer

#### E.90.1.4 Settings

Table E.90-1. Data collection settings.

Source Energy	120 kV
Current	0.60 mA
Magnification	1.80 X
Filter	Copper
# Rotational angles	1410
Exposure time / frame	500 ms
Frame Binning	2
Spatial Resolution ( $\mu\text{m}$ )	111 $\mu\text{m}$
Array Dimensions (pixels)	2048 × 2048

#### E.90.1.5 Laboratory Setup

The DRC utilizes an YXLON Modular CT System. This system has the capability to utilize various X-ray sources for varying applications, including a 450-kV source, a microfocus source, and a nanofocus source. The microfocus source used has a variable focal spot size of less than 4  $\mu\text{m}$  and is suitable for magnifications up to 10X, with the nanofocus ranging up to 187X. The detector has 3 DOFs, allowing the effective detector area to be increased through combined scans. The

manipulator controls the position of the detector, object, and source. It has 7 DOFs including a rotating stage to rotate the object during the scan. The entire system includes the source, detector, manipulator, control and reconstruction computers, and user control station. The computers and control station are outside of the radiation enclosure (vault) and utilize a safety interlock system to operate. Cameras are located in the vault to allow the operator to monitor the part from outside the enclosure.

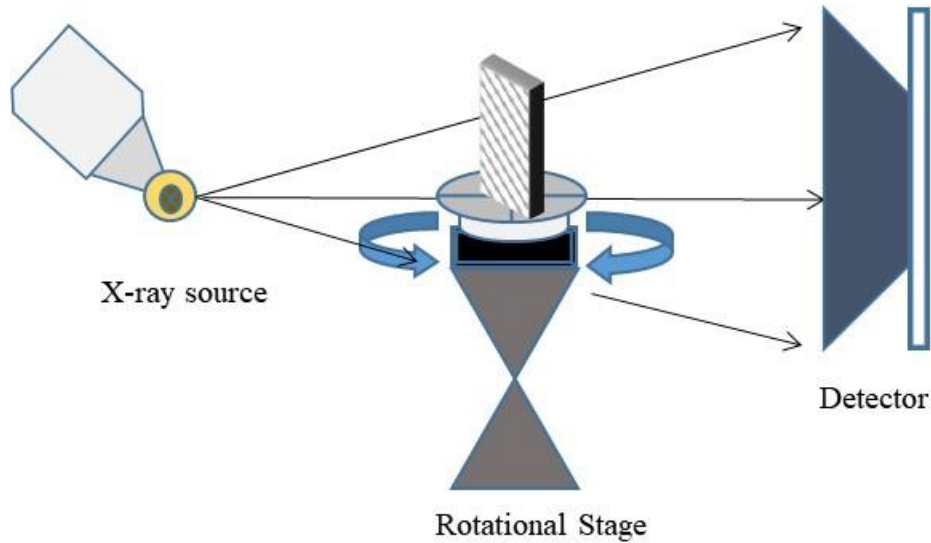


*Figure E.90-2. XCT system components.*

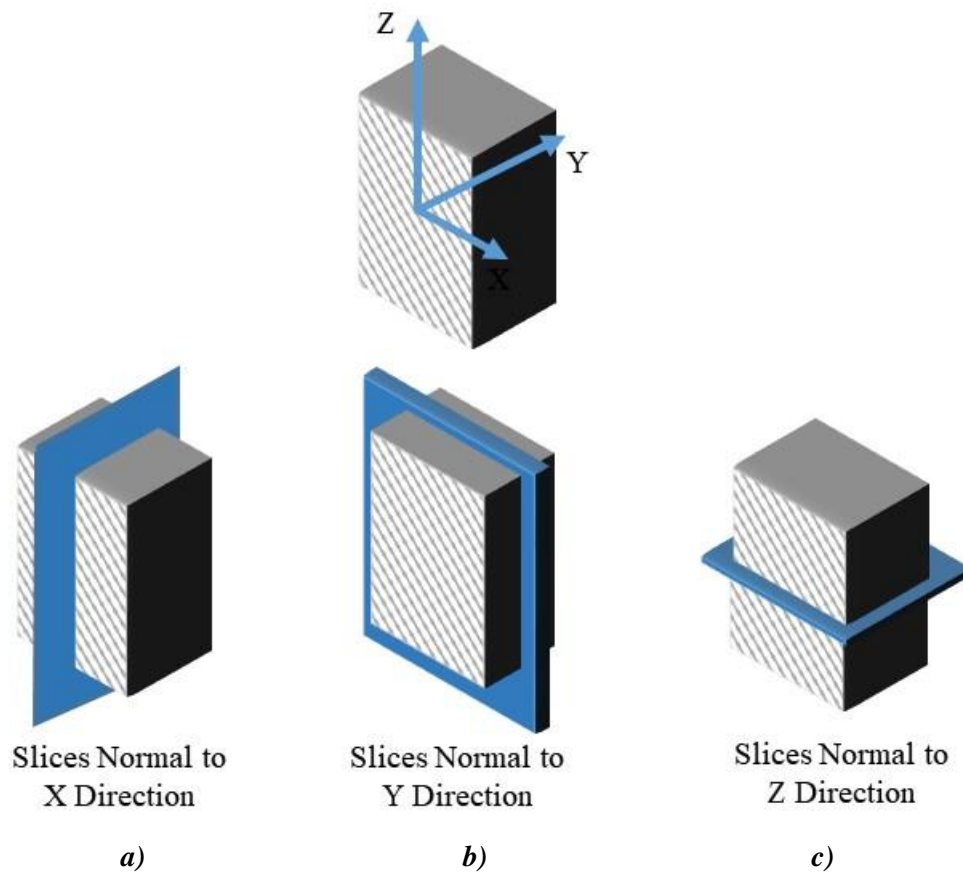


*Figure E.90-3. Slice direction nomenclature.*

To reduce overall scan time, the standard panels of the same thickness were stacked together, separated by light foam sheets and held together with tape. This allowed three parts to be scanned at once and analyzed separately in post-processing. The panel bundle was then secured in a foam fixture. The position of the specimen, source, and detector are controlled to produce geometric magnification of the image and increase the spatial resolution. The image data are gathered as X-rays penetrate the part and expose the detector for a set amount of time. For each scan, these image data are collected at 1410 different angles throughout a 360° rotation. These images are then reconstructed to create the 3D volume dataset. This dataset is viewed and analyzed in Volume Graphics, a volume rendering software, to identify the relevant components.

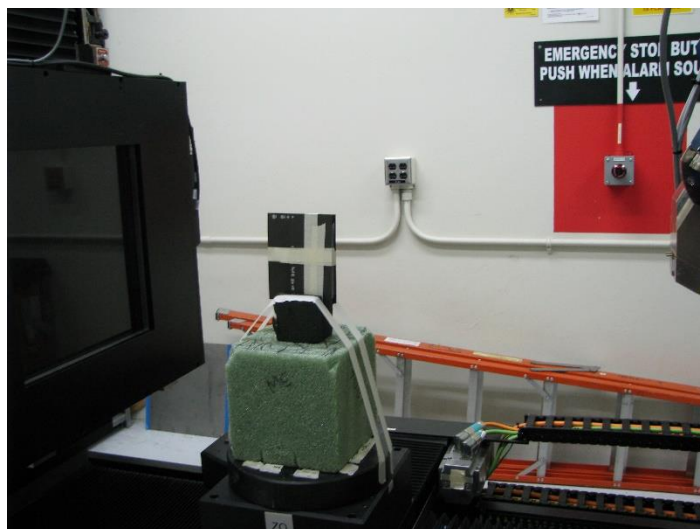


*Figure E.90-4. Microfocus XCT setup for impact damage standards.*

### E.90.1.6 Inspection Results

Unlike 2D X-ray imaging, CT shows slice views of the object that are not superimposed. This allows for improved detection of flaws. In the case of the impact panels, the damage would show as a slightly dented region at the near surface. Figure E.90-5 shows a slice view at the near surface of each panel. The dark spot in the center of Figure E.90-5b and c indicates less dense or lack of material, caused by the indentation of the impact on Panels 91 and 92. The tape used to hold the panels together for the scan is visible in Figure E.90-5a, with similar impact damage visible in the center for Panel 90.

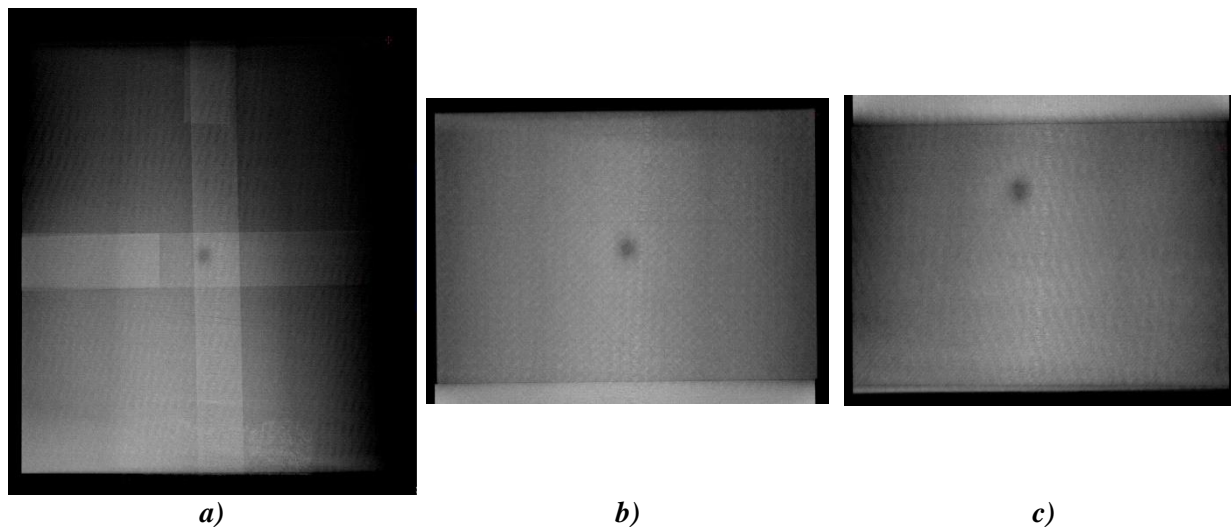


*Figure E.90-5. CT slice view of 24-ply impact damage panels 90 (a), 91 (b), and 92 (c).*

## E.90.2 Method: X-ray Computed Radiography (CR)

### E.90.2.1 Partner: Boeing

### E.90.2.2 Technique Applicability: ☆☆☆

X-ray CR is unable to reliably detect the impact damage.

### E.90.2.3 Equipment List and Specifications:

- Philips 160 kV X-Ray source, 0.4-mm focal spot size
- IPS Phosphorus Imaging Plate
- GE CRxFlex Scanner, 50- $\mu$ m resolution
- GE Rhythm Review 5.0 visualizing software

### E.90.2.4 Settings

*Table E.90-2. Imaging and exposure parameters.*

Source Energy	40 kV
Current	2 mA
Source-Detector Distance	60 in
Magnification	1X
Exposure time	35 s
Resolution ( $\mu$ m)	50 $\mu$ m
Imaging Area (in)	14 $\times$ 17

### E.90.2.5 Laboratory Setup

The DRC has a small X-ray enclosure (vault) for the primary purpose of 2D X-ray imaging. It includes a Philips 160-kV X-ray source and the ability to use film, CR, and digital detector arrays. The CR imaging plates are placed on a table and the source, suspended from the ceiling by a 3-axis crane, can be positioned to control the Source to Object Distance. Outside of the enclosure are the controls for the source, utilizing a safety interlock system. These controls allow the user to set the energy, current, and exposure time for the source. In addition to the vault, the DRC utilizes a CRxFlex system to scan and erase the CR imaging plates, storing the images on a computer. The phosphorus imaging plates, after exposure to X-rays, will luminesce the images when exposed to red light, allowing the 50- $\mu$ m scanner to create digital versions and “erase” the plates using bright white light to be used again. The CR digital images are then reviewed using Rhythm Review.

The three panels of the same thickness, each containing an impact damaged point, were placed directly on the plastic cassette containing the imaging plate with the X-ray source directly overhead (Figure E.90-6). The source was located 60 inches from the specimen and imaging plate to reduce geometric distortion. Lead markers were used to label the image, showing up in the results as bright white.



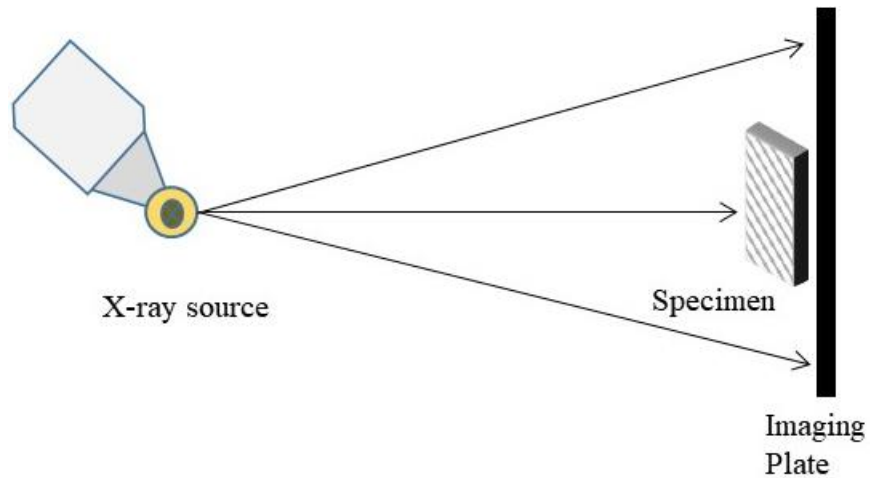


*Figure E.90-6. X-ray CR imaging.*

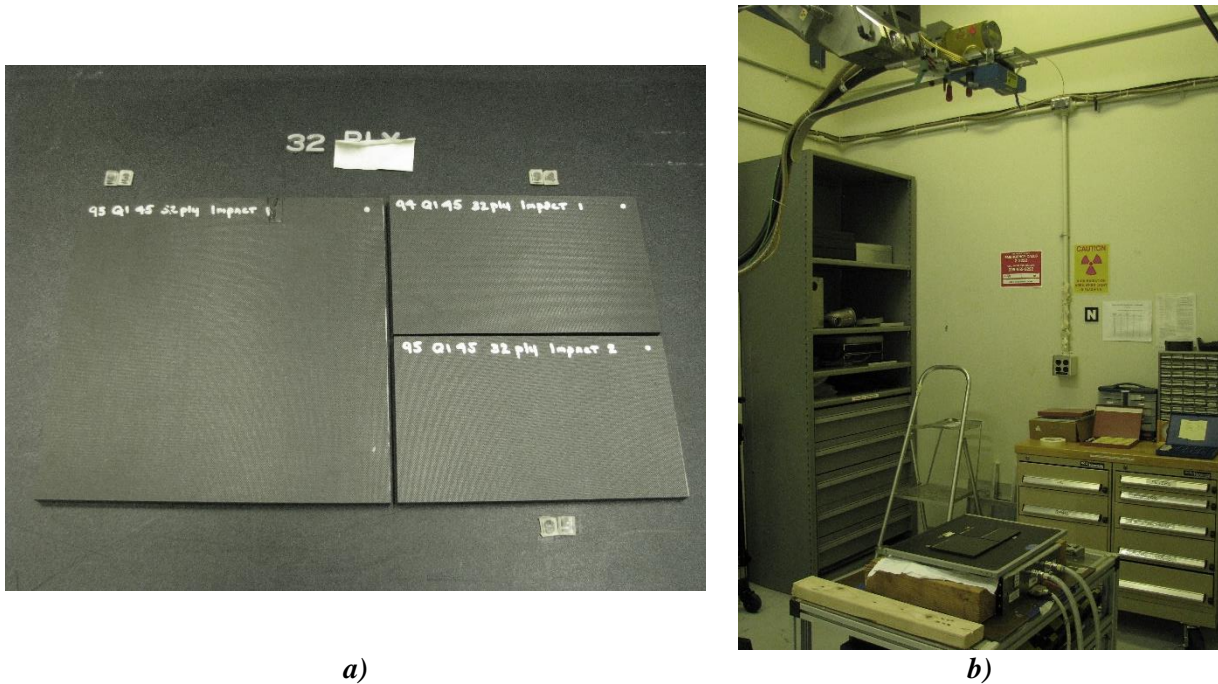


*Figure E.90-7. Laboratory setup of impact plate standards for CR imaging.*

### E.90.2.6 Inspection Results

CR imaging is dependent on the superimposed density of the part being imaged. In the case of the impact damage, the damaged portion tends to get indented, slightly compressing the material underneath the indent. Therefore, the superimposed density remains approximately the same. This makes the detection of impact damage by an operator using 2D radiography such as CR very difficult. As seen in Figure E.90-8, the impact damage is not easily visible. Given knowledge of the locations, an operator may be able to discern damage but contrast from the damage is not enough to be detected in a general case.



*Figure E.90-8. Flash filtered CR image of 24-ply impact panels.*

### **E.90.3 Method: Pulse-Echo Ultrasound Testing (PEUT)**

#### **E.90.3.1 Partner: NASA**

#### **E.90.3.2 Technique Applicability: ★★ ★**

PEUT detected the impact damage in this sample.

#### **E.90.3.3 Laboratory Setup**

Immersion Ultrasonic Testing: NASA LaRC uses a custom-designed single-probe ultrasonic scanning system. The system has an 8-axis motion controller, a multi-axis gantry robot mounted above a medium-size water tank, a dual-channel, 16-bit, high-speed digitizer, and an off-the-shelf ultrasonic pulser receiver. The system can perform TTUT and PEUT inspections. TT inspection employs two aligned ultrasonic probes, one transmitter, and one receiver, placed on either side of a test specimen. Pulse-echo inspection is a single-sided method where a single ultrasonic probe is both transmitter and receiver. In each method, data are acquired while raster scanning the ultrasonic probe(s) in relation to a part. Figure E.90-9 shows a simplified block diagram of a scanning Pulse-echo inspection

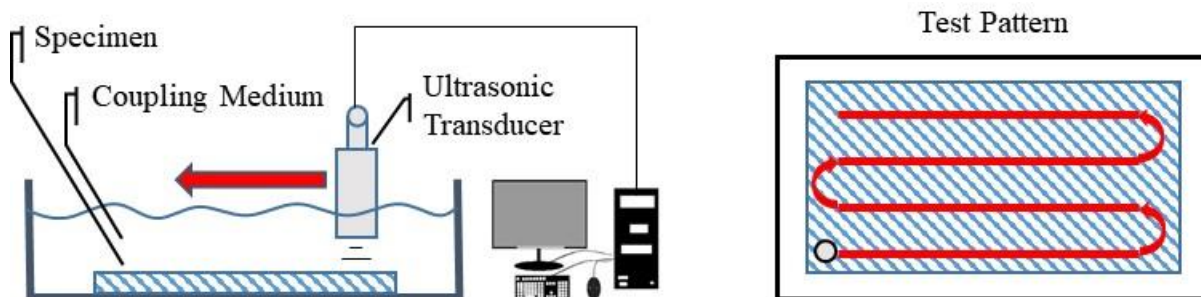


*Figure E.90-9. Ultrasonic system components.*

#### E.90.3.4 Equipment List and Specifications:

- Pulsar/Receiver: Olympus 5073PR
- Digitizer: AlazarTech ATS9462, dual channel, 16 bit, 180 MS/s
- Sensor: Olympus 2-inch spherical focus immersion ultrasonic transducer
- Motion system: open looped stepper motor based X-YY-Z gantry robot
- Motion Controller: Galil DMC-4183
- Acquisition Software: FastScan, custom developed at NASA LaRC
- Signal Processing Software: DataViewer, custom developed at NASA LaRC

#### E.90.3.5 Settings

*Table E.90-3. Post-impact inspection settings.*

Resolution (horz) [in/pixel]	0.01
Resolution (ver) [in/pixel]	0.01
Probe frequency [MHz]	10
Focal Length [in]	2
Array Dimensions [pixels]	601 × 601

The specimen is placed flat against the zero position of the tank raised above the glass bottom by several metal washers. The test probe is computer-controlled and correlated to the position on the sample. It is also focused to a point 1 mm below the surface of the test material. The specimen remains in place while the transducer follows a preprogrammed test grid across the surface as indicated in Figure E.90-10. At each point, ultrasonic data are collected from individual pulses. Larger step sizes between data collection result in lower image resolution. These data points are reconstructed into a data cube displaying spatial coordinates as time progresses. 2D reconstruction of the collection of ultrasonic responses create flattened slices at varying depths within the material.

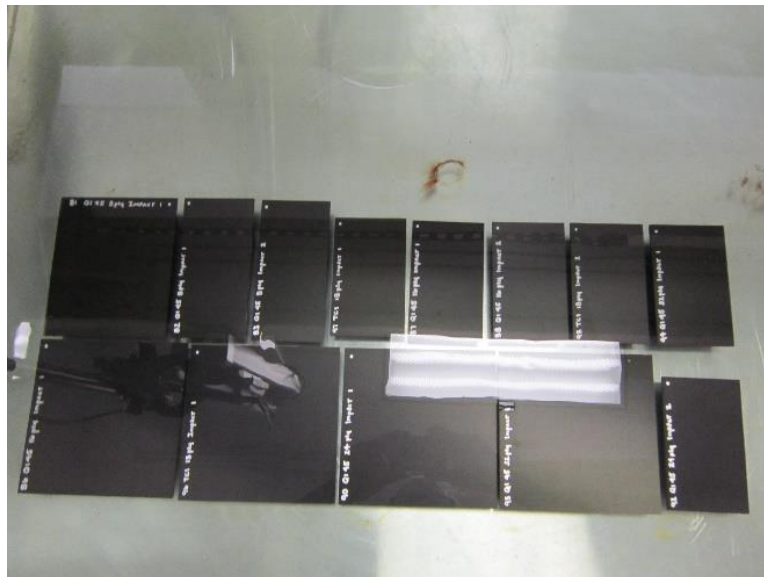
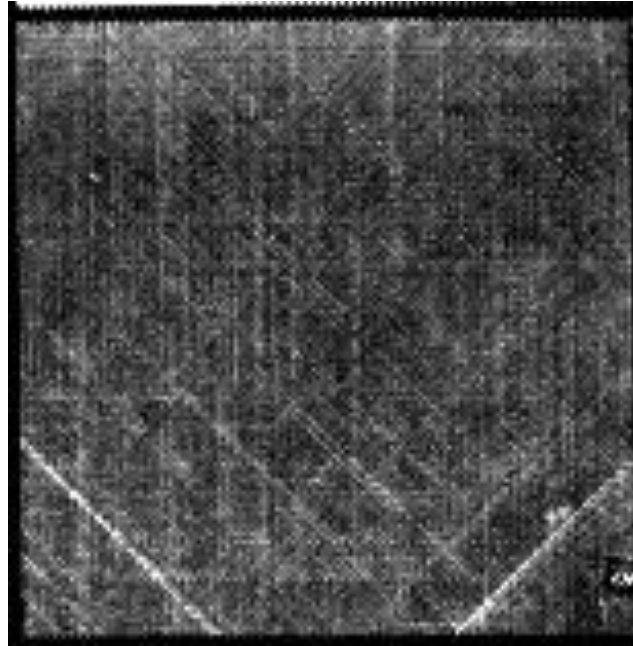


*Figure E.90-10. Specimen baseline inspection orientation.*

### E.90.3.6 Inspection Results

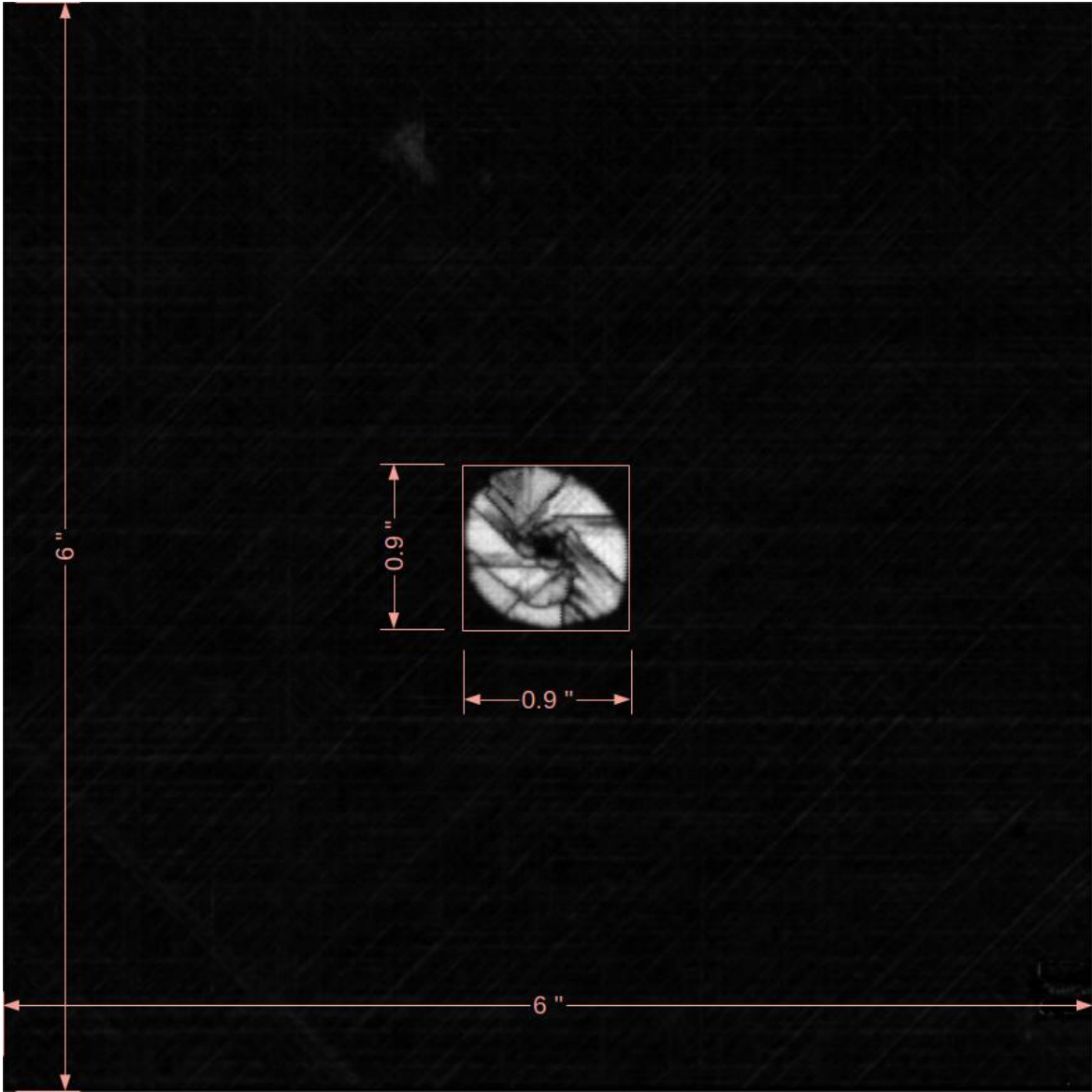
Specimen #90 is a 6 by 6-inch, 24-ply flat panel with a 1-inch impact. PEUT was performed on this specimen in NASA's immersion tank specified above.

Figure E.90-11 shows a back side surface amplitude image of the sample in its pre-impacted state. Small voids are visible in the upper left and lower right of the sample. There is also an indication from visible damage near the lower right corner.



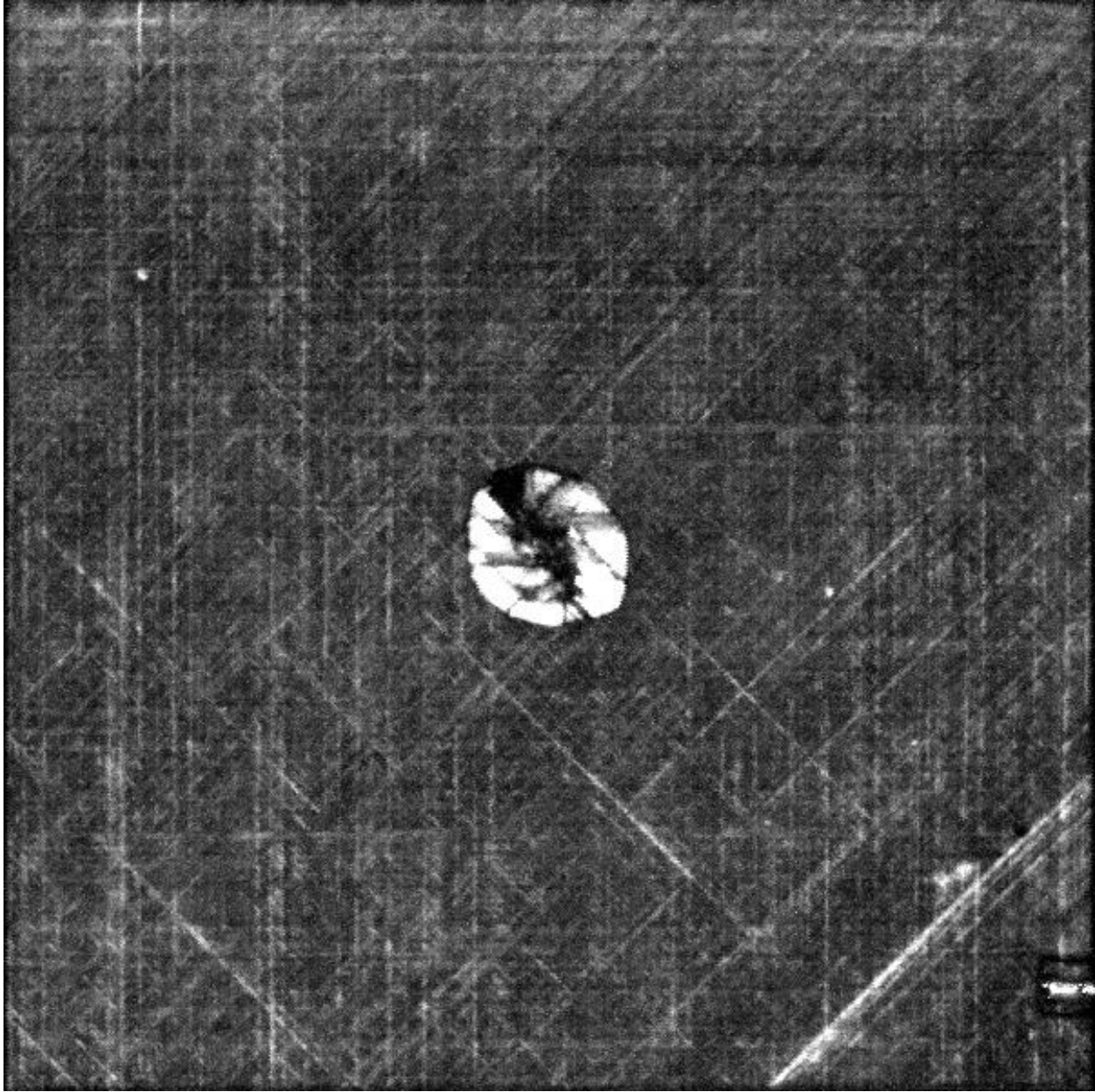
*Figure E.90-11. 10-MHz baseline image.*

Figure E.90-12a shows an internal reflection amplitude image of the sample in its post-impacted state. The gate region is selected to highlight reflections from the delaminations caused by the impact. The impact damage region is identified with measurements. Figure E.90.12b shows the same time gated region as above allowing the high-amplitude delamination reflections to saturate revealing the internal flaws noted on the pre-impact inspection.



*a)*





b)

*Figure E.90-12. 10-MHz post-impact image.*

**E.91 Specimen #91: Boeing Impact QI\_45 24ply 3x5 Impact 1**

Structure	Material	Details	Dimensions (inches)	Partner Methods	
24 plies	IM7/8552	Single Impact Location	6 × 6 5 × 3	NASA	E.91.1 PEUT E.91.2 XCT

## E.91.1 Method: Pulse-Echo Ultrasound Testing (PEUT)

### E.91.1.1 Partner: NASA

### E.91.1.2 Technique Applicability: ★★ ★

PEUT detected the impact damage in this sample.

### E.91.1.3 Laboratory Setup

Immersion Ultrasonic Testing: NASA LaRC uses a custom-designed single-probe ultrasonic scanning system. The system has an 8-axis motion controller, a multi-axis gantry robot mounted above a medium-size water tank, a dual-channel, 16-bit, high-speed digitizer, and an off-the-shelf ultrasonic pulser receiver. The system can perform TTUT and PEUT inspections. TT inspection employs two aligned ultrasonic probes, one transmitter, and one receiver, placed on either side of a test specimen. Pulse-echo inspection is a single-sided method where a single ultrasonic probe is both transmitter and receiver. In each method, data are acquired while raster scanning the ultrasonic probe(s) in relation to a part. Figure E.91-1 shows a simplified block diagram of a scanning Pulse-echo inspection.

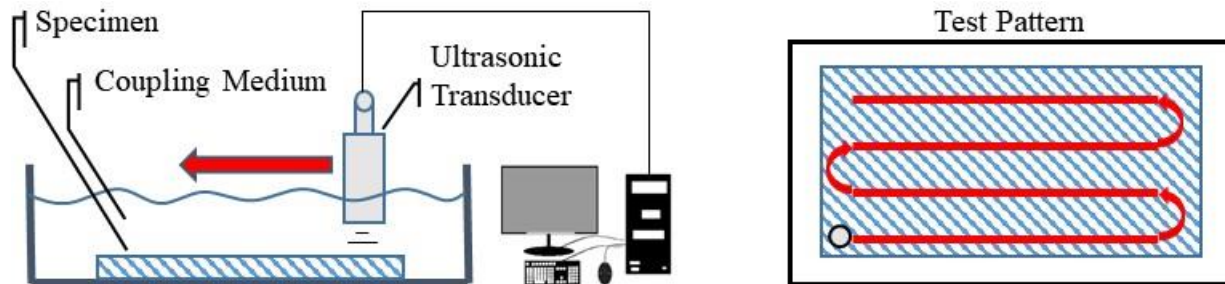


Figure E.91-1. Ultrasonic system components.

### E.91.1.4 Equipment List and Specifications:

- Pulser/Receiver: Olympus 5073PR
- Digitizer: AlazarTech ATS9462, dual channel, 16 bit, 180 MS/s
- Sensor: Olympus 2-inch spherical focus immersion ultrasonic transducer
- Motion system: open looped stepper motor based X-YY-Z gantry robot
- Motion Controller: Galil DMC-4183
- Acquisition Software: FastScan, custom developed at NASA LaRC
- Signal Processing Software: DataViewer, custom developed at NASA LaRC

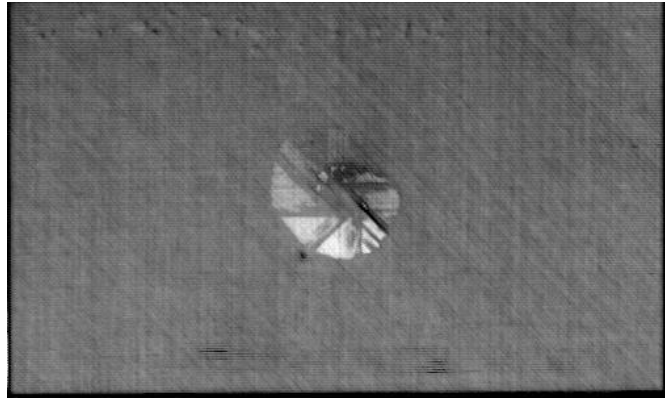
### E.91.1.5 Settings

Table E.91-1. Post-impact inspection settings.

Resolution (horz) [in/pixel]	0.01
Resolution (ver) [in/pixel]	0.01
Probe frequency [MHz]	10
Focal Length [in]	2
Array Dimensions [pixels]	500 × 301

The specimen is placed flat against the zero position of the tank raised above the glass bottom by several metal washers. The test probe is computer-controlled and correlated to the position on the sample. It is also focused to a point 1 mm below the surface of the test material. The specimen

remains in place while the transducer follows a preprogrammed test grid across the surface as indicated in Figure E.91-2. At each point, ultrasonic data are collected from individual pulses. Larger step sizes between data collection result in lower image resolution. These data points are reconstructed into a data cube displaying spatial coordinates as time progresses. 2D reconstruction of the collection of ultrasonic responses create flattened slices at varying depths within the material.



*Figure E.91-2. Specimen post-impact inspection orientation.*

#### **E.91.1.6 Inspection Results**

Specimen #91 is a 3 by 5-inch, 24-ply flat panel with a 1.11-inch impact. Only post-impacted PEUT was performed on this specimen in NASA's immersion tank specified above.

Figure E.91-3 shows a photograph of the pre-impacted sample. NASA did not perform baseline PEUT on this sample.

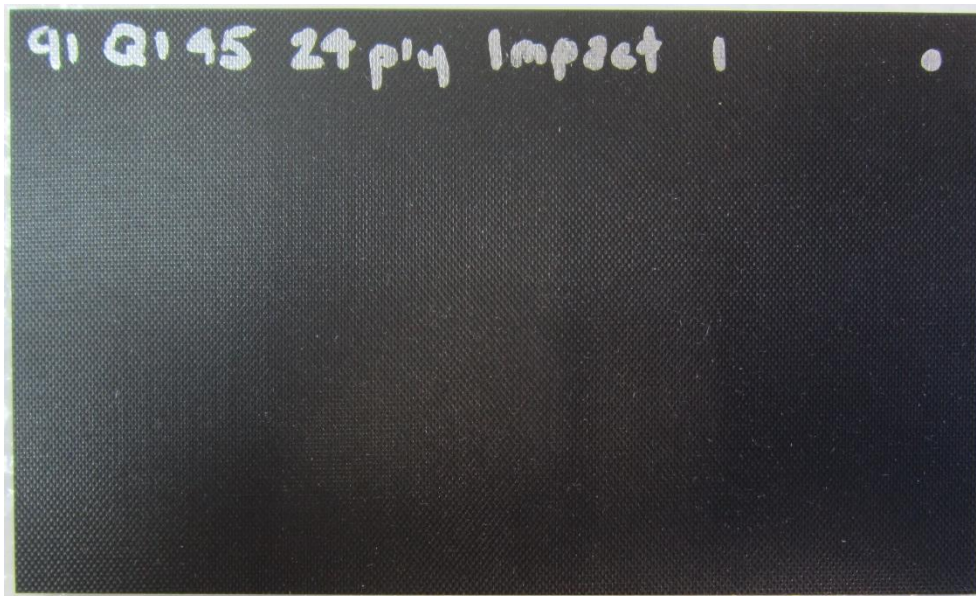
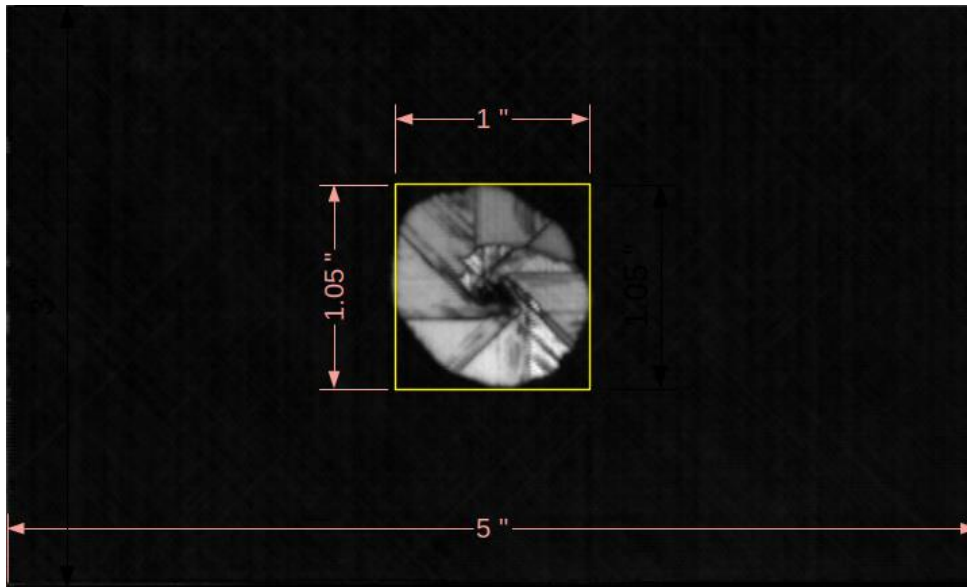


*Figure E.91-3. Baseline PEUT was not performed on this sample.*

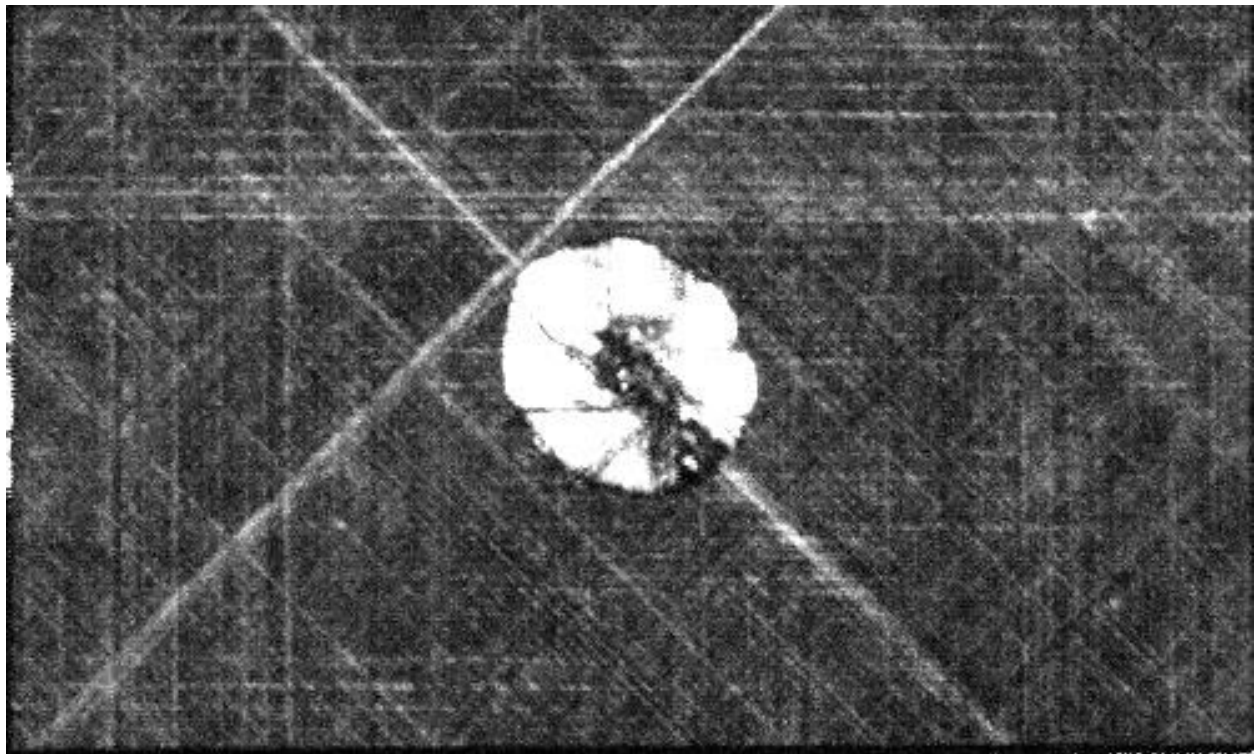
Figure E.91-4a shows an internal reflection amplitude image of the sample in its post-impacted state. The gate region is selected to highlight reflections from the delaminations caused by the impact. The impact damage region is identified with measurements. Figure E.91.4b shows the same



time gated region as above allowing the high-amplitude delamination reflections to saturate revealing the internal features.



a)



b)

*Figure E.91-4. 10-MHz post-impact image.*

## E.91.2 Method: X-ray Computed Tomography (XCT)

### E.91.2.1 Partner: NASA

### E.91.2.2 Technique Applicability: ★★★

XCT is capable of imaging and quantifying the damage due to low-impact energy in this specimen

### E.91.2.3 Laboratory Setup

The microfocus XCT system at NASA LaRC is a commercially available Avonix (Nikon C2) Metrology System designed for high-resolution NDE inspections. The system is an advanced microfocus X-ray system, capable of resolving details down to 5  $\mu\text{m}$ , and with magnifications up to 60X. The system is supplied as a complete, large-dimension radiation enclosure, with X-ray source, specimen manipulator, and an amorphous silica detector as shown in Figure E.91-5. The imaging controls are housed in a separate control console. The detector is a Perkin-Elmer 16-bit amorphous silicon digital detector with a  $2000 \times 2000$ -pixel array.

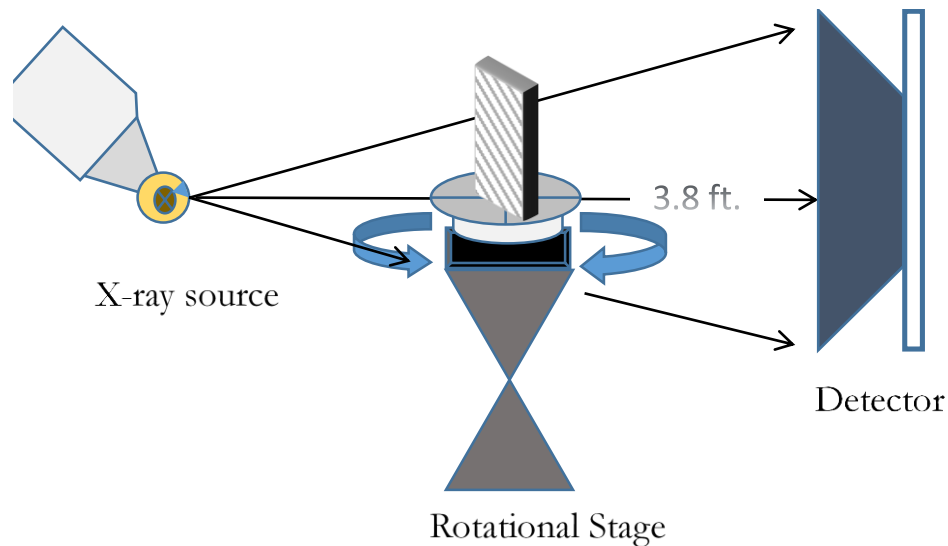


*Figure E.91-5. XCT system components.*

A consistent Cartesian coordinate system is used to define slice direction as illustrated in Figure E.91-6. Slices normal to the X, Y, and Z-directions are shown in Figure E.91-6a, b, and c, respectively.



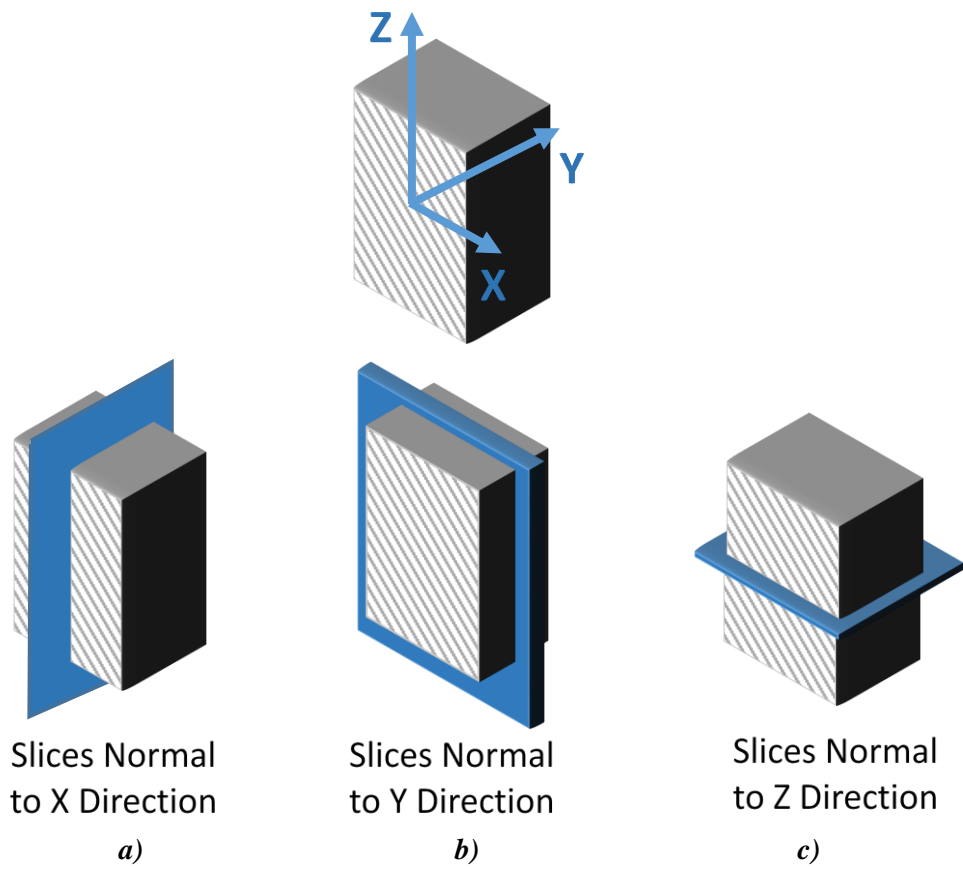


*Figure E.91-6. Slice direction nomenclature.*

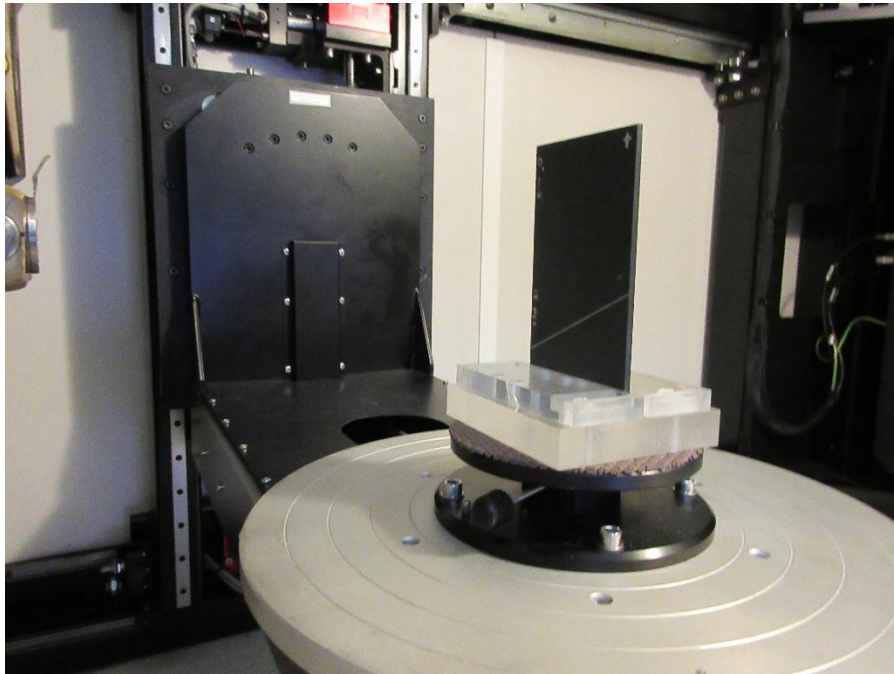


*Figure E.91-7. Impact specimen test stand setup.*

#### E.91.2.4 Equipment List and Specifications:

- Avonix 225 CT System
- 225 kV microfocus X-ray source with 5  $\mu\text{m}$  focal spot size
- 15 or 30kg Capacity 5 axis fully programmable manipulator.
- Detector: Perkin Elmer XRD 1621 – 2000  $\times$  2000 pixels with 200  $\mu\text{m}$  pitch
- 10  $\mu\text{m}$  spatial resolution for specimens 1.5 cm wide
- Thin panels 10-inch  $\times$  10-inch – full volume 200  $\mu\text{m}$  spatial resolution

#### E.91.2.5 Settings

*Table E.91-2. Data collection settings.*

Source Energy	160 kV
Current	37 $\mu\text{A}$
Magnification	5.0 X
Filter	0.125 Sn
# Rotational angles	3142
Exposure time / frame	1.0 sec
Max Histogram Grey Level	54.8 K
# Averages	8
Resolution ( $\mu\text{m}$ )	40.04 $\mu\text{m}$
Array Dimensions (pixels)	1999 $\times$ 305 $\times$ 1998

The specimen is placed vertically (rotated about the smallest dimension) on the rotational stage located between the radiation source and the detector. The rotational stage is computer-controlled and correlated to the position of the sample. As the sample is rotated the full 360° (~0.11° increments), the detector collects radiographs at each rotated angle as the X-ray path intersects the sample. 3D reconstruction of the collection of radiographs produces a volume of data that can then be viewed along any plane in the volume. The closer the sample can be placed to the X-ray source, the higher the spatial resolution that can be obtained.

#### E.91.2.6 Data and Results

Specimen #91, is a 3 by 5-inch 24-ply flat panel with a BVID impact. XCT was performed on this specimen in NASA LaRC's CT system with the settings defined in Table E-91.2.

The damage caused by the impact can be clearly seen from all viewing directions as shown in Figure E.91-8. There is a very small surface indication of an impact. Damage extends almost completely through the thickness of the specimen.

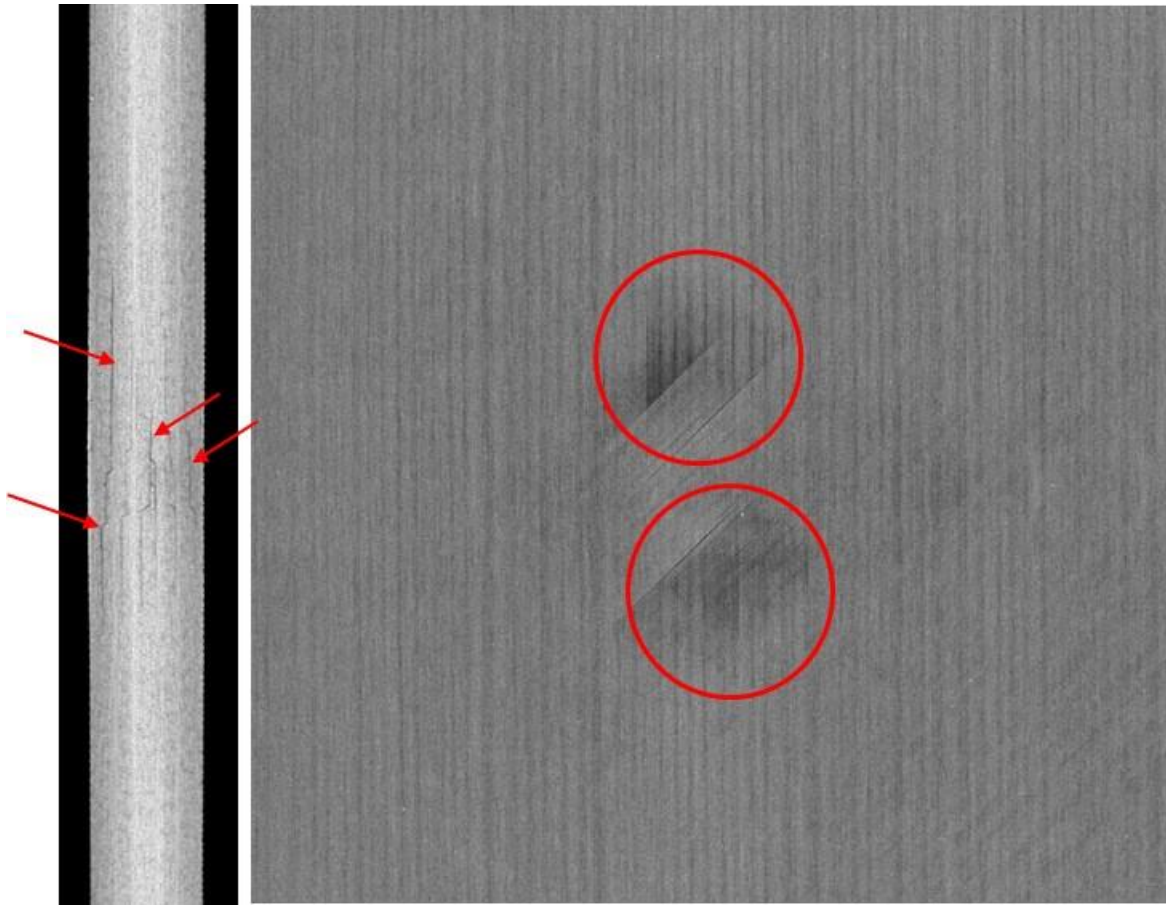


*Figure E.91-8. CT slice normal to the thickness direction show delaminations and matrix cracking (left). CT slice normal to the front surface shows delaminations between plies (right).*

## E.92 Specimen #92: Boeing Impact QI\_45 24ply 3x5 Impact 2

Structure	Material	Details	Dimensions (inches)	Partner Methods	
24 plies	IM7/8552	Single Impact Location	6 × 6 5 × 3	NASA	E.92.1 PEUT E.92.2 XCT

### E.92.1 Method: Pulse-Echo Ultrasound Testing (PEUT)

#### E.92.1.1 Partner: NASA

#### E.92.1.2 Technique Applicability: ★★★

PEUT detected the impact damage in this sample.

#### E.92.1.3 Laboratory Setup

Immersion Ultrasonic Testing: NASA LaRC uses a custom-designed single-probe ultrasonic scanning system. The system has an 8-axis motion controller, a multi-axis gantry robot mounted above a medium-size water tank, a dual-channel, 16-bit, high-speed digitizer, and an off-the-shelf ultrasonic pulser receiver. The system can perform TTUT and PEUT inspections. TT inspection employs two aligned ultrasonic probes, one transmitter, and one receiver, placed on either side of a test specimen. Pulse-echo inspection is a single-sided method where a single ultrasonic probe is both transmitter and receiver. In each method, data are acquired while raster scanning the

ultrasonic probe(s) in relation to a part. Figure E.92-1 shows a simplified block diagram of a scanning Pulse-echo inspection

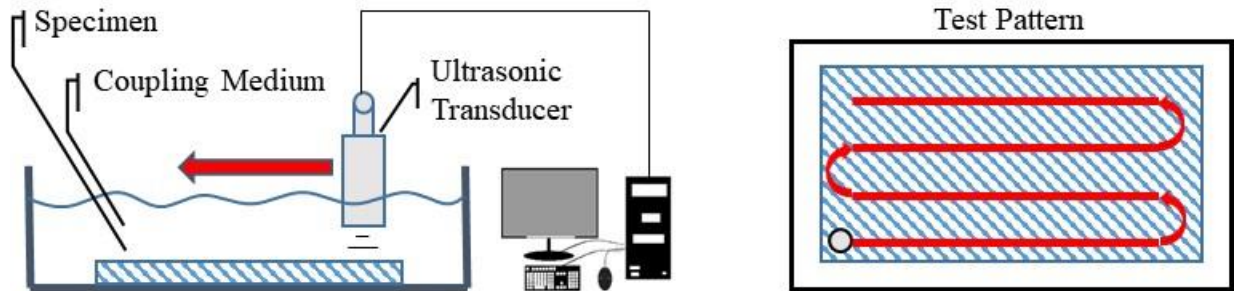


Figure E.92-1. Ultrasonic system components.

#### E.92.1.4 Equipment List and Specifications:

- Pulsar/Receiver: Olympus 5073PR
- Digitizer: AlazarTech ATS9462, dual channel, 16 bit, 180 MS/s
- Sensor: Olympus 2-inch spherical focus immersion ultrasonic transducer
- Motion system: open looped stepper motor based X-YY-Z gantry robot
- Motion Controller: Galil DMC-4183
- Acquisition Software: FastScan, custom developed at NASA LaRC
- Signal Processing Software: DataViewer, custom developed at NASA LaRC

#### E.92.1.5 Settings

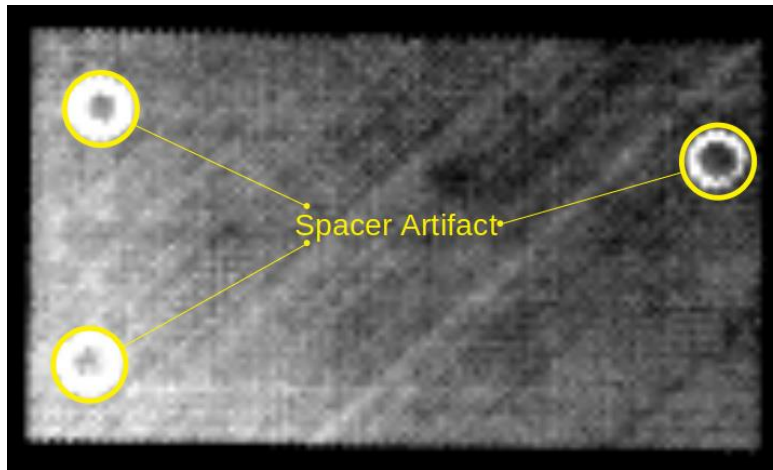
Table E.92-1. Post-impact inspection settings.

Resolution (horz) [in/pixel]	0.01
Resolution (ver) [in/pixel]	0.01
Probe frequency [MHz]	10
Focal Length [in]	2
Array Dimensions [pixels]	500 × 301

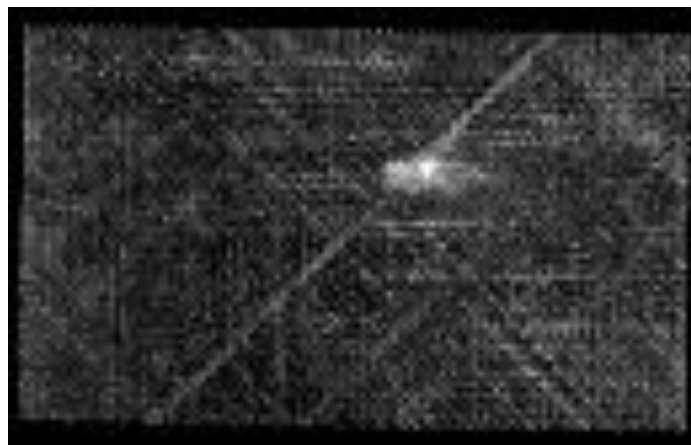
The specimen is placed flat against the zero position of the tank raised above the glass bottom by several metal washers. The test probe is computer-controlled and correlated to the position on the sample. It is also focused to a point 1 mm below the surface of the test material. The specimen remains in place while the transducer follows a preprogrammed test grid across the surface as indicated in Figure E.92-2. At each point, ultrasonic data are collected from individual pulses. Larger step sizes between data collection result in lower image resolution. These data points are reconstructed into a data cube displaying spatial coordinates as time progresses. 2D reconstruction of the collection of ultrasonic responses create flattened slices at varying depths within the material.







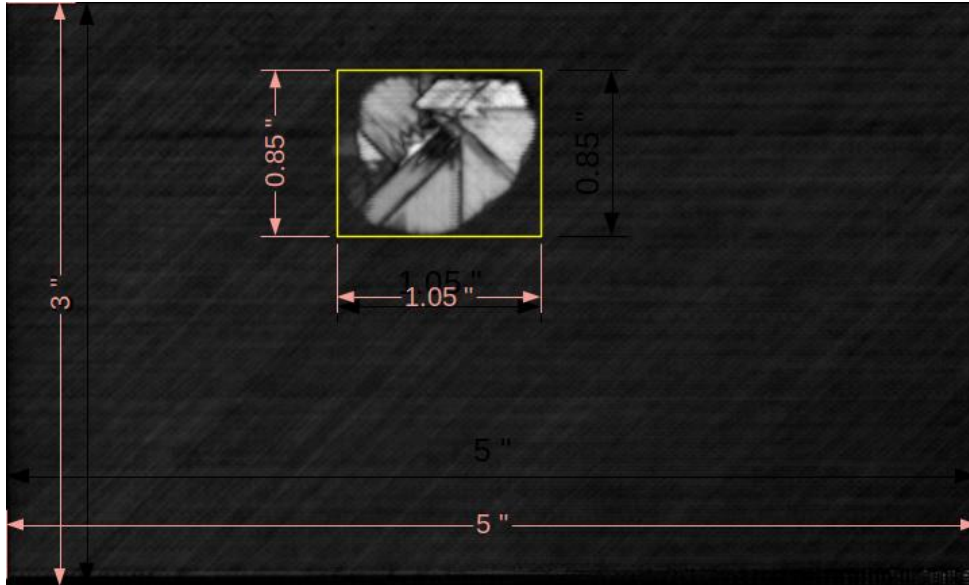
*a) Back side surface amplitude image.*



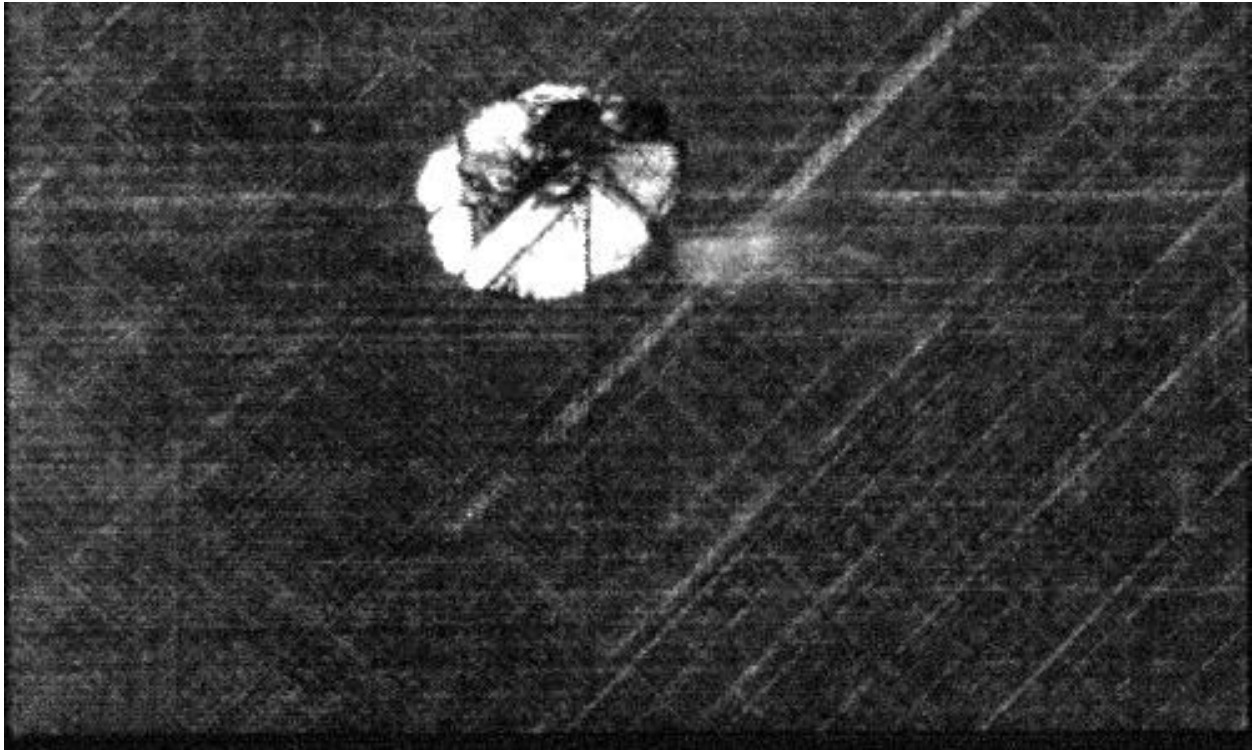
*b) High-amplitude sub-surface reflection.*

*Figure E.92-3. 10-MHz baseline image.*

Figure E.92-4a shows an internal reflection amplitude image of the sample in its post-impacted state. The gate region is selected to highlight reflections from the delaminations caused by the impact. The impact damage region is identified with measurements. Figure E.92.4b shows the same time gated region as above allowing the high-amplitude delamination reflections to saturate revealing the internal flaws noted on the pre-impact inspection. The high-amplitude region above and right of center appears unchanged after impact.



a)



b)

*Figure E.92-4. 10-MHz post-impact image.*

**E.92.2 Method: X-ray Computed Tomography (XCT)**

**E.92.2.1 Partner: NASA**

**E.92.2.2 Technique Applicability: ★★★**

XCT is capable of imaging and quantifying the damage due to low-impact energy in this specimen

### E.92.2.3 Laboratory Setup

The microfocus XCT system at NASA LaRC is a commercially available Avonix (Nikon C2) Metrology System designed for high-resolution NDE inspections. The system is an advanced microfocus X-ray system, capable of resolving details down to 5  $\mu\text{m}$ , and with magnifications up to 60X. The system is supplied as a complete, large-dimension radiation enclosure, with X-ray source, specimen manipulator, and an amorphous silica detector as shown in Figure E.92-5. The imaging controls are housed in a separate control console. The detector is a Perkin-Elmer 16-bit amorphous silicon digital detector with a  $2000 \times 2000$ -pixel array.

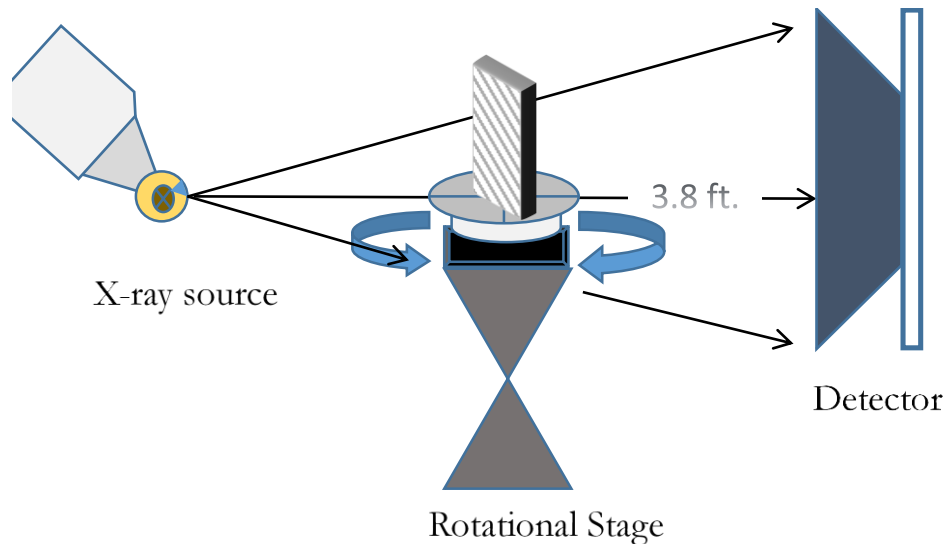


*Figure E.92-5. XCT system components.*

A consistent Cartesian coordinate system is used to define slice direction as illustrated in Figure E.92-6. Slices normal to the X, Y, and Z-directions are shown in Figure E.92-6a, b, and c, respectively.



#### E.92.2.4 Equipment List and Specifications:

- Avonix 225 CT System
- 225 kV microfocus X-ray source with 5  $\mu\text{m}$  focal spot size
- 15 or 30kg Capacity 5 axis fully programmable manipulator.
- Detector: Perkin Elmer XRD 1621 – 2000  $\times$  2000 pixels with 200  $\mu\text{m}$  pitch
- 10  $\mu\text{m}$  spatial resolution for specimens 1.5 cm wide
- Thin panels 10-inch  $\times$  10-inch – full volume 200  $\mu\text{m}$  spatial resolution

#### E.92.2.5 Settings

*Table E.92-2. Data collection settings.*

Source Energy	160 kV
Current	37 $\mu\text{A}$
Magnification	5.0 X
Filter	0.125 Sn
# Rotational angles	3142
Exposure time / frame	1.0 sec
Max Histogram Grey Level	55 K
# Averages	8
Resolution ( $\mu\text{m}$ )	40.04 $\mu\text{m}$
Array Dimensions (pixels)	1999 $\times$ 259 $\times$ 1998

The specimen is placed vertically (rotated about the smallest dimension) on the rotational stage located between the radiation source and the detector. The rotational stage is computer-controlled and correlated to the position of the sample. As the sample is rotated the full 360° (~0.11° increments), the detector collects radiographs at each rotated angle as the X-ray path intersects the sample. 3D reconstruction of the collection of radiographs produces a volume of data that can then be viewed along any plane in the volume. The closer the sample can be placed to the X-ray source, the higher the spatial resolution that can be obtained.

#### E.92.2.6 Data and Results

Specimen #92, is a 3 by 5-inch 24-ply flat panel with a BVID impact. XCT was performed on this specimen in NASA LaRC's CT system with the settings defined in Table E-92.2.

The damage caused by the impact can be clearly seen from all viewing directions as shown in Figure E.92-8. There is no surface indication of an impact. Damage extends all the way through the thickness of the specimen. The impact location is in the lower left portion of the FOV, and the impacted side is on the left in left hand image of Figure E.92-8. There is a very small inclusion in the image (yellow arrow).



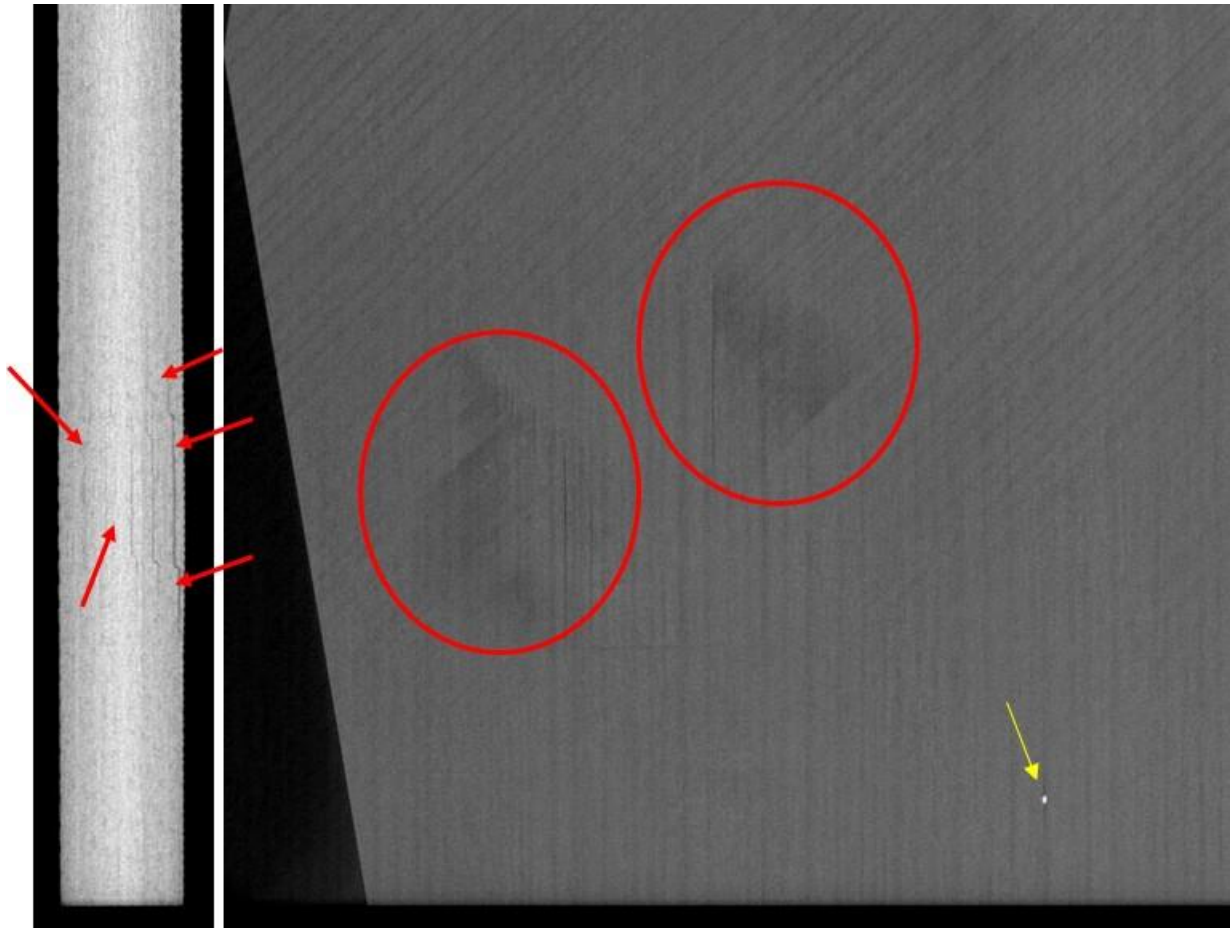


Figure E.92-8. CT slice normal to the thickness direction show delaminations and matrix cracking (left). CT slice normal to the front surface shows delaminations between plies (right).

**E.93 Specimen #93: Boeing Impact QI\_45 32ply 6x6 Impact 1**

Structure	Material	Details	Dimensions (inches)	Partner Methods	
32 plies	IM7/8552	Single Impact Location	6 × 6 5 × 3	Boeing	E.93.1 XCT E.93.2 X-ray CR
				NASA	E.93.3 PEUT

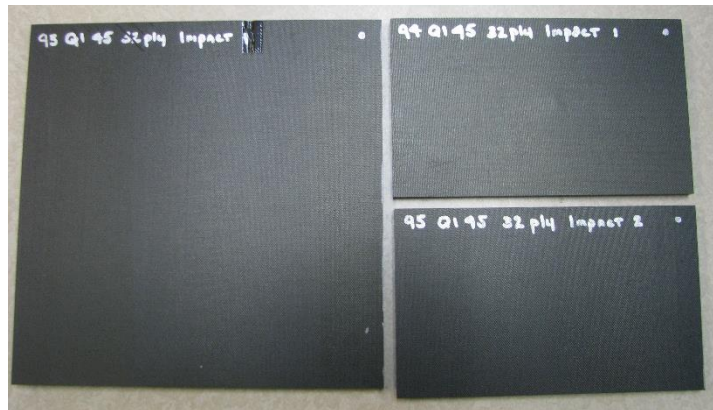


Figure E.93-1. Photographs of radii delamination standard.

### E.93.1 Method: X-ray Computed Tomography

#### E.93.1.1 Partner: Boeing

#### E.93.1.2 Technique Applicability: ★★☆☆

XCT is able to detect impact damage on some of the panels.

#### E.93.1.3 Equipment List and Specifications:

- YXLON Modular CT System
- 225 kV Microfocus X-ray source with variable focal spot size
- 100 kg capacity 7-axis granite based manipulator
- XRD 1621 Detector- 2048 × 2048 pixels with 200- $\mu\text{m}$  pitch, 400 × 400-mm active area
- 111  $\mu\text{m}$  spatial resolution for impact panel scan
- Volume Graphics 3.0 visualizing software
- Reconstruction Computer

#### E.93.1.4 Settings

*Table E.93-1. Data collection settings.*

Source Energy	125 kV
Current	0.60 mA
Magnification	1.80 X
Filter	Copper
# Rotational angles	1410
Exposure time / frame	500 ms
Frame Binning	2
Spatial Resolution ( $\mu\text{m}$ )	111 $\mu\text{m}$
Array Dimensions (pixels)	2048 × 2048

#### E.93.1.5 Laboratory Setup

The DRC utilizes an YXLON Modular CT System. This system has the capability to utilize various X-ray sources for varying applications, including a 450-kV source, a microfocus source, and a nanofocus source. The microfocus source used has a variable focal spot size of less than 4  $\mu\text{m}$  and is suitable for magnifications up to 10X, with the nanofocus ranging up to 187X. The detector has 3 DOFs, allowing the effective detector area to be increased through combined scans. The manipulator controls the position of the detector, object, and source. It has 7 DOFs including a rotating stage to rotate the object during the scan. The entire system includes the source, detector, manipulator, control and reconstruction computers, and user control station. The computers and control station are outside of the radiation enclosure (vault) and utilize a safety interlock system to operate. Cameras are located in the vault to allow the operator to monitor the part from outside the enclosure.

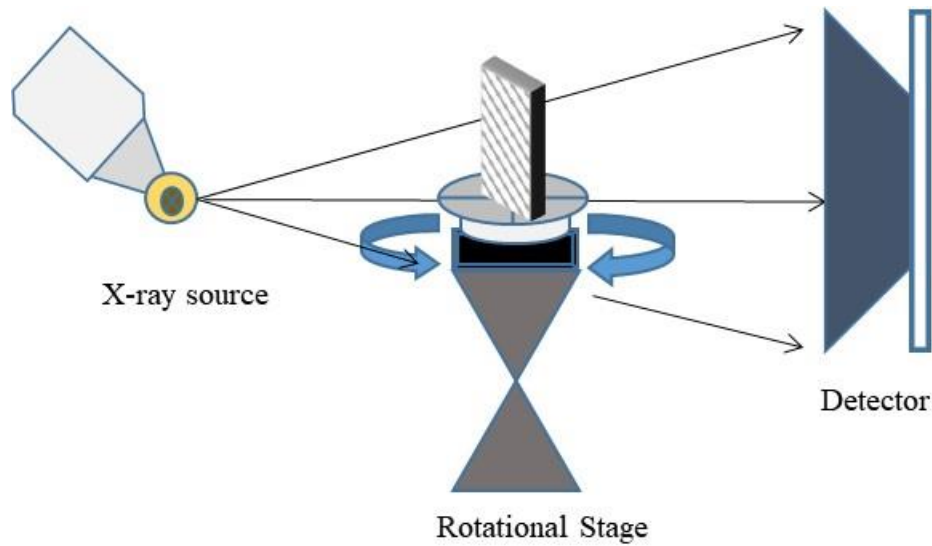


*Figure E.93-2. XCT system components.*

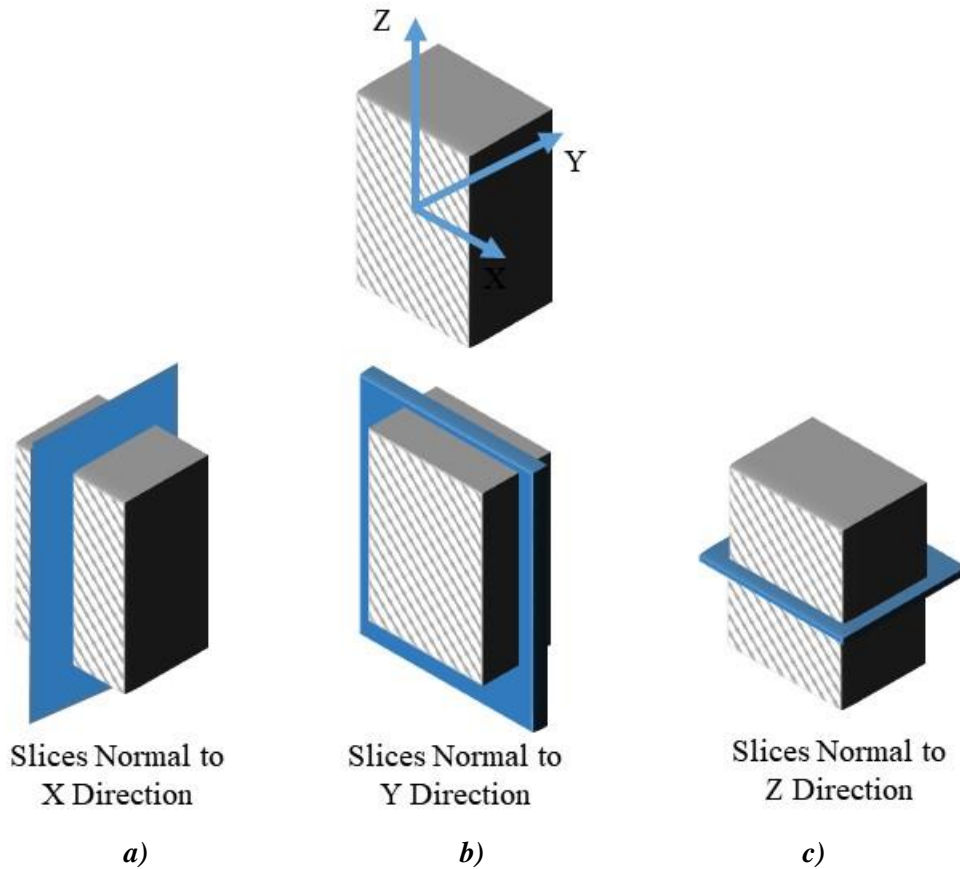


*Figure E.93-3. Slice direction nomenclature.*

To reduce overall scan time, the standard panels of the same thickness were stacked together, separated by light foam sheets and held together with tape. This allowed three parts to be scanned at once and analyzed separately in post-processing. The panel bundle was then secured in a foam fixture. The position of the specimen, source, and detector are controlled to produce geometric magnification of the image and increase the spatial resolution. The image data are gathered as

X-rays penetrate the part and expose the detector for a set amount of time. For each scan, these image data are collected at 1410 different angles throughout a 360° rotation. These images are then reconstructed to create the 3D volume dataset. This dataset is viewed and analyzed in Volume Graphics, a volume rendering software, to identify the relevant components.

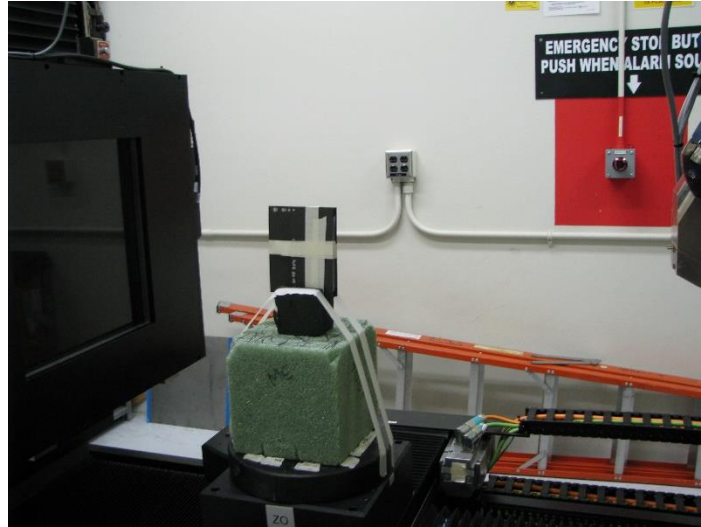


*Figure E.93-4. Microfocus XCT setup for impact damage standards.*

#### **E.93.1.6 Inspection Results**

Unlike 2D X-ray imaging, CT shows slice views of the object that are not superimposed. This allows for improved detection of flaws. In the case of the impact panels, the damage would show as a slightly dented region at the near surface. Figure E.93-5 shows a slice view at the near surface of each panel. The dark spot in the center of Figure E.93-5b indicates less dense or lack of material, caused by the indentation of the impact on Panel 94. A surface gouge is visible in Figure E.93-5a, however there is no detected impact damage for Panel 93 or Panel 95 (Figure E.93-5c).

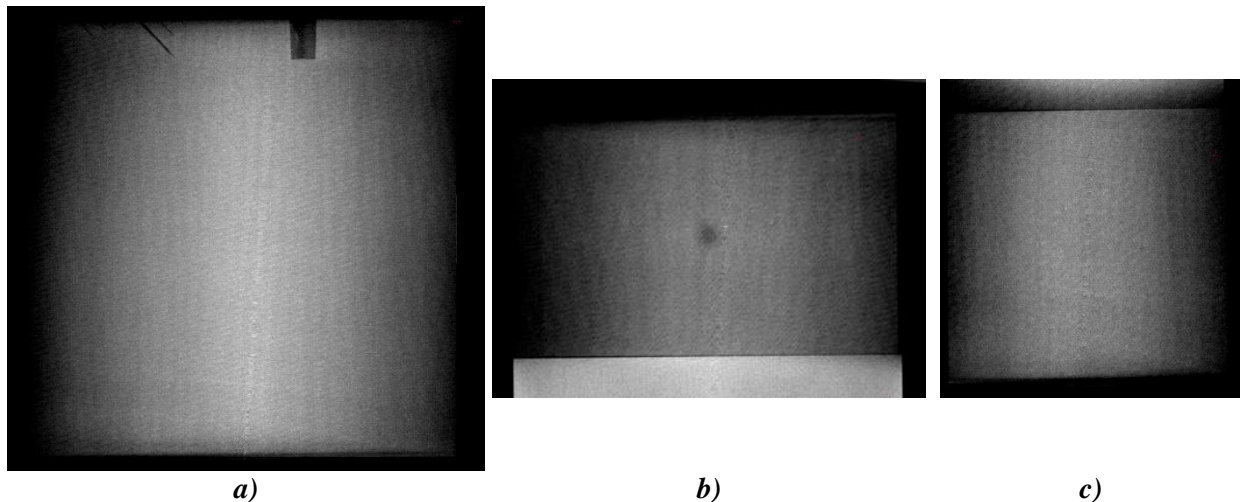


*Figure E.93-5. CT slice view of 32-ply impact damage panels 93 (a), 94 (b), and 95 (c).*

## E.93.2 Method: X-ray Computed Radiography (CR)

### E.93.2.1 Partner: Boeing

### E.93.2.2 Technique Applicability: ★★★

X-ray CR is unable to reliably detect the impact damage.

### E.93.2.3 Equipment List and Specifications:

- Philips 160 kV X-Ray source, 0.4-mm focal spot size
- IPS Phosphorus Imaging Plate
- GE CRxFlex Scanner, 50- $\mu\text{m}$  resolution
- GE Rhythm Review 5.0 visualizing software

### E.93.2.4 Settings

*Table E.93-2. Imaging and exposure parameters.*

Source Energy	40 kV
Current	2 mA
Source-Detector Distance	60 in
Magnification	1X
Exposure time	38 s
Resolution ( $\mu\text{m}$ )	50 $\mu\text{m}$
Imaging Area (in)	14 $\times$ 17

### E.93.2.5 Laboratory Setup

The DRC has a small X-ray enclosure (vault) for the primary purpose of 2D X-ray imaging. It includes a Philips 160-kV X-ray source and the ability to use film, CR, and digital detector arrays. The CR imaging plates are placed on a table and the source, suspended from the ceiling by a 3-axis crane, can be positioned to control the Source to Object Distance. Outside of the enclosure are the controls for the source, utilizing a safety interlock system. These controls allow the user to set the energy, current, and exposure time for the source. In addition to the vault, the DRC utilizes a CRxFlex system to scan and erase the CR imaging plates, storing the images on a computer. The phosphorus imaging plates, after exposure to X-rays, will luminesce the images when exposed to red light, allowing the 50- $\mu\text{m}$  scanner to create digital versions and “erase” the plates using bright white light to be used again. The CR digital images are then reviewed using Rhythm Review.



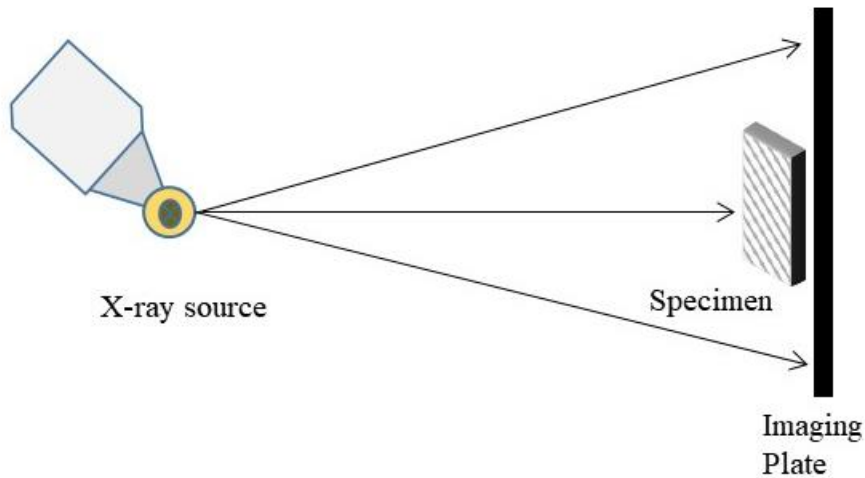
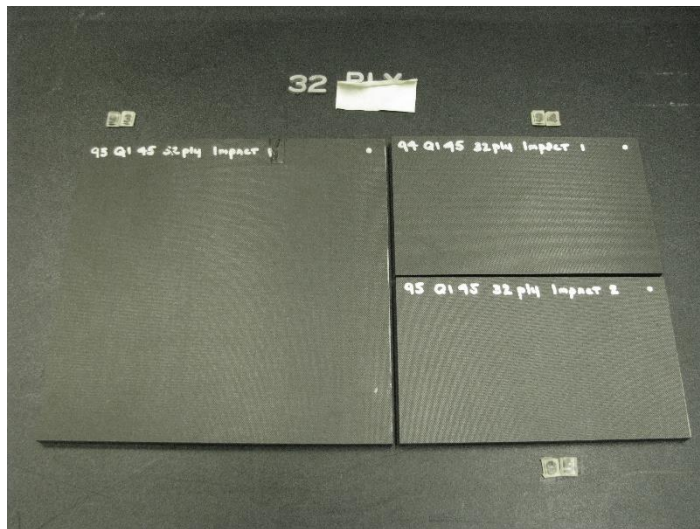


*Figure E.93-6. X-ray CR imaging.*

The three panels of the same thickness, each containing an impact damaged point, were placed directly on the plastic cassette containing the imaging plate with the X-ray source directly overhead (Figure E.93-7). The source was located 60 inches from the specimen and imaging plate to reduce geometric distortion. Lead markers were used to label the image, showing up in the results as bright white.



*a)*



*b)*

*Figure E.93-7. Laboratory setup of impact plate standards for CR imaging.*

### **E.93.2.6 Inspection Results**

CR imaging is dependent on the superimposed density of the part being imaged. In the case of the impact damage, the damaged portion tends to get indented, slightly compressing the material underneath the indent. Therefore, the superimposed density remains approximately the same. This makes the detection of impact damage by an operator using 2D radiography such as CR very difficult. As seen in Figure E.93-8, the impact damage is not easily visible. Given knowledge of

the locations, an operator may be able to discern damage but contrast from the damage is not enough to for detection in a general case.



*Figure E.93-8. Flash filtered CR image of 32-ply impact panels.*

### **E.93.3 Method: Pulse-Echo Ultrasound Testing (PEUT))**

#### **E.93.3.1 Partner: NASA**

#### **E.93.3.2 Technique Applicability: ★★ ★**

PEUT detected the impact damage in this sample.

#### **E.93.3.3 Laboratory Setup**

Immersion Ultrasonic Testing: NASA LaRC uses a custom-designed single-probe ultrasonic scanning system. The system has an 8-axis motion controller, a multi-axis gantry robot mounted above a medium-size water tank, a dual-channel, 16-bit, high-speed digitizer, and an off-the-shelf ultrasonic pulser receiver. The system can perform TTUT and PEUT inspections. TT inspection employs two aligned ultrasonic probes, one transmitter, and one receiver, placed on either side of a test specimen. Pulse-echo inspection is a single-sided method where a single ultrasonic probe is both transmitter and receiver. In each method, data are acquired while raster scanning the ultrasonic probe(s) in relation to a part. Figure E.93-9 shows a simplified block diagram of a scanning Pulse-echo inspection.

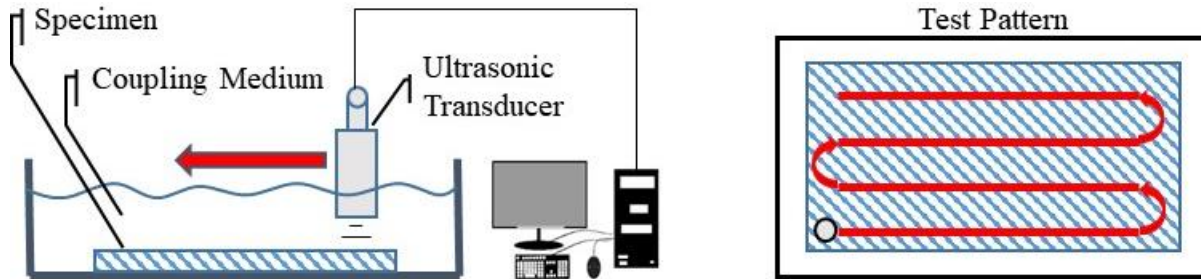


Figure E.93-9. Ultrasonic system components.

#### E.93.3.4 Equipment List and Specifications:

- Pulsar/Receiver: Olympus 5073PR
- Digitizer: AlazarTech ATS9462, dual channel, 16 bit, 180 MS/s
- Sensor: Olympus 2-inch spherical focus immersion ultrasonic transducer
- Motion system: open looped stepper motor based X-YY-Z gantry robot
- Motion Controller: Galil DMC-4183
- Acquisition Software: FastScan, custom developed at NASA LaRC
- Signal Processing Software: DataViewer, custom developed at NASA LaRC

#### E.93.3.5 Settings

Table E.93-3. Post-impact inspection settings.

Resolution (horz) [in/pixel]	0.01
Resolution (ver) [in/pixel]	0.01
Probe frequency [MHz]	10
Focal Length [in]	2
Array Dimensions [pixels]	601 × 601

The specimen is placed flat against the zero position of the tank raised above the glass bottom by several metal washers. The test probe is computer-controlled and correlated to the position on the sample. It is also focused to a point 1 mm below the surface of the test material. The specimen remains in place while the transducer follows a preprogrammed test grid across the surface as indicated in Figure E.93-10. At each point, ultrasonic data are collected from individual pulses. Larger step sizes between data collection result in lower image resolution. These data points are reconstructed into a data cube displaying spatial coordinates as time progresses. 2D reconstruction of the collection of ultrasonic responses create flattened slices at varying depths within the material.

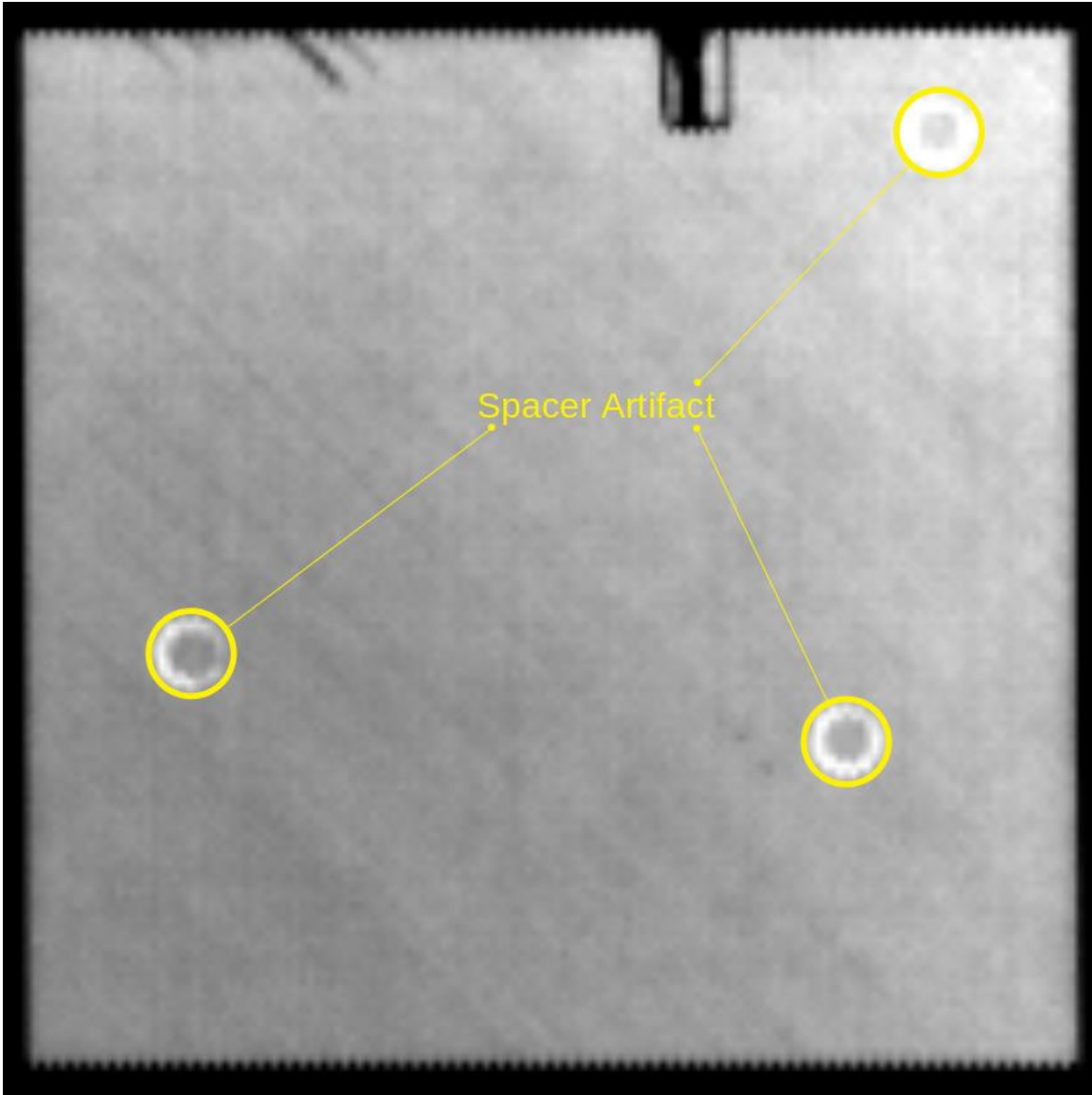


*Figure E.93-10. Specimen baseline inspection orientation.*

#### **E.93.3.6 Inspection Results**

Specimen #93 is a 6 by 6-inch, 32-ply flat panel with a 0.23-inch impact. PEUT was performed on this specimen in NASA's immersion tank specified above.

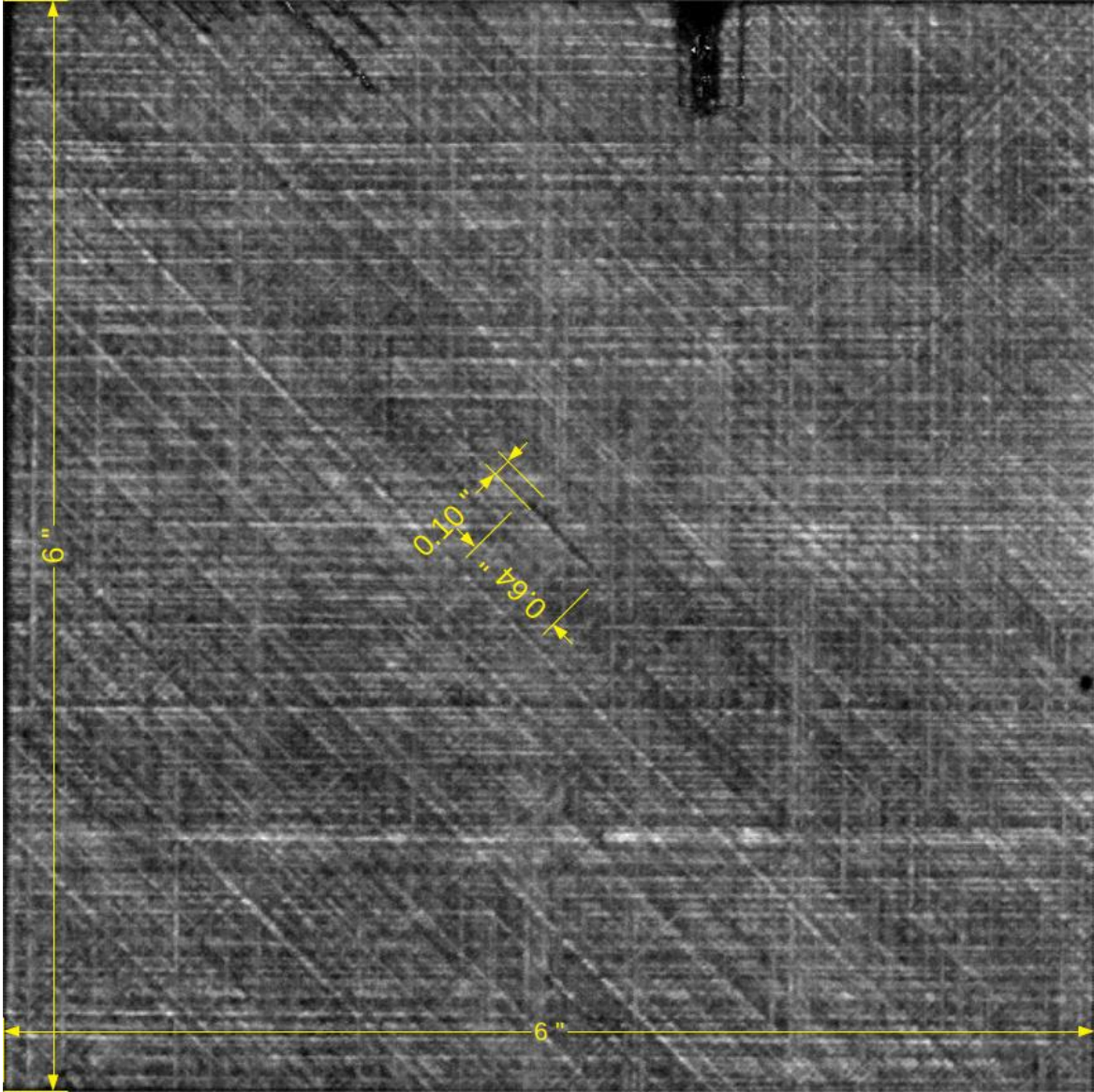
Figure E.93-11 shows a back side surface amplitude image of the sample in its pre-impacted state. No significant internal flaws were noted. The highlighted areas above are high-amplitude reflections from the three spacers used to position the sample above the bottom of the immersion tank.



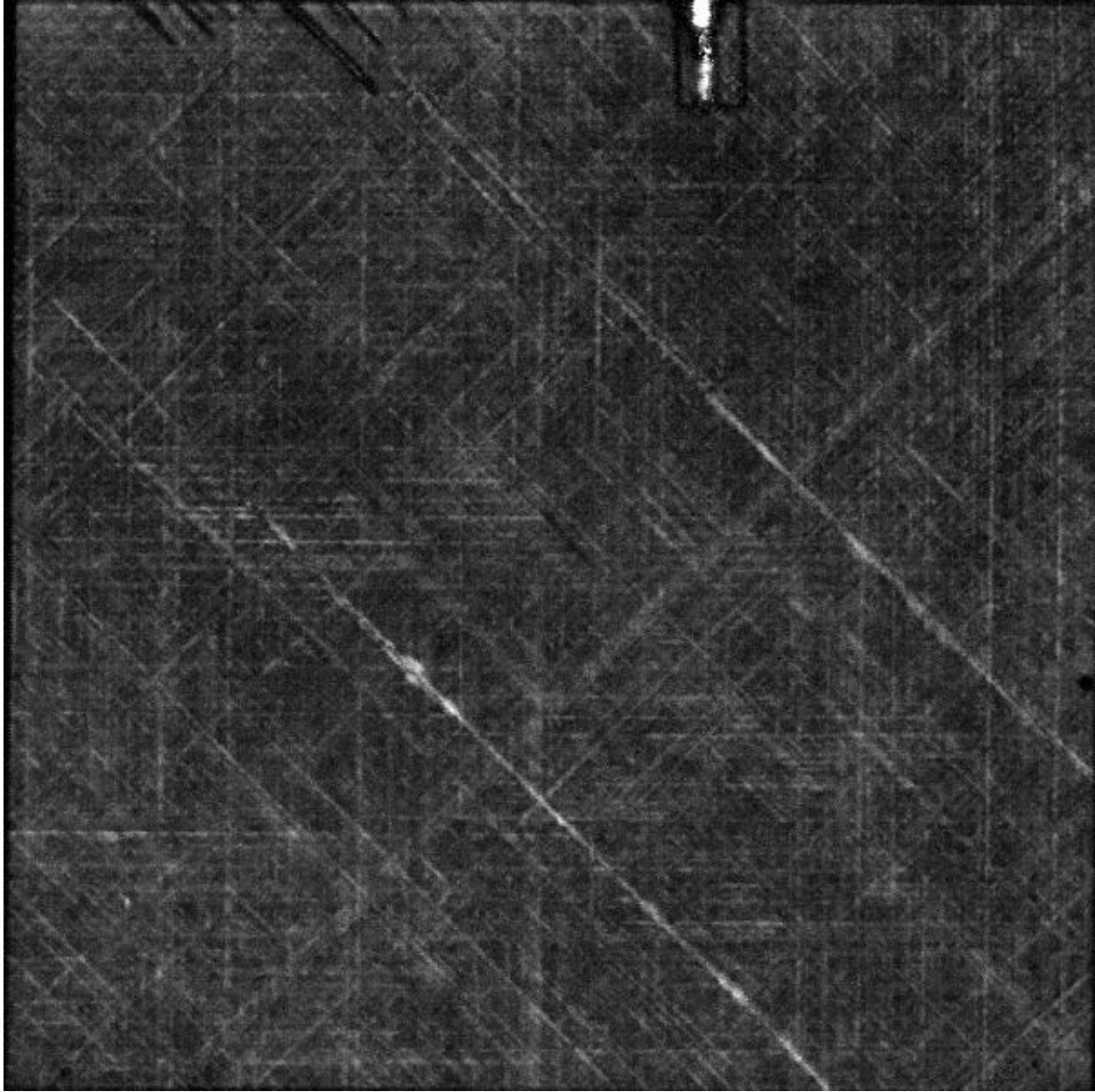
*Figure E.93-11. 10-MHz baseline image.*

Figure E.93-12a shows a back side surface amplitude image of the sample in its post-impacted state. The barely visible impact damage region is identified with measurements. Figure E.93-12b is an internal reflection amplitude image. The gate region is selected to highlight reflections from an indication to the left of center consistent with a twisted tow.





*a) Back side surface amplitude image.*



*b) Internal reflection amplitude image.  
Figure E.93-12. 10-MHz post-impact image.*

**E.94 Specimen #94: Boeing Impact QI 45 32ply 3x5 Impact 1**

Structure	Material	Details	Dimensions (inches)	Partner Methods	
32 plies	IM7/8552	Single Impact Location	6 × 6 5 × 3	NASA	E.94.1 PEUT E.94.2 XCT

**E.94.1 Method: Pulse-Echo Ultrasound Testing (PEUT)**

**E.94.1.1 Partner: NASA**

**E.94.1.2 Technique Applicability: ★★★**

PEUT detected the impact damage in this sample.

### E.94.1.3 Laboratory Setup

Immersion Ultrasonic Testing: NASA LaRC uses a custom-designed single-probe ultrasonic scanning system. The system has an 8-axis motion controller, a multi-axis gantry robot mounted above a medium-size water tank, a dual-channel, 16-bit, high-speed digitizer, and an off-the-shelf ultrasonic pulser receiver. The system can perform TTUT and PEUT inspections. TT inspection employs two aligned ultrasonic probes, one transmitter, and one receiver, placed on either side of a test specimen. Pulse-echo inspection is a single-sided method where a single ultrasonic probe is both transmitter and receiver. In each method, data are acquired while raster scanning the ultrasonic probe(s) in relation to a part. Figure E.94-1 shows a simplified block diagram of a scanning Pulse-echo inspection

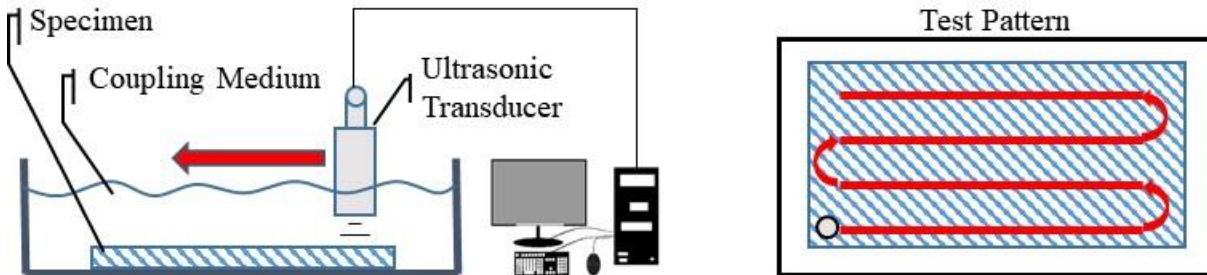


Figure E.94-1. Ultrasonic system components.

### E.94.1.4 Equipment List and Specifications:

- Pulser/Receiver: Olympus 5073PR
- Digitizer: AlazarTech ATS9462, dual channel, 16 bit, 180 MS/s
- Sensor: Olympus 2-inch spherical focus immersion ultrasonic transducer
- Motion system: open looped stepper motor based X-YY-Z gantry robot
- Motion Controller: Galil DMC-4183
- Acquisition Software: FastScan, custom developed at NASA LaRC
- Signal Processing Software: DataViewer, custom developed at NASA LaRC

### E.94.1.5 Settings

Table E.94-1. Post-impact inspection settings.

Resolution (horz) [in/pixel]	0.01
Resolution (ver) [in/pixel]	0.01
Probe frequency [MHz]	10
Focal Length [in]	2
Array Dimensions [pixels]	497 × 304

The specimen is placed flat against the zero position of the tank raised above the glass bottom by several metal washers. The test probe is computer-controlled and correlated to the position on the sample. It is also focused to a point one mm below the surface of the test material. The specimen remains in place while the transducer follows a preprogrammed test grid across the surface as indicated in Figure E.94-2. At each point, ultrasonic data are collected from individual pulses. Larger step sizes between data collection result in lower image resolution. These data points are reconstructed into a data cube displaying spatial coordinates as time progresses. 2D reconstruction of the collection of ultrasonic responses create flattened slices at varying depths within the material.

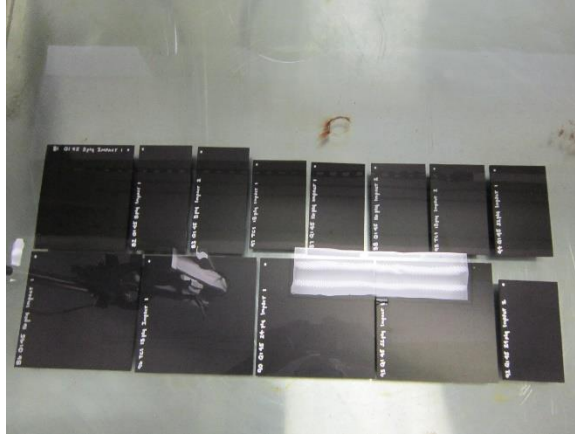
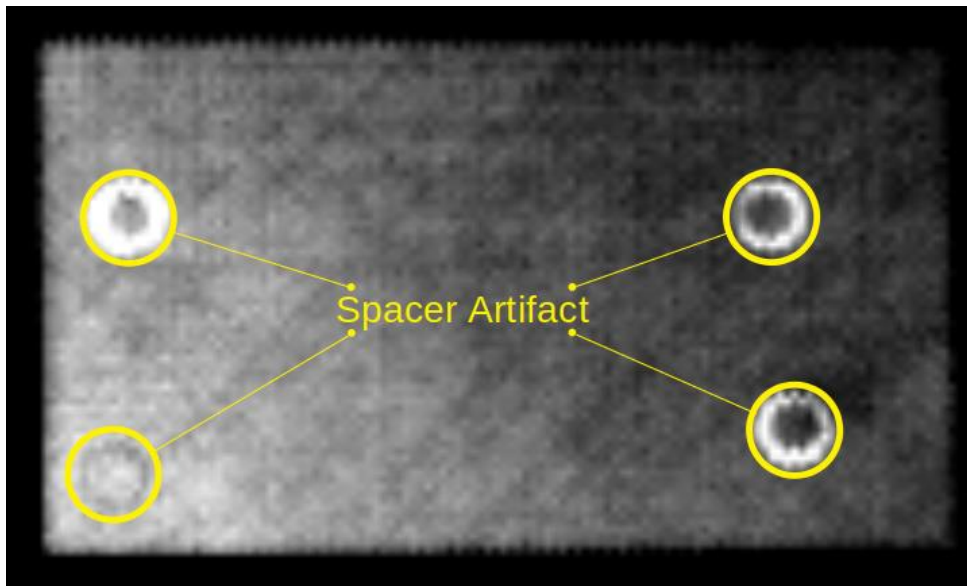


*Figure E.94-2. Specimen baseline inspection orientation.*

### **E.94.1.6 Inspection Results**

Specimen #94 is a 3 by 5-inch, 32-ply flat panel with a 1.12-inch impact. PEUT was performed on this specimen in NASA's immersion tank specified above.

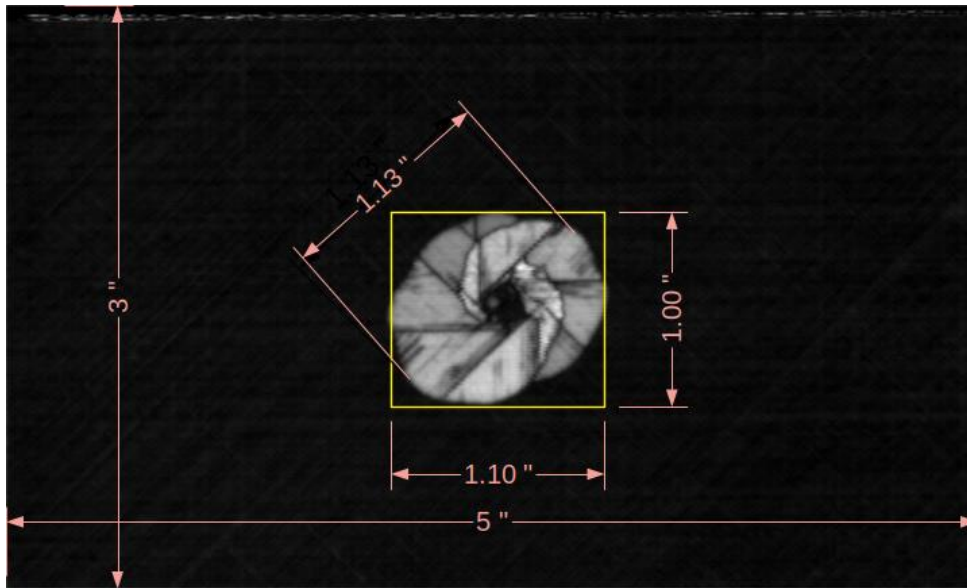
Figure E.94-3 shows a back side surface amplitude image of the sample in its pre-impacted state. No significant internal flaws were noted. The highlighted areas above are high-amplitude reflections from the four spacers used to position the sample above the bottom of the immersion tank.



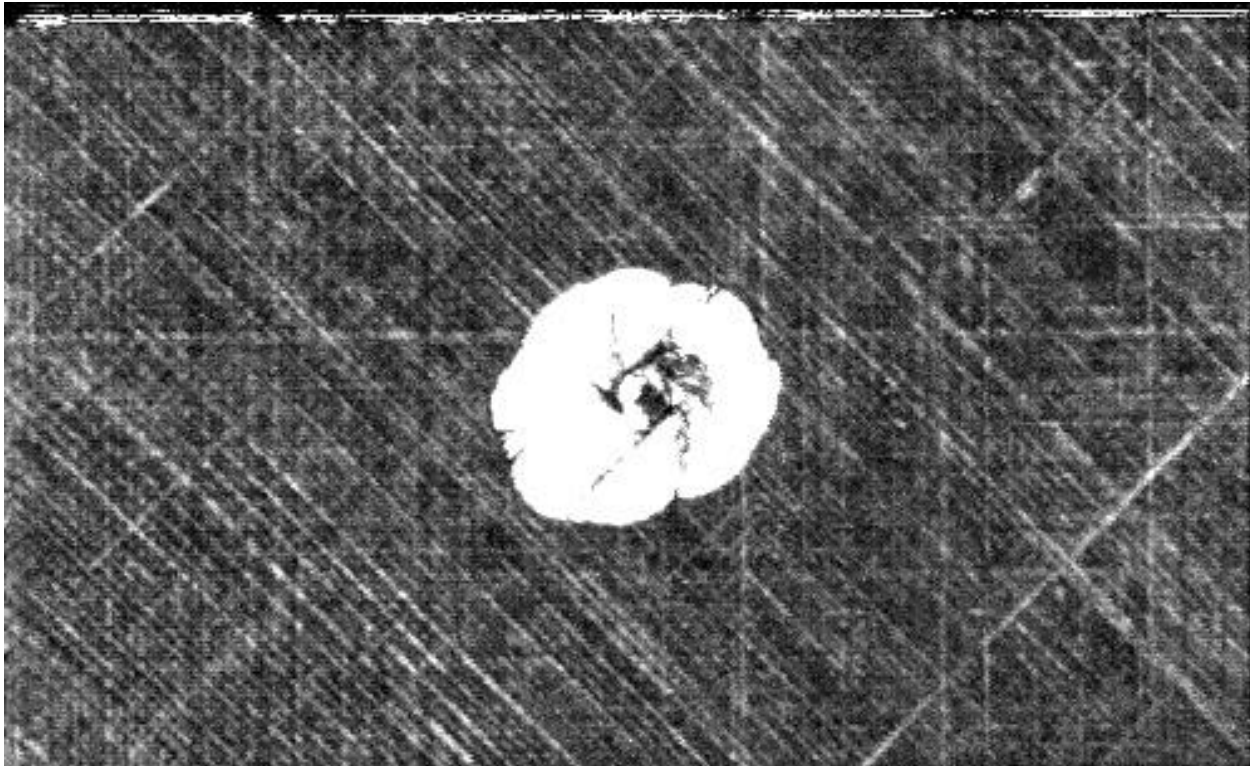
*Figure E.94-3. 10-MHz baseline image.*

Figure E.94-4a shows an internal reflection amplitude image of the sample in its post-impacted state. The gate region is selected to highlight reflections from the delaminations caused by the impact. The impact damage region is identified with measurements. Figure E.94.4b shows the same time gated region as above allowing the high-amplitude delamination reflections to saturate revealing the internal layup features.





a)



b)

*Figure E.94-4. 10-MHz post-impact image.*

**E.94.2 Method: X-ray Computed Tomography (XCT)**

**E.94.2.1 Partner: NASA**

**E.94.2.2 Technique Applicability: ★★★**

XCT is capable of imaging and quantifying the damage due to low-impact energy in this specimen.



### E.94.2.3 Laboratory Setup

The microfocus XCT system at NASA LaRC is a commercially available Avonix (Nikon C2) Metrology System designed for high-resolution NDE inspections. The system is an advanced microfocus X-ray system, capable of resolving details down to 5  $\mu\text{m}$ , and with magnifications up to 60X. The system is supplied as a complete, large-dimension radiation enclosure, with X-ray source, specimen manipulator, and an amorphous silica detector as shown in Figure E.94-5. The imaging controls are housed in a separate control console. The detector is a Perkin-Elmer 16-bit amorphous silicon digital detector with a  $2000 \times 2000$ -pixel array.

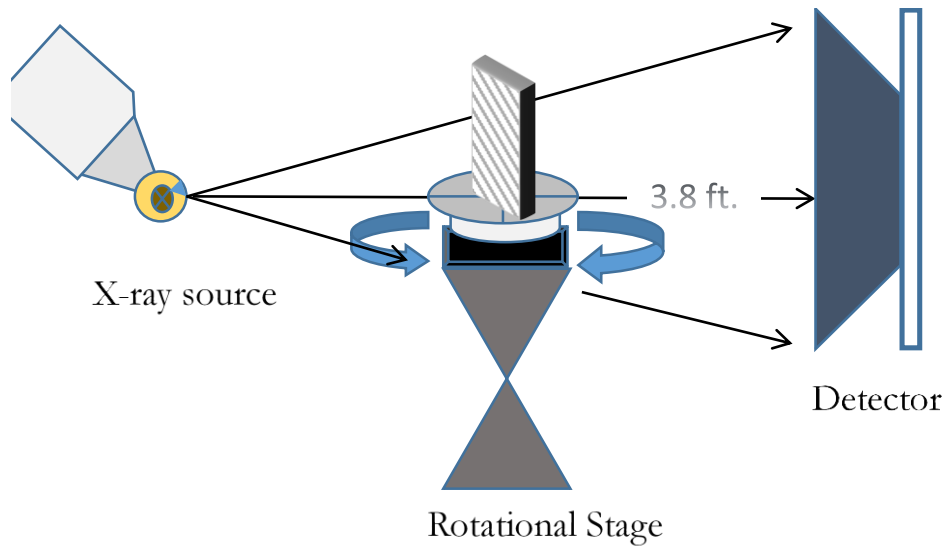


*Figure E.94-5. XCT system components.*

A consistent Cartesian coordinate system is used to define slice direction as illustrated in Figure E.94-6. Slices normal to the X, Y, and Z-directions are shown in Figure E.94-6a, b, and c, respectively.

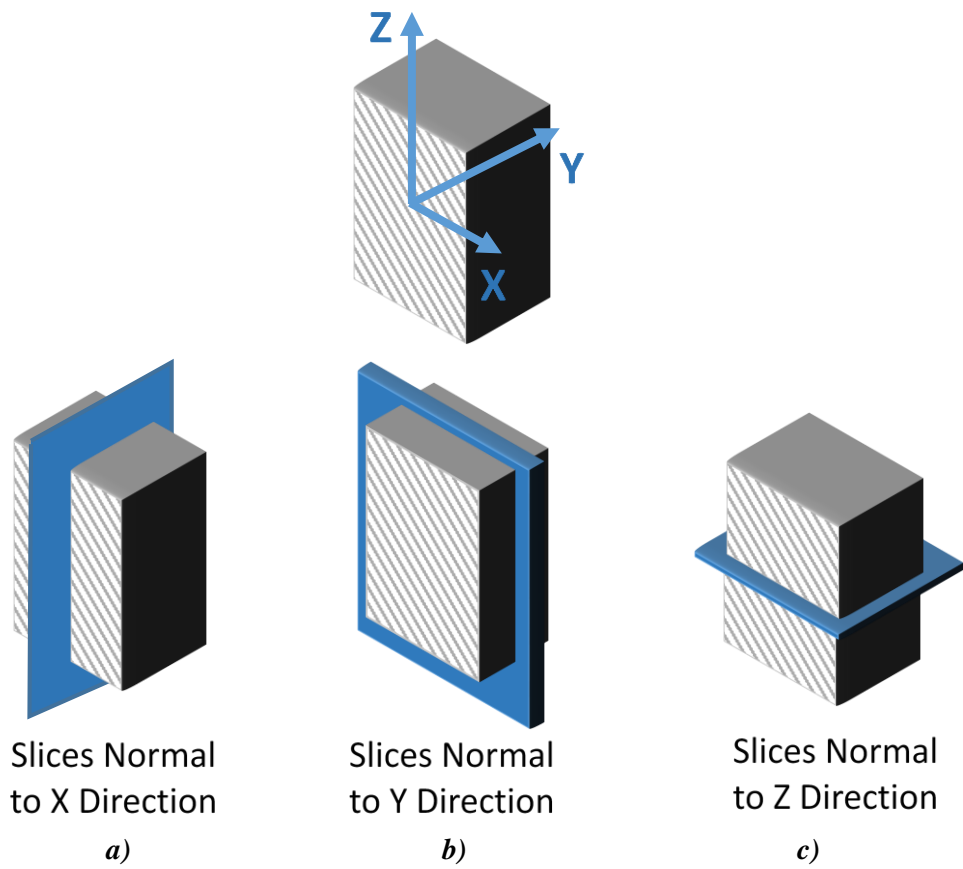


*Figure E.94-6. Slice direction nomenclature.*

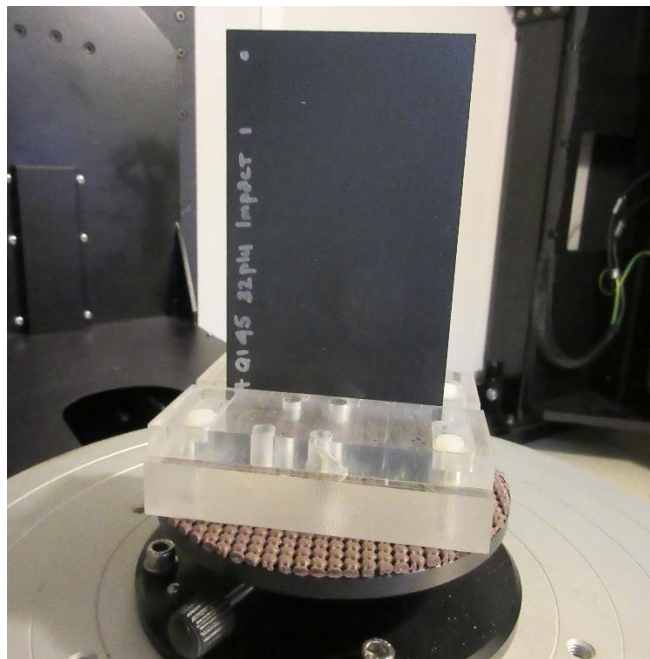


*Figure E.94-7. Impact specimen test stand setup.*

#### E.94.2.4 Equipment List and Specifications:

- Avonix 225 CT System
- 225 kV microfocus X-ray source with 5  $\mu\text{m}$  focal spot size
- 15 or 30kg Capacity 5 axis fully programmable manipulator.
- Detector: Perkin Elmer XRD 1621 – 2000  $\times$  2000 pixels with 200  $\mu\text{m}$  pitch
- 10  $\mu\text{m}$  spatial resolution for specimens 1.5 cm wide
- Thin panels 10-inch  $\times$  10-inch – full volume 200  $\mu\text{m}$  spatial resolution

#### E.94.2.5 Settings

*Table E.94-2. Data collection settings.*

Source Energy	160 kV
Current	37 $\mu\text{A}$
Magnification	5.0 X
Filter	0.125 Sn
# Rotational angles	3142
Exposure time / frame	1.0 sec
Max Histogram Grey Level	50 K
# Averages	8
Resolution ( $\mu\text{m}$ )	40.04 $\mu\text{m}$
Array Dimensions (pixels)	1999 $\times$ 303 $\times$ 1998

The specimen is placed vertically (rotated about the smallest dimension) on the rotational stage located between the radiation source and the detector. The rotational stage is computer-controlled and correlated to the position of the sample. As the sample is rotated the full 360° (~0.11° increments), the detector collects radiographs at each rotated angle as the X-ray path intersects the sample. 3D reconstruction of the collection of radiographs produces a volume of data that can then be viewed along any plane in the volume. The closer the sample can be placed to the X-ray source, the higher the spatial resolution that can be obtained.

#### E.94.2.6 Data and Results

Specimen #94, is a 3 by 5-inch 32-ply flat panel with a BVID impact. XCT was performed on this specimen in NASA LaRC's CT system with the settings defined in Table E-94.2.

The damage caused by the impact can be clearly seen from all viewing directions as shown in Figure E.94-8. There is no surface indication of an impact. Damage extends all the way through the thickness of the specimen.

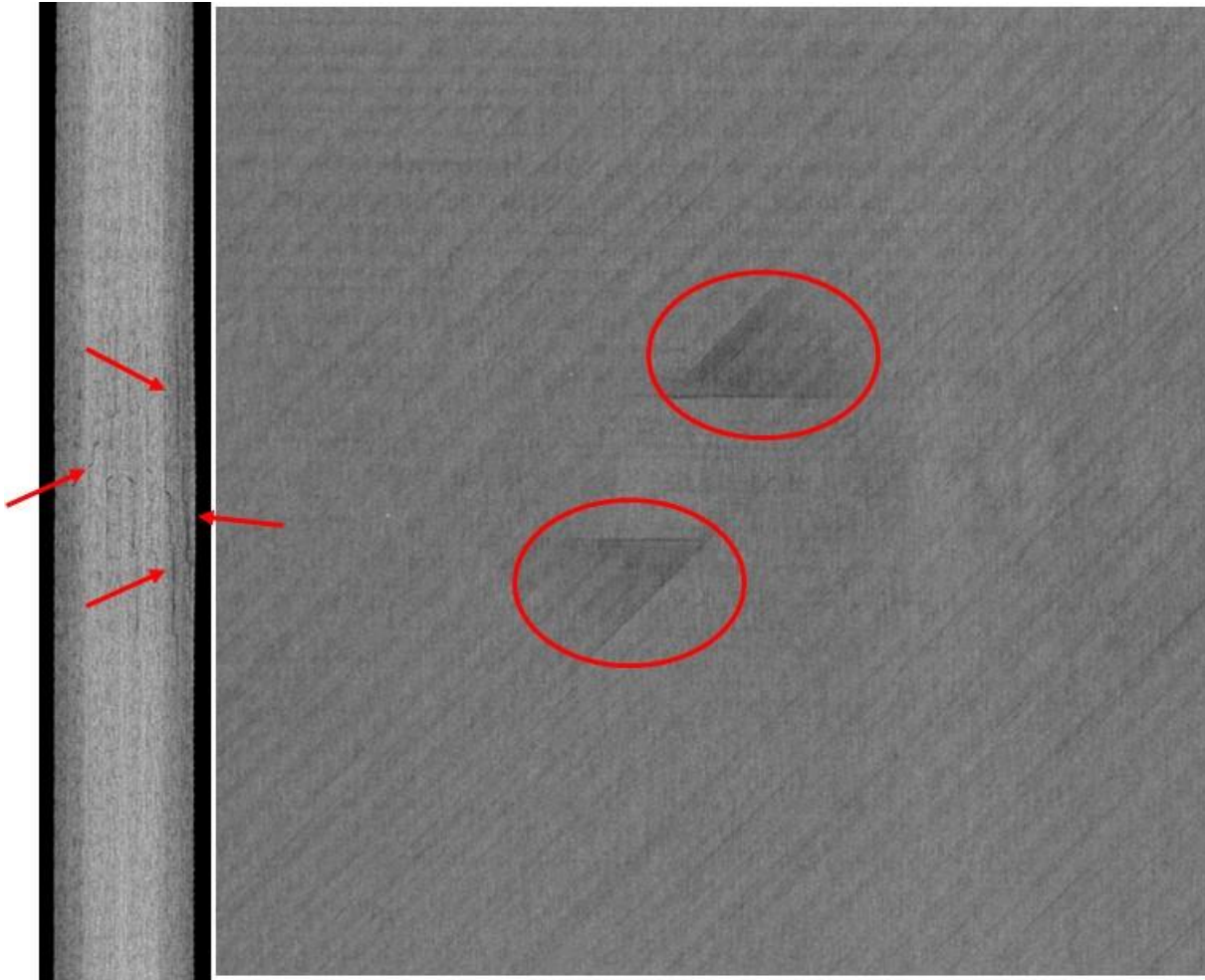


*Figure E.94-8. CT slice normal to the thickness direction show delaminations and matrix cracking (left). CT slice normal to the front surface shows delaminations between plies (right).*

**E.95 Specimen #95: Boeing Impact QI\_45 32ply 3x5 Impact 2**

Structure	Material	Details	Dimensions (inches)	Partner Methods	
32 plies	IM7/8552	Single Impact Location	6 × 6 5 × 3	NASA	E.95.1 PEUT E.95.2 XCT

**E.95.1 Method: Pulse-Echo Ultrasound Testing (PEUT)**

**E.95.1.1 Partner: NASA**

**E.95.1.2 Technique Applicability: ★★ ★**

PEUT detected the impact damage in this sample.

**E.95.1.3 Laboratory Setup**

Immersion Ultrasonic Testing: NASA LaRC uses a custom-designed single-probe ultrasonic scanning system. The system has an 8-axis motion controller, a multi-axis gantry robot mounted above a medium-size water tank, a dual-channel, 16-bit, high-speed digitizer, and an off-the-shelf ultrasonic pulser receiver. The system can perform TTUT and PEUT inspections. TT inspection employs two aligned ultrasonic probes, one transmitter, and one receiver, placed on either side of

a test specimen. Pulse-echo inspection is a single-sided method where a single ultrasonic probe is both transmitter and receiver. In each method, data are acquired while raster scanning the ultrasonic probe(s) in relation to a part. Figure E.95-1 shows a simplified block diagram of a scanning Pulse-echo inspection.

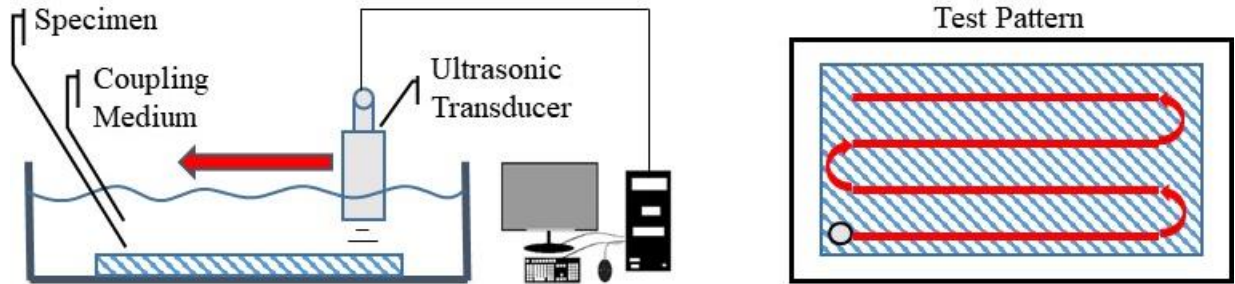


Figure E.95-1. Ultrasonic system components.

#### E.95.1.4 Equipment List and Specifications:

- Pulsar/Receiver: Olympus 5073PR
- Digitizer: AlazarTech ATS9462, dual channel, 16 bit, 180 MS/s
- Sensor: Olympus 2-inch spherical focus immersion ultrasonic transducer
- Motion system: open looped stepper motor based X-YY-Z gantry robot
- Motion Controller: Galil DMC-4183
- Acquisition Software: FastScan, custom developed at NASA LaRC
- Signal Processing Software: DataViewer, custom developed at NASA LaRC

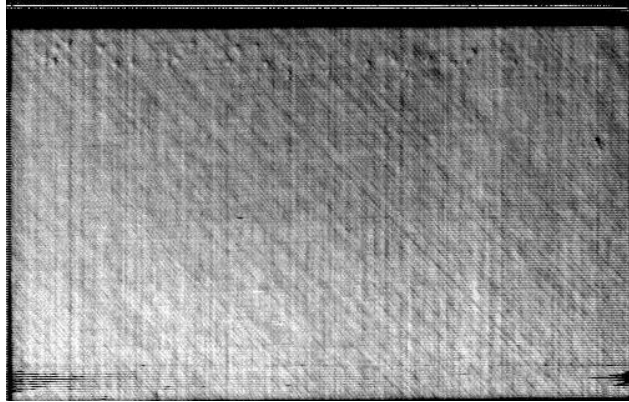
#### E.95.1.5 Settings

Table E.95-1. Post-impact inspection settings.

Resolution (horz) [in/pixel]	0.01
Resolution (ver) [in/pixel]	0.01
Probe frequency [MHz]	10
Focal Length [in]	2
Array Dimensions [pixels]	502 × 306

The specimen is placed flat against the zero position of the tank raised above the glass bottom by several metal washers. The test probe is computer-controlled and correlated to the position on the sample. It is also focused to a point 1 mm below the surface of the test material. The specimen remains in place while the transducer follows a preprogrammed test grid across the surface as indicated in Figure E.95-2. At each point, ultrasonic data are collected from individual pulses. Larger step sizes between data collection result in lower image resolution. These data points are reconstructed into a data cube displaying spatial coordinates as time progresses. 2D reconstruction of the collection of ultrasonic responses create flattened slices at varying depths within the material.



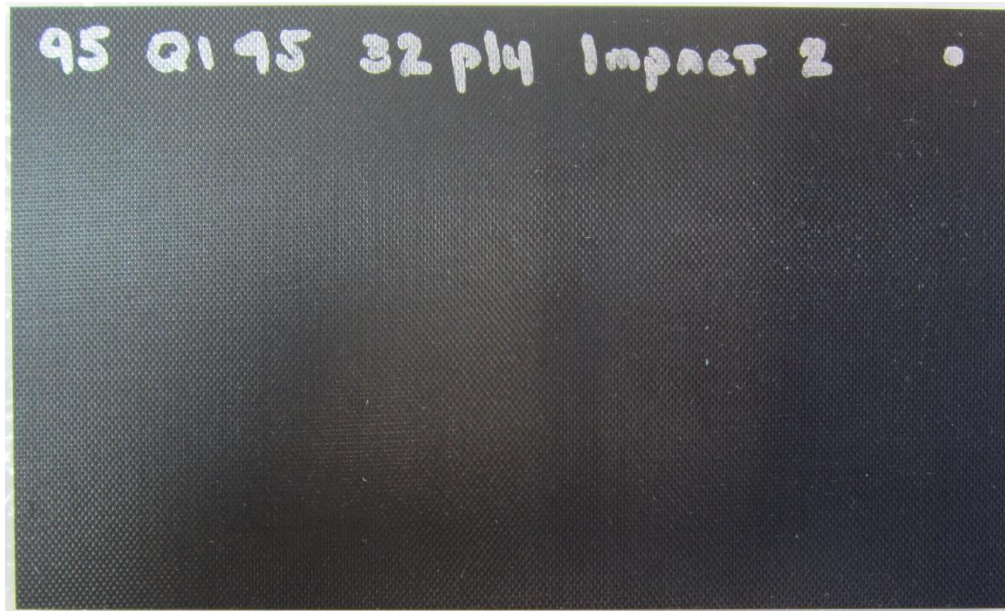


*Figure E.95-2. Specimen baseline inspection orientation.*

#### **E.95.1.6 Inspection Results**

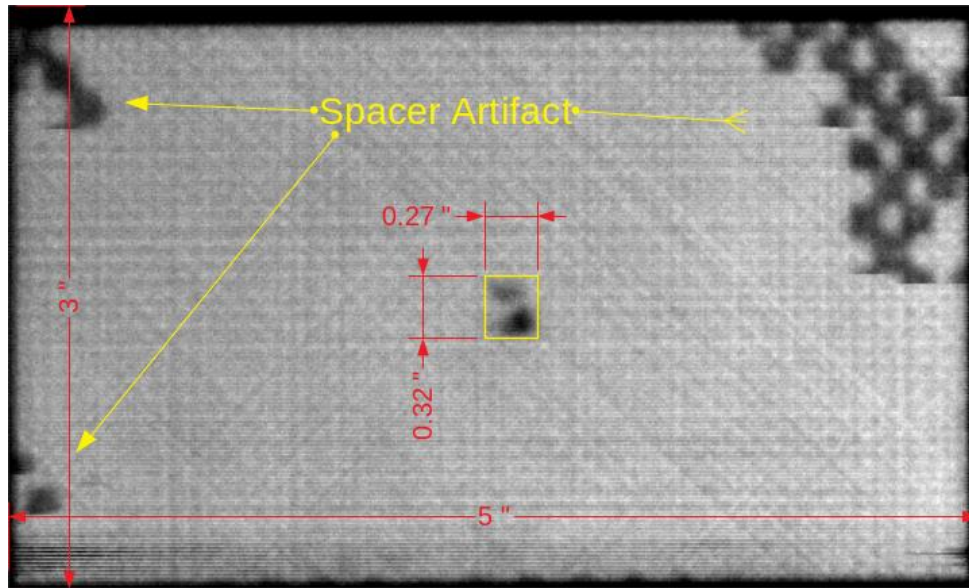
Specimen #95 is a 3 by 5-inch, 32-ply flat panel with a 0.25-inch impact. Only post-impacted PEUT was performed on this specimen in NASA's immersion tank specified above.

Figure E.95-2 above shows a photograph of the pre-impacted sample. NASA did not perform baseline PEUT on this sample.

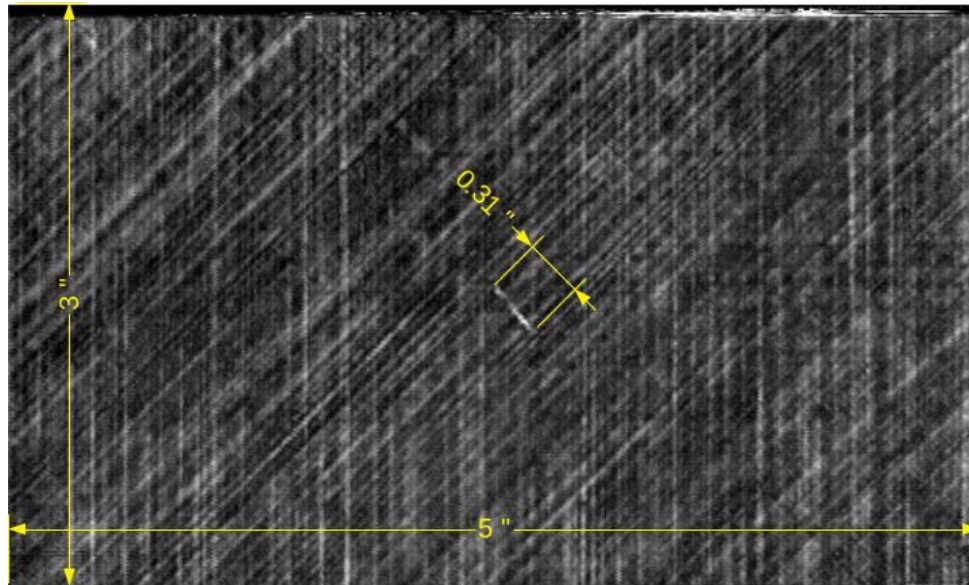


*Figure E.95-3. Baseline PEUT was not performed on this sample.*

Figure E.95-4a shows a back side surface amplitude image of the sample in its post-impacted state. The impact damage region is identified with measurements. Dark artifacts caused by a sound absorbing spacer under the sample are also noted. Figure E.95-4b is an internal reflection amplitude image. The gate region is selected to highlight reflections from the delaminations caused by the impact.



a)



b)

*Figure E.95-4. 10-MHz post-impact image.*

**E.95.1.7 Method: X-ray Computed Tomography (XCT)**

**E.95.1.8 Partner: NASA**

**E.95.1.9 Technique Applicability: ★★★**

XCT is capable of imaging and quantifying the damage due to low-impact energy in this specimen.

**E.95.1.10 Laboratory Setup**

The microfocus XCT system at NASA LaRC is a commercially available Avonix (Nikon C2) Metrology System designed for high-resolution NDE inspections. The system is an advanced microfocus X-ray system, capable of resolving details down to 5  $\mu\text{m}$ , and with magnifications up to 60X. The system is supplied as a complete, large-dimension radiation enclosure, with X-ray

source, specimen manipulator, and an amorphous silica detector as shown in Figure E.95-5. The imaging controls are housed in a separate control console. The detector is a Perkin-Elmer 16-bit amorphous silicon digital detector with a  $2000 \times 2000$ -pixel array.

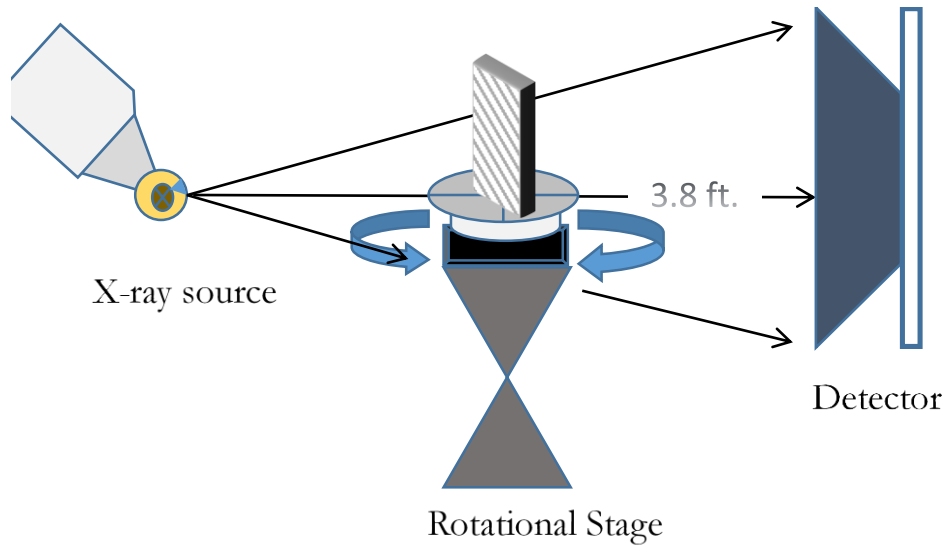


*Figure E.95-5. XCT system components.*

A consistent Cartesian coordinate system is used to define slice direction as illustrated in Figure E.95-6. Slices normal to the X, Y, and Z-directions are shown in Figure E.95-6a, b, and c, respectively.



#### E.95.1.11 Equipment List and Specifications:

- Avonix 225 CT System
- 225 kV microfocus X-ray source with 5  $\mu\text{m}$  focal spot size
- 15 or 30kg Capacity 5 axis fully programmable manipulator.
- Detector: Perkin Elmer XRD 1621 – 2000  $\times$  2000 pixels with 200  $\mu\text{m}$  pitch
- 10  $\mu\text{m}$  spatial resolution for specimens 1.5 cm wide
- Thin panels 10-inch  $\times$  10-inch – full volume 200  $\mu\text{m}$  spatial resolution

#### E.95.1.12 Settings

*Table E.95-2. Data collection settings.*

Source Energy	160 kV
Current	37 $\mu\text{A}$
Magnification	5.0 X
Filter	0.125 Sn
# Rotational angles	3142
Exposure time / frame	1.0 sec
Max Histogram Grey Level	55 K
# Averages	8
Resolution ( $\mu\text{m}$ )	40.04 $\mu\text{m}$
Array Dimensions (pixels)	1999 $\times$ 253 $\times$ 1998

The specimen is placed vertically (rotated about the smallest dimension) on the rotational stage located between the radiation source and the detector. The rotational stage is computer-controlled and correlated to the position of the sample. As the sample is rotated the full 360° (~0.11° increments), the detector collects radiographs at each rotated angle as the X-ray path intersects the sample. 3D reconstruction of the collection of radiographs produces a volume of data that can then be viewed along any plane in the volume. The closer the sample can be placed to the X-ray source, the higher the spatial resolution that can be obtained.

#### E.95.1.13 Data and Results

Specimen #95, is a 3 by 5-inch 32-ply flat panel with a BVID impact. XCT was performed on this specimen in NASA LaRC's CT system with the settings defined in Table E-95.2.

Impact specimen #95 contained no detectable impact damage as shown in Figure E.95-8. There is no surface indication of an impact.





*Figure E.95-8. CT slice normal to the thickness direction show no damage (left). CT slice normal to the front surface shows no damage plies (right).*

**E.96 Specimen #96: Boeing Impact TC1 18ply 6x6 Impact 1**

Structure	Material	Details	Dimensions (inches)	Partner Methods	
18 plies	IM7/8552	Single Impact Location	6 × 6 5 × 3	Boeing	E.96.1 XCT
				NASA	E.96.2 X-ray CR
					E.96.3 PEUT

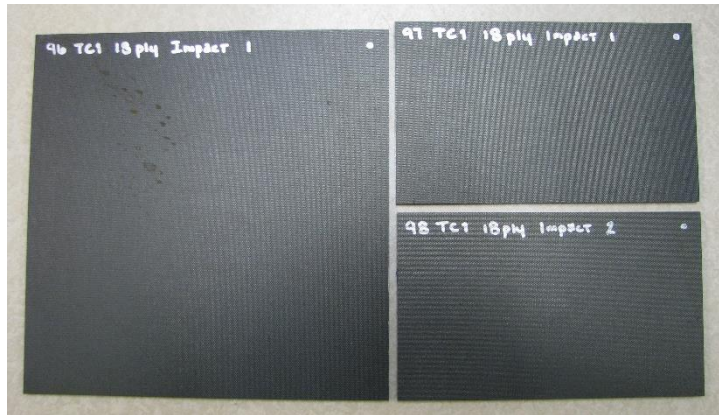


*Figure E.96-1. Photographs of radii delamination standard.*

**E.96.1 Method: X-ray Computed Tomography (XCT)**

**E.96.1.1 Partner: Boeing**

**E.96.1.2 Technique Applicability: ★★☆☆**

XCT is able to detect impact damage on some of the panels.

**E.96.1.3 Equipment List and Specifications:**

- YXLON Modular CT System
- 225 kV microfocus X-ray source with variable focal spot size
- 100 kg capacity 7-axis granite based manipulator
- XRD 1621 Detector – 2048 × 2048 pixels with 200- $\mu\text{m}$  pitch, 400 × 400-mm active area
- 111- $\mu\text{m}$  spatial resolution for impact panel scan
- Volume Graphics 3.0 visualizing software
- Reconstruction Computer

**E.96.1.4 Settings**

*Table E.96-1. Data collection settings.*

Source Energy	120 kV
Current	0.60 mA
Magnification	1.80 X
Filter	Copper
# Rotational angles	1410
Exposure time / frame	500 ms
Frame Binning	2
Spatial Resolution ( $\mu\text{m}$ )	111 $\mu\text{m}$
Array Dimensions (pixels)	2048 × 2048

**E.96.1.5 Laboratory Setup**

The Digital Radiography Center (DRC) utilizes an YXLON Modular CT System. This system has the capability to utilize various X-ray sources for varying applications, including a 450-kV source, a microfocus source, and a nanofocus source. The microfocus source used has a variable focal spot size of less than 4  $\mu\text{m}$  and is suitable for magnifications up to 10X, with the nanofocus ranging up to 187X. The detector has 3 DOFs, allowing the effective detector area to be increased through

combined scans. The manipulator controls the position of the detector, object, and source. It has 7 DOFs including a rotating stage to rotate the object during the scan. The entire system includes the source, detector, manipulator, control and reconstruction computers, and user control station. The computers and control station are outside of the radiation enclosure (vault) and utilize a safety interlock system to operate. Cameras are located in the vault to allow the operator to monitor the part from outside the enclosure.

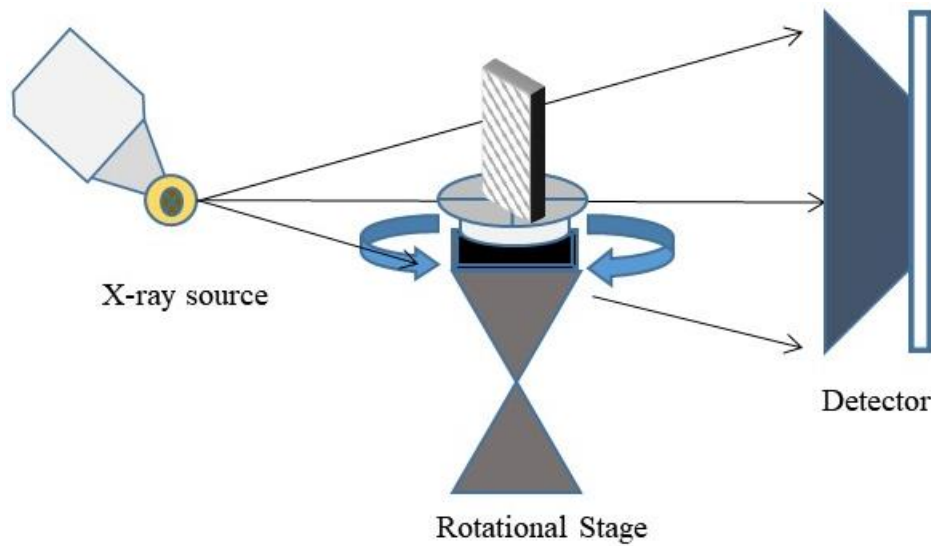


*Figure E.96-2. XCT system components.*

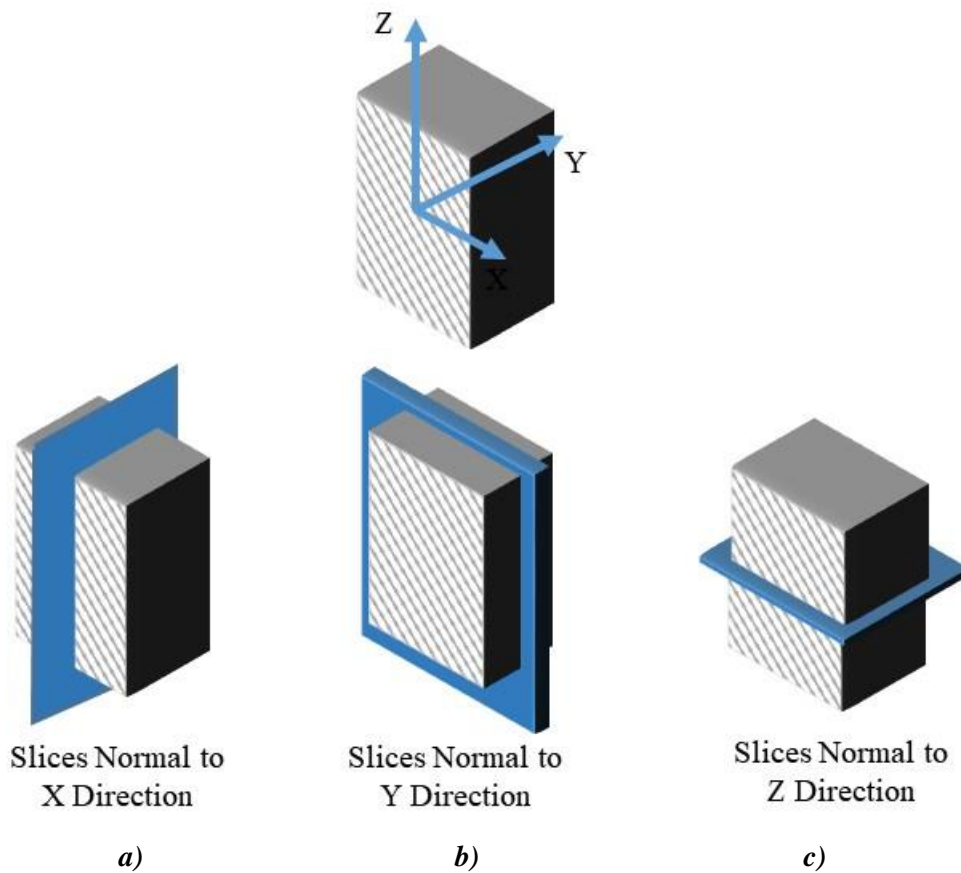


*Figure E.96-3. Slice direction nomenclature.*

To reduce overall scan time, the standard panels of the same thickness were stacked together, separated by light foam sheets and held together with tape. This allowed three parts to be scanned at once and analyzed separately in post-processing. The panel bundle was then secured in a foam fixture. The position of the specimen, source, and detector are controlled to produce geometric magnification of the image and increase the spatial resolution. The image data are gathered as X-rays penetrate the part and expose the detector for a set amount of time. For each scan, these image data are collected at 1410 different angles throughout a 360° rotation. These images are then reconstructed to create the 3D volume dataset. This dataset is viewed and analyzed in Volume Graphics, a volume rendering software, to identify the relevant components.

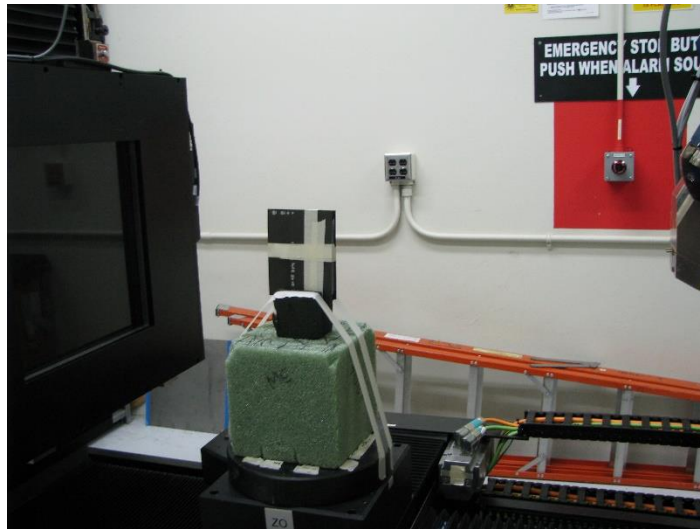


*Figure E.96-4. Microfocus XCT setup for impact damage standards.*

### E.96.1.6 Inspection Results

Unlike 2D X-ray imaging, CT shows slice views of the object that are not superimposed. This allows for improved detection of flaws. In the case of the impact panels, the damage would show as a slightly dented region at the near surface. Figure E.96-5 shows a slice view at the near surface of each panel. The dark spot in the center of Figure E.96-5b and c indicates less dense or lack of material, caused by the indentation of the impact on Panels 97 and 98. Figure E.96-5a shows no detectable impact damage on Panel 96.

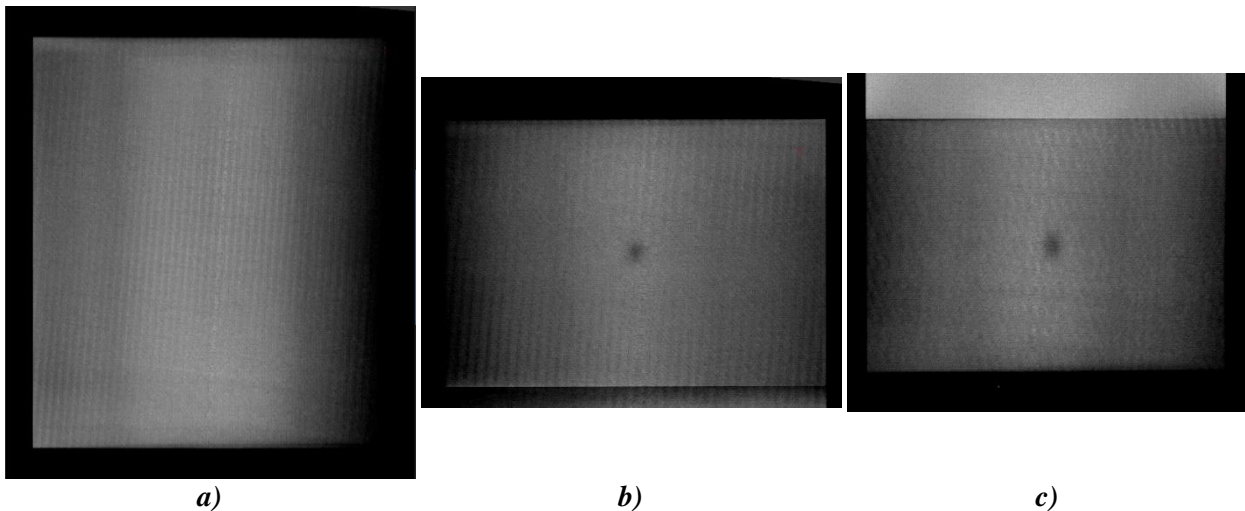


*Figure E.96-5. CT slice view of 18-ply impact damage panels 96 (a), 97 (b), and 98 (c).*

### E.96.2 Method: X-ray Computed Radiography (CR)

#### E.96.2.1 Partner: Boeing

#### E.96.2.2 Technique Applicability: ☆☆☆

X-ray CR is unable to reliably detect the impact damage.



### E.96.2.3 Equipment List and Specifications:

- Philips 160 kV X-Ray source, 0.4-mm focal spot size
- IPS Phosphorus Imaging Plate
- GE CRxFlex Scanner, 50- $\mu\text{m}$  resolution
- GE Rhythm Review 5.0 visualizing software

### E.96.2.4 Settings

*Table E.96-2. Imaging and exposure parameters.*

Source Energy	40 kV
Current	2 mA
Source-Detector Distance	60 in
Magnification	1X
Exposure time	30 s
Resolution ( $\mu\text{m}$ )	50 $\mu\text{m}$
Imaging Area (in)	14 $\times$ 17

### E.96.2.5 Laboratory Setup

The DRC has a small X-ray enclosure (vault) for the primary purpose of 2D X-ray imaging. It includes a Philips 160-kV X-ray source and the ability to use film, CR, and digital detector arrays. The CR imaging plates are placed on a table and the source, suspended from the ceiling by a 3-axis crane, can be positioned to control the Source to Object Distance. Outside of the enclosure are the controls for the source, utilizing a safety interlock system. These controls allow the user to set the energy, current, and exposure time for the source. In addition to the vault, the DRC utilizes a CRxFlex system to scan and erase the CR imaging plates, storing the images on a computer. The phosphorus imaging plates, after exposure to X-rays, will luminesce the images when exposed to red light, allowing the 50- $\mu\text{m}$  scanner to create digital versions and “erase” the plates using bright white light to be used again. The CR digital images are then reviewed using Rhythm Review.

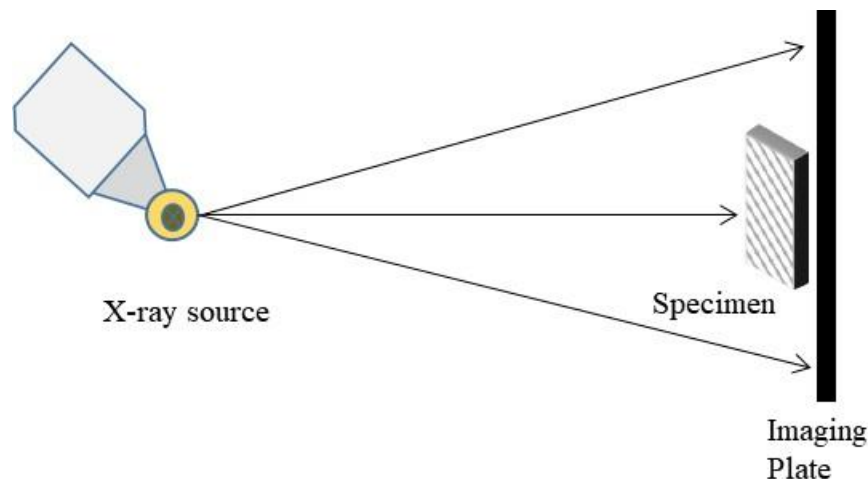
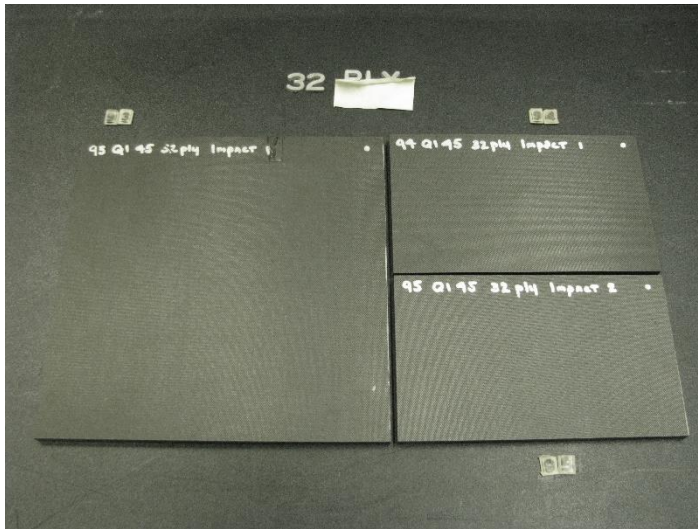


*Figure E.96-6. X-ray CR imaging.*

The three panels of the same thickness, each containing an impact damaged point, were placed directly on the plastic cassette containing the imaging plate with the X-ray source directly overhead (Figure E.96-7). The source was located 60 inches from the specimen and imaging plate to reduce

geometric distortion. Lead markers were used to label the image, showing up in the results as bright white.



a)



b)

*Figure E.96-7. Laboratory setup of impact plate standards for CR imaging.*

### **E.96.2.6 Inspection Results**

CR imaging is dependent on the superimposed density of the part being imaged. In the case of the impact damage, the damaged portion tends to get indented, slightly compressing the material underneath the indent. Therefore the superimposed density remains approximately the same. This makes the detection of impact damage by an operator using 2D radiography such as CR very difficult. As seen in Figure E.96-8, the impact damage is not easily visible. Given knowledge of the locations, an operator may be able to discern damage but contrast from the damage is not enough to be detected in a general case.

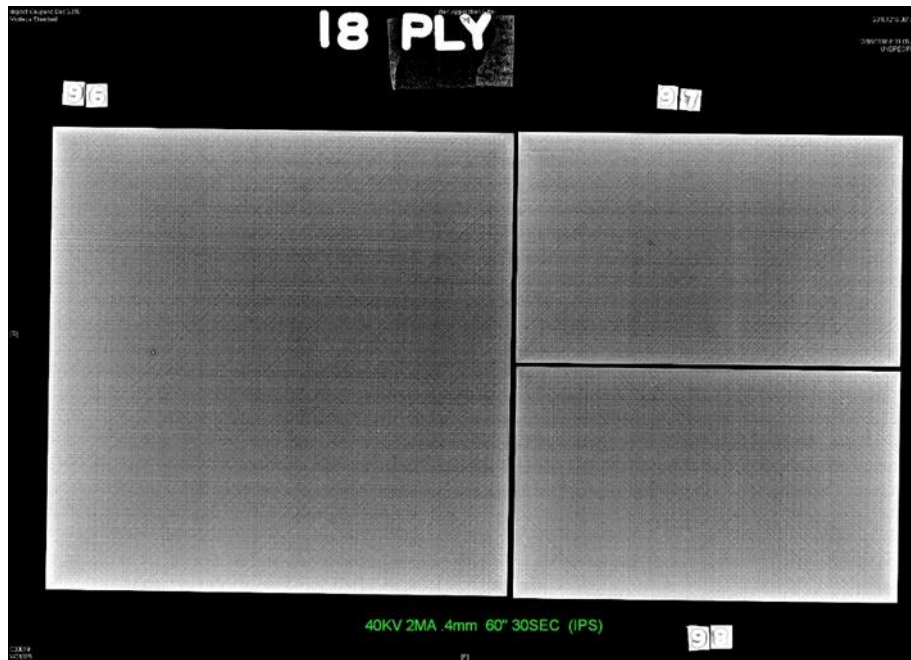


Figure E.96-8. Flash filtered CR image of 18-ply impact panels.

**E.96.3 Method: Pulse-Echo Ultrasound Testing (PEUT)**

**E.96.3.1 Partner: NASA**

**E.96.3.2 Technique Applicability: ★★ ★**

PEUT detected the impact damage in this sample.

**E.96.3.3 Laboratory Setup**

Immersion Ultrasonic Testing: NASA LaRC uses a custom-designed single-probe ultrasonic scanning system. The system has an 8-axis motion controller, a multi-axis gantry robot mounted above a medium-size water tank, a dual-channel, 16-bit, high-speed digitizer, and an off-the-shelf ultrasonic pulser receiver. The system can perform TTUT and PEUT inspections. TT inspection employs two aligned ultrasonic probes, one transmitter, and one receiver, placed on either side of a test specimen. Pulse-echo inspection is a single-sided method where a single ultrasonic probe is both transmitter and receiver. In each method, data are acquired while raster scanning the ultrasonic probe(s) in relation to a part. Figure E.96-9 shows a simplified block diagram of a scanning Pulse-echo inspection.

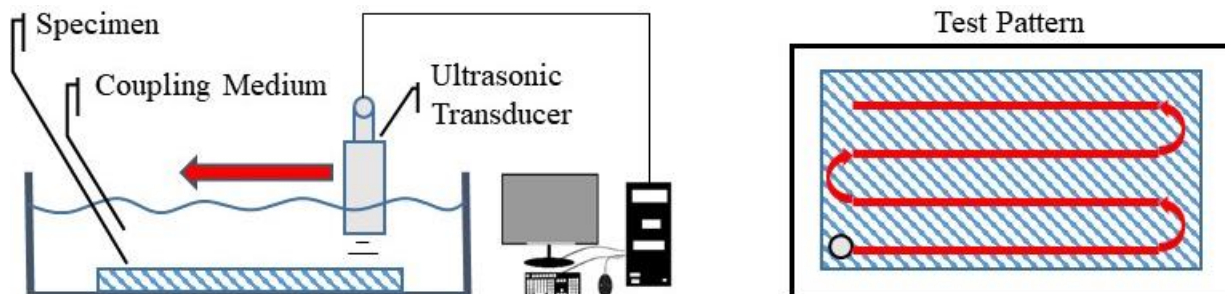
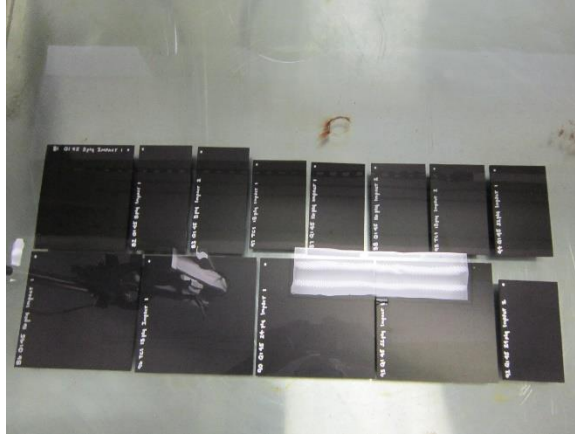


Figure E.96-9. Ultrasonic system components.



*Figure E.96-10. Specimen baseline inspection orientation.*

#### **E.96.3.4 Equipment List and Specifications:**

- Pulsar/Receiver: Olympus 5073PR
- Digitizer: AlazarTech ATS9462, dual channel, 16 bit, 180 MS/s
- Sensor: Olympus 2-inch spherical focus immersion ultrasonic transducer
- Motion system: open looped stepper motor based X-YY-Z gantry robot
- Motion Controller: Galil DMC-4183
- Acquisition Software: FastScan, custom developed at NASA LaRC
- Signal Processing Software: DataViewer, custom developed at NASA LaRC

#### **E.96.3.5 Settings**

*Table E.96-3. Post-impact inspection settings.*

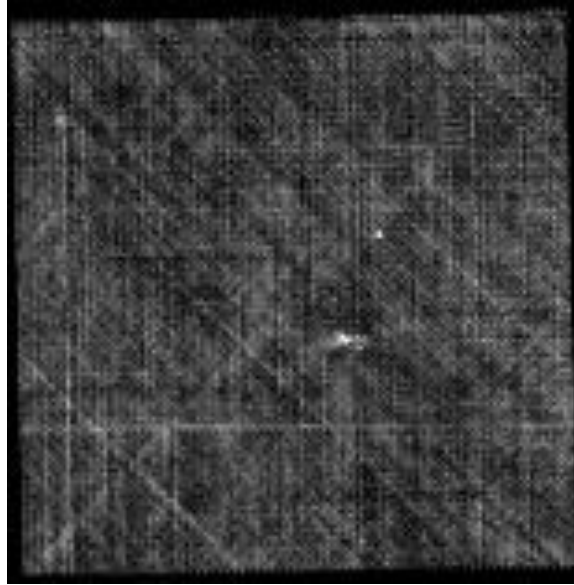
Resolution (horz) [in/pixel]	0.01
Resolution (ver) [in/pixel]	0.01
Probe frequency [MHz]	10
Focal Length [in]	2
Array Dimensions [pixels]	601 × 601

The specimen is placed flat against the zero position of the tank raised above the glass bottom by several metal washers. The test probe is computer-controlled and correlated to the position on the sample. It is also focused to a point 1 mm below the surface of the test material. The specimen remains in place while the transducer follows a preprogrammed test grid across the surface as indicated in Figure E.96-9. At each point, ultrasonic data are collected from individual pulses. Larger step sizes between data collection result in lower image resolution. These data points are reconstructed into a data cube displaying spatial coordinates as time progresses. 2D reconstruction of the collection of ultrasonic responses create flattened slices at varying depths within the material.

#### **E.96.3.6 Inspection Results**

Specimen #96 is a 6 by 6-inch, 18-ply flat panel with a 0.3-inch impact. PEUT was performed on this specimen in NASA's immersion tank specified above.

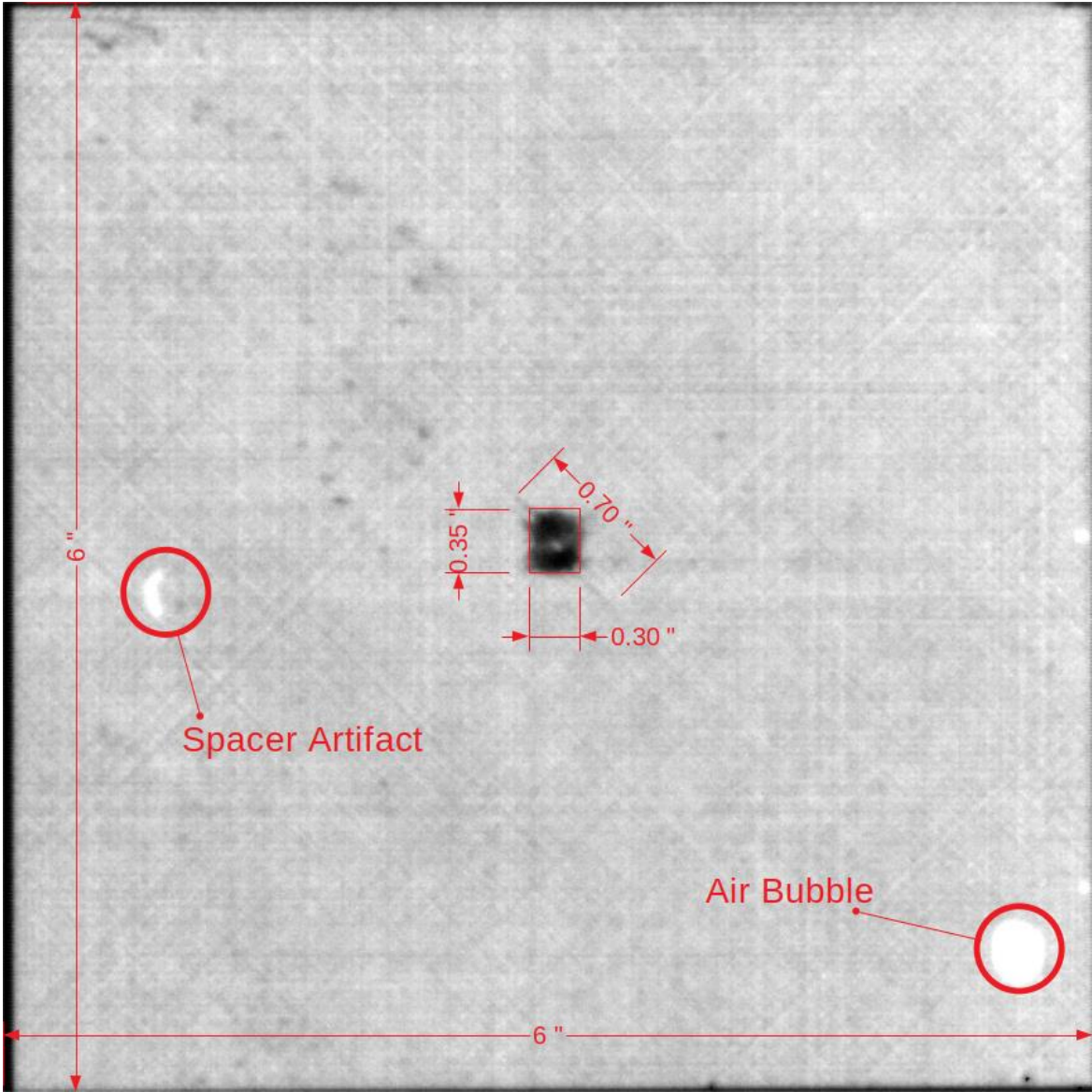
Figure E.96-11 shows an interior echo amplitude image of the sample in its pre-impacted state. One small void and a feature consistent with a twisted tow were noted.



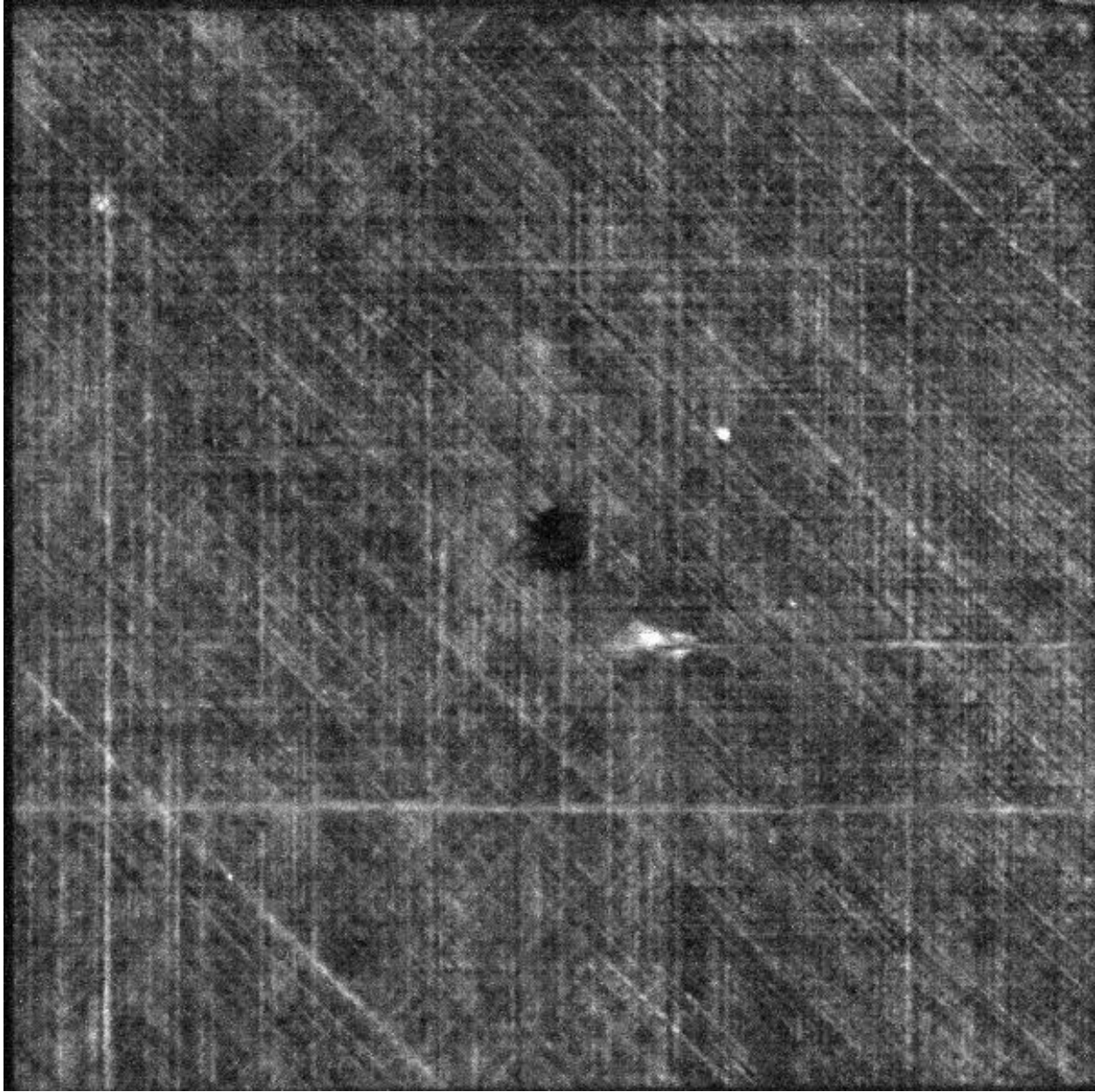
*Figure E.96-11. 10-MHz baseline image.*

Figure E.96-12a shows a back side surface amplitude image of the sample in its post-impacted state. The impact damage region is identified with measurements. An air bubble and a spacer on the under side of the sample in the immersion tank is also noted. Figure E.96-12b below is an internal reflection amplitude image. The gate region is selected to highlight reflections from the void and twisted tow noted above. These features appear unchanged by the impact.





a)



b)

*Figure E.96-12. 10-MHz post-impact image.*

**E.97 Specimen #97: Boeing Impact TC1 18ply 3x5 Impact 1**

Structure	Material	Details	Dimensions (inches)	Partner Methods	
18 plies	IM7/8552	Single Impact Location	6 × 6 5 × 3	NASA	E.97.1 PEUT E.97.2 XCT

## E.97.1 Method: Pulse-Echo Ultrasound Testing (PEUT)

### E.97.1.1 Partner: NASA

### E.97.1.2 Technique Applicability: ★★ ★

PEUT detected the impact damage in this sample.

### E.97.1.3 Laboratory Setup

Immersion Ultrasonic Testing: NASA LaRC uses a custom-designed single-probe ultrasonic scanning system. The system has an 8-axis motion controller, a multi-axis gantry robot mounted above a medium-size water tank, a dual-channel, 16-bit, high-speed digitizer, and an off-the-shelf ultrasonic pulser receiver. The system can perform TTUT and PEUT inspections. TT inspection employs two aligned ultrasonic probes, one transmitter, and one receiver, placed on either side of a test specimen. Pulse-echo inspection is a single-sided method where a single ultrasonic probe is both transmitter and receiver. In each method, data are acquired while raster scanning the ultrasonic probe(s) in relation to a part. Figure E.97-1 shows a simplified block diagram of a scanning Pulse-echo inspection.

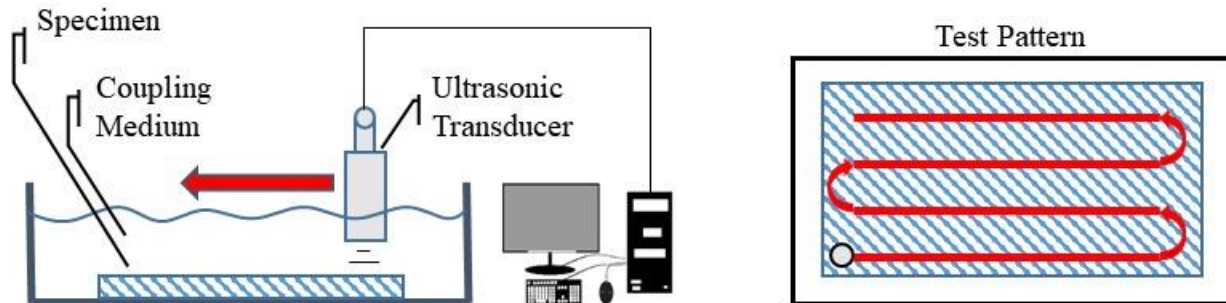


Figure E.97-1. Ultrasonic system components.

### E.97.1.4 Equipment List and Specifications:

- Pulser/Receiver: Olympus 5073PR
- Digitizer: AlazarTech ATS9462, dual channel, 16 bit, 180 MS/s
- Sensor: Olympus 2-inch spherical focus immersion ultrasonic transducer
- Motion system: open looped stepper motor based X-YY-Z gantry robot
- Motion Controller: Galil DMC-4183
- Acquisition Software: FastScan, custom developed at NASA LaRC
- Signal Processing Software: DataView, custom developed at NASA LaRC

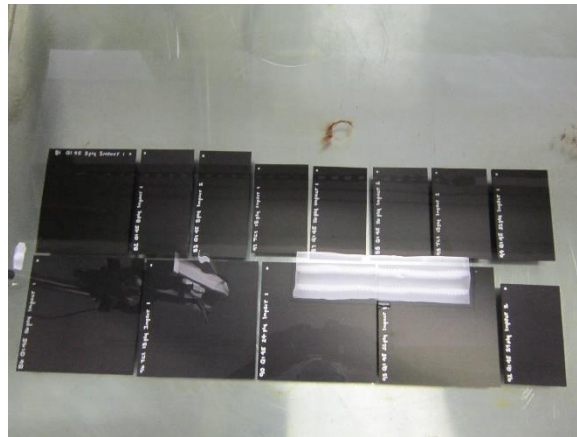
### E.97.1.5 Settings

Table E.97-1. Post-impact inspection settings.

Resolution (horz) [in/pixel]	0.01
Resolution (ver) [in/pixel]	0.01
Probe frequency [MHz]	10
Focal Length [in]	2
Array Dimensions [pixels]	496 × 310

The specimen is placed flat against the zero position of the tank raised above the glass bottom by several metal washers. The test probe is computer-controlled and correlated to the position on the

sample. It is also focused to a point 1 mm below the surface of the test material. The specimen remains in place while the transducer follows a preprogrammed test grid across the surface as indicated in Figure E.97-1. At each point, ultrasonic data are collected from individual pulses. Larger step sizes between data collection result in lower image resolution. These data points are reconstructed into a data cube displaying spatial coordinates as time progresses. 2D reconstruction of the collection of ultrasonic responses create flattened slices at varying depths within the material.



*Figure E.97-2. Specimen baseline inspection orientation.*

#### **E.97.1.6 Inspection Results**

Specimen #97 is a 3 by 5-inch, 18-ply flat panel with a 0.92-inch impact. PEUT was performed on this specimen in NASA's immersion tank specified above.

Figure E.97-3 shows a back side surface amplitude image of the sample in its pre-impacted state. No significant internal flaws were noted. The highlighted areas above are high-amplitude reflections from the three spacers used to position the sample above the bottom of the immersion tank. The bright indication in the lower right is from an air bubble under the sample.

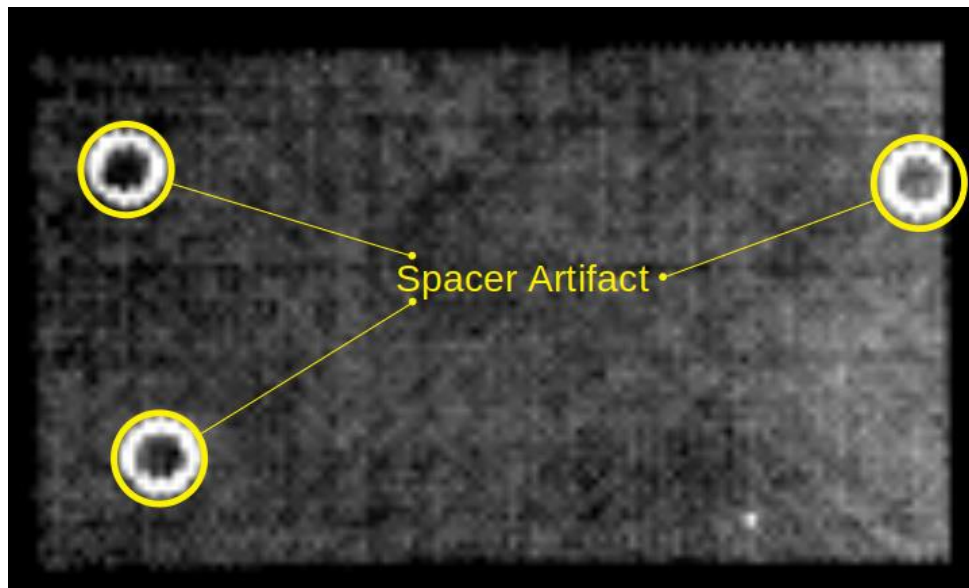


*Figure E.97-3. 10-MHz baseline image.*



Figure E.97-4 shows an internal reflection amplitude image of the sample in its post-impacted state. The gate region is selected to highlight reflections from the delaminations caused by the impact. The impact damage region is identified with measurements.

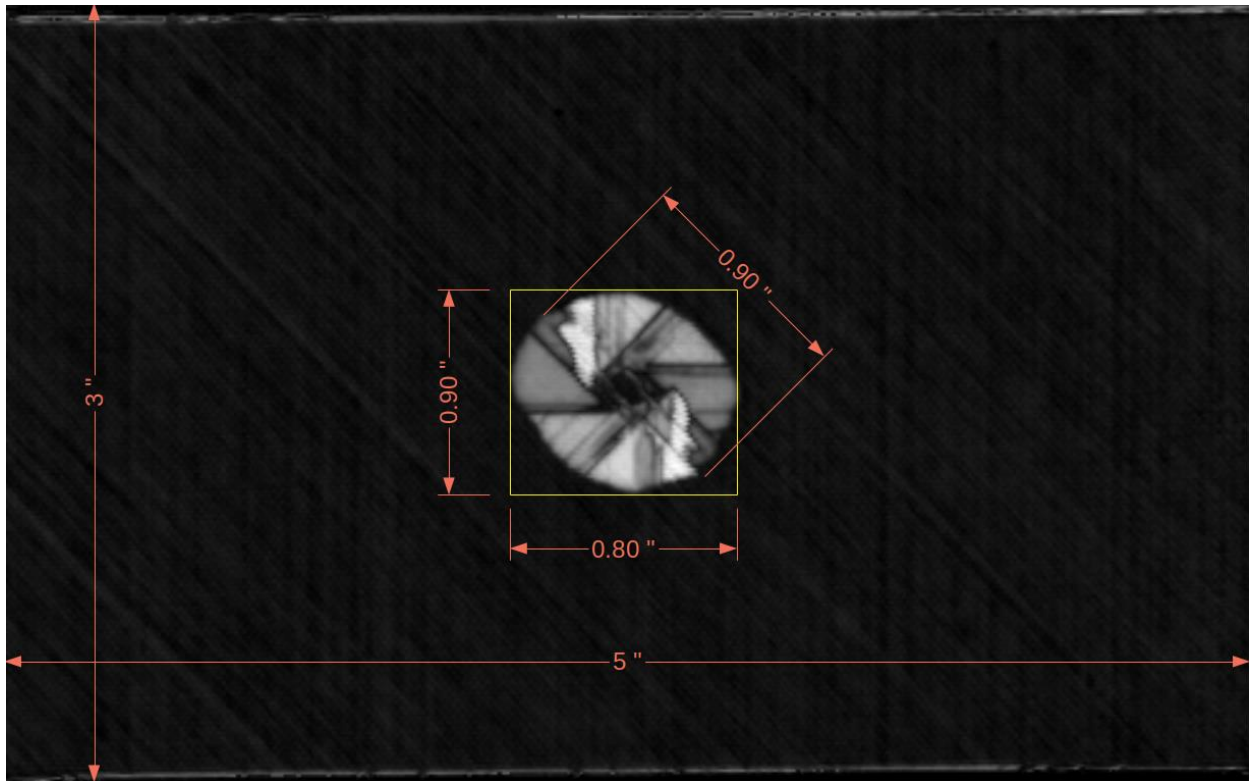


*Figure E.97-4. 10-MHz post-impact image.*

**E.97.2 Method: X-ray Computed Tomography (XCT)**

**E.97.2.1 Partner: NASA**

**E.97.2.2 Technique Applicability: ★★★**

XCT is capable of imaging and quantifying the damage due to low-impact energy in this specimen.

**E.97.2.3 Laboratory Setup**

The microfocus XCT system at NASA LaRC is a commercially available Avonix (Nikon C2) Metrology System designed for high-resolution NDE inspections. The system is an advanced microfocus X-ray system, capable of resolving details down to 5  $\mu\text{m}$ , and with magnifications up to 60X. The system is supplied as a complete, large-dimension radiation enclosure, with X-ray source, specimen manipulator, and an amorphous silica detector as shown in Figure E.97-5. The imaging controls are housed in a separate control console. The detector is a Perkin-Elmer 16-bit amorphous silicon digital detector with a 2000  $\times$  2000-pixel array.



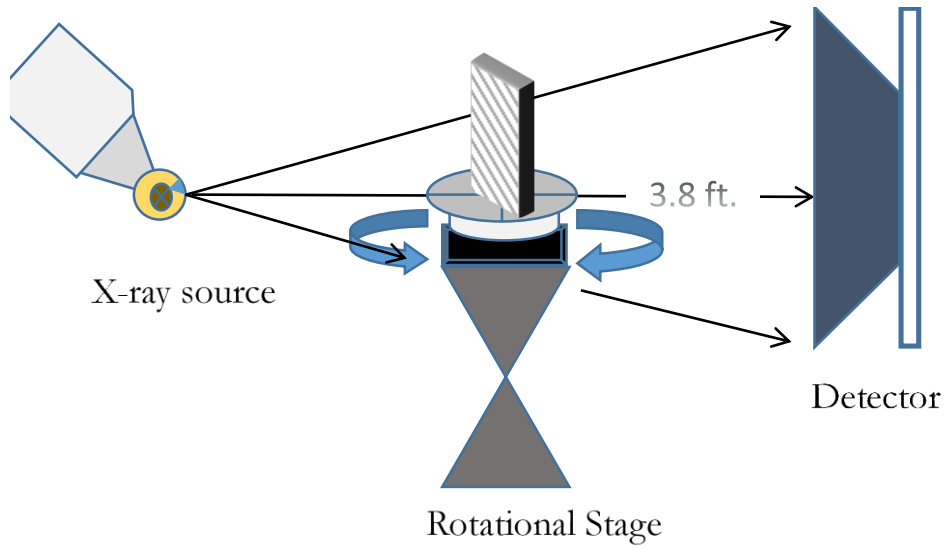


**Figure E.97-5. XCT system components.**

A consistent Cartesian coordinate system is used to define slice direction as illustrated in Figure E.97-6. Slices normal to the X, Y, and Z-directions are shown in Figure E.97-6a, b, and c, respectively.

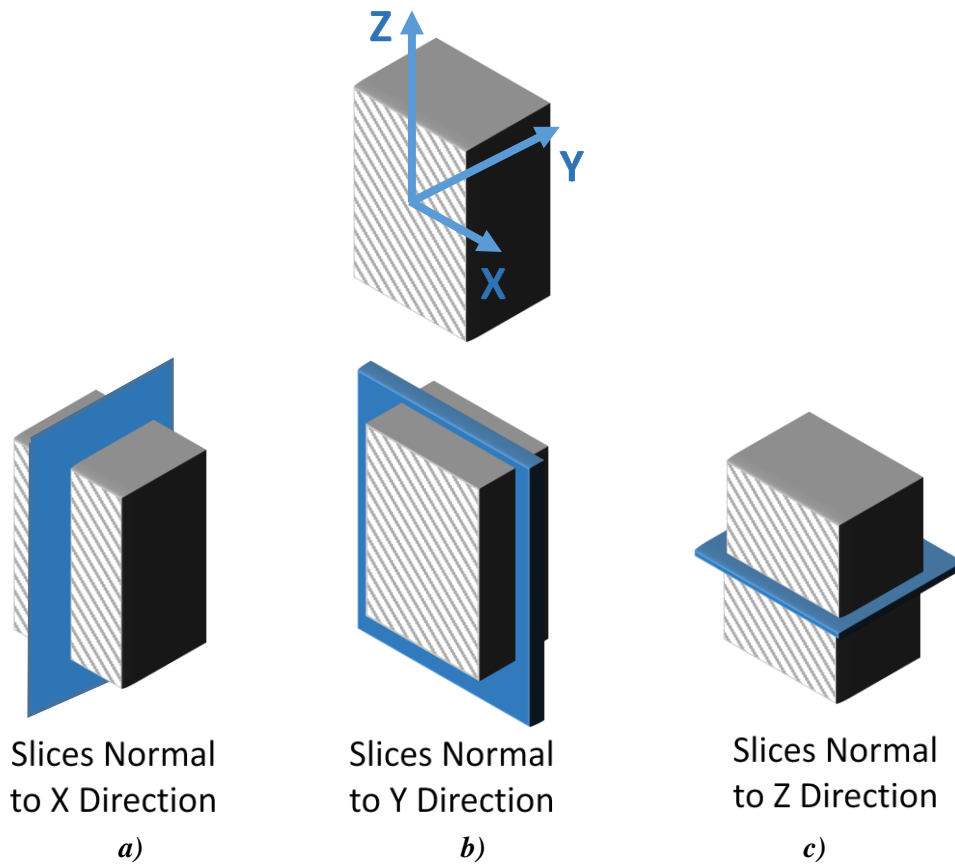


**Figure E.97-6. Slice direction nomenclature.**

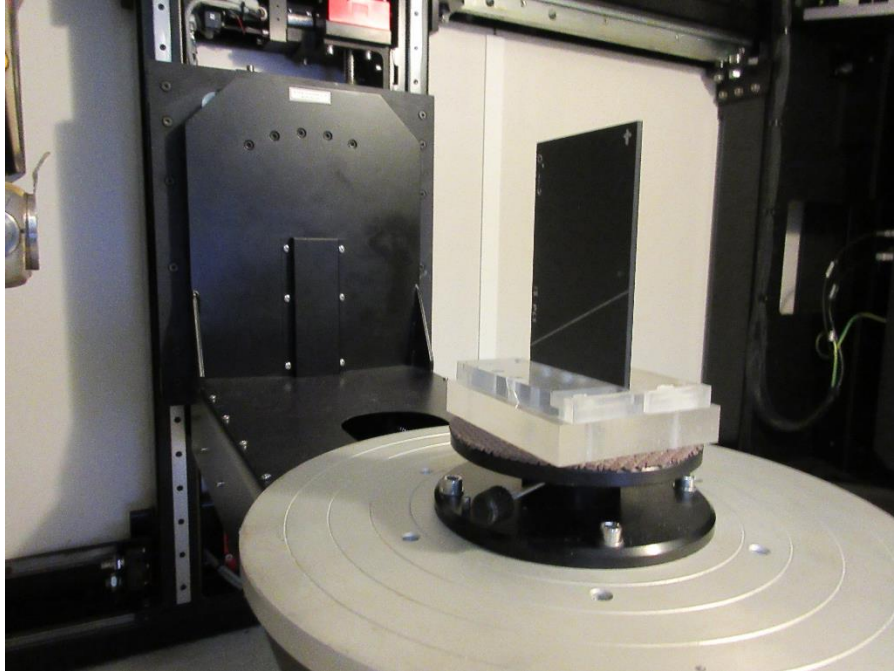


*Figure E.97-7. Impact specimen test stand setup.*

#### **E.97.2.4 Equipment List and Specifications:**

- Avonix 225 CT System
- 225 kV microfocus X-ray source with 5  $\mu\text{m}$  focal spot size
- 15 or 30kg Capacity 5 axis fully programmable manipulator.
- Detector: Perkin Elmer XRD 1621 – 2000  $\times$  2000 pixels with 200  $\mu\text{m}$  pitch
- 10  $\mu\text{m}$  spatial resolution for specimens 1.5 cm wide
- Thin panels 10-inch  $\times$  10-inch – full volume 200  $\mu\text{m}$  spatial resolution

#### **E.97.2.5 Settings**

*Table E.97-2. Data collection settings.*

Source Energy	160 kV
Current	37 $\mu\text{A}$
Magnification	5.0 X
Filter	0.125 Sn
# Rotational angles	3142
Exposure time / frame	1.0 sec
Max Histogram Grey Level	52.7 K
# Averages	8
Resolution ( $\mu\text{m}$ )	40.04 $\mu\text{m}$
Array Dimensions (pixels)	1999 $\times$ 201 $\times$ 1998

The specimen is placed vertically (rotated about the smallest dimension) on the rotational stage located between the radiation source and the detector. The rotational stage is computer-controlled and correlated to the position of the sample. As the sample is rotated the full 360° (~0.11° increments), the detector collects radiographs at each rotated angle as the X-ray path intersects the sample. 3D reconstruction of the collection of radiographs produces a volume of data that can then

be viewed along any plane in the volume. The closer the sample can be placed to the X-ray source, the higher the spatial resolution that can be obtained.

### E.97.2.6 Data and Results

Specimen #97, is a 3 by 5-inch 18-ply flat panel with a BVID impact. XCT was performed on this specimen in NASA LaRC’s CT system with the settings defined in Table E-97.2.

The damage caused by the impact is clearly seen from all viewing directions as shown in Figure E.97-8. There is no surface indication of an impact. Damage extends almost completely through the thickness of the specimen, getting wider at depths furthest from the impacted side. As can be seen in Figure E.97-8 (left), the delaminations are also getting wider at depths furthest from the impacted side.

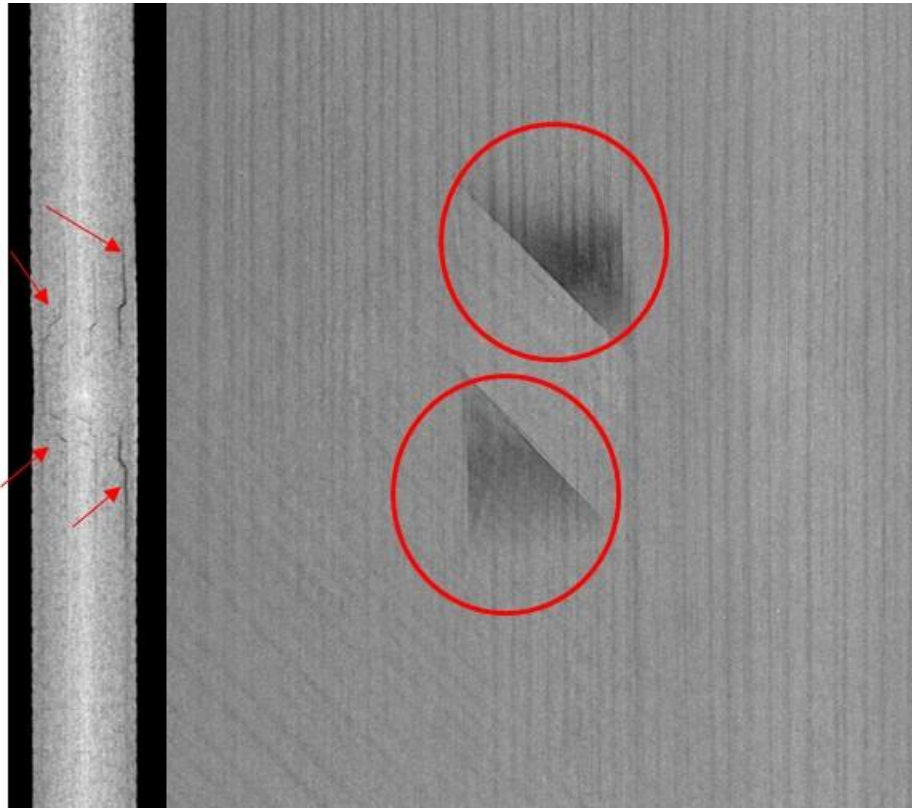


*Figure E.97-8. CT slice normal to the thickness direction show delaminations and matrix cracking (left). CT slice normal to the front surface shows delaminations between plies (right).*

### E.98 Specimen #98: Boeing Impact TC1 18ply 3x5 Impact 2

Structure	Material	Details	Dimensions (inches)	Partner Methods	
18 plies	IM7/8552	Single Impact Location	6 × 6 5 × 3	NASA	E.98.1 PEUT E.98.2 XCT

#### E.98.1 Method: Pulse-Echo Ultrasound Testing (PEUT)

##### E.98.1.1 Partner: NASA

##### E.98.1.2 Technique Applicability: ★★★

PEUT detected the impact damage in this sample.

### E.98.1.3 Laboratory Setup

Immersion Ultrasonic Testing: NASA LaRC uses a custom-designed single-probe ultrasonic scanning system. The system has an 8-axis motion controller, a multi-axis gantry robot mounted above a medium-size water tank, a dual-channel, 16-bit, high-speed digitizer, and an off-the-shelf ultrasonic pulser receiver. The system can perform TTUT and PEUT inspections. TT inspection employs two aligned ultrasonic probes, one transmitter, and one receiver, placed on either side of a test specimen. Pulse-echo inspection is a single-sided method where a single ultrasonic probe is both transmitter and receiver. In each method, data are acquired while raster scanning the ultrasonic probe(s) in relation to a part. Figure E.98-1 shows a simplified block diagram of a scanning Pulse-echo inspection.

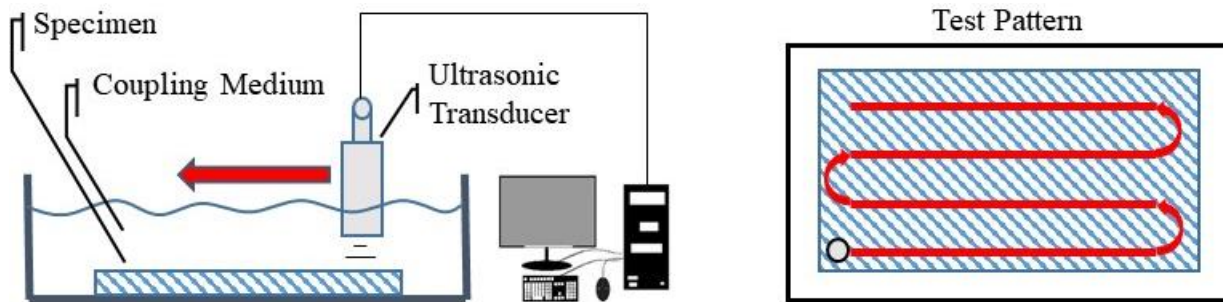


Figure E.98-1. Ultrasonic system components.

### E.98.1.4 Equipment List and Specifications:

- Pulser/Receiver: Olympus 5073PR
- Digitizer: AlazarTech ATS9462, dual channel, 16 bit, 180 MS/s
- Sensor: Olympus 2-inch spherical focus immersion ultrasonic transducer
- Motion system: open looped stepper motor based X-YY-Z gantry robot
- Motion Controller: Galil DMC-4183
- Acquisition Software: FastScan, custom developed at NASA LaRC
- Signal Processing Software: DataViewer, custom developed at NASA LaRC

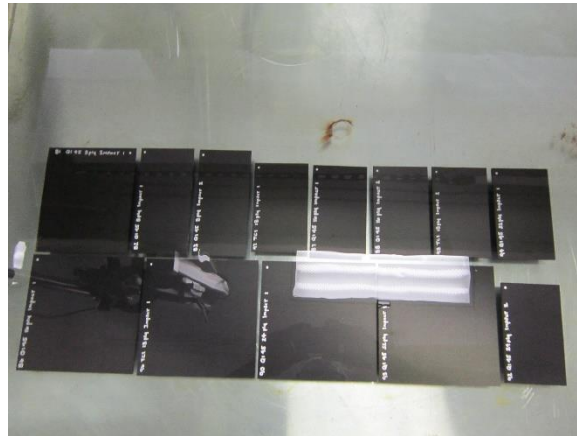
### E.98.1.5 Settings

Table E.98-1. Post-impact inspection settings.

Resolution (horz) [in/pixel]	0.01
Resolution (ver) [in/pixel]	0.01
Probe frequency [MHz]	10
Focal Length [in]	2
Array Dimensions [pixels]	504 × 309

The specimen is placed flat against the zero position of the tank raised above the glass bottom by several metal washers. The test probe is computer-controlled and correlated to the position on the sample. It is also focused to a point 1 mm below the surface of the test material. The specimen remains in place while the transducer follows a preprogrammed test grid across the surface as indicated in Figure E.98-2. At each point, ultrasonic data are collected from individual pulses. Larger step sizes between data collection result in lower image resolution. These data points are reconstructed into a data cube displaying spatial coordinates as time progresses. 2D reconstruction

of the collection of ultrasonic responses create flattened slices at varying depths within the material.

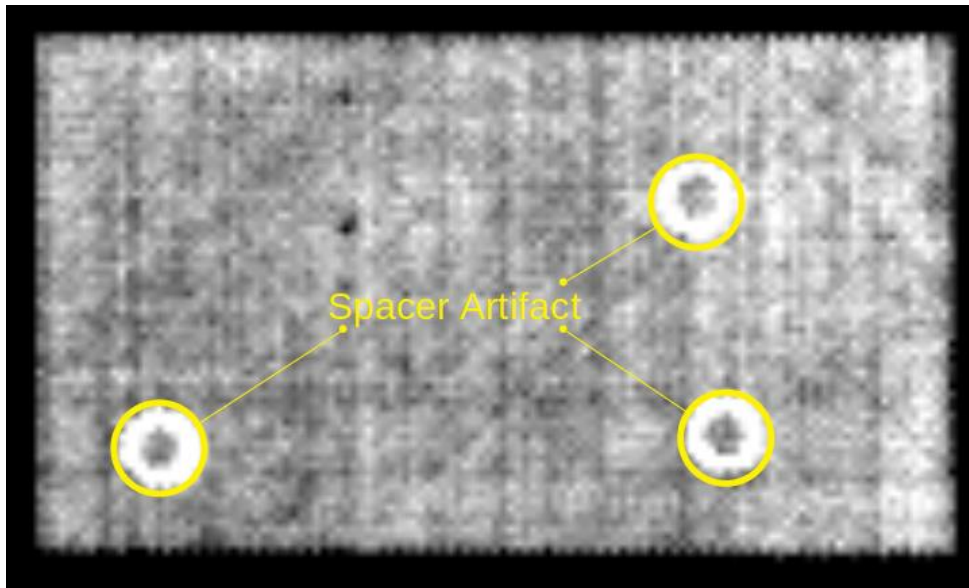


*Figure E.98-2. Specimen baseline inspection orientation.*

### **E.98.1.6 Inspection Results**

Specimen #98 is a 3 by 5-inch, 18-ply flat panel with a 0.96-inch impact. PEUT was performed on this specimen in NASA's immersion tank specified above.

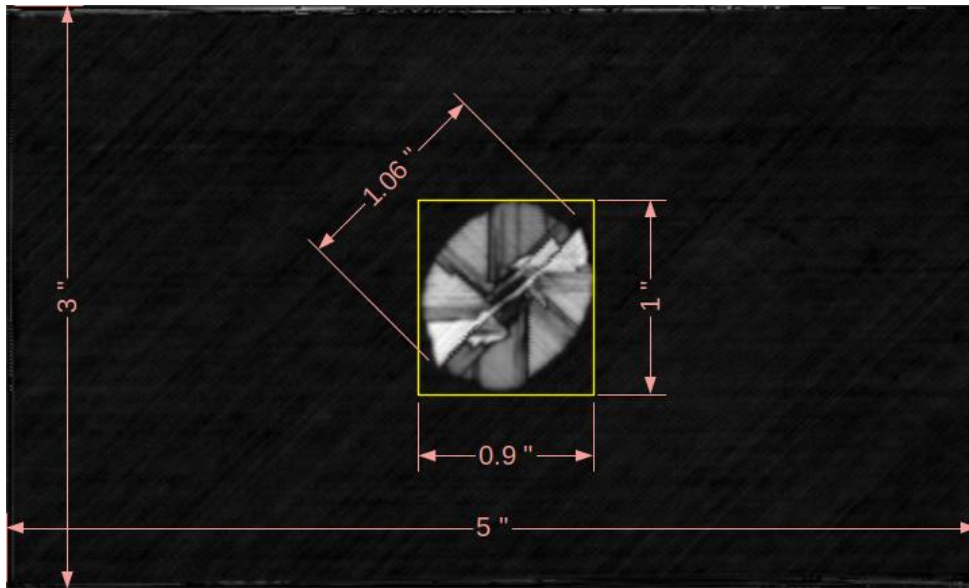
Figure E.98-3 shows a back side surface amplitude image of the sample in its pre-impacted state. No significant internal flaws were noted. The highlighted areas above are high-amplitude reflections from the three spacers used to position the sample above the bottom of the immersion tank.



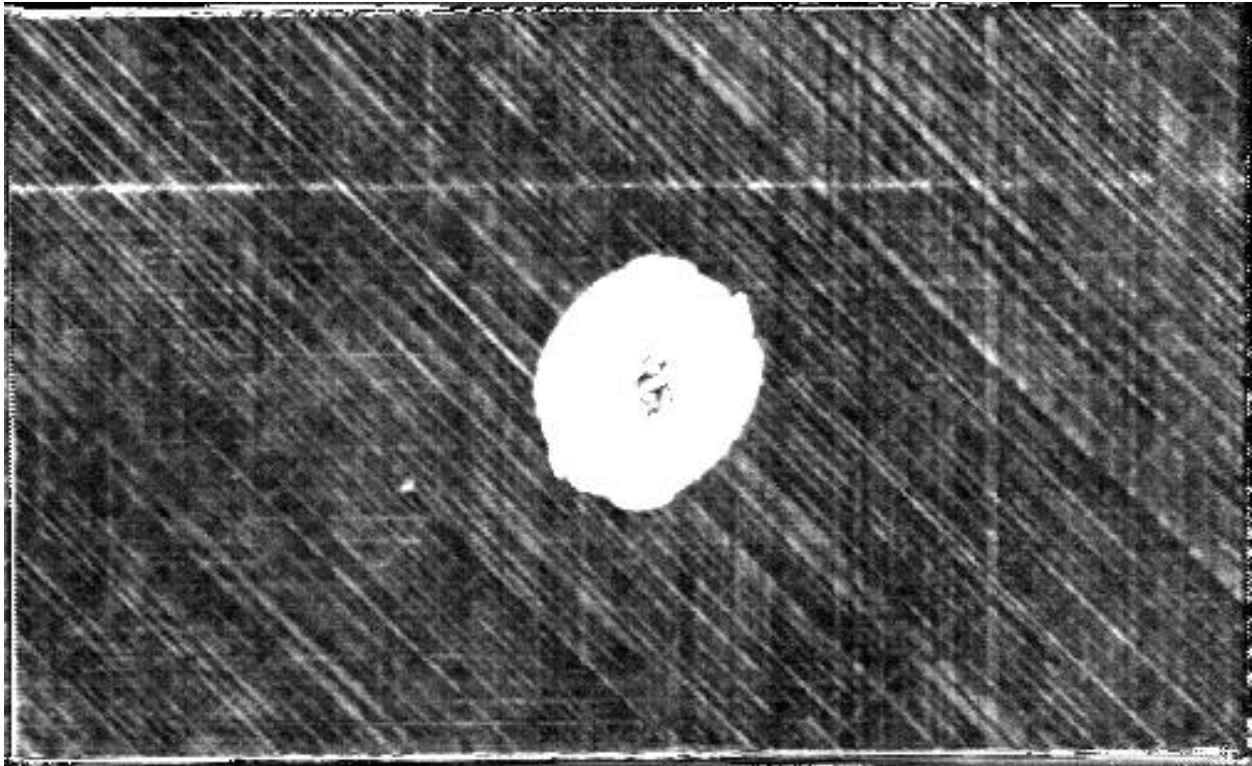
*Figure E.98-3. 10-MHz baseline image.*

Figure E.98-4a shows an internal reflection amplitude image of the sample in its post-impacted state. The gate region is selected to highlight reflections from the delaminations caused by the impact. The impact damage region is identified with measurements. Figure E.98.4b shows the same time gated region as above allowing the high-amplitude delamination reflections to saturate revealing the internal features.





a)



b)

*Figure E.98-4. 10-MHz post-impact image.*

**E.98.2 Method: X-ray Computed Tomography (XCT)**

**E.98.2.1 Partner: NASA**

**E.98.2.2 Technique Applicability: ★★★**

XCT is capable of imaging and quantifying the damage due to low-impact energy in this specimen.

### E.98.2.3 Laboratory Setup

The microfocus XCT system at NASA LaRC is a commercially available Avonix (Nikon C2) Metrology System designed for high-resolution NDE inspections. The system is an advanced microfocus X-ray system, capable of resolving details down to 5  $\mu\text{m}$ , and with magnifications up to 60X. The system is supplied as a complete, large-dimension radiation enclosure, with X-ray source, specimen manipulator, and an amorphous silica detector as shown in Figure E.98-5. The imaging controls are housed in a separate control console. The detector is a Perkin-Elmer 16-bit amorphous silicon digital detector with a  $2000 \times 2000$ -pixel array.

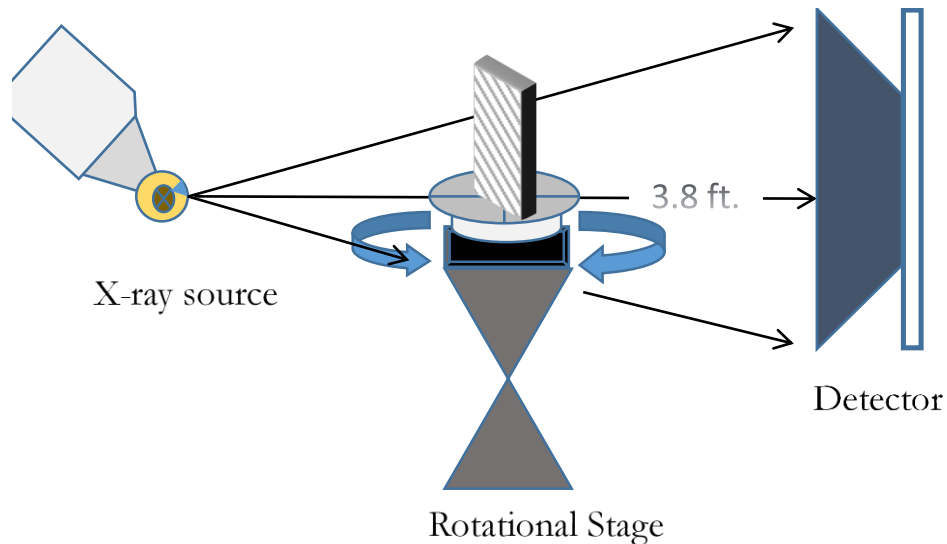


*Figure E.98-5. XCT system components.*

A consistent Cartesian coordinate system is used to define slice direction as illustrated in Figure E.98-6. Slices normal to the X, Y, and Z-directions are shown in Figure 98-6a, b, and c, respectively.



#### E.98.2.4 Equipment List and Specifications:

- Avonix 225 CT System
- 225 kV microfocus X-ray source with 5  $\mu\text{m}$  focal spot size
- 15 or 30kg Capacity 5 axis fully programmable manipulator
- Detector: Perkin Elmer XRD 1621 – 2000  $\times$  2000 pixels with 200  $\mu\text{m}$  pitch
- 10  $\mu\text{m}$  spatial resolution for specimens 1.5 cm wide
- Thin panels 10-inch  $\times$  10-inch – full volume 200  $\mu\text{m}$  spatial resolution

#### E.98.2.5 Settings

*Table E.98-2. Data collection settings.*

Source Energy	160 kV
Current	37 $\mu\text{A}$
Magnification	5.0 X
Filter	0.125 Sn
# Rotational angles	3142
Exposure time / frame	1.0 sec
Max Histogram Grey Level	53 K
# Averages	8
Resolution ( $\mu\text{m}$ )	40.04 $\mu\text{m}$
Array Dimensions (pixels)	1999 $\times$ 221 $\times$ 1998

The specimen is placed vertically (rotated about the smallest dimension) on the rotational stage located between the radiation source and the detector. The rotational stage is computer-controlled and correlated to the position of the sample. As the sample is rotated the full 360° (~0.11° increments), the detector collects radiographs at each rotated angle as the X-ray path intersects the sample. 3D reconstruction of the collection of radiographs produces a volume of data that can then be viewed along any plane in the volume. The closer the sample can be placed to the X-ray source, the higher the spatial resolution that can be obtained.

#### E.98.2.6 Data and Results

Specimen #98, is a 3 by 5-inch 18-ply flat panel with a BVID impact. XCT was performed on this specimen in NASA LaRC's CT system with the settings defined in Table E-98.2.

The damage caused by the impact can be clearly seen from all viewing directions as shown in Figure E.98-8. There is no surface indication of an impact. Damage extends most of the way through the thickness of the specimen.

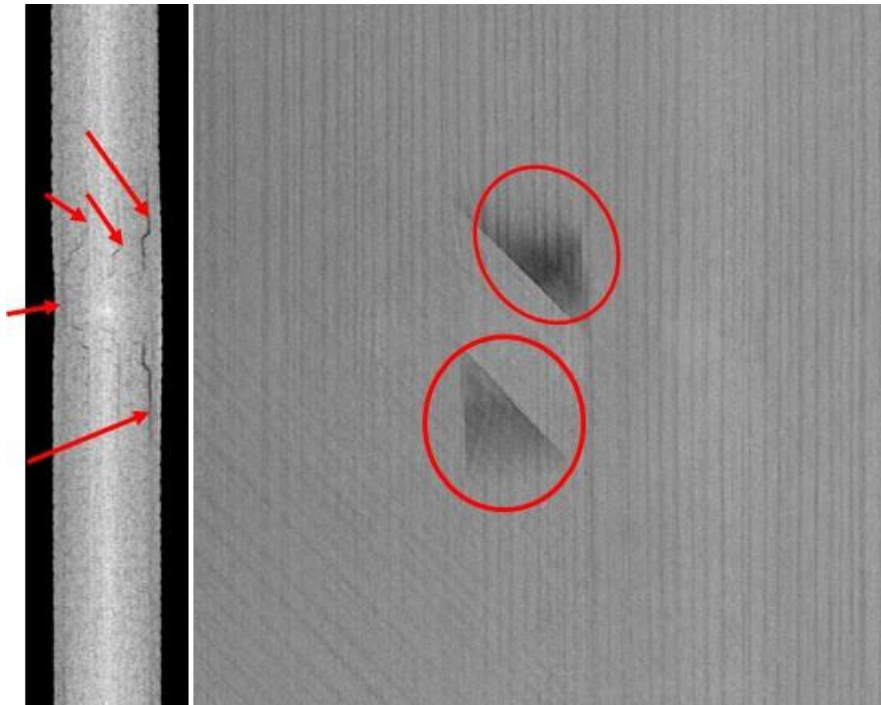


*Figure E.98-8. CT slice normal to the thickness direction show delaminations and matrix cracking (left). CT slice normal to the front surface shows delaminations between plies (right).*